

UNCLASSIFIED

AD 403 387

*Reproduced
by the*

DEFENSE DOCUMENTATION CENTER

FOR

SCIENTIFIC AND TECHNICAL INFORMATION

CAMERON STATION, ALEXANDRIA, VIRGINIA



UNCLASSIFIED

NOTICE: When government or other drawings, specifications or other data are used for any purpose other than in connection with a definitely related government procurement operation, the U. S. Government thereby incurs no responsibility, nor any obligation whatsoever; and the fact that the Government may have formulated, furnished, or in any way supplied the said drawings, specifications, or other data is not to be regarded by implication or otherwise as in any manner licensing the holder or any other person or corporation, or conveying any rights or permission to manufacture, use or sell any patented invention that may in any way be related thereto.

63-3-3

403387

ASD-TDR-62-731

FIBER OPTICS IN AEROSPACE VEHICLE HAZARD DETECTION

ACTUAL
CATALOGUE

TECHNICAL DOCUMENTARY REPORT ASD-TDR-62-731

December 1962

Directorate of Aeromechanics
Aeronautical Systems Division
Air Force Systems Command
Wright-Patterson Air Force Base, Ohio

Project No. 6075, Task No. 607506

ASTIA

MAY 8 1963

ASTIA

(Prepared under Contract No. AF 33(616)-8165
by Fenwal Incorporated, Ashland, Massachusetts
Author: Alan C. Traub)

**Best
Available
Copy**

NOTICES

When Government drawings, specifications, or other data are used for any purpose other than in connection with a definitely related Government procurement operation, the United States Government thereby incurs no responsibility nor any obligation whatsoever; and the fact that the Government may have formulated, furnished, or in any way supplied the said drawings, specifications, or other data, is not to be regarded by implication or otherwise as in any manner licensing the holder or any other person or corporation, or conveying any rights or permission to manufacture, use, or sell any patented invention that may in any way be related thereto.

Qualified requesters may obtain copies of this report from the Armed Services Technical Information Agency, (ASTIA), Arlington Hall Station, Arlington 12, Virginia.

This report has been released to the Office of Technical Services, U.S. Department of Commerce, Washington 25, D.C., in stock quantities for sale to the general public.

Copies of this report should not be returned to the Aeronautical Systems Division unless return is required by security considerations, contractual obligations, or notice on a specific document.

FOREWORD

51 Report on

This is the final report on work done by Fenwal Incorporated, Ashland, Massachusetts, under Air Force Contract No. AF 33(61)-8165, Project No. 6075, Task No. 607506. This program, entitled "Investigation of Fiber Optics for Hazard Detection" was conducted between 8 March 1961 and 30 June 1962 and was administered under the direction of the Hazards Protection Section, Environmental Branch, Flight Accessories Laboratory, Aeronautical Systems Division. Mr. T. M. Trumble was Task Engineer for the Air Force, with Dr. A. C. Traub serving as Project Engineer for the contractor.

A portion of the work, involving certain optical aspects of glass fibers, was subcontracted to American Optical Company. Another subcontract, concerning image tube studies, was let privately to Mr. R. M. Burley of Concord, Massachusetts.

The author wishes to acknowledge the personal interest and assistance of the several engineers and scientists who have made major contributions to this effort and of the many technical personnel who supported their work; in particular:

- 1.) Messrs. G. T. Beery and T. M. Trumble of the Flight Accessories Laboratory, who initiated and supervised the project and whose personal interest and co-operation were extremely helpful.
- 2.) Mr. R. M. Burley of Concord, Massachusetts, who expended considerable personal effort in assembling most of the material on image converters and intensifiers.
- 3.) Dr. W. P. Siegmund, Dr. M. G. Brown, and Mr. E. S. Carpenter of American Optical Company who have made substantial contributions of optical information, both contractually and of their own accord.
- 4.) Mr. J. W. Hicks, Jr., of Mosaic Fabrications Incorporated, who has offered valuable assistance.

Within Fenwal Incorporated, acknowledgement is made to Mr. C. F. Rockwell who provided most of the material on radiation detection systems, with contributions by Messrs. L. H. Walbridge and L. F. Clark, Jr.; to Messrs. S. Dalzell, J. J. Gassmann, T. S. Jess and C. H. Mellor, and to Miss J. E. Sylvester for major contributions on the mechanical and thermal aspects of fiber optic systems. The author's appreciation is also extended to Messrs. J. J. Foley and R. J. Bassett for invaluable assistance in the preparation of most of the drawings and photographs.

FOREWORD

This is the final report on work done by Fenwal Incorporated, Ashland, Massachusetts, under Air Force Contract No. AF 33(616)-8165, Project No. 6075, Task No. 607506. This program, entitled "Investigation of Fiber Optics for Hazard Detection", was conducted between 8 March 1961 and 30 June 1962 and was administered under the direction of the Hazards Protection Section, Environmental Branch, Flight Accessories Laboratory, Aeronautical Systems Division. Mr. T. M. Trumble was Task Engineer for the Air Force, with Dr. A. C. Traub serving as Project Engineer for the contractor.

A portion of the work, involving certain optical aspects of glass fibers, was subcontracted to American Optical Company. Another subcontract, concerning image tube studies, was let privately to Mr. R. M. Burley of Concord, Massachusetts.

The author wishes to acknowledge the personal interest and assistance of the several engineers and scientists who have made major contributions to this effort and of the many technical personnel who supported their work; in particular:

- 1.) Messrs. G. T. Beery and T. M. Trumble of the Flight Accessories Laboratory, who initiated and supervised the project and whose personal interest and co-operation were extremely helpful.
- 2.) Mr. R. M. Burley of Concord, Massachusetts, who expended considerable personal effort in assembling most of the material on image converters and intensifiers.
- 3.) Dr. W. P. Siegmund, Dr. M. G. Brown, and Mr. E. S. Carpenter of American Optical Company who have made substantial contributions of optical information, both contractually and of their own accord.
- 4.) Mr. J. W. Hicks, Jr., of Mosaic Fabrications Incorporated, who has offered valuable assistance.

Within Fenwal Incorporated, acknowledgement is made to Mr. C. F. Rockwell who provided most of the material on radiation detection systems, with contributions by Messrs. L. H. Walbridge and L. F. Clark, Jr.; to Messrs. S. Dalzell, J. J. Gassmann, T. S. Jess and C. H. Mellor, and to Miss J. E. Sylvester for major contributions on the mechanical and thermal aspects of fiber optic systems. The author's appreciation is also extended to Messrs. J. J. Foley and R. J. Bassett for invaluable assistance in the preparation of most of the drawings and photographs.

ABSTRACT

Light-transmitting glass fiber bundles in various configurations have been subjected to extensive optical, mechanical and thermal testing and to various other analyses. The report provides important information on fiber optic characteristics as well as design considerations for developing optimum systems.

System configurations are recommended which would extend the capabilities of the basic fiber bundle in meeting the diverse requirements of installation, operation and maintenance in various applications. An experimental fiber optic system for flame detection is described. It uses a 25 foot long bundle and incorporates a special photoelectric detection system and other embodiments of our findings.

This report has been reviewed and is approved.

William C. Savage
WILLIAM C. SAVAGE
Chief, Environmental Branch
Flight Accessories Laboratory

TABLE OF CONTENTS

Section	Page
INTRODUCTION	1
SUMMARY.....	2
1. PRELIMINARY CONSIDERATIONS	3
1.1 History of Fiber Optics	3
1.2 The Hazard Detection Problem	5
1.2.1 Fiber Optics Capabilities	5
1.2.2 Fiber Optics Limitations	6
1.2.3 Scope of Study	7
2. PROPERTIES OF INDIVIDUAL FIBERS	9
2.1 Optical Properties.....	9
2.1.1 Transmittance.....	9
2.1.2 End Surface Losses	11
2.1.3 Cladding Losses	12
2.1.4 Numerical Aperture	13
2.1.5 Multifibers	14
2.1.6 Measurement Results and Discussion	15
2.2 Mechanical Properties	20
2.2.1 Tensile Strength	20
2.2.2 Shear Strength.....	23
2.2.3 Minimum Bend Radius	24
2.3 Thermal Properties	24
3. PROPERTIES OF FIBER BUNDLES	28
3.1 Optical Image Transmission	28
3.1.1 Attenuation vs. Length	28
3.1.2 Interstitial Losses	34
3.1.3 Resolution	36
3.1.4 Effects of Fiber Diameter.....	38
3.1.5 Coherent vs. Incoherent Bundles	39
3.1.6 Color Distortion in Fiber Bundles	40
3.1.7 Viewing Conditions.....	44
3.1.8 Fused vs. Potted End Faces	44
3.1.9 Exit Angle	45
3.1.10 Non-Glass Fibers.....	46
3.1.11 Summary of Optical Properties.....	46
3.2 Mechanical Properties	49
3.2.1 Tensile Strength	50

Section	Page
3.2.2 Vibration Resistance	51
3.2.3 Other Mechanical Tests	57
3.3 Thermal Properties	59
4. FIBER OPTIC DETECTION SYSTEMS	62
4.1 Terminal Optics.....	62
4.1.1 Objective Lenses.....	62
4.1.2 Magnifying Eyelenses	65
4.2 Radiation Detection	69
4.2.1 Determination of a Detection-Mode Philosophy	69
4.2.2 Evaluation of Existing Photodetectors	82
4.2.3 Photodetection Circuitry	85
4.2.4 Combined Photo and Thermal Detection	87
4.2.5 Detector-to-Fiber-Bundle Couplings	88
4.3 Unusual Bundle Configurations	90
4.4 Bundle-to-Bundle Couplings	91
4.5 Self-Cleaning Windows	93
4.5.1 Thermal Methods	94
4.5.2 Pneumatic Methods	97
4.5.3 Electromechanical Methods	98
4.6 Image Tubes	100
4.7 Test Circuits	102
4.8 Dynamic Scanning Devices	103
5. AN EXPERIMENTAL MODEL.....	105
5.1 Design Considerations.....	105
5.2 Configuration of Experimental Model	106
5.3 Operation of Experimental Model.....	107
6. CONCLUSIONS AND RECOMMENDATIONS	109
APPENDIX	171
DRAWINGS AND FIGURES.....	110
BIBLIOGRAPHY AND REFERENCES	197

LIST OF ILLUSTRATIONS

Figure		Page
1a	End Faces of Monofilament Fiber Bundles at Various Magnifications.....	110
1b	Several Fused Fiber Faceplates under Various Magnifications and Lighting Conditions	110
1c	Multifibers under High Magnification.....	110
2	Spectral Transmittance of Two Types of Schott Glass in Four Inch Thicknesses	111
3	Spectral Transmittance of Solid Glass Extrapolated to 6 and 50 Foot Thicknesses from Measurements on a 4 Inch Block.....	112
4	Spectral Transmittance of Solid Glass Extrapolated to 6 and 50 Foot Thicknesses from Measurements on a 4 Inch Block.....	113
5	Spectral Transmittance of Solid Glass Extrapolated to 6 and 50 Foot Thicknesses from Measurements on a 4 Inch Block.....	114
6	Spectral Transmittance of Solid Glass Extrapolated to 6 and 50 Foot Thicknesses from Measurements on a 4 Inch Block.....	115
7	Spectral Transmittance of Solid Glass Extrapolated to 6 and 50 Foot Thicknesses from Measurements on a 4 Inch Block.....	116
8	Spectral Transmittance of Solid Glass Extrapolated to 6 and 50 Foot Thicknesses from Measurements on a 4 Inch Block.....	117
9	Fiber Radiation Pattern with 17° Input Cone	118
10	Fiber Radiation Pattern with 74° Input Cone	119
11	Frequency of Breakage vs. Tension for Three Groups of Fibers.....	120

LIST OF ILLUSTRATIONS

Figure		Page
12	Shear Strength Apparatus	121
13	Distribution of Shear Points for Mono-Fibers of Various Diameters.....	122
14	Test for Minimum Bend Radius of Glass Fibers.....	123
15	Frequency of Breakage vs. Radius for Several Fiber Diameters.....	124
16	Typical Fiber Viscosities vs. Temperature.....	125
17	Typical Viscosity-Time Curves	126
18	Comparison of Core and Clad-Core Transmittance (Theoretical).....	127
19	Theoretical Spectral Transmittance of Four Fiber Bundles with 70% Area Factor.....	128
20	Reproduction of Direct Spectrophotometric Curves for Four Fiber Bundles, Including Lens Losses	129
21	Typical Arrangement for Fiber Image Studies.....	130
22	Appearance of Engine Fire through Simulated Thicknesses of Fused Fiber Faceplate.....	131
23	Appearance of Engine Fire through Simulated Lengths of Multifiberscope	132
24	Low Resolution Flame Image Transmitted by Simulated Lengths of Monofilament Fiberscope	133
25	Small Flame and Glowing Turbine Casing Seen through Simulated Lengths of Multifiberscope.....	134
26	Closely Packed Array of Fiber Ends, Typical of Light Pipes.....	135

LIST OF ILLUSTRATIONS

Figure		Page
27	End Face Array Typical of Monofilament Fiberscope	136
28a	Test Pattern Imaged by Fused Faceplate with "Four Mil" Fibers	137
28b	Test Pattern Imaged by Fused Faceplate with "Two Mil" Fibers	137
28c	Test Pattern Imaged by Fused Faceplate with "Half Mil" Fibers	137
29	Image Clarity as Affected by Number of Fibers per Image.....	138
30	Perceptibility of Incandescent Turbine Casing vs. Apparent Image Size	139
31	Color Test Chart Photographed Directly and through 25 Foot Fiberscope	140
32	Pair of Joined 12-1/2 Foot Fiberscopes Used in Preparing Figure 31	141
33	Color Effects of 6-1/4 Foot Long Fiber Bundle on Selected Blackbody Temperatures	142
34	Color Effects of 12-1/2 Foot Long Fiber Bundle on Selected Blackbody Temperatures	143
35	Color Effects of 25 Foot Long Fiber Bundle on Selected Blackbody Temperatures	144
36	Color Effects of 50 Foot Long Fiber Bundle on Selected Blackbody Temperatures	145
37	Color Effects of 100 Foot Long Fiber Bundle on Selected Blackbody Temperatures	146
38	"Image Washout" Due to Ambient Light Falling on End Face.....	147

LIST OF ILLUSTRATIONS

Figure		Page
39	Increased Image Mottling with Reduced Objective Lens Aperture.....	148
40	Image Brightness vs. Viewing Angle and Objective Lens Aperture Ratio.....	149
41	Typical Vibration Test Arrangement, Showing Shaker Table and Control Console.....	150
42	Effect of Varying the Objective Lens Focal Length	151
43	Effect of Varying the Eyepiece Magnification.....	152
44	Photodetection Circuit Used in Experimental Breadboard	153
45	Three Possible Multiple Bundle Configurations.....	154
46	Self-Cleaning Window Test Arrangement	155
47	One Form of Thermal Self-Cleaning Window.....	156
48	Another Form of Thermal Self-Cleaning Window.....	157
49	Various Self-Heated Test Windows.....	158
50	Two Other Forms of Self-Cleaning Windows	159
51	Self-Cleaning Windows; Air Flow Devices	160
52	Self-Cleaning Windows; Air Flow Devices.....	161
53	Self-Cleaning Windows; Air Flow Devices.....	162
54	Operation of Electromechanical Self-Cleaning Window. Exterior View.....	163
55	Operation of Electromechanical Self-Cleaning Window. Interior View.....	164
56	An Infrared Image Converter, A Reference Photograph, and Two Converted Images.....	165

LIST OF ILLUSTRATIONS

Figure		Page
57	Control Photographs and Converted Infrared Images of Various Scenes Containing Organic Diffusion Flames.....	166
58	Alarm Unit Adaptor; Connector; and Test Assembly.....	167
59	Control Unit (Experimental Optical Detection System)	168
60	Experimental Fiber Optic Hazard Detection System	169
61	Half-Power Spectral Ranges and Peak Response Wave- Lengths of Various Photodetectors Compared with Spectral Line-Transmittance of a 6 Foot Fiber Bundle.....	170

LIST OF TABLES

Table	Page
1 Tensile Strength Test Results on Single Fibers.....	21
2 Thermal Properties of Two Glasses	25
3 Corrected Transmittance Values for Curves Shown in Figure 20.....	32
4 Color Temperatures of Various Light Sources.....	43
5 Typical Applications of Various Fiber Bundle Configurations	49
6 Vibration Test Results on Two Fiber Bundles.....	53
7 Compressional Test Results on Various Jacketed Configurations.....	58
8 Angular Field for Various Objective Lens Focal Lengths and Fiberscope End Face Dimensions	64
9 Comparison of Photodetectors.....	84

INTRODUCTION

The routine operation of an aircraft requires that the pilot have immediate and reliable information in the event of a vehicle malfunction so that corrective action may be taken quickly. At present, the occurrence of a hazardous situation is communicated to the pilot through an array of electrical or electronic devices, such as engine fire or overheat detectors, smoke detectors, fuel and oil pressure gauges, landing-gear down-lock indicators and others.

Although these devices are highly reliable and effective, they are known to malfunction occasionally and to provide the pilot with false information, or with not enough information, such as whether an engine fire is an especially violent one or is fairly localized and can be controlled. A vital ingredient which these devices lack is the ability to put the pilot into close psychological touch with the occurrence. He must rely upon his instruments and often wonders if they themselves are operating properly. Pilots have been known to remark that if they could see into an engine compartment "with their own eyes", then they would believe what the instruments are telling them.

Accordingly, it was the purpose of this effort "to put the pilot's eye into the engine compartment" or other remote location so that he personally might evaluate the visual information and form his own judgment of whether an alarm condition existed.

Our purpose has been to determine whether the fairly new science of fiber optics might provide solutions to certain problems in the detection of engine fires and other hazards by aircraft crew members during flight.

Manuscript released by the author on 28 September 1962 for publication as an
ASD Technical Documentary Report

SUMMARY

This study has attempted to establish the effectiveness of various fiber optic system configurations in providing positive visual identification of certain flight hazards; it has also examined the compatibility of such systems with the environmental rigors of airborne operation.

It is not the purpose of a fiber bundle to serve as a primary alarm device, for this would imply the need for continuous monitoring by the pilot or other crew member. Instead, the bundle is intended for operation in support of associated or separate malfunction detectors in order to provide highly reliable verification or supplemental information.

The findings of this study are that fiber optic systems can be used to great advantage in providing flight crews with reliable knowledge of certain hazardous conditions in remote areas of the flight vehicle. The effectiveness of the system is limited only by the degree of refinement specified by the designer. When good visual acuity must be provided, such as if the operation of a landing-gear down-lock must be observed, a fiber system can be specified which will provide an image quality comparable to that of the finest color television system. Where one simply wants to identify a flickering yellow fire in an otherwise dark engine compartment, considerable savings in weight and cost may be realized by the use of a very simple "light pipe" (or scrambled fiber bundle) configuration.

Laboratory tests conducted as a part of this program have indicated that such systems, when properly designed, should be extremely adaptable to the adverse mechanical, thermal and other influences which accompany airborne and aerospace vehicle operations.

SECTION 1

PRELIMINARY CONSIDERATIONS

This section presents a definition and brief historical review of fiber optics, limited to those events which are of interest to the present problem. It also discusses the hazard detection problem, those optical features of fiber bundles which clearly lend themselves to solutions of the problem, and the known physical properties of fiber bundles which had to be more fully investigated in order to establish the limits on the capabilities which the fiber science could offer.

1.1 History of Fiber Optics

Fiber optics is the science dealing with the transmission of electromagnetic radiation through transparent filaments which are long compared with their diameters. The fiber diameters of interest are small enough to permit substantial bending without breakage and therefore they allow the possibility of flexible fiber bundles which can transmit light from one place to another along a curved path.

If the fibers are intentionally arranged in an orderly manner in a fiber bundle, so that the opposite ends of each fiber occupy corresponding positions in the end faces of the bundle, an entire optical image can be transmitted. The bundle transmits the image by means of "static scanning", or simultaneous point by point transmission of each element of the image. This is to be contrasted with dynamic scanning as is used in television and facsimile transmission in which the image points are scanned consecutively and transmitted by a single channel.

It has been known for many years that smooth-walled, transparent cylinders, such as glass or plastic rods, have the ability to conduct light from one end to the other by means of multiple internal reflections. This conduction phenomenon occurs even within narrow, flexible filaments of such materials and, moreover, the filaments may be rather sharply bent without seriously reducing the light transmission.

Such a filament can be used to conduct light from one point to another, although the emergent light is simply a spot of one color and intensity only and does not include any pictorial information which may have been contained in the light striking it. This is because the multiple reflections from the walls, which appear shiny from the inside, have the property of averaging out any color and intensity variations which may exist over the end face as the light enters it.

In 1920, a review of electromagnetic wave propagation through transparent filaments was presented by Schriever (9)*. In the mid-1920's, patents were

*Numerals in parentheses refer to published works in Bibliography and References

applied for by Baird (12) and by Hansell (15) which suggested the use of many such filaments in parallel to conduct the many, separate spots of light which make up the entire image of an object. The idea was apparently first reduced to practice by Lamm (7) in the late 1920's.

At that time, little was known about practical means for making and aligning small, transparent fibers and preventing light leakage between walls of adjacent fibers. Consequently, the art did not advance appreciably for several decades, although many ideas were proposed and patented involving the use of light-conducting filaments for television systems, endoscopes and so forth.

In 1953, van Heel (10) in Holland reported on a method of optically insulating small glass fibers, following this with another paper (11) in 1954. In that year, Hopkins and Kapany (3) in England described a practical method of aligning the fibers and apparently coined the name "fiberscope". Meanwhile, work was under way by O'Brien in the U.S. on fiber cladding and other improvements and a patent application describing improved fiberscopes was filed in 1954 (17).

Shortly thereafter, serious research in fiber optics was begun at American Optical Company, Bausch & Lomb Optical Company, and the University of Rochester; this was followed shortly by work at Armour Research Foundation, the University of Michigan, American Cystoscope Makers Incorporated and Mosaic Fabrications Incorporated.

The efforts of these and other highly competent groups soon brought fiber bundles to the stage of commercial feasibility; the bundles could be made reproducibly, the image quality was good, and the cost was within reach of many potential users. As industry became aware of the technical possibilities of the fiberscope and its non-image-bearing counterpart, the "light pipe", increasing numbers of diverse applications were suggested and experimental fiber bundles were prepared in various configurations for evaluation.

In 1958, the possible use of fiber bundles as aircraft hazard detection devices was suggested. Research was initiated on the use of fiber bundles in providing flight crews with indisputable visual evidence of possible malfunction conditions in remote parts of flight vehicles. Other objectives of this effort were to develop packaging configurations which would render the fibers suitable for the rigors of aerospace operating environments and to combine the image-transporting capabilities of fiber bundles with the known capabilities of various photoelectric detection systems for aircraft fire warning applications.

Many problems remained to be solved, however, for the environmental problems

and the bundle length requirements for aircraft use introduced complications which had not been considered during the earlier efforts. Also, the optical capabilities and limitations of various fiber bundle configurations had to be scrutinized closely so that the system would not be over- or underdesigned to meet the requirements of any given aircraft application.

The problems were outlined in detail in an unsolicited proposal submitted to WADC by Fenwal in 1959. A modified version of this proposal to WADD in 1960 led to the present contract.

1.2 The Hazard Detection Problem

Most of the malfunctions which occur in aircraft engines or elsewhere are detectable visually from some appropriate nearby vantage point; an engine fire, a smoky oil leak onto a hot surface, a landing-gear locking pin not in position, and many others, can be seen plainly by an eye located in the proper place. Other types of malfunction are not as readily apparent; a hot gas leak in a burner-can may not be very luminous; an engine part may become seriously overheated without being hot enough to glow, and so forth.

The intended purpose of a fiber bundle is not to make invisible occurrences become visible (although one phase of this program does examine the possibility of infrared-to-visible image converters for use with certain bundles). Instead, its function is merely to transmit an image of "anything that the eye can see", and to do so efficiently, reliably and economically.

Consequently, this study has concentrated on the ability of fiber bundles to transmit specific types of visual information, with primary attention being paid to large and small flickering or steady yellow flames, such as might result from a fuel leak. Attention has also been paid to blue flames typifying high altitude diffusion flames or certain luminous hot gas leaks, and to the ability of fiberscopes of various sizes and shapes to transmit clear, detailed images of engine structural parts and accessories, for cases in which these need to be monitored.

Auxiliary studies were concerned with photodetection equipment for specific use with fiber bundles in order to provide automatic notification of a possible fire condition or other unusual light-level situation requiring visual inspection by the pilot.

1.2.1 Fiber Optics Capabilities

Although the known capabilities of fiber optics are not rightly a part of the problem, they are listed here in order to provide a setting against which the subsequent sections may be viewed in proper perspective.

A well-designed and manufactured fiberscope has the ability to transmit extremely

high quality images over distances of several feet. The image quality can be comparable to that of the finest closed-loop color television system, if a suitable number of fibers is used, and yet the bundle is completely inert, requiring no operating power or circuitry components. Objects are rendered in natural, lifelike appearance, except for some color distortion which is noticeable in bundles of about ten feet or longer; this distortion is caused by the greenish color of the optical glass used in the fibers but is easily corrected with color compensating filters (see Paragraph 3.1.6).

A typical diameter for each fiber used in such devices is 0.002". In such diameters, glass fibers are extremely soft and flaxen-like and are capable of withstanding much more severe mechanical abuse than one would expect for glass in its ordinary forms. Moreover, the softening point for most fiber optic glasses is in the neighborhood of 1000°F, so that the glass itself is not the limiting factor in the use of fiber bundles for most aircraft applications involving high temperatures.

1.2.2 Fiber Optics Limitations

A principle limitation in the effectiveness of fiberscopes and light pipes is imposed by the inevitable light absorption of the glass or other material of which the fibers are composed. A further transmittance loss occurs because of microscopic irregularities in the wall finish of each fiber, and these are an almost unavoidable feature of present day fiber drawing techniques. Typical transmittance losses in fibers amount to about fifty per cent per seven foot section (on the basis of the amount of light entering that section) although under optimum manufacturing conditions losses of only fifty per cent in twelve feet have been claimed. Further losses occur as "packing losses" because the round fiber ends do not make full use of the end face area; also, minor reflectance losses occur at the fiber ends as light passes into or out of the fibers.

It was beyond the scope of this effort to effect improvements in fiber transmittance. Instead, it was our purpose to determine how serious these light losses would be in view of the fiber bundle lengths which might be needed in many modern aircraft. As will be seen in Paragraph 3.1.11, today's fiber bundles are recommended for use in maximum lengths of between fifty and one hundred feet, depending upon the brightness of the target and the suitability of the viewing conditions.

A possible limitation which had to be examined was the ability of glass fibers to withstand severe mechanical environments. Although the yarn-like softness of the fiber material would lead one to expect good durability under normal aircraft operating conditions, the extent of this durability had not been measured, in terms of standard military specifications. It was our purpose, therefore, to study the resistance of glass fibers to various mechanical stresses, particularly to vibration, as influenced by the type of jacketing in which they were contained.

and thus to establish a firm quantitative basis for any considerations regarding the suitability of fiber bundles for aircraft environments.

Although the glass fibers themselves can tolerate environmental temperatures of about 1000°F, the epoxy resins which are customarily used for potting the end faces begin to deteriorate at much lower temperatures. It was in this area that one of the few advancements in the art was proposed as a part of this effort; accordingly, a study of high temperature potting compounds was undertaken, with results which we feel have justified the effort, as will be seen in Paragraph 3.3.

A possible problem was anticipated in the case where a particularly long fiber bundle might have to be installed in an aircraft as a single element. The difficulty of threading a twenty-five or fifty foot bundle through a circuitous path involving bulkheads and firewalls, and the possibility that a single break during installation would render the entire bundle useless, made it desirable for us to consider the possibility of a fiber bundle assembled in place by the coupling together of modular lengths. The particular problem was focused upon the coupling joint, for no knowledge existed as to how a mechanical coupling should be made which would be practical and yet which would satisfy the difficult optical requirements of minimum degradation of the image as it passed out of one bundle end face and into the next. Moreover, in anticipation of the possible use of automatic alarm and test circuits in a practical fiber bundle system, it would be necessary to provide electrical power leads integrally with the fiber bundle assembly in order to allow test lights within the pickup head to be energized. The mating connectors therefore had to provide electrical continuity between power leads and return leads, besides meeting other criteria which we had arbitrarily established, such as their being readily demountable, reliable, economical and capable of automatically aligning the bundle end faces with optical precision.

A connector study was therefore included as a part of this effort, and its results are reported in Paragraph 4.4.

A large part of the effort was concerned with the question of just how refined a fiber bundle design need be for a particular detection problem. One would not want to specify a high resolution fiberscope for the simple detection of a yellow flame in a dark jet-engine compartment, nor a low resolution light pipe where high visual acuity was needed. The question of overdesign versus underdesign is not regarded here as a limitation of fiber bundles themselves, but rather as a limitation in one's knowledge of them, for no scientific foundation existed as the basis for one's selecting the proper fiber bundle for a particular use. This question is examined in detail in Paragraph 3.1 which is accompanied by photographic documentation intended to illustrate optical effectiveness as a function of the bundle parameters.

1.2.3 Scope of Study

The scope of this study is logically divided into three categories, reported on

separately in Sections 2, 3 and 4.

Section 2 deals with the basic optical, mechanical and thermal properties of the individual fibers themselves, without regard for the group properties which fibers assume in a co-operative configuration. This section reports the results of tests conducted on individual fibers, there being no reference to image properties, protective jackets and so forth.

Section 3 treats the group aspects of fiber behavior and reports the results of tests on actual fiber bundles, both coherent and incoherent and in various jacketings. This section again considers optical, mechanical and thermal properties, although these have a different meaning from that associated with an individual fiber. The Section 3 study is concerned with the basic fiber bundle, in a suitable protective jacket, and is limited to a consideration of what occurs within the bundle itself, between end faces.

By contrast with studies of the basic fiber and the basic fiber bundle, Section 4 considers the properties of various fiber bundle systems which arise when one adds to the fiber bundle such appurtenances as terminal optics, radiation detectors, image tubes, mechanical couplings and others.

In Sections 3 and 4 it was the purpose of the studies to examine the capabilities and limitations of fiber bundles in view of typical operating and environmental problems anticipated in various aerospace vehicle applications. The matter of optical image quality which can be transmitted by a particular fiber bundle configuration has received especially detailed attention, the results being illustrated in a series of photographs which should enable the reader to gain a subjective impression of such matters.

Section 5 describes the design and construction of a particular breadboard system configuration, selected to illustrate many of the findings resulting from this study; the design incorporates and integrates many features which are, we believe, appropriate to the needs of typical aerospace hazard identification problems.

SECTION 2

PROPERTIES OF INDIVIDUAL FIBERS

A knowledge of the physical properties of individual fibers is necessary to an understanding of fiber bundles. Much can be said about the properties of a single fiber before one goes on to discuss the properties which these fibers assume collectively. The single-fiber properties most interesting to this discussion are the optical, mechanical, and thermal properties; these will be discussed separately in the following paragraphs.

2.1 Optical Properties

The optical properties of the single fiber are important to the ultimate question of image transmission in the fiber bundle, which in turn is the most critical issue involved in a determination of the suitability of fiber bundles for use in aircraft hazard detection.

2.1.1 Transmittance

Light is conducted through a transparent fiber by means of multiple internal reflections which occur at the interface, provided that the rays strike the interface within a certain angle of it, called the "critical angle". The conduction phenomenon is described extensively in the literature (for example, 3, 11, 17, 26, 86, 94, 95, 97, 105, 111, and 118) and will not be elaborated upon here.

In an ideal, cylindrical fiber with perfectly smooth walls, each reflection occurs with virtually perfect efficiency. However, as light travels through a fiber, a part of it is lost because of the imperfect transmission of all known fiber materials, including the many types of glass. Although glass is commonly regarded as a highly transparent material in the usual forms in which it appears, it should be remembered in considering glass fibers many feet long that one is effectively "looking through" a glass block many feet thick. In the case of the fiber, as in the case of the glass block, the path length traveled by a given ray would be the axial length times the secant of the angle which the ray makes with the axis. Thus, a ray inclined at 60 degrees to the axis will have traveled through twice as much glass as an axial ray.

Assuming perfect wall reflectivity and a bulk absorption coefficient of α for the fiber material, it can be shown (3) that the transmittance, T , of a fiber of length L is given by the equation $\log_e T = -\alpha L \sec \theta$ for a ray making an angle of θ with the fiber axis.

The bulk absorption of glass is responsible for only a part of the light loss occurring in an actual fiber. A major source of loss is the fact that actual glass fibers, as they are made today, do not have perfectly reflecting walls or interfaces. This is due to various influences, particularly to the lack of perfect

smoothness in the walls. Thus, an individual light ray which is initially contained within the critical angle may, upon striking a surface irregularity, be outside the critical angle at the point of incidence and will thus escape through the fiber wall.

Hopkins and Kapany (3) point out that in a "one mil" (0.001" diameter) glass fiber of refractive index 1.50, a ray inclined at 10° to the axis will undergo 116 reflections per inch. Only one of these reflections need be incomplete in order for some of the light from a ray to be irrevocably lost.

Surface irregularities, surface contaminants, and absorption within the surrounding material (which is important in the case of clad fibers) all combine to modify the efficiency of the reflection process. Extrapolations from experimental measurements, according to Potter (41, 42), show an equivalent or average interfacial reflectivity of only 99.93% for certain clad fibers. Assuming the conditions stated in the previous paragraph, it is apparent that a 10° ray would traverse a one-inch length of fiber with a reflection efficiency of only $(0.9993)^{116}$ or 85%, without absorption losses being taken into account.

In addition to bulk absorption losses and imperfect interfacial reflectance, modern fibers suffer from a third defect which impairs transmission, notably the presence of solid impurities, refractive index variations, and minute air bubbles which partly absorb or scatter the light striking them. These inclusions are random phenomena and occur, on the average, only among a small percentage of fibers for every few feet of length.

If one end of a bare fiber bundle is brightly illuminated in a darkened laboratory and the bundle is examined visually along its length, the bundle should appear perfectly dark if all of the light is proceeding from the lighted end to the other end (except for bulk absorption). What is generally seen, however, are spots and patches of light emanating from various points and sections along certain fibers. The escaping light indicates fiber defects, including impurities and surface irregularities. The net effect is the appearance of "grey" fibers as one examines the end face of a uniformly illuminated fiber bundle.

Such fibers are noticeable in the photographs of Figure 1. They are especially apparent when a bundle end is illuminated uniformly but are ordinarily submerged by high contrast image detail. The middle photograph of Figure 1a is a view of a coarse but high contrast image transmitted by a short, partly oriented fiber bundle. If the reader views this photograph from a distance, he may barely discern a broadside view of a brightly illuminated jet engine. In this example, the grey fibers are not obtrusive. Nonetheless, they can detract from the efficacy of the fiber bundle, and are a specific technical area in which improvements could be made through subsequent research and development.

Single fiber transmission measurements are difficult to make or to interpret. The measurement results vary, depending upon the geometry of the illumina-

tion, whether the fiber is straight or curved, etc., and each result has a different meaning. A few such measurements have been performed by Potter (41, 42) and have yielded transmittance values of the order of 70% for typical fibers in lengths of about one foot. The reader is referred to the above references and to Paragraph 2.1.6 for a detailed account of these and other measurements and their interpretations.

The light losses which occur within glass fibers are not the same for light of all wavelengths. In particular, the bulk absorption of glass in the visible spectrum is greatest in the violet, blue, and red regions. The result is that present day fibers transmit most efficiently in the yellow-green region, an important factor when one considers the effects of chromatic distortion upon the recognition of images whose original color is important. For example, it is highly possible to recognize the scrambled fiber bundle image of a yellow diffusion flame against a steady background of almost any color, provided that the distinctive flame color is preserved. The flame image is characterized as an array of flickering yellow spots which, although scrambled, strongly suggest the presence of a flame. If the greenish tinge of a long fiber bundle is superimposed upon the flame color, the scrambled image loses one of its identifying characteristics, and the observer's recognition of the flame is less positive.

Color distortion and means of compensating for it are discussed more fully in Paragraph 3.1.6 dealing with fiber bundles. For the present, we shall merely indicate that the color distortion and light losses now occurring in a typical single fiber would greatly limit the effectiveness of fiber bundles in most hazard detection applications where lengths greater than 75 to 100 feet are concerned.

2.1.2 End Surface Losses

A small amount of light incident upon the end face of a glass fiber is reflected and does not enter the fiber. This effect, known as a "Fresnel reflection", occurs at all abrupt interfaces between transparent media of unequal refractive indexes and is responsible for the luster of everyday transparent objects.

The Fresnel losses account for only a small proportion of the light lost in fibers whose lengths are greater than several feet but are important in shorter fibers and at fiber bundle couplings (to be considered in Paragraph 4.4). The magnitude of the loss increases with the steepness of the angle which the entering ray makes with the perpendicular to the surface; it is also greater between media of more widely different refractive indexes. For a ray in air entering a medium of index N at right angles to its surface ("normal" incidence), the Fresnel reflectance is equal to $(N - 1)^2 / (N + 1)^2$. For a typical glass fiber of index 1.62, this would amount to 5.6%. The same relative loss occurs as an axial ray leaves the far end of a fiber. Moreover, considering that most of the useful light entering a fiber does so at other than normal incidence, the average Fresnel loss over a given acceptance cone would be appreciably greater.

2.1.3 Cladding Losses

Almost all optical fibers now manufactured consist of a light-conducting glass core surrounded by a thin layer of glass with a lower refractive index. This layer, known as the cladding, serves as optical insulation and preserves the surface finish of the core, keeping it out of optical contact with other core surfaces so as to minimize light leakage.

In order to provide effective optical insulation, the cladding must have no less than a certain minimum thickness. This is of the order of a few wavelengths of light and amounts to a very small fraction of a thousandth of an inch. For fibers whose diameters are greater than a few mils, the cladding cross section can be made small enough to occupy almost a negligible proportion of the end face area, although it becomes relatively important in the case of half mil fibers or smaller.

In fibers of ordinary lengths, the cladding is totally ineffective as a conductor of light from end to end. Of the light incident upon a clad fiber, that part which enters the cladding is free to escape into any surface which touches it. The cladding cross section must therefore be regarded as exacting a toll from the incident light.

The fiber diameters of concern to this study are in the two to three mil range. Fibers smaller than this are difficult to manufacture effectively, and in smaller diameters they become poor conductors of light. Fibers larger than about three mils were found to be less able to withstand vibration and bending tests as appropriate to aircraft installation and operation. Fortunately, the cladding losses in fibers of two to three mil diameters would be trivial by comparison with the other losses. For long fiber bundles, as might be used in aircraft, fibers with a minimum of necessary cladding thickness should be specified. Fibers now being made for short-length applications are frequently provided with a cladding thickness equal to about one-tenth the core diameter. This is done for convenience of manufacture and, in the case of two or three mil fibers, provides an unnecessarily large proportion of cladding area in the bundle cross-section. The resulting light loss is not important in short bundles but would be of concern in aerospace applications where the highest possible area-utilization were desirable.

There is one instance in which cladding losses are of concern to this study, and that is in the case of the multifiber, to be described in Paragraph 2.1.5. Figure 1c shows a photomicrograph of several "six by six" multifiber arrays, each about two mils square and containing 36 separate optical channels. Each channel is so narrow that a relatively thick cladding must be provided. The cladding appears as grey areas between channels and would undoubtedly appear much darker if greater fiber lengths were used. It is clear in this case that, of the image-bearing light striking the end face, the proportion lost in the cladding would be substantial.

2.1.4 Numerical Aperture

The solid angle over which an optical fiber accepts light entering the end face is limited. Light rays entering from outside this "acceptance angle" gradually escape the fiber walls upon subsequent reflections.

The angular diameter of the acceptance cone is related to the critical angle for total reflection within the fiber, and this in turn depends upon the ratio of the refractive indexes on both sides of the boundary. Quantitatively, the acceptance angle is conveniently described in terms of "numerical aperture", (76) a dimensionless quantity used in lens optics to describe light-gathering power. If N_1 is defined as the refractive index of the core material and N_2 refers to the cladding (or other surrounding medium in the case of an unclad fiber), then the numerical aperture, or N.A., can be shown to be equal to $(N_1^2 - N_2^2)^{1/2}$.

For the photographically-inclined reader, the familiar "f-number" of a camera lens is $1/(2N.A.)$, where a small f-number or high N.A. indicates a large light-gathering power. The N.A. is also equal to the sine of the half-angle of the acceptance cone in air. Thus, for a square-ended fiber in air, the maximum numerical value of N.A. having physical meaning is unity, corresponding to f/0.5, meaning that a light ray entering the fiber end at any angle will be retained by the fiber.

The N.A. of a clean, unclad fiber in air ($N_2 = 1$) is larger than that of any clad fiber. For example, with $N_1 = 1.62$, then all rays entering the fiber end will be retained.

With a typical cladding glass of $N_2 = 1.52$, the N.A. is reduced to 0.565, corresponding to about f/0.9, or an included acceptance angle of 69°.

In considering the total amount of light transmitted by a fiber, one must ordinarily take into account the angle over which the fiber accepts light from a source. A fiber with twice the N.A. of another fiber will accept light over a solid angle four times as great and therefore, in principle, will conduct four times the total light energy. This statement applies with certain reservations, notably:

- (1) The source illuminating the fiber must be "Lambertian"; that is, its emitted light must fill a hemispherical angle and the light intensity must be proportional to the cosine of the angle from the normal. It will thus look equally bright from all directions.
- (2) The increasing Fresnel losses for rays entering the fiber at steeper angles must be ignored.
- (3) The increased transmission losses for steeper rays must be ignored.

- (4) It must be noted that a fiber which conducts more total light than another will not necessarily appear brighter at the exit end; rather, the light is merely visible over a broader viewing angle.

The first and last statements, together with certain considerations pertinent to the hazard detection problem, serve to de-emphasize the need for high numerical apertures in the fibers of interest to us in this study. The reasons are twofold, depending upon the fact that the use of both objective lenses and magnifying eyepieces is anticipated in aerospace applications of fiber bundles. The explanation is given in the following paragraphs.

It must first be understood that, in principle, assuming a straight cylindrical fiber with flat end faces, a ray entering an end face at a given angle to the axis will emerge from the other end face at the same angle. From this principle, one can deduce the fact that the acceptance and emittance angles at the end faces should be equal. In practice, this is not strictly true, for inhomogeneities and bends in a fiber introduce a certain amount of distortion in the geometry of the rays traversing the fiber. The result is that axial rays entering the fiber may emerge at steep angles, and conversely; in general, the effect is that the entrant cone of light becomes somewhat enlarged and diffused upon leaving the fiber.

It is apparent that the emergent cone need be no larger than necessary to fill the magnifying eyepiece. A typical eyepiece may have a lens "speed" of from $f/1$ to $f/1.5$, corresponding to numerical apertures of 0.50 to 0.33. Any emergent light falling outside the eyepiece area is wasted. The incident cone therefore need not have an N.A. greater than about 0.33; that is, the objective lens need be no "faster" than about $f/1.5$ if an $f/1.5$ eyepiece is used. A mitigating circumstance is that the incident cone does become distorted as it traverses the fiber; one can therefore profit by using an objective lens of somewhat higher N.A. than the eyepiece in order that the latter be completely filled with light at all viewing angles. This subject is discussed further in Paragraph 3.1.9 which considers the effects of objective N.A. upon the visibility of the image at the viewing end of a fiber bundle.

2.1.5 Multifibers

A recent development in the fiber optics art is the multifiber which, mechanically, is a single strand of glass but which contains many optically insulated light channels. A typical multifiber end face, shown in Figure 1c, is comprised of a "6 x 6" array of optical channels, although other arrays are easily produced. In the photograph, the bright areas correspond to the core glass in a typical single fiber, whereas the dark areas represent the cladding.

The advantage of the multifiber is that it provides many image points, or high resolution (see 3.1.3), while retaining a physical size (such as 2 or 3 mils on

a side) which can be readily handled without breakage during manufacturing. Another advantage is that the process of making multifibers lends itself readily to the production of square or rectangular fibers which utilize the end face area of a fiber bundle more efficiently than do round single fibers. Aside from affording more image points per cross section, multifibers manifest similar optical properties and essentially the same mechanical, and thermal properties as individual glass fibers with the same core and cladding. Multifibers have therefore not received special attention during the course of this effort; only casual mention will be made of them throughout the remainder of the report.

2.1.6 Measurement Results and Discussion

As noted in Paragraph 2.1.1, transmission measurements on a single fiber have a valid meaning only with regard to the specific set of measurement conditions under which the data were obtained. For example, the transmittance of an individual fiber might arbitrarily be expressed as the ratio of the amount of light emerging from one end to the amount incident upon the other. However, in the case of a diffuse illumination source, all of the light incident upon the fiber end might not be accepted by the fiber because of numerical aperture limitations. Therefore, one might arbitrarily use as a criterion for transmittance the amount of light accepted by (rather than incident upon) a fiber end face. Moreover, even within the acceptance angle, it is possible to illuminate a fiber in a number of different ways for transmission measurements, from the case of a highly convergent beam contained within the acceptance angle to the case of a collimated beam containing only rays parallel to the fiber axis. With each of these modes of illumination the measured transmittance will be different, for the higher-angle light is transmitted over a longer optical path and with many more reflections than is the axial light. Moreover, the observed transmittance value is further influenced by whether the test fiber is straight or curved; in the latter case, incident collimated rays become decollimated and affect the measured values.

Of the variety of possible illumination conditions, a specially-apertured diffuse source was selected as the light source for a series of measurements under this study. The source was arranged so that the steepest rays incident upon the fiber were within the acceptance angle. Such a source was considered to be fairly inclusive of the conditions under which a fiber might be illuminated by an objective lens in an aircraft installation.

At the exit face of the fiber, the emergent light was collected on a photographic film, by contrast with Potter's method of using an integrating sphere (41). Through densitometric measurements and calculations, the photographic record lends itself to integration of the total transmitted energy, as does the integrating sphere, but in addition it provides a record of the angular distribution of the light as it emerges from the fiber.

After tests on many different samples, it became apparent that glass fibers as currently manufactured show appreciable differences in the output pattern and

integrated transmittance, and that no randomly selected fiber could be regarded as typical of a given batch. The reasons are apparently due to the localized defects mentioned in Paragraph 2.1.1.

It then appeared reasonable to study the bulk spectral transmittance properties of the glass itself, using techniques which would yield comparative transmittance values between various types of glass and which would not be subject to the imperfections inherent in currently manufactured fibers. Of the many different glass formulations available commercially, a selection was made from among several which have been used for optical fiber manufacture as well as from those which have not. (It should be noted that the glass types now used in commercial fibers are selected on the basis of other properties besides transmittance, particularly melting point, thermal expansion coefficient, availability, and so forth. We wish to stress the fact that most present commercial fibers are made in lengths less than a few feet, for specific purposes, and that high transmittance in great lengths was apparently not an objective until the aircraft hazard detection problem arose.)

For the purpose of these measurements, glass blocks of various types were obtained in four-inch lengths, the length-limiting factor being due to the physical capacity of the spectrophotometric instruments used for the measurements. As will be noted shortly, the test results indicated that for purposes of very long fiber bundles, where glass transmittance is a compelling factor, the possible use of several commercial glasses which have not been used for fibers should be investigated further. The test results also indicated that different melts, or batches, of supposedly the same glass yielded slight short-length bulk transmittance differences which, when extrapolated to greater lengths, became appreciable (compare Figures 3, 4, and 5); further work is thus indicated on the quality control of currently manufactured optical glass.

In order to appreciate the significance of the test results, the reader should be aware of one phenomenon in particular. If we consider two four-inch lengths of glass which transmit, respectively, 99% and 97%, the difference does not appear appreciable. However, in extrapolating these transmittance values to twenty-five foot (300 inch) lengths, by raising the four-inch transmittance values to the 75th power, one finds the respective values to be 47% and 10%. Further, a four-inch block transmitting 90% would transmit only 0.04% in a 25-foot length. Thus, slight differences in the measured values for four-inch blocks become highly accentuated when extrapolated to 25-foot lengths. Figure 2 shows manufacturer's data on two types of Schott glass in four-inch lengths. If extrapolated to, say, 25-foot lengths, the transmittances of these glasses would differ greatly.

Several of the glasses which have been used as core glasses in fiber-optic systems have been manufactured in accordance with specifications developed in recent years for glass shields for gamma ray protection. This radiation protection application is similar to the fiber optics application in the requirement for high transmittance in glasses which also have high refractive index. The curves shown in Figure 2, from Schott Glass Company, are for their standard

SF 6 glass and their special SF 6/FA Strahlenschutzgläser and show the improvement in clarity that has been made for the radiation shielding glass. The low residual color of these glasses makes a very great improvement in the transmittance of long light pipes or fiberscopes in comparison with standard glasses. There probably is no other application of optical glass so demanding of highest clarity as the long fiberscope or light pipe.

The sample blocks used in the bulk transmittance measurements for this study were 1" x 1" x 4" in size, the measurements being made through the four-inch dimension, with the side walls being painted black. Absolute spectrophotometric data were obtained in the 400 to 1000 millimicron range through use of a General Electric Recording Spectrophotometer, and relative values in the 600 to 1800 millimicron range were yielded by a Model 14 Cary Recording Spectrophotometer, the latter curves being matched to the former to yield absolute values. The observed values were corrected for reflectance losses at the end faces and were extrapolated by machine computation to six-foot and fifty-foot lengths, the results being plotted in Figures 3 through 8. The vertical axes represent line transmittance, indicating that this is the bulk transmittance of the glass itself and does not take into account end losses, including the packing losses which would occur if these measurements had been made on actual fiber bundles.

A particularly interesting result will be observed in Figure 6, in which the integrated spectral transmittance of Schott SF 4/FA glass, extrapolated to 50-foot lengths, is appreciably greater than that of the other glasses tested. The difference is not as noticeable in the visible spectral region, from 400 to 700 millimicrons, but it is appreciable in the 700 to 1300 millimicron region where infrared flame detectors and image converters might be used in conjunction with fiber bundles (see Paragraphs 4.2 and 4.6). This glass has not heretofore been studied for possible use in fibers.

It is stressed that the data presented in these figures arise from measurements on solid glass blocks and cannot be extrapolated to fiber transmittance values unless the properties of the cladding material are taken into account. The nature of the total internal reflection phenomenon is such that even the rays which are retained by the core do penetrate very slightly into the cladding upon each reflection; consequently, any absorptivity in the cladding will attenuate a ray progressively each time it is reflected at the interface.

The influence of absorption by the cladding glass on the spectral transmission of a fiber optic system is not as limiting as that of the core glass. However, the cladding transmittance influence is not negligible. We have inferred the effect of the cladding glass transmission properties from the difference in the transmittance of the core glass alone and the transmittance of actual fiberscopes of the same length. At the present time the selection of glass type for cladding optical fibers is generally limited to commercially available glass tubing. The glass used for this tubing is noticeably green in color even in lengths of a few inches and appears black in lengths such as used for fiber optic systems. The

effect of this absorption appears as a distortion of the spectral transmittance of the fiber bundle in comparison with the core glass spectral transmittance. This distortion is particularly noticeable as a relative lowering of transmission in the far red and near infrared regions. This is the best region for transmission of some of the specially selected core glasses but in fiber bundles this region becomes less highly transmitting than in the visible region (500 - 600 m μ). There are two "windows" in long lengths of core glass:

- (1) The visible region from 500 to 600 m μ , and
- (2) The far red and near infrared region from 700 to 1000 m μ .

The second "window" actually extends to 1350 m μ with a decreasing transmittance in the case of some core glasses but this region is most highly transmitting in the 700 to 1000 m μ region. Although this second "window" is of little use for visual observation, it lies in a wavelength region where physical detectors such as S-1 response phototubes, image converters, and near-infrared-sensitive photodetectors are highly sensitive. (The application of these devices to fiber optic hazard detection systems is discussed in Section 4.)

There is a commercially available tubing (KG-12 glass) with about one-fourth the absorption of the standard tubing (R-6 glass). The KG-12 glass has a higher refractive index (1.56 compared with 1.52 for R-6) so that with the same core glass, the acceptance angle of the fiber optic component will be reduced. However, a combination of a 1.7552 index core glass (SF4/FA) or a 1.7174 core glass (SF1/FA) and the 1.56 cladding glass would have both a higher transmittance in the near infrared and a higher numerical aperture than the standard combination of 1.62 index core with 1.52 index cladding. These combinations would have a more yellowish tinge due to the short wavelength absorption limit extending further into the visible region but would have superior transmission properties in all other spectral regions.

There are also factors other than the higher cladding glass transmittance which would yield higher transmittance by this combination. With a higher refractive index difference between core and cladding, there would be less penetration of the light into the cladding glass upon internal reflection so that the absorption at each reflection would be less. Moreover, with a higher index core glass the angle of light to the axis is less for a given input angle so that there would be fewer reflections than in a lower index core under the same conditions. The use of "color free" glass for the cladding would require the provision of special facilities for producing small amounts of glass tubing from optical grade glass rather than from the large installations for commercial glass tubing. For highest fiber transmission and best mechanical properties, this special production facility would be required as well as great care in the production of high clarity glass for use as the core material.

Another factor of interest is the radiation pattern of a typical fiber, that is, the angular distribution of the emitted light under a given set of light-input conditions. Two radiation patterns for a particular type of fiber are shown as Figures 9 and 10, the difference between them being the matter of cone width of the entrance illumination. The fibers used in this measurement consisted of a Schott SF 4 core ($n = 1.755$) and a Kimble R-6 cladding ($n = 1.520$), in six-foot lengths. This refractive index ratio provides a numerical aperture of 0.86, corresponding to an acceptance half-angle of 46° . The input light source was so apertured as to provide illuminating cones with half-angles of $8\frac{1}{2}^\circ$ and 37° respectively, both being within the acceptance angle of the fibers. Figure 10 shows a more severe loss of rays at the edges of the input cone than does Figure 9; this is attributed to absorption in the cladding, which the steeper rays penetrate more frequently during interfacial reflections.

The data were obtained through use of the photographic technique described earlier in connection with the transmittances of single fibers. However, because of random fiber defects and the fact that no two fibers are alike, the measurements were made on a group of 100 fibers in order to average out the variations. The emitted light was collected on a photographic film a few inches from the output end, and the degree of blackening on various parts of the processed film constituted the raw data. The film density was measured point by point with an Eastman Kodak Model 31A Densitometer and with a modified Kipp Recording Densitometer. These measurements, along with data pertaining to the film exposure characteristics, provided the basis for calculation of the intensity-vs.-angle properties of the emitted light.

The radiation patterns of Figures 9 and 10 thus constitute a form of fiber transmittance data, showing the percent of transmitted intensity for each ray direction through the fiber on the basis of the input intensity being 100% for each angle within the entrance cone. Although the total transmittance (integrated over the exit cone) was not computed, its value could be determined from the information contained in the figures. This would involve a double integration in order to convert the intensity information in the diagrams into the energy values upon which transmittance values are based.

Fiber radiation patterns are of interest in two respects. A knowledge of the pattern is helpful in the selection or evaluation of a magnifying eyepiece for use with a fiber bundle; for greatest eye freedom during viewing, the eyepiece diameter should be large enough to collect all of the emitted light, but it need not be appreciably larger than this for no light will appear on the bundle end face if it is viewed at too steep an angle. Secondly, the fact that the exit cone is somewhat restricted seems to have a bearing on the mottling which occurs even with high quality fiberscope images when, for some reason, the exit cones of some fibers are deflected away from the fiber axes. This will be discussed more fully in Paragraph 3.1.9 since it is appropriate to fiber bundles rather than to single fibers.

2.2 Mechanical Properties

With regard to a single fiber, the mechanical properties of greatest interest to possible aerospace applications are tensile strength, shear strength, and minimum bend radius. The following sections describe tests conducted here on such properties and are supplemented with further information from other sources. The tests were made on typical round clad fibers supplied by American Optical Company, with a core of Schott F 2 glass ($N = 1.62$) and a cladding of Kimble R-6 glass ($N = 1.52$). (All refractive indexes are given in terms of the sodium D line.) Fiber diameters were confined to the 0.001" to 0.010" range. Most of the tests were conducted on monofilaments, although some tensile strength measurements were made on multifibers.

2.2.1 Tensile Strength

One of the more pertinent questions regarding the mechanical properties of glass fibers for aircraft use concerns tensile strength. It is understandable that for a given fiber, there is a limiting length beyond which the fiber could not support its own weight if suspended vertically. This limitation could be important in the case of a long fiber bundle running the length of an aircraft which was in a steep nose-up attitude. The limitation would be more severe in level flight under thrust values greater than one g. (These arguments apply to cases where the glass fibers are affixed to their container only at the ends but lie loosely within it in between.) Nonvertical aircraft attitudes would permit a gravitational component perpendicular to the fiber axes, tending to hold the fibers together and to provide a small amount of static friction between them and the container wall. However, the static friction between glass fibers is known to be quite small, unless the fibers are extremely clean, and it cannot be relied upon to prevent individual fibers from stretching in response to an axial force.

Tensile strength tests were performed on individual, round fibers of nominal diameters ranging from 1 mil to 9 mils. Ten-inch lengths were used, with the fibers being suspended vertically from a support and with a 1000 gram capacity Chatillon scale being used in series with the applied tensile force. Breaking forces were observed through use of a maximum-force indicator with which the scale is equipped.

Several methods of gripping the fiber ends were evaluated before one was selected which afforded sufficient gripping force without fracturing the fiber. The selected method was to sandwich about two inches of each end between two strips of electrical tape which were placed together face to face; the free ends of the tape were then attached respectively to a fixed support and to the scale, and the breaking force was applied manually. Breaks which did not occur in the six-inch free length of fibers were discounted.

The test result averages are given in Table I.

<u>Nominal Fiber Diameter</u>	<u>Number of Fibers Tested</u>	<u>Average Breaking Force (pounds weight)</u>	<u>Average Tensile Strength (psi)</u>
0.001"	20	0.084	88,100
0.002"	30	0.266	73,133
0.003"	10	0.474	58,000
0.008"	20	1.55	30,800
0.009"	10	1.77	28,800

Table 1. Tensile strength test results on single fibers.

Among the fibers in any group, substantial variations in breaking force were observed, the standard deviation often amounting to twenty per cent of the average value. However, the average values show a distinct trend toward increased breaking forces and, oddly, reduced tensile strengths with increasing fiber diameters.

The reason for the reduced tensile strengths of larger fibers is not known. These values are much lower than the published values for bulk glass (see Reference 125 and Page 202 of Reference 127). Consultation with the subcontractor has led to the speculation that the slower cooling of the larger fibers, immediately after they are drawn, leads to steeper thermal gradients and residual stresses; by contrast, the more uniform cooling of the smaller fibers (throughout their cross sections) may be likened to a more careful annealing process. As will be seen subsequently, there is also reason to believe that the manner in which a newly drawn fiber cools in air leads to a tempered condition, which is less evident in larger fibers.

The distribution of breaking point values within groups of twenty samples prompted an inquiry into the possible effects which an annealing procedure might have on the fibers. To this end, various groups of 20 fibers in 2 mil and 3 mil diameters were annealed for fifteen minutes at 860°F and tested for breaking point. It was found that annealing had the effect of lowering the tensile strength substantially for fibers of both diameters; it was also seen to have little effect on leveling the distribution of breaking forces and actually increased it in the group of 3 mil fibers tested.

The reduction of tensile strength after annealing was an unexpected result but was supported in Reference 125 by the assertion that "... the breaking strength of fibers results largely from their surfaces being free from flaws of perceptible magnitude. The partial or complete annealing of glass fibers will reduce their strengths materially, which may be caused by chemical action at the surface or the spontaneous formation of flaws during the process of stabilization." The author confines his discussion to fibers of one-half mil diameter or

less, which, he states, are unlikely to emerge from the drawing process in a tempered condition because the high cooling rates do not allow the necessary transient temperature differences to exist between the fiber surface and its interior. The claim may not be true of fiber diameters in our present range of interest and we believe it likely that some tempering does occur; consequently, annealing acts as to undo these effects, as well as to introduce surface flaws. We conclude, therefore, that annealing can serve only as a disruptive influence where tensile strength is of concern.

The subcontractor has recently completed a private study program with the objective of improving the tensile strength of optical fibers. Their study has revealed that a glass fiber is strongest when it is freshly drawn; subsequent contact with any solid surface, such as that of another fiber, induces countless, tiny surface flaws, any one of which can become the nucleus of a rupture when the glass is stressed. Fiber strength was found to be improved by the application of various protective films to the surface of each freshly drawn fiber. Tensile strength values up to 170,000 psi were reported for typical fibers.

Other tensile strength studies were concerned with the effects of glass drawing rate and temperature at the time the fibers are formed, and with the effects of the relative values of the core and cladding thermal expansion coefficients. The studies indicated no major effects over the range through which the parameters were varied. Figures 11a and 11b compare the tensile strength test results on two sets of multifibers made under different conditions but which were otherwise similar. The drawing temperatures differed by 100°F for the two sets, with the drawing speeds being adjusted so that 2.4 mil square fibers were yielded in both cases. Each fiber comprised a 6 x 6 array of optical channels, each channel with a core of Schott F 2 glass, a cladding of Kimble R-6 glass, and an overcoating of Kimble KG-12 glass which was used as the binder.

Seventy-five fibers each, in five-inch lengths, were subjected to tensile stresses; the frequency of breakages occurring at a given tension is plotted in Figures 11a and 11b. In the latter figure, which pertains to the fibers drawn at a lower temperature, the "center of mass" of the plotted values is seen to shift toward the lower values. This result may not be experimentally significant; the high degree of irregularity in both curves indicates that a statistical sample larger than 75 fibers should be used in such tests. The randomness of these test results, and of others to be discussed shortly, support the view that presently made fibers are highly non-uniform in all of their properties and that further research is needed in this direction.

Figure 11c presents tensile strength test results on 50 monofibers of a different composition. The basic difference in mechanical properties between these fibers and the multifibers concerns the nature of the internal stresses. The relative thermal expansion coefficients of the glasses used in the multifibers were such

that the claddings were in tangential tension (see Paragraph 2.3). It is generally believed that the greatest fiber strength results from the surface being in tangential compression, with the core in radial tension, much like the forces that exist in a bicycle wheel when the spokes are tight. The monofibers depicted in Figure 11c were made of materials selected to provide such stresses, but the figure does not show a significant improvement in tensile strength as compared with the multifibers.

Except for the fact that the tensile strength of a fiber reflects somewhat its general mechanical condition, the typical tensile strength values observed in these studies are largely of academic interest with regard to the present problem. The values observed are comfortably high, so that the question of axial g-force limitations need not be of concern here. Calculation has shown that a fiber with a tensile strength of only 30,000 psi and a typical specific gravity of 2.5 will support itself in lengths up to 27,000 feet in a one g field.

2.2.2 Shear Strength

A special test device was designed and constructed to allow shear point measurements on single fibers as a function of fiber diameter. The device is shown in Figure 12 and consists of a base plate and backing plate upon which a fiber mounting plate and clamp are fixed; the shearing of each fiber is effected by an air-pressure-driven shearing pin whose end protrudes from a pressure cylinder. The shearing force is controlled and observed by means of a conventional pressure regulator and gauge.

The fibers tested were of the type described in Paragraph 2.2. The following test procedure was used:

- (1) A fiber was placed on the mounting plate and clamped in position with the shearing pin resting lightly on the fiber.
- (2) The air pressure was increased slowly on the rear of the shearing pin, causing the pin to bear more heavily on the fiber.
- (3) The pressure increase was halted as soon as shear occurred. At that instant, a momentary pressure drop was indicated as the pin plunged downward, but the regulator would soon restore the shearing pressure value. This value was recorded and was converted to a total force applied by the shearing pin (including its own weight) necessary to break the fiber.

Several hundred fibers, in diameters of 2, 3, 5, 8, and 10 mils, were tested in accordance with the above procedure. The distribution of shear points for each diameter is shown in Figure 13. As expected, the distribution shifts toward the higher breaking point values when the fiber diameter is increased.

The irregularities in the distributions are attributed to fiber inhomogeneities and to the random surface flaws mentioned earlier. No special attempts had been made to prevent formation of these flaws; the fibers were subjected to handling procedures typical of those prior to assembly of a commercial fiber bundle.

2.2.3 Minimum Bend Radius

Breaking radius tests have been performed upon several hundred fibers through use of a simple test device constructed for the purpose. As in the shear point tests, fibers of 2, 3, 5, 8, and 10 mil diameters were used and were of the same composition as before.

The test device consisted of a base plate to which was attached a vertical scale calibrated in sixteenths of an inch; a guide pin and a hollowed-out guide ring completed the assembly, which is shown in Figure 14.

The following test procedure was used to determine the minimum bend radius of each fiber:

- (1) The test fiber was guided around the inside diameter of the guide ring to form a circular loop.
- (2) The fiber ends were grasped manually and pulled past the guide pin in opposite directions along a straight line to decrease the size of the loop.
- (3) The loop diameter was observed continuously with reference to the scale, and the last value observed before fiber breakage was recorded as the breaking diameter. Breakages which occurred elsewhere than within the loop were not recorded.

Figure 15 presents the test data in graphical form. As in the case of shear strength measurements, there is again a rather broad distribution of breaking radii for fibers of a given diameter. As before, this is attributed to fiber inhomogeneities and to surface flaws.

2.3 Thermal Properties

With regard to the individual fiber, the thermal properties of greatest interest to aerospace applications are the softening temperature and the thermal expansion properties. The former imposes a limit on environmental temperatures, while the latter is of concern to the degree of stress which occurs within a clad fiber as its temperature is varied.

The thermal properties of glass have been amply documented in the literature (for example, References 124 to 128) and will be reviewed only briefly here.

The softening point of glass is most usually defined in terms of its viscosity, a characteristic of glass which varies with time, temperature, and composition and which is quite important to the fabrication and performance characteristics of glass. Several reference viscosities have been established by the American Society for Testing Materials. Examples are:

- (1) Softening point. This is the temperature at which glass will deform under its own weight and corresponds to a viscosity of $10^{7.8}$ to 10^8 poises.
- (2) Annealing point. At this temperature, the internal strains in glass are reduced to an acceptable commercial limit within 15 minutes; it is characterized by a viscosity of 10^{18} poises.
- (3) Strain point. This is defined as the temperature at which the internal stresses will be reduced to low values in four hours. The corresponding viscosity is $10^{14.8}$ poises.

Figure 16, drawn from material in Reference 125, shows the viscosities of several types of newly drawn fibers versus temperature; the strain and annealing points are indicated according to the ASTM values.

The coefficient of thermal expansion is of interest because when two different glasses are fused together, as in the case of a clad fiber, any difference in their expansion coefficients will produce residual stresses when the fiber is cooled. The thermal expansion coefficient of glass is expressed as the fractional change in length per unit of temperature difference and is generally the mean value observed over the range 0 to 300°C.

In this study, our interest is confined to the Schott F 2 core glass and Kimble R-6 cladding glass which are quite commonly used in optical fibers. The F 2 is a lead alkali silica glass with a refractive index of 1.62 while the R-6 is a soda lime silica composition with an index of 1.52. The expansion, annealing point, and softening point data for these glasses are:

	<u>Schott F 2</u>	<u>Kimble R-6</u>
Expansion coefficient	$86 \times 10^{-7}/^\circ\text{C}$	$93 \times 10^{-7}/^\circ\text{C}$
Annealing point	438°C	522°C
Softening point	593°C	702°C

Table 2. Thermal properties of two glasses.

Because of the fairly well matched expansion coefficients, little difficulty has been experienced with clad fibers fracturing during manufacture or ordinary

handling. It will be observed, in this case, that the cladding glass has a higher coefficient and should be expected to shrink more tightly around the core as the fiber is cooled to ever lower temperatures. To our knowledge, extensive tests have not been performed on the influence of differential expansion in weakening fibers at low temperatures; however, tests performed here in another connection indicated that clad fibers can be temperature-cycled rapidly between -100° F and 1000° F with no apparent deterioration.

Theoretical considerations indicate that from the standpoint of mechanical strength, fibers of improved qualities should result if the order of thermal expansion coefficients were the reverse of the one in the widely used F 2, R-6 pair. If the core material had the higher coefficient, then upon cooling from the molten state it would tend to shrink more and to pull the cladding tightly toward it. The cladding, not being able to contract as much, would be left in a condition of tangential and linear compression, which in principle should yield a stronger fiber.

The values given in Table 2 refer to glass in the bulk state. It is widely held that differences do exist between glass in the fiber form vs. the massive form because of differences in their cooling rates from the molten state. The high chilling rates of fibers leave the glass structure in an unstabilized condition, implying that further changes will occur with time, at a given temperature. The effect of these changes upon viscosity is especially noticeable, as shown in Figure 17, which is based on data in Reference 125.

Measurements of the physical properties of the same glass in different physical forms indicate that a fiber of 0.0005" in diameter may have a strain point 200° C to 300° C under the corresponding temperature of massive glass and a difference of 10×10^{-7} per °C in the coefficient of expansion.

While all the properties of glass in fiber form are materially different from those shown by the same compositions in massive form, the properties of fibers tend to return to the values established for bulk glass as stresses in the fibers are released. This stress release can occur at room temperature over a period of several weeks or in the annealing range. While many of the properties of glass in fiber form can be predicted with some certainty, much remains to be learned about the mechanical strength of fibers. The properties of glass under stress are in no way similar to those of metals. Glass, unlike metal, fails abruptly without yield or deformation. Failure always results from a tensile component of stress even though a load may be applied in compression. There seems to be no effect on the fatigue of glass whether a load is static or cyclic.

It has been generally accepted for some time that small surface flaws are the starting points of a fracture when glass breaks under stress. These flaws are submicroscopic in size and are caused by chemical action on the surface of the glass, or are scratches caused by contact with other pieces of material. The flaws become the focal points of stress concentrations since glass does not yield

under stress as the metals do. Tests on large samples of fibers have led to the belief that no accurate prediction of the breaking stress can be made since the surface of the glass is so dependent on its past history. In the case of the very fine glass fibers which are drawn for textile applications, observed tensile strength values are much higher than for optical fibers or for bulk glass. Freshly drawn, untouched fibers have been found to have breaking strengths up to 900,000 psi, while measurements on fibers of production runs have an average value of about 250,000 to 300,000 psi. Partial or complete annealing of fibers will reduce this value very substantially, probably because of chemical actions on the surfaces of the fibers and because it may relieve certain desirable stresses which contribute to fiber strength.

SECTION 3

PROPERTIES OF FIBER BUNDLES

The term "fiber bundle", as used here, pertains to a cooperative configuration of transparent fibers fulfilling some light-transmitting function which a single fiber cannot perform. As a result, the properties and behavior of a fiber bundle are quite different from those of a single fiber and often cannot be predicted from a knowledge of the latter's properties. Moreover, when one considers the mechanical configuration of the end faces and the mechanical considerations introduced by the protective jacket which is normally provided, it is apparent that the study of fiber bundles includes aspects which are totally foreign to the study of an individual fiber.

We are using the term "fiber bundle" to include both the image-bearing "fiberscope" and the light-bearing "light pipe". The ensuing discussion will concern itself with both forms, their common ingredient being the ability to transmit visual information, whether it is pictorial or "scrambled". As in Section 2, we shall consider optical, mechanical, and thermal properties, but this time in relation to the group aspects of fiber behavior, with some reference to and unavoidable repetition of Section 2 material.

3.1 Optical Image Transmission

The following paragraphs will emphasize the image-bearing aspects of bundles of optical fibers and the way in which image quality is affected by various influences such as bundle length, fiber packing factors, number of fibers, and so forth. We use the term "image" in its broad sense to include scrambled or incoherent images as well as pictorial presentations, and we shall differentiate between them by use of the terms "coherent image" and "incoherent image".

3.1.1 Attenuation vs. Length

The most important single factor in any discussion of fiber bundles for aerospace applications regards the maximum lengths which may be used for effective image transmission. Depending upon the brightness of the scene to be imaged, and upon the viewing conditions and other factors, there is a maximum possible length beyond which any fiber bundle loses its effectiveness.

The length limitation is imposed by the losses of radiant energy which occur within optical fibers as a result of bulk absorption by the materials themselves and as a result of scattering and of other losses introduced by fiber defects. The purpose of this Paragraph is to examine the extent of these losses for various fiber bundles and to speculate as to practical length limitations for various viewing situations.

In the study of optical fibers by Potter (41, 42), six parameters were listed as having significant effects on the transmittance of a single fiber:

- (1) Fiber core diameter;
- (2) Fiber length;
- (3) Refractive index of core glass;
- (4) Refractive index of surround glass;
- (5) Reflectivity at interface; and
- (6) Absorption coefficient of core glass.

These are assuredly the important ones, but to them we would add the absorption of the surround glass and the presence of contaminants within the core or cladding, both factors being especially important in the case of long fibers. Potter has made measurements with the purpose of deducing typical values of interfacial reflectivity and has arrived at values of the order of 99.93%; it is possible that this value takes into account the effects of any interfacial defects or others.

The parameters listed above are exclusive of fixed losses which occur in a fiber bundle in the form of packing or interstitial losses which are dealt with elsewhere in this report.

In Paragraph 2.1.6 we reported the results of transmittance measurements on solid blocks of various types of glass, as shown in Figures 2 through 8. A later series of measurements was concerned with the spectral transmittance of clad fibers with F 2 glass cores and R-6 glass cladding for comparison with the data on solid F 2 blocks. This series comprised spectral transmittance measurements on 2, 4, 6, and 12 $\frac{1}{2}$ -foot long light pipes, using the General Electric spectrophotometer. In this instrument, the light beam in the position of the sample is 5/8" high by 3/16" wide; a lens was used to converge this beam to about 3/16" by 1/16" in order that it would be contained within the 4" diameter light pipe end faces. The marginal rays in this case were 7° from axial, which is well within the acceptance angle of the fibers. The output end of the fibers was directed into the integrating sphere of the instrument so that all of the emitted light was collected and utilized in the measurement. All fibers were approximately two mils in diameter.

The recorded data were then corrected for end face reflectance losses in order to convert them into line-transmittance so that they could be extrapolated to a common length for comparison with each other. In addition, the data were adjusted for computed values of entrant light which was lost in falling between fibers (see Paragraph 3.1.2), falling on the cladding end faces, and falling on "dead" or missing fibers. This is equivalent to subtracting from the reference

light beam a small part of its cross-sectional area containing that part of the light which falls between the fiber cores, thereby raising the measured transmittance values to what they would be for a hypothetical bundle of clad fibers with no interstitial spaces. It is important to realize that these adjustments serve to eliminate the effect of absorption of incident light by the integrated end face area of the claddings, but the adjusted transmittance values nonetheless include the effects of cladding absorption of rays which initially entered the cores themselves but which "leaked" into the cladding during the multiple reflection process. The purpose of these adjustments was to eliminate variations in the "area factor" (fraction of incident light falling on the cores only) which varies appreciably from one fiber bundle to another; only in this way could the measured values be reduced to a common basis for comparison.

The computed results are shown in Figure 18. The uppermost curve is a reproduction of one shown in Figure 5 and pertains to a particular melt of Schott F 2 glass extrapolated to a six-foot length. The lower solid curve is the computed transmittance of a six-foot light pipe, assuming no interstitial losses, and is based on the average of the spectrophotometric measurements on the 2, 4, 6, and 12½-foot long light pipes. Both curves represent line-transmittance only, and would have to be revised downward slightly to accommodate end surface reflectance losses.

Because the lower curve is corrected for interstitial losses, the only remaining causes of the disparity between the two solid curves should be (1) light losses within the fibers because of scattering, (2) imperfect interfacial reflectance between core and cladding, and (3) the apparently substantial absorption by the cladding. There is, in addition, a further slight source of disparity due to a circumstance of the experimental set up, notably that the incident light beam in the case of the upper curve was fairly well collimated, being contained within a very few degrees of the fiber axis, while the beam in the lower case was somewhat convergent, with the marginal rays being incident at about $\pm 7^\circ$ off axis. The effect of this convergence was to increase the total path length of many rays through the fiber (according to the relationship $L \sec \theta$; see Paragraph 2.1.1) and is reflected in the fact that the transmittance curve is somewhat lower than it should be.

We observe that in the visible spectral region the lower curve approaches within 80% of the upper curve, but in the infrared region this value drops to about 68%. This implies the presence of some dispersive or wavelength-sensitive phenomenon which arises when one proceeds to clad a core material and draw it into fibers. If we assume, reasonably, that the scattering phenomena and the interfacial defects are non-dispersive, then the only remaining cause of appreciable infrared loss would be absorption by the cladding; the known infrared losses within presently used cladding materials bear this out. The importance of these curves is that they apparently verify (1) the theoretical prediction that a light ray which is totally reflected at a dielectric interface does indeed penetrate into the second

medium for a finite distance and therefore (2) that to achieve highly transmitting fibers of considerable length, where many reflections are involved, it is extremely important to specify high transmittance not only in the core material but in the cladding as well.

Also shown in Fig. 18, as broken lines, are partial transmittance measurement values for "F 2, R-6" light pipes of three different qualities, extrapolated to six foot lengths and adjusted upward for interstitial and end losses. The lowest curve originates from a light pipe whose core material was from a melt of F 2 glass which apparently contained inclusions, to which fibers are very sensitive. The middle broken curve represents fibers with F 2 cores from a higher quality melt, and the uppermost broken curve is for fibers with cores of the better F 2 melt but with a different area factor as well. A word of explanation is necessary with regard to the computed area factors and their effect on possible uncertainties in the broken curves. For each light pipe measured, a photomicrograph of the end face was studied carefully in order to allow an estimate of the usable end-face fractional area. Reference to Fig. 1a will reveal that, although the area factor averaged over a given light pipe has a specific meaning, it shows wide local variations over the end face. In the spectrophotometric measurements, the illuminating beam was contained within the fiber bundle end face and illuminated only a portion of it. During the measurement, it was not possible to determine which part of the end face was being illuminated. Thus, an average area factor value computed for a given light pipe was not necessarily applicable to that part of the end face area which was actually used in the measurements. Consequently, the adjustments in the curves, which were achieved by dividing the observed transmittance value at each wavelength by the area factor, are not necessarily the appropriate ones. In the case of the highest broken curve, the computed area factor was only 52%; this may have been unduly low, leading to an unnecessarily large correction in the original transmittance curve. The area factors for the three broken curves were, respectively, 52%, 66.5%, and 70%, reading from the top downward, which is a fairly large variation considering the small number of samples.

Figure 19 presents computed transmittance values for light pipes in 12 $\frac{1}{2}$, 25, 50, and 100 foot lengths. These values were extrapolated from measurements on shorter light pipes with F 2 cores and R-6 claddings. After extrapolation of the line-transmittance values to the various lengths, appropriate deductions were made to allow for end surface reflectance losses (wavelength by wavelength) and for an arbitrary area factor of 70%. These curves are thus intended to portray, somewhat realistically, the transmittance values of actual light pipes in the lengths indicated.

Figure 20 presents the results of direct spectrophotometric measurements on several light pipes and on a fiberscope composed of multifibers. In the latter case, the cross-sectional cladding area would be expected to occupy an appreciably greater proportion of the entrance area than it would in a light pipe; this

is very likely the reason that the 48" light pipe shows a higher transmittance than does the 36" fiberscope. The curves shown include the effects of reflectance losses introduced by a condensing lens used in the measurements. Without the lens, the curves would be somewhat higher, as indicated by the corrected values shown below for 550 m μ :

TRANSMITTANCE AT 550 MILLIMICRONS:

	<u>Observed</u>	<u>Corrected for Lens</u>
24-inch light pipe	46%	53%
48-inch light pipe	40%	46%
36-inch fiberscope	34%	39%
12 $\frac{1}{2}$ foot light pipe	17%	20%

Table 3. Corrected transmittance values for curves shown in Figure 20.

The corrections for the lens reflectance are seen to become less important, in a relative sense, in the longer fiber bundles where the line-losses predominate.

We turn now to the question of the effect which a reduced transmittance would have in the practical case of a fiber bundle being used in an aerospace application. It is difficult to specify a certain maximum usable fiber bundle length for any application, for this length will depend upon the scene brightness, the degree of visual recognition demanded by the observer, and several other factors. Instead, we can only hope to convey a subjective impression of the manner in which an image deteriorates as it is transferred through increasingly greater bundle lengths.

To this end, we have prepared a series of photographs, under laboratory conditions, attempting to show the progress of the image deterioration with increasing bundle lengths. The photographic subjects consisted of live scenes or photographs representing typical situations which might be viewed in aerospace hazard detection problems, such as an engine fire. The subjects were imaged upon fused faceplates or fiber bundles of various configurations by means of appropriate objective lenses. The image transmitted by the fiber optic device was photographed by conventional means; the effect of an increasing optical bundle length was simulated by the introduction of appropriate optical filters before the camera.

One of several laboratory photographic setups is shown in Fig. 21. The subject in this case is a laboratory mockup of a jet engine section, with a propane burner flame being introduced to simulate the appearance of an accidental engine fire. An objective lens (in this case, a variable focus or "Zoom" lens) forms an image of the subject upon a thin fiberscope faceplate

whose purpose is to superimpose upon the image a mosaic pattern characteristic of a fiberscope of given quality or resolution. The image transmitted to the rear surface of the faceplate was photographed at close range as the eye might see it with an eyepiece magnifier of reasonable power. This setup was also used in other photographic studies to be described later.

Figure 22 presents a series of views of an engine fire as it might appear through increasing lengths of fiberscope. It is not possible to specify the precise fiberscope length which is simulated in each of the photographs but only to suggest a series of approximate lengths. The reasons are several, including the fact that fiberscopes differ among themselves in apparent transmittance per unit length and it is not possible to specify a "typical" fiberscope transmittance. A more important reason is that the ability of the eye to accommodate for various brightnesses in viewing a fiberscope image is not at all effective when viewing a series of photographs of such images. Thus, the image which appears darkest in the photographs might actually appear somewhat brighter to the eye in an actual viewing situation, and conversely. The observer's viewing conditions and state of dark-adaptation strongly influence what he will "see" in viewing a fiberscope image. Therefore, a series of photographs cannot hope to duplicate an actual visual situation but only to indicate trends.

Tentatively, therefore, we suggest that the progression of darker, greener images of Figure 22 depicts what an observer might see in viewing an engine fire successively through 5, 10, 15, and 20 foot fiberscopes of average quality under laboratory viewing conditions. The suggested lengths are based upon visual estimates by the author who has had an opportunity to make observations through several long fiberscopes during this study; however, these estimates are subjective and include an uncertainty of perhaps $\pm 25\%$ in the length values.

The image detail visible in these photographs is typical of a high quality fiberscope with fused end faces. Approximately one million fibers are represented over the area of each photograph, each being too small to be visible. By contrast, Figure 23 presents a similar sequence of photographs taken with an actual multifiberscope. The multifibers themselves are visible in the first photograph (although they are out of focus in the later ones); however, the thirty-six individual channels within each multifiber are again too small to be resolved here. As an extreme example of a low resolution image, the photographs of Figure 24 depict a similar sequence as transmitted by only a few thousand fibers. This sequence was prepared through use of an intentionally coarse faceplate specially prepared for this purpose. The fibers were of eight mil diameters and were potted in epoxy resin, rather than being fused together; their outlines are therefore highly discernible and their group appearance would be (except for their random arrangement) somewhat typical of a monofilament fiberscope viewed under high magnification.

Although the subject of the number of fibers per image belongs in Paragraph 3.1.3 on resolution, it is introduced here so that we can examine the limitations imposed upon image clarity due to the combined effects of low resolution and high attenuation. To add a further element of poor image quality, we have provided a de-focused image of the flame on the faceplate shown in Figure 24; although the fiber ends are themselves well resolved in the photographs, the flame image and the engine parts are blurred. Thus, Figures 22 and 24 depict the effect of an increase in bundle length on both a high quality and a low quality fiberscope.

There is no question of the superior image quality seen in Figure 22. However, the question which must be asked, in comparing these figures, reverts to the matter of the intended function of a fiberscope. That question is, "Apart from the matter of poor image quality, is there any doubt that a flame is visible in the last photograph of Figure 24, assuming an engine compartment in which no other light source should be present?". (It must be remembered that in an actual viewing situation, the normal motion of the flame would add a further dimension of reality which is not possible in a photograph.)

If the reader agrees that the flame is recognizable here, then in cases where a fiberscope is used simply to provide a pilot with the knowledge of fire-vs.-no-fire in an engine compartment, it is suggested that the reduced image quality of the low resolution fiberscope can become secondary to the matter of the reduced weight and cost which would be afforded by the smaller number of fibers.

A final sequence of progressively attenuated photographs is presented as Figure 25. In this case the visual situation differs in that a smaller flame is seen against an incandescent engine surface. The sequence of simulated fiberscope lengths is approximately as before, except that the characteristic green tinge of long fiberscopes was not introduced into these photographs. It is observed that the flame is still visible in the final photograph although the hot surface is not. (Paragraph 4.6 on image tubes will discuss means of rendering the hot surface visible in this situation.) The estimated lengths are 10, 20, 30 and 40 ft.

3.1.2 Interstitial Losses

Because only the core of a clad fiber is an effective transmitter of light, any incident light which falls between the cores at the end face is lost, including that which falls on the cladding ends.

In the case of round fibers, the integrated area of the interstices occupies a measurable fraction of the end face area. At the viewing end, the image (whether coherent or not) is seen with a reduced average brightness, as though one were viewing a scene through a dark window screen. The apparent brightness loss depends upon the fiber spacing in the end faces and is greater with more loosely spaced fibers.

Figure 26 shows the case of maximum packing density (or area factor) which is realizable in the case of a light pipe with round fibers, whereas Figure 27 shows the more open spacing which results with current methods of monofilament fiberscope manufacture in which straight rows of fiber ends are laid down successively.

In the former case, where each fiber is surrounded closely by six others and the lines connecting their centers make angles of 60° or 120° with each other, it can be shown that

$$\text{Area Factor} = \frac{\pi}{3.47} \times \frac{(\text{Core diameter})^2}{(\text{Spacing})^2}$$

where the fiber spacing is the distance between their centers.

In practice, the fibers do not embed as closely, particularly in the fiberscope case. If each fiber were surrounded by five others, on the average, then the 60°, 120° relationship would be replaced by a 72°, 108° one and we would have:

$$\text{Area Factor} = \frac{\pi}{3.80} \times \frac{(\text{Core diameter})^2}{(\text{Spacing})^2}$$

With actual light pipes, one finds the average number of fibers surrounding a given fiber to be somewhere between five and six so that for computation of the area factor, one would use a value for the factor in the denominator somewhere intermediate to those shown.

In the ideal packing situation, depicted in the first formula above, it is seen that if the fibers were not clad and the cores were in contact, then the fiber spacing would equal the core diameter, and the area factor would be $\pi/3.47$ or about 91%. Thus, in the ideal case, the interstices would cause about a 9% loss of the incident light.

Somewhat different considerations apply to fiberscopes made of multifibers, which are normally more square or rectangular than circular and which therefore utilize the end face area more effectively (see Figure 1c). However, although the spaces between fibers are not as great, the ratio of cladding cross section to total area may be greater, depending upon the size and construction of the basic multifiber.

The above considerations imply that the highest utilization of the bundle end face area would be achieved through the use of fibers with square cores and a minimum of cladding. However, other considerations involving the geometry of internally reflected rays show that the transmittance is not as high through square fibers as through round ones because of a greater tendency for light to escape through the corners of each fiber.

There is, however, an alternative approach to higher end face utilization which involves fusing the fibers together only at the end faces, leaving them round over most of their lengths. Figure 1b shows the dense packing which is attainable by fusing.

The process is done under vacuum conditions in order to eliminate air gaps, and heretofore it has lent itself more readily to short, solid faceplates than to fiber bundle ends. Progress is being made, however, in overcoming certain manufacturing difficulties and particularly the brittleness of the transition zone between the solid end face and the loose fibers immediately behind it.

3.1.3 Resolution

Figures 28a, b, and c show the improvement in image clarity which is obtained as one transmits a given image through a larger number of smaller fibers. The definition of detail is obviously improved as one dissects an image into an ever greater number of smaller elements for transmission purposes. The fiber bundles used here were fused faceplates containing fibers of 4 mil, 2 mil, and $\frac{1}{2}$ mil diameters, respectively.

In these photographs, it is particularly evident that a single fiber cannot convey picture information over its end face; instead, any image detail falling on a fiber end is averaged out in its course through the fiber and appears at the far end as an area of uniform color and intensity. Consequently, a fiber bundle can transmit only as many picture elements as the number of fibers which it contains. The number of fibers is often referred to as the "resolution" of the bundle.

Bundle resolution does not depend on fiber size, for two bundles which have the same number of differently-sized fibers will transmit the same number of picture elements.

The matter of the degree of bundle resolution required for a given aerospace detection problem depends upon the amount of picture information which must be conveyed, and since this varies broadly from one situation to another, no quantitative recommendation can be made concerning each. For example, the subject may be an engine section, as in Figure 22, containing considerable detail and which may have to be monitored for a small oil leak; in such a case, a million fibers (as in the photograph) may not be too many, although there is no advantage to using more fibers than the eye can resolve individually, for image clarity does not improve beyond the point where the individual fiber can no longer be distinguished. (This assumes that the picture area remains constant in size and that the fiber diameters are reduced as their number is increased.)

On the other hand, the same engine section may happen to be the subject in a case where the viewing requirement is not as critical, as in the detection of a small accidental fire and of its size and location. In this case, a quarter

million fibers would provide an image of quality comparable to a television image under good conditions of reception, while only 100,000 image points (as in Figure 23) might be adequate.

At the other extreme, the engine details may not be at all of interest but only the question of whether a fire, large or small, exists in the compartment. In such a case, a few thousand fibers would provide enough shape recognition (see Figure 24) to allow the flame to be distinguished from any spurious light source which might be present, such as sunlight entering through a louver. In a typical jet engine compartment which is well sealed against outside light sources, and where flame detection (and not discrimination) is the only problem anywhere from a few fibers to a few hundred may suffice, depending largely upon the angular coverage which is desired, for this in turn depends upon the relationship between the bundle diameter and the focal length of the objective lens. In the simplest of flame detection situations, there is very little sacrifice of image realism if one specifies a light pipe instead of a fiberscope, for the sparkling, scrambled yellow dots by which the light pipe conveys a flame image leave no doubt that one is observing the color and flicker characteristics of a flame and that form recognition is not necessary. Laboratory observations through a very small light pipe containing only 33 two-mil fibers have indicated to us how few image points are necessary in providing convincing information that a flame is being observed.

Figure 29 illustrates the recognizability of a flame under progressively worse image conditions. The fiber bundles used were, respectively, fused and potted faceplates containing increasingly coarser fibers; a slight reduction in fiber orientation is evident in one of the faceplates.

It is important to recognize that the presence of a flame is clearly discernible in all cases, especially when one considers the characteristic flame motion which is visible in the actual case. Where the problem is simply one of detecting flame versus no-flame, the difference in image quality becomes less emphatic and all four faceplates in the figure can be considered to be performing with equal effectiveness.

Although the sequence of photographs depicts an image of constant size as transmitted by increasingly coarser faceplates, it may also be regarded as a progression of smaller images formed on smaller sections of the same faceplate but photographed at progressively higher magnifications. In view of this consideration, it is clear that the use of fewer fibers does not necessarily imply larger fibers but rather a smaller fiber bundle, with its attendant savings in weight and in cost. In our opinion, the fiber bundle user may tend to specify too large a number of fibers for a given application, being understandably influenced by the thought of a clearer image; we wish to stress the economies which may be enjoyed if one uses no more fibers than are necessary for a given function.

This discussion of resolution has concerned itself largely with coherent images as transmitted by fiberscopes; to a lesser extent, the information-transmitting ability of a fiberscope increases with the number of fibers, but because light pipes are recommended here largely for "go, no-go" flame detection applications, there would be little advantage afforded by a larger number of smaller fibers. Indeed, we have observed the effect of the scintillating, scrambled flame image to be more dramatic with larger, fewer fibers because the spots tend to move around the bundle end face more freely; when too many fibers are used, clusters of them scintillate in unison but the visual effect is not as striking. A quarter-inch diameter light pipe containing about a thousand 5-mil fibers is quite effective for flame detection, although our studies have indicated that, from the standpoint of mechanical durability, five-mil fibers are not likely to be as suitable for aerospace environments as are two or three mil fibers. The principal advantage, then, of specifying a flame-detection light pipe with many finer fibers would be a matter of mechanical survival.

3.1.4 Effects of Fiber Diameter

We consider two fiberscopes with equal numbers of fibers but differing in fiber diameter and thus in bundle cross section. We assume, also, that they are used with objective lenses whose focal lengths are proportional to the respective fiber sizes so the fiberscope fields of view are identical; the respective image sizes of a given object will thus be in proportion to the fiberscope sizes.

Aside from the obvious ways in which these devices differ mechanically, cost-wise, and so forth, we are interested in how they differ optically. With one stipulation, the main difference is simply in the total amount of light transmitted and the effect which this has on the ease of viewing. The stipulation is that the fiber sizes must be at least large enough so that waveguide effects do not predominate; that is, the fiber diameters must exceed a few wavelengths of light. If they are larger than a few microns (1 mil = 25.4 microns) the fiber transmittance will be largely independent of fiber diameter.

The suggestion that the larger fiberscope transmits more total light automatically implies a certain desirability, but the exact nature of this advantage should be understood by the reader. It does not imply that one image will be brighter than the other, for the additional flux is merely distributed over a larger end surface area; similarly, the angular distributions of emergent rays will not differ if the objective N.A.'s. are the same. The essential difference between the two fiberscope images is that the larger one will require less eyepiece magnification to convert it to a given angular size than will the smaller one. As will be shown in Paragraph 4.1.1, the advantage of a lower eyepiece magnification is that the magnified image is visible from steeper angles, allowing a greater freedom of head movement by the observer. Essentially, then, the extra radiant flux carried by the larger bundle can be directed into a larger solid angle at the observer's end, providing him with an image of the same angular size but one which is more easily viewed.

On the other hand, with a larger initial image at his disposal the system designer may elect to specify the same eyepiece magnification as he would for the smaller fiberscope image. In this case, the observed image will appear larger but will be confined to the same viewing angle as with the smaller image.

Figure 30 presents a sequence of photographs depicting a difficult viewing situation requiring the recognition of a barely luminous, incandescent turbine casing as seen through a fiberscope. The three photographs are identical except for differences of magnification. It will perhaps be observed that the largest photograph affords the quickest, most positive identification of the subject. The magnifications are in the ratio 1:2:3 and represent the apparent image sizes provided by three fiberscope-objective-lens systems scaled up in that ratio but all viewed through the same eyepiece. A different choice of relative eyepiece magnifications could yield images of the same angular size but differing in the restrictions on the observer's head movements.

3.1.5 Coherent vs. Incoherent Bundles

The distinguishing feature of the incoherent fiber bundle, or light pipe, is the ability to transmit color and intensity information in cases where shape information is not necessary, and to do so at a fraction of the component cost compared with its image-bearing counterpart, the fiberscope.

In detection applications, its intended use is therefore the transmission of scrambled light patterns where the only item of concern is whether or not light is present in a given color, intensity, or motion pattern in a remote area under surveillance. In the realm of aerospace hazard detection, the light pipe is ideally suited to the visual monitoring of accidental fires whose color and flicker characteristics are so singular as to permit recognition without the need of shape information.

In the case where a light pipe is used for flame recognition, the motion of the scrambled image resulting from flame flicker is a vital ingredient in the recognition process. It would thus be meaningless for us to try to portray the effect through the use of still photographs, although the interested reader can provide himself quite economically with a small light pipe and lenses in order to demonstrate the effect to his own satisfaction. (Light pipes in various configurations are listed as standard products by American Optical Company, Southbridge, Massachusetts, and other fiber optics suppliers can very likely make them to order.)

As in the case of a fiberscope, the flame-detection light pipe should be used with an objective lens to form an image on its input face. Although light guides will accept radiation directly from a luminous source, the absence of a lens yields a uniform light distribution over the end face, and the pattern of scintillating spots which characterizes the flame would not be seen.

A feature of modern commercial light pipes is that the degree of fiber disorder varies in a random way from one sample to another. The disorder does not result from a methodical scrambling procedure during manufacture but occurs naturally during the handling process prior to potting of the end faces. Shorter fiber bundles are characterized by lesser degrees of disorder, so that entire groups of fibers are interspersed throughout one another, rather than individual fibers.

Our laboratory studies have indicated that the observer's attention and recognition are greatly abetted when the degree of disorder of a scrambled flame image is the highest possible. We therefore recommend that light pipes for such applications be specified with a high degree of fiber scrambling and that the supplier give special attention to this feature during manufacture.

The flames referred to in this discussion are restricted to the orange-yellow to whitish-yellow flickering diffusion flames characteristic of ordinary "fuel puddle" fires under various degrees of ventilation. These fires might result from leaks or ruptures in lines or tanks bearing petroleum-derivative fuels or other hydrocarbon fluids such as hydraulic or lubricating oils. Many other types of accidental fire are possible in aerospace operations, many of them not being highly self-luminous or readily visible. These would include certain exotic fuel flames, hydrogen flames, hot exhaust gas leaks as in jet engine afterburners, premixed hydrocarbon flames, and even certain hydrocarbon diffusion flames at high altitudes where they are known to lose much of their incandescent carbon particle emission and fade to a pale blue.

Such flames, if at all observable, would most likely require the picture-carrying ability of a fiberscope for recognition, especially if the background or viewing conditions were at all adverse. In the case of an invisible flame, it is hardly necessary to point out that visual observation through a fiberscope would serve no purpose, it being a general guiding principle that if an object can be detected visually, it can generally be seen through a fiber bundle but not otherwise. However, in Paragraph 4.6 on image tubes, methods of expanding the image capabilities of fiber bundles are discussed, utilizing the high transmittance of glass and other materials in the infrared spectrum.

3.1.6 Color Distortion in Fiber Bundles

Figures 22 through 24 indicate the loss of image brightness which makes it difficult to recognize objects through long fiberscopes. The figures also show the distortion of the natural colors of objects due to the inherent color in most glasses which becomes noticeable in great lengths.

Where shape recognition is the principle function provided by a fiberscope, color distortion becomes a matter of secondary concern. However, the color of an object is often an important aid to recognition, as in the perception of a

flame or of an overheated surface. In the latter case, the incandescent color of the surface as seen directly would provide the observer with some intuitive knowledge of the surface temperature; if the color is distorted in passing through a long fiberscope, the observer may lose his ability to judge the actual color and the level of surface temperature in order to decide whether he is viewing a normal, an abnormal, or a highly abnormal temperature condition.

In flame perception through fiberscopes, some color distortion can be tolerated because the shape and flicker information alone are sufficient for recognition. In light pipes, however, where color and motion are the essential clues in flame recognition, a scintillating pattern of greenish-yellow dots would provide much less convincing evidence of a flame than would the more familiar orange-yellow dots.

It is difficult to be specific about the amount of color distortion which can be tolerated in a given situation. A tolerance might be established in terms of whether it does or does not (statistically) prevent an observer from identifying a given object or condition; however, the tolerance depends upon so many parameters of the viewing situation that an attempt to put it on a quantitative foundation is outside of the scope of this study. In general, however, it may be stated that a given amount of color distortion becomes increasingly less objectionable as the number of familiar objects increases in the object field, for then the eye becomes less dependent upon the perceived color of an object as an aid to identification. Moreover, the ability of the eye to compensate for color distortions in familiar scenes would tend to suppress the apparent distortion greatly.

Because color distortions are perceived differently by the eye than by color photographic processes, they are difficult to depict photographically as the eye would see them. To some extent this is true in Figures 22 through 24, in which each sequence of photographs does not appear to become as progressively green as the original scenes did when viewed directly in the laboratory. However, a distinction must be introduced here between what the eye sees and what the mind perceives, for the two do not always coincide. An individual may be wearing yellow sunglasses and still recognize a white sheet of paper as being white. If queried on this, he may admit that the paper "looks" yellow but that he "knows" that it is white, although he may never have seen that particular sheet before. He is able to make this identification because of the presence of familiar objects in the scene, his color-memory of these objects serving to establish a new color reference scale which undoes the effects of the yellow sunglasses. However, he would not be able to make a correct color identification if the same sheet of paper were the only illuminated object in his field of view and if he had no knowledge of what colored sunglasses he was wearing.

Returning to Figures 22 through 24, it is probably more correct to say that each sequence of images appears as the mind would perceive it, rather than as the eye would see it, because for an unknown reason in the rendering of the color prints from the original transparencies, an unanticipated degree of color compensation appeared in each sequence.

The same is true of Figure 31 which compares the direct and indirect views of the color test chart appearing in the 1960 edition of the Eastman Kodak Color Dataguide. The lower photograph was made through a 25-foot length of multifiberscope, comprising two 12-1/2 foot sections with their end faces held together mechanically, as shown in Figure 32. The reduced brightness of the fiberscope image was compensated for somewhat during the photographic exposure in order to suppress the brightness difference and to allow a better evaluation of the chromaticity change. The lower photograph therefore conforms more closely to the psychologically-perceived image after a "mental" brightness correction has been made.

The reader will have little difficulty in recognizing the progression of colors in the test photograph and in agreeing that they appear to represent the same sequence as in the control photograph. This is largely because of his subconscious awareness that the color reference background in both cases is supposed to "look" white, and as his mind links the reference colors together, the color test strips appear more nearly to match. The reader can perform a simple test which will eliminate the effect of this psychological "bias" and which will allow an objective evaluation of the color change; he need only mask off all but the yellow rectangles in both photographs, preferably by cutting slots in a sheet of white or yellow paper, in order to perceive more nearly the actual color difference.

To summarize, the visual perception mechanism can accommodate rather wide color distortions provided that the scene contains elements which are recognizable through features other than color, but in the absence of other clues, the observer's recognition depends much more strongly upon an accurate color rendition of the object being viewed. As applied to the aerospace problem, this means that the color distortion arising in a given length of fiber bundle would be less disruptive in the case of a fiberscope image of a well lighted scene containing familiar objects than it would in the case of a scrambled flame image transmitted by a light pipe.

From line-transmittance measurements made earlier on F 2/R-6 fibers (see Paragraph 3.1.1), computations have been made in order to determine quantitatively the extent of color distortion imposed upon various blackbody color temperatures by selected lengths of fiber bundles. Length values were extrapolated to 5-1/4, 12-1/2, 25, 50 and 100 feet. The results are shown in Figures 33 through 37 where they are plotted in the C.I.E. (Commission Internationale de l'Eclairage) chromaticity diagram. (See Handbook of

Colorimetry, prepared by the M. I. T. Color Measurement Laboratory under the direction of A. C. Hardy, The Technology Press, Massachusetts Institute of Technology, 1936, or any standard text on colorimetry.)

Each point within the horseshoe-shaped figure represents the chromaticity of some visible color, that is, the hue and saturation aspects without regard for brightness. The locations of pure spectral colors are designated at the periphery by their wavelengths in millimicrons. The solid curve contained within each figure shows the continuum of "trichromatic coefficients" or chromaticity coordinates corresponding to blackbody color temperatures from 1000° K to infinity, with the corresponding temperatures being indicated at intervals.

Each figure shows the chromaticity shifts for several color temperatures for a given fiber bundle length. The shifts are seen to be in the direction of the yellow-green portion of the spectral locus and are greater as the bundle length is increased; this is in accord with the known color of F 2/R-6 fibers.

Of the many colors whose shifts might have been the subject of this study, the blackbody colors are the most interesting, for they typify the colors arising in many aerospace hazard situations involving incandescent surfaces and flames. The observed color of each of these emitters can generally be approximated by the color of a blackbody source at a given temperature and plotted on the C. I. E. diagram. The approximate color temperatures of various standard light sources, practical light sources, and familiar surfaces are given in Table 4.

<u>SOURCE</u>	<u>APPROXIMATE COLOR TEMPERATURE, °K.</u>
Incipient red heat	770 - 820
Dark red heat	920 - 1020
Bright red heat	1120 - 1220
Orange heat	1320 - 1420
Yellow heat, including many hydrocarbon diffusion flames	1400 - 2000
Standard British candle	1930
Freezing point of platinum	2042
Tungsten lamps	2500 - 3200
Photoflood lamp	3400
Carbon arc	4000 - 5000
Cloudy sky	6500
Hazy sky	9000
Average blue sky	12,000 - 18,000
Clear blue sky	25,000

Table 4. Color temperatures of various light sources.

The color distortions introduced by fiber bundles can be corrected to some extent but only at the expense of image brightness. The correction is achieved by introducing an appropriate optical absorption filter anywhere in the image path. There is a variety of colored filter materials available from several sources, including glass filters and gelatin filters. Although methods are available for calculating the precise color filter needed in a given situation, it is much more convenient and quite satisfactory to make the selection empirically, using several observers to judge, in the laboratory, when a given fiber bundle has been satisfactorily color corrected.

3.1.7 Viewing Conditions

The principal viewing condition which can affect the perception of a fiberscope image is the ambient light level at the viewing end. The ideal viewing situation would be a darkened enclosure, especially in the case of longer fiber bundles or less intense images.

A high ambient light level can affect image perception in two ways. First, it implies the presence of bright surfaces in the observer's field of view, and these tend to compete with the image brightness and to lessen the observer's dark adaptation. Secondly, any ambient light which is able to reach the viewing end face of the bundle will be partly reflected and scattered by it, thereby illuminating the shadow areas and diluting the image.

Extreme cases of "image washout" are shown in Figure 38 which was prepared by illuminating a fiberscope end face at various levels as the image was being photographed. The highest ambient light level shown corresponds to the case of direct sunlight falling on the fiberscope end face. The object field was moderately illuminated with photoflood lamps and the image was slightly attenuated in traversing the three-foot fiberscope. With longer fiberscopes or lower scene brightnesses, the washout effect would be even more objectionable.

Fortunately, most ordinary fiber bundle viewing conditions do not involve especially adverse ambient light levels. In cases where they do, the recommended remedy would be the use of an appropriate eye shield, such as a viewing hood or a molded rubber eyeguard or face-adapter.

3.1.8 Fused vs. Potted End Faces

Paragraph 3.1.2 discussed the desirability of a high area factor in order to provide maximum utilization of the fiber bundle cross section. It is apparent, from a comparison of Figures 1a and 1b, that a substantially higher area factor would be provided by a fiber bundle with fused end faces so that the interstitial areas would be minimal.

As mentioned earlier, manufacturing difficulties have thus far delayed the commercial availability of flexible fiber bundles with fused end faces. A particular difficulty is the brittleness of the transition zone just between the fused mass at the bundle end and the free fibers. However, various strain-relief methods are being perfected by at least one manufacturer, and fused-end fiberscopes should become available in the near future.

3.1.9 Exit Angle

The radiation patterns of Figures 9 and 10 demonstrate that some distortion occurs in the geometry of the light rays which traverse a fiber. The cases illustrated are for straight fibers, the distortions being more severe and less symmetrical for curved ones. Moreover, these figures show the average effect of 100 fibers, and the results of individual fiber defects are not apparent.

As the eye views a fiber bundle image in which the individual fibers are resolvable, the effects of individual fiber defects become noticeable. Such defects are not fully understood, but they have the effect of deflecting the exit cones of light away from the fiber axes in a random way so that the image may appear mottled. The mottling is especially noticeable at steeper viewing angles, and it also increases as the numerical aperture of the objective lens is decreased.

Figure 39 illustrates the increase in mottling which is observed as the objective lens diaphragm is "stopped down". Figure 40 shows the combined effects of both lens diaphragm and viewing angle. The left-hand column of figures shows the progression of mottling as seen on-axis with objective lens aperture ratios of f/1.5, f/2, and f/8. The 20° off-axis viewing situation, shown in the right-hand photographs, is much more sensitive to a narrowing of the incident cone; although aperture ratios of f/1.5 and f/2 do not pose a problem, a reduction to f/2.8 greatly limits the amount of light available at 20° and accentuates the differences among fibers.

As stated, the origin of the fiber differences is not known, but speculations as to their identities have included the internal fiber defects discussed earlier as well as possible end-face chips or fractures incurred during grinding and polishing, leading to prismatic surfaces which deflect the emergent light noticeably off axis. It is known that conventional glass polishing techniques do not produce as satisfactory a finish on potted fiber end faces as they do on glass. The reason is that the difference in the relative hardnesses of the fibers and of the material in which they are embedded exerts a disruptive influence upon the polishing mechanism, particularly with regard to relative removal-rates of the materials and the embedding of abrasive particles within the softer material.

3.1.10 Non-glass Fibers

The subject matter of this report is concerned with optical fibers made of the ordinary glass materials. Although many plastic and other glassy materials in fiber form are suitable for conducting radiation, conventional glass fibers constitute the bulk of modern, commercial fiber bundle materials.

The almost exclusive use of glass is a situation which has evolved after many years of patient investigation by the fiber manufacturers concerning the properties of other candidate materials. Several plastic materials have been studied and are suitable for certain short-length applications; however, (1) they do not have high enough refractive indexes to allow them to be clad with a material of a low index; (2) they do not offer as high a line-transmittance as many glasses; and (3) plastic fibers cannot be made with walls as smooth as can be provided by glass, it being recalled that wall defects have an adverse effect on the multiple internal reflection process. Several of the references authored by Potter describe the properties of plastic fibers used as scintillators in high-energy-radiation studies. A particularly applicable paper is Potter, R. J., *Absorption measurements on a plastic scintillator*, *Rev. Sci. Instr.* 32, 286-288 (March, 1961).

Fused quartz has also been considered for optical fiber use and it offers the advantage of a much broader spectral transmission band than those of most glasses. However, its low refractive index of 1.54 makes it difficult to find a suitable cladding material which is physically compatible with it, and it is therefore not recommended for use in applications requiring lengths greater than a few feet.

For special problems requiring the transmission of infrared radiation, a newly-investigated glasslike material has shown interesting properties. The material is arsenic trisulfide, which lends itself to fabrication in fiber form and has a high enough refractive index to be readily clad. Arsenic trisulfide fibers are described in References 30, 51, 75, and 109.

Other materials are discussed in Reference 105, including certain exotic glasses and standard crystalline materials but, as observed by the author, they have not lent themselves to successful fiber manufacture and their uses are limited to highly specialized applications.

3.1.11 Summary of Optical Properties

The data and comments offered in the foregoing paragraphs are intended as a general guide to the selection of a fiber bundle design for each specific application or as a guide to the evaluation of a given bundle design in terms of its optical performance. However, there is not always a precise answer to the question of whether a given bundle will or will not perform satisfactorily

in a given situation. For each fiber bundle, there is a realm of visual situations with which it can definitely cope, and another one with which it cannot. Between the two realms is a vast, nebulous one where the ability of the bundle to transmit useful visual information depends upon several factors external to the bundle itself such as the viewing conditions, the acuity and attitude of the observer, and subtle features of the scene being viewed.

Consequently, only general suggestions can be offered as to the performance capabilities of a given bundle or the choice of bundle design to meet a given situation.

With regard to image brightness versus length, it may be stated that fiberscopes in lengths up to about 25 feet would be useful in transmitting recognizable images of non-self-luminous objects which would ordinarily be visible upon direct observation. As shown in Figure 19, the transmittance of such fiberscopes is about 15% in the yellow-green region (or approximately that of a pair of ordinary sunglasses), and the corresponding brightness reduction is in many cases well within the capability of the eye to accommodate with little loss of visual acuity. (It should be noted that the approximately logarithmic response of the eye to brightness changes is responsible for the fact that a surface with only a twenty percent reflectance appears to be mid-grey, or about half way between white and black. See Ref. 130.) Obviously, if the object scene is brightly illuminated, or if the demand upon visual recognition is not as high, much greater fiberscope lengths may be used. Experiments here have shown that under good viewing conditions and with a large field of view available, the eye can recognize room objects as viewed casually through a neutral density filter transmitting only three percent. If the eye is shielded from room light, that figure may be reduced to about one percent. Moreover, a self-luminous object such as a candle flame is clearly recognizable when seen through a filter transmitting 0.1% under room light conditions or as low as 0.01% when the eye is shielded.

The latter statement has a bearing upon the upper length limit on fiberscopes and light pipes used for flame recognition. As shown in Figure 19, a 100-foot fiber bundle made under current techniques is predicted to transmit a substantial fraction of a percent in the yellow-green region. Again, the logarithmic response of the eye should make it highly possible to recognize a yellow diffusion flame through such lengths, especially under favorable viewing conditions.

With regard to light pipes only, their recommended use is confined to applications requiring the recognition of yellow flickering flames in darkened or moderately lighted compartments, where their characteristic scintillating, scrambled patterns offer a high degree of conviction that a flame is being observed. Moreover, light pipes may be used in great lengths for such purposes, up to 100 feet or so, and in cases where (1) it is possible to afford a high degree of eyepiece magnification and where (2) a high degree of back-

ground light is not present, appreciable flame recognition is afforded by only a very few fibers. Experiments conducted here on the perceptibility of scrambled flame images transmitted by 20 or 30 two-mil fibers have been very encouraging regarding the possible use of very narrow light pipes for flame verification. It is very inviting to contemplate the use of a flame-detection light pipe housed in a protective jacket of only 0.100" O. D. and appearing no larger than an electrical lead wire, as were the ones which we tested.

It should also be possible for light pipes to transmit images of fairly bright incandescent surfaces in lengths up to 25 feet where the detection of extreme overheat conditions is necessary.

As a tentative guide to the optical performance capabilities of fiber bundles in various configurations, we offer the following table which correlates fiber bundle configurations with typical object scenes for which they might be used.

<u>FIBER BUNDLE CONFIGURATION</u>	<u>IMAGE TO BE TRANSMITTED</u>
Monofilament or multifiber scope transmitting 1 million to 100,000 image points, in lengths to 25 feet.	Highly detailed image of engine parts or ordinary scenes requiring high degree of recognition similar to direct view.
Same, in lengths to 50 feet.	Same, but requiring less recognition of fine detail or involving brightly illuminated scene.
Same, in lengths to 100 feet	Same, but involving recognition of self-luminous objects, such as flames.
Same, but transmitting only 100,000 to 10,000 image points.	Same as above sequence but requiring recognition of coarse detail only, such as flames, incandescent surfaces, smoke clouds arising from oil leaks, etc.
Monofilament light pipes, 10,000 to 1,000 fibers, in lengths to 50 feet.	Yellow-flame or very hot surface recognition in compartments with moderate background lighting, requiring broad angular coverage.
Same, in lengths to 100 feet.	Large, violent flames in darkened compartments, with good viewing conditions.

Same, but 1,000 to 10 fibers	Same, but with less angular coverage required.
Same as above sequences but with color-correcting filters.	Same as above, but where color-compensation is necessary, with the sacrifice of image brightness.

Table 5. Typical applications of various fiber bundle configurations.

The above correlations were estimated on the basis of monofilaments or multifibers in two to three mil diameters and assume moderate eyepiece magnification (5 to 10X; see Paragraph 4.1.1) and average viewing conditions with regard to cockpit lighting and viewing arrangement. They assume fiber transmittances as afforded by current manufacturing techniques and that the fiber bundles are formed in continuous lengths or with a very few optical couplings (see Paragraph 4.4). Variations in any of the above conditions will alter the applications appropriately.

3.2 Mechanical Properties

A question of great importance to the possible aerospace use of glass fibers concerns their ability to survive in adverse mechanical environments. One does not ordinarily think of glass as being a durable material under extremes of shock or vibration; however, if one examines the physical texture of a skein of two mil glass fibers, for example, he will find them to be extremely soft and flexible, suggesting a very good possibility of sufficient compliance under mechanical stress as to be quite durable.

Supplementing the tests on individual fibers described in Paragraph 2.2, we have performed mechanical tests on fiber bundles in order to determine the severity of the environments which they might withstand in appropriate jacketing materials. The tests were concerned primarily with the possible effects of vibration, for this is regarded as the greatest single threat to fiber integrity once the bundle is installed. There was reduced emphasis on testing of jacketed fibers for resistance to compression, impact, and flexural influences, for it is felt that these are suffered largely during installation and can be held to a minimum with normal care.

The most important finding of these tests was that suitably jacketed fibers in the diameter range of one to two mils are extremely durable with regard to the applicable portions of vibration evaluations specified in MIL-E-5272C and FAA TSO C11C and to more extreme vibration tests designed here in attempts to test the fibers to destruction. With the exception of a single occurrence involving a sample with a possible inclusion of a metallic fragment, all samples survived all vibration tests with only minor fiber damage;

more generally, the testing was halted when the jacketing material itself ruptured, which generally occurred at a supporting fixture as might be expected.

In general, it was found that fibers laid loosely in Teflon-lined braided shielding conduit or in stainless steel or aluminum tubing enjoyed ample protection, and more so when further protected with vinyl "spaghetti" before mounting within the jackets.

3.2.1 Tensile Strength

As a corollary to the tensile strength measurements on single fibers, similar tests were performed on unjacketed bundles of fibers. For this purpose, groups of loose fibers were assembled into bundles with their ends potted into brass collars with epoxy resin. The bundles were suspended vertically by the upper collar, with tension being applied manually to the lower one and being measured by an appropriate scale.

Although it was expected that a bundle of fibers could withstand a greater tensile force than a single fiber, preliminary tests showed that, in lengths up to twelve inches at least, such was not the case. It was soon apparent that minor variations in fiber length between the potted ends resulted in most of the tensile force being sustained by very few fibers at a time, causing the fibers to rupture gradually in a succession of small groups.

It was then expected that fibers greater than several feet in length would show sufficient elasticity to absorb the effects of small length variations without breakage. Assuming an elastic modulus of 9.8×10^8 , it was calculated that a six-foot fiber with a tensile strength of only 50,000 psi should be able to stretch by as much as 0.368" when subjected to its breaking load, allowing the possibility that minor length variations would be "smoothed out" in bundles of greater lengths.

A test was then conducted on a six-foot long bundle containing 569 two-mil fibers, as determined by a count of a photographic enlargement.

When the tensile force reached 25 pounds, rupture of the fibers began to occur at various points as indicated by the onset of a gradual and continuing increase in the bundle length. The break did not occur abruptly at any one point along the bundle; the slowness of the stretching was most likely due to cohesive forces between fiber surfaces which added some support to the lower end even though many fibers had broken. The lengthening of the bundle continued until the lower end reached the floor, whereupon the test was halted even though the rupture was not complete.

It is difficult to evaluate the results of the above test, for it is not known whether all fibers in the bundle broke at once or whether the rupture was gradual and progressive after the shortest ones broke; it is the latter case which we suspect. However, assuming the former situation to be the case, calculation shows that a 25 lb. breaking force on 569 two-mil fibers corresponds to a tensile strength of 0.0439 lb/fiber or 13,980 psi. It will be recalled that tests on individual two-mil fibers indicated tensile strengths of 88,100 psi (see Table 1, Paragraph 2.2.1) of which the above value constitutes only about 19%. This contradiction can be resolved if one were to assume, reasonably, that at the onset of fiber rupture only about 19% of the fibers were supporting the 25 lb. load and that when these broke, further deterioration was rapid and progressive.

The conclusion is that even a six-foot bundle does not afford enough "stretch" to level out the non-uniformities in fiber length, although it is a considerable improvement over the twelve-inch bundles which were effectively no stronger than a single fiber.

It is fully expected that any tensile strength limitations on bare fiber bundles will not be a problem in aerospace applications. The tensile strengths of the recommended jacketing materials will allow sufficient protection to the fibers during ordinary handling. In the case of jacketed fibers supported at their ends only and subjected to severe axial accelerating forces, it was pointed out earlier that typical fibers can support themselves in lengths of many thousands of feet under axial forces corresponding to several g's.

3.2.2 Vibration Resistance

Vibration evaluations were performed here on fiber bundles in various jacketing configurations, using Ling Sine-O-Matic equipment (Model CP5/6 with a 1500 pound force output and with an A175 Shaker rated at 68 g's at 4000 cps for the bare table). The test criteria were the relative number of fibers surviving each test, as indicated by a visual inspection or by actual count of a photographic enlargement of the end face, with the other end face being uniformly illuminated.

The first tests were performed on $\frac{1}{4}$ -inch diameter bundles in two types of $\frac{9}{16}$ " diameter braided conduit, one being "Dash 8" Titeflex lined with a Teflon sleeve, the other being S-143 Braided Shielding Conduit with a metallic bellows interior surface. The two-mil fibers were laid loosely within these containers, with the ends potted in place and ground and polished to allow visual inspection of the number of intact fibers at the beginning and end of each test.

The jacketed bundles were 59" long, each containing several thousand fibers. A 17" span in the center of each bundle was subjected to vibration, the ends of the span being clamped to the shaker table. The extreme ends of each

bundle were variously grounded to the shaker frame, suspended from overhead supports, or clamped to the shaker table.

The equipment and a test arrangement are depicted in Figure 41. In this case, the bundle ends are seen to be supported from overhead.

Vibration was conducted in two transverse planes for one set of tests and confined to one plane thereafter because of the rotational symmetry of the bundles. The testing schedule was based largely on Vibration Procedures II and XII of MIL-E-5272C, with the exception that the tests were conducted at room temperature only and that vibration was confined to one plane after the first series. The tests included extended exposures to vibration at the resonant frequency using 0.060" displacements.

The results of these tests appear in Table 6, the fiber survival data being based upon visual estimates.

VIBRATION TEST & REMARKS	PERCENTAGE OF FIBERS SURVIVING	
	In -8 Titeflex Teflon Braided Conduit	In S-143 Braided Shielding Conduit
1. Resonant search, 5 to 500 cps 0.036" D.A. or 10G, bundle ends suspended from ceiling supports	100%	100%
2. Cycling, 15 to 500 to 15 cps in 9.55 min., 4 cycles, 0.036" D.A. or 10G	100% (Ends tied to frame)	100% (Ends suspended)
3. Cycling, 5 to 15 to 5 cps in 5.45 min., 4 cycles, 0.08" D.A.	100% (Ends tied to frame)	100% (Ends suspended)
4. Endurance, 30 min., at resonance, 0.036" D.A., ends suspended in test 4 through 10	100%	100%
5. Repeat 2 cycling six times	100%	100%
6. Repeat 3 cycling six times	100%	100%

(Next four tests conducted in other transverse plane)

(continued)

7. Repeat 1	100%	not tested
8. Repeat 2 cycling ten times	100%	not tested
9. Repeat 3 cycling ten times	100%	not tested
10. Repeat 4	100%	not tested
11. Ends clamped to table frame, repeat all tests above but in one plane only	100%	not tested
12. Repeat 11 but with ends clamped to shaker table	100%	not tested
13. Four hours at resonance, 0.060" D.A. (20G)	100%	approximately 30%
14. Repeat 13	not tested	approximately 10%
15. Repeat 14	not tested	approximately 1%

Table 6. Vibration test results on two fiber bundles.

The results shown in the second column apply to a possible "freak" bundle mentioned earlier which may have contained a metallic fragment which severed the glass fibers under prolonged vibration. A subsequent dissection and examination of this bundle showed that all fibers ruptured near the center of the test span where the amplitude of vibration was at its maximum. A gray, metallic dust accumulation was evident in this area.

The encouraging results with Teflon-lined conduit, indicated in the first column above, suggested a further examination of the effects of bellows-lined conduit on glass fibers under vibration. Accordingly, an identical bundle was prepared and subjected to similar vibration tests, with the unexpected result that no fiber deterioration was noticeable visually. The tests were continued in an effort to establish the degree of vibration exposure which this sample would endure. The significant tests conducted were:

MIL-E-5272C, Procedure II (4 hours at resonance, 20G),
repeated for a total of 20 hours.

FAA TSO C11C, four 15-minute cycles, 5-1000-5 cps, 10G, and one hour at resonance at 10G, the resonant frequency varying between 41 and 49 cps throughout the tests.

At the end of these tests, a visual inspection revealed no noticeable damage to the fibers. A more sensitive photographic comparison method was invoked, involving the superposition of a negative of the bundle end face before testing upon a positive photograph of the same end face after testing. This subtractive process results in an optical cancellation of all fibers which were intact at the beginning and end of the test but clearly highlights any individual fibers which were destroyed. The photographic test result showed that less than a few dozen of the original several thousand fibers were severed.

The same photographic comparison process was applied to the Teflon-lined sample referred to in Table 6 and revealed no broken fibers. A second Teflon-lined sample was then prepared, similar to the first, and was subjected to four hours of resonant vibration at 20 g's, followed by four 15-minute cycles from 5 to 1000 to 5 cps at 0.036" double amplitude or 10 g's and finally one hour of resonant vibration at 10 g's. Again, no fiber damage was observed under a visual check.

The same vibration test schedule was then applied to a third sample of fibers jacketed in the S-143 bellows-lined Titeflex, and again no damage was noted visually.

Another sample of the same dimensions but in a rigid stainless steel tube was then tested. The tubing selected was Type 304, 1/8 hard, with a 3/8" O.D. and a 0.020" wall thickness. The same tests as above were applied, with no evidence of fiber damage at the end of the tests.

All samples tested to this point had been composed of 2-mil fibers. Two new samples were then prepared using, respectively, 1 mil and 8-mil fibers in "Dash 8" Teflon-lined Titeflex. Each sample was cycled for 2½ hours from 5 to 500 to 5 cps at 0.036" D.A. or 10 g's; this was followed by ½ hour at resonance at 10 g's and four hours at 20 g's. Finally, each sample was subjected to four 15-minute cycles from 5 to 1000 to 5 cps at 0.036" D.A. or 10 g's and a one hour resonant frequency vibration at 10 g's. At the end of all tests, no fiber damage was evident.

It is pointed out that in the latter tests, the photomicrographic comparison method used earlier was not applied. It was felt that the possible loss of a very small percentage of fibers would be trivial and would not affect the function of the bundle, and the visual check was therefore adopted as the more valid and less time-consuming criterion.

In the early stages of planning these tests, it had been expected that substantial damage might occur to fibers laid loosely within jackets and subjected to severe vibration, especially in the case of the eight-mil fibers. Therefore, plans had been made to conduct subsequent tests on samples filled with viscous damping agents, including silicone oils and various gels, in order to lessen the destructive effects of vibration. When the tests on loose fibers revealed no observable damage, there was felt to be no need for tests using damping agents and these were subsequently canceled.

During the period over which these tests were being performed, considerable thought was being given to the question of a bundle jacketing configuration to be recommended ultimately for general aerospace use. The test results continued to verify that the choice of a loose fiber bundle mounted within braided conduit and potted at the ends would be a logical one. However, other developments during the general effort suggested that a somewhat different design might have merit with regard to other considerations, and the question of the mechanical durability of the new design was raised.

Briefly, the new jacketing design achieved certain simplifications and economies in the assembly process and also provided a reliable means of incorporating an electrical lead wire within the bundle in cases where a test light would be necessary at the far end. (A fuller explanation is given in Section 5 describing an experimental breadboard which incorporates the new design.)

The suggested modification involved the inserting of the fibers into a sleeve of vinyl "spaghetti" before installing them in the protective jacket. In cases where an electrical lead was to be required, the vinyl-clad bundle would be further covered with wire braiding before insertion into the jacket.

The question was raised as to whether the "tighter" configuration of the pre-wrapped fibers might introduce problems during vibration, by contrast with the "fluffy" configuration of the loose fibers. It was believed that the clad bundle would vibrate as a unit within the protective jacket and that if it showed any elasticity under lateral displacement, it would have a resonant frequency which would most likely differ from that of a typical span of the jacket around it.

A single sample was prepared for vibration testing in order to provide at least preliminary information on its behavior. The fiber bundle was $\frac{1}{4}$ " in diameter and 18" long, containing two-mil fibers. In order not to favor the test outcome, and also to provide information on another jacketing material, rigid aluminum tubing was selected as the protective cover. The vinyl-clad bundle was inserted into a $\frac{1}{2}$ -inch O.D. aluminum tube with an approximately 0.030" wall thickness and the ends were fixed in place with epoxy resin. The sample ends were clamped rigidly to the shaker table.

Testing of this sample was conducted according to the vibration requirements of Procedure XII, MIL-E-5272C (2.5 hours of cycling and 0.5 hour of resonant vibration); Procedure II, MIL-E-5272C (4 hours of resonant vibration at 20 g's); and Paragraph 7.3 of FAA TSO C11C (one hour of cycling at 10 g's between 5 and 1000 cps and one hour of resonance at 10 g's). During the testing, structural fatigue of the aluminum tubing was evidenced by changes in the resonant frequency of the unsupported span until the frequency leveled off at 320 cps during the third test. There was no evidence of damage either to the fibers or to the aluminum jacket.

The applied accelerating force was then increased to 30 g's at the resonant frequency. After five minutes of exposure, the resonant frequency was observed to drop sharply whereupon the unit was removed from the fixture and examined. Fractures were observed around the circumference of both ends of the tubing where they protruded from the mounting fixture bushings. A pair of longer bushings was then fabricated and installed in order to support the fracture zones, and the testing was resumed. The new resonant frequency was observed to be 575 cps but dropped off sharply after several minutes and finally became erratic so that the testing was discontinued.

To this point, the ends of the unit had been secured rigidly to the shaker table with a U-clamp arrangement. A new mounting configuration was then proposed, using Adel mounting clamps (No. 432SS8-8) with synthetic rubber cushions. The fiber bundle was then inserted into a new aluminum tube and vibrated at resonance (185 cps) at 20 g's. After ten hours, no visible deterioration had occurred to either the fibers or the tubing. The applied acceleration was then increased to 35 g's and the sample was resonated for approximately six hours. No damage to the unit was yet in evidence and the test was halted. One of the Adel clamps was observed to have fractured along the base, near the mounting hole.

A final vibration test was concerned with a different bundle configuration. Optical tests being conducted concurrently had indicated that extremely narrow light pipes containing only a few dozen two-mil fibers might be highly useful in certain flame detection applications while offering substantial savings in size and weight. Consequently, an 18" long group of such fibers contained in vinyl spaghetti was mounted in a 0.100" O.D. inconel tube and subjected to eight hours of vibration at 0.060" double amplitude or 20 g's of applied acceleration. The resonant amplitude (D.A.) at the center of the test sample was observed to vary from 3/4" to just over 1" during the test. At the end of the test, the end of the inconel tubing secured by the mounting clamp had broken off completely. However, a photomicrographic examination of the bundle end face showed that of the original 26 fibers in the bundle, 25 were intact.

The evidence afforded by the vibration tests points strongly to a good possibility of fiber survival under many aerospace conditions; as mentioned earlier, the question of the suitability of tiny glass fibers for severe mechanical en-

vironments was a serious one which, to our knowledge, had not previously been answered. It was therefore gratifying to witness what we consider to be a favorable test outcome.

3.2.3 Other Mechanical Tests

Several tests were originally proposed under this heading, all but one having been finally ruled out for reasons that they were not applicable to aerospace mechanical environments or would offer information of limited value. For example, impact resistance tests on various jacketed bundle configurations would largely duplicate the effects of sustained resonant vibration, both being a matter of exposure to lateral accelerating forces; indeed, the forces applied during the vibration tests described above were deemed to be more severe than those required by many shock test specifications, and so such tests were held to be redundant. Similarly, torque resistance tests had been planned until it became clear that the jacketing materials of greatest interest (braided conduit and rigid stainless steel or aluminum tubing) were highly "twistproof" from the standpoint of ordinary handling and would transmit little torsional stress to the bundle within. Moreover, if torque were to be transmitted to a fiber bundle itself, it would result largely in stretching forces on the individual fibers, but since these are generally loaded into their containers with appreciable, intentional slack, there is a considerable margin of safety with regard to the accidental torquing of a fiber bundle assembly.

It was also originally proposed to study the minimum allowable bend radius for various jacketed configurations. It was then realized that there is a favorable disparity between the amount of bending which a bare fiber bundle can survive and the minimum radius of curvature which might be effected manually upon the recommended jacketing materials, and so such testing was deemed unnecessary.

It should be pointed out that the mechanical severities to which a fiber bundle might be subjected in aerospace use can fall into two classes. The first class concerns the normal environmental hazards during vehicle operation, involving largely the possibility of severe axial accelerational forces and adverse vibrational influences. Our tests have indicated that the inherent tensile strength of fibers renders them suitable for high axial thrusts in great unsupported lengths, and that the vibration levels suggested in military and civil aircraft specifications pose little problem. The second class of hazards concerns possible mechanical abuse during handling, installation, and maintenance, and this could be by far the greatest threat to the physical survival of a fiber bundle. We therefore stress the fact that a jacketed fiber bundle can definitely be damaged by being dropped or stepped upon, being bent unduly, being hammered upon or sawed into, or being subjected to other abuses as a result of carelessness. With normal care, a fiber bundle should

provide extremely satisfactory service; it need not be "coddled", but the attitude that it is more fragile than most aircraft cables and conduits would be quite helpful in prolonging its usefulness.

The single test series conducted under this heading involved the compression resistance of $\frac{1}{4}$ " diameter by 12" long fiber bundles in "Dash 8" (Teflon-lined) and S-143 (bellows-lined) Titeflex. Fibers were tested in one, two, and eight mil diameters. During testing, each sample was placed on an aluminum block on the middle plate of a Dillon dynamometer. A smaller, second plate was placed upon the sample bearing on a four-inch length of it; the sharp, lower edges at the ends of this plate were rounded off to a $\frac{1}{4}$ " radius in order to eliminate possible shearing forces under pressure. As pressure was applied, the condition of the fibers was monitored visually with the aid of a light source placed at one end. The test results are presented in Table 7:

<u>Test Sample</u>	<u>Maximum Compressional Force (lbs.)</u>	<u>Sample Condition After Compression</u>
1 mil fibers, -8 Titeflex	9000	Partial deterioration
1 mil fibers, S-143 Titeflex	9000	" "
2 mil fibers, -8 Titeflex	9000	Complete deterioration
2 mil fibers, S-143 Titeflex	9000	" "
8 mil fibers, -8 Titeflex	1100	" "
8 mil fibers, S-143 Titeflex	3000	" "

Table 7. Compressional test results on various jacketed configurations.

The length of the four-inch pressure plate was selected in order to duplicate the effects of the pressure applied when a bundle assembly lying on a hard surface was accidentally stepped upon. The test results indicate that ordinary compressional forces applied by the human foot should pose no problem. This is not to imply, however, that unsupported spans of the material can withstand human weights, for under such conditions undue tensile forces would be exerted which could stretch the jacketing sufficiently to snap the fibers.

It is believed that a substantial influence upon compression resistance is exerted by the tightness of fiber packing within the outer jacket. This belief is extrapolated from the knowledge that the minimum bend radius of a jacketed bundle is affected by the degree of packing. If a constrained bundle of fibers is subjected to bending forces, the outer fibers tend to stretch whereas compressional forces are applied to the inner ones. The low ductility and compressibility of glass do not permit appreciable compliance and the fibers tend, instead, to ribbon out into a flat band. They are permitted to do this only if there is sufficient space within the confines of the constraining surface; otherwise, the outer ones will be subjected to tensile forces beyond

their capacity, while the inner ones will be compressed until they yield by sharp, localized bending which fractures them. We suspect that a loose packing affords sufficient freedom for the fibers to slip laterally during compression of the jacket as to afford a greater compression resistance than in the case of a fully packed jacket, although tests were not performed to bear this out.

3.3 Thermal Properties

The thermal properties of glass fibers themselves have been described in Paragraph 2.3. The present discussion is concerned with all other factors pertinent to a fiber bundle assembly which would limit its use in high temperature environments.

Because the fibers themselves, as currently made, are not recommended for continuous exposures above 1000°F, we shall be concerned only with the abilities of the various fabrication materials to survive this temperature. In particular, we are concerned with the pickup end of the bundle only, assuming that this end may frequently be situated in a high temperature zone but that the remainder of the bundle and the readout module would be located in cooler regions. Thus, for high temperature use, we visualize a conventional fiber optic system with a special, high temperature section comprising the pickup end and being coupled to the main system. Alternatively, the entire bundle length can be designed for high temperature use, although this may impose certain restrictions on the choice of materials.

Regarding the choice of jacketing materials, those considered for normal temperature operation have included rigid stainless steel or aluminum tubes and various aircraft-type hoses with plastic or metallic interior surfaces. For high temperature use, the choice would be limited to the stainless steel tubing and to aircraft hoses of an all-metal construction.

Conventional test lights in the pickup head would not be usable at 1000°F and this feature would have to be forsaken.

The use of cemented objective lenses would not be possible at 1000°F and it is questionable whether even a simple "singlet" lens used as the objective would hold its shape at this temperature. The solution to this problem might be provided by use of an objective lens made of quartz or other high temperature optical material.

The principal problem in the suitability of fiber bundles for high temperature use has been the limitations imposed by the materials customarily used to cement the fiber ends together prior to grinding and polishing. Such materials were selected on the basis of their properties at room temperature, there never having been a need for high temperature binding agents.

A study was therefore conducted here in a search for potting materials with high temperature stability in addition to other requirements listed below:

- (1) Chemical and thermal stability over the temperature range from -100° F to 1000° F;
- (2) Compatibility with glass working techniques used in the preparation of optically-finished surfaces;
- (3) Thermal expansion properties intermediate to those of glass and metal;
- (4) Good "wetting" properties with regard to both glass and metal.

The investigation was conducted according to the following outline:

- (1) Materials were chosen from three groups of adhesive compounds; solders that contain indium (referred to as "glass solders"), materials referred to as "high temperature plastics", and cements intended for high temperature applications (examples are the ceramic cements and aluminum phosphide cements).
- (2) Of the materials chosen, each was tested to determine if it showed any chemical action upon lead glass at any temperature above ambient up to 1000° F. Failure was indicated by a change in color or shape of the glass fibers.
- (3) Each material was formed into suitable samples using glass fibers, cured at about 600° F, and ground and polished on standard metallographic equipment to determine if it had properties suitable for producing an optical surface usable in a fiber bundle.
- (4) Each material was tested to determine if it would wet both glass and metal and adhere to these materials after curing. Brass collars of about $\frac{1}{4}$ " I. D. were prepared and used to contain each test bundle of fibers. A test was considered negative if, after curing, any air spaces existed between the collars and the bundle, or between the fibers. This test also established the wetting power of the sample material; the material was considered to have failed if all voids were not filled.
- (5) If a material passed tests 3 and 4, we concluded that there was no problem with regard to thermal expansion differences.

At the end of a preliminary investigation, most of the materials initially chosen had been eliminated. Categorically, the reasons were as follows:

- (1) The indium solders had two main shortcomings. First, they would not flow around the fibers so that wetting was very difficult and, more important, their melting points were very low.
- (2) Of the cements, three ceramic cements and three aluminum phosphide cements were investigated. All of these materials showed two common faults and were therefore abandoned. They were coarse, gritty materials, not able to wet either the glass fibers or the metal rings and they all attacked the glass chemically.

Attention was then focused on the high temperature plastics, with encouraging results. The manufacturer's data on the first material tested is as follows:

Curing time: 6 hours at 600°F
Maximum service temperature: 1200°F
Continuous service temperature: 600°F

This material, when cured according to the manufacturer's directions, proved to be the best material tested. All of the requirements for a potting material as described in the test were met.

The next group of materials tested had the following characteristics:

Curing time: 6 hours at 600°F
Maximum service temperature: 1000°F
Continuous service temperature: 600°F

These materials cure hard enough to polish to a good optical surface. The materials passed all other tests as well and can be considered satisfactory for high temperature potting compounds.

In most of the high temperature tests, a discoloration of the potting materials was observed, but this had little adverse effect on the light transmission of the test sample.

SECTION 4. FIBER OPTIC DETECTION SYSTEMS

In this section we consider the fiber optic detection system as a complete entity, starting with the objective lens, ending with the magnifying eyepiece, and including radiation detection devices, image tubes, optical couplings, and other aids to the application of the basic fiber bundle to the hazard detection problem.

4.1 Terminal Optics

This term applies to the objective lens which forms the initial image on the receiving end of the fiber bundle and to the magnifying lens which is generally used in order to present a larger apparent image at the viewing end. Certain features of both are of interest to fiber optics applications and are reviewed in the following paragraphs as a possible aid to the system designer in making an appropriate selection for a given application.

4.1.1 Objective Lenses

Two quantities are of primary interest in the selection of the objective lens which is to image an object field onto the receiving face of a fiber bundle.

The more important quantity is the focal length of the lens with respect to the bundle end face dimensions, for this ratio determines whether a large part of the scene will be included at relatively low magnification or a small part at higher magnification. The wide-field or wide-angle case is associated with a shorter focal length lens than is the narrow-field or telephoto case. For a fiber bundle end face of given size, the magnification and angular field width are complementary quantities and a compromise must be chosen depending upon the needs of a given viewing situation. Figure 42 shows the effect of a progressive increase in objective lens focal length, wherein it is apparent that the wide-field case presents a more complete image of the scene but with less magnification of detail.

The other quantity of interest in the selection of a lens is the maximum aperture compared with its focal length -- that is, the "lens speed" which ordinarily determines the brightness of an image formed upon a photographic film. This is the lens diameter expressed units of the lens focal length; for example, the diameter of a 10mm diameter lens with a 20mm focal length might be expressed as a "focal length divided by 2" or simply "f/2". Thus, another name for lens speed is focal ratio and the purpose of this quantity is to provide a basis for the comparison of image brightness produced by various photographic lenses of various diameters and focal lengths; that is, an f/2 lens of 25mm focal length will produce a larger image than an f/2, 13mm lens, but one of the same brightness.

It is important to note that a lens with a high focal ratio, such as f/1.5, produces a broader convergent cone of light on the receiving surface than does, say, an f/3.5 lens. This means more total light reaching the surface which, if it happens to be a diffusely reflecting surface, will appear brighter to the eye. However, because there is no diffusion ordinarily involved in the transmission of light through a glass fiber, a large focal ratio, or "fast" lens, has a different meaning here. It simply means that the image-forming light will be transmitted through the fiber as a family of steeper rays than with a "slower" lens and will leave the other end with a broader angular spread; the reason is that the angular characteristics of the light rays entering a fiber are approximately preserved as the light travels through the fiber -- the more so if the fiber core is smooth-walled and straight. Thus, a faster lens will not produce a brighter image through a fiber bundle, but merely one which can be seen over a wider angle at the viewing end.

The selection of objective lens speed, then, is determined by the desired angular spread of the emergent light. This, in turn, is generally determined by the focal ratio of the magnifying eyepiece. Provided that the emergent cone is broad enough to fill the eyepiece with light, it generally does not pay to use a faster objective lens than is necessary to produce such a cone although some extra cone width can be helpful in allowing for some shift in the direction of the emergent cone as a result of any bends in the fiber bundle. If the objective lens speed is too "slow" and the eyepiece is not filled with light, then at extreme viewing angles the fiber end face may be seen through the magnifier but no image will appear on it. (For example, See Figure 40)

Returning to the subject of focal length selection, the fiber optic system designer must first consider the physical dimensions of the bundle end face with which he is dealing and must then decide upon the angular width of the object field to be included in the image. Simple geometrical considerations will then indicate the appropriate focal length for the objective lens. For example, a reasonable end face or "frame" size in many fiberscope applications is 5 x 5mm, corresponding very closely to the 4 x 5mm frame size of an 8mm motion picture film. The usual 8mm movie camera lens has a focal length of 13mm, providing an angular coverage of 2 ($\arctan 2.5/13$) or 22° in the horizontal plane. Other focal lengths are available in such lenses -- the most common being from 5 to 9mm for wide angle use and 25mm or greater for telephoto use. For a 5 x 5mm fiberscope, it is thus convenient to use any of the standard 8mm movie camera lenses as the objective lens and to employ the same angular field terminology regarding wide-angle or telephoto images. Indeed, custom-fabricated fiberscopes in the 5 x 5mm size range are often specified with an end fitting designed to receive the threads of an 8mm movie camera lens and to provide an in-focus image on the end face when the lens is tightened into position. Such threads have been standardized by most manufacturers and are referred to as "D" mount threads. Similarly, the accepted thread standard for 16mm movie camera lenses is described as the "C" mount. (Copies of "C" mount and "D" mount thread specifications are available at 25 cents each from

the American Standards Association, Incorporated, 10 East 40th Street, New York 16, New York. The specification is No. PH22.76-1960 and is entitled "Threaded Lens Mounts for 16mm and 8mm Motion-Picture Cameras".)

Another typical fiberscope frame size which may be convenient in many aerospace applications is 8 x 10mm, corresponding identically to the frame size of a 16mm motion picture film. For such fiberscopes it is especially convenient to specify "C" mount threads and to use any of the variety of 16mm movie camera lenses which are available commercially.

The angular width, θ , of the object field provided across any dimension, D, of a fiberscope end face by a lens of focal length, L, can be determined from the formula $\tan(1/2)\theta = (1/2)D/L$ or $\theta = 2(\arctan D/2L)$. Typical values for various frame sizes and focal lengths are presented in Table 8:

Standard "D" Mount Focal Lengths	Angular Field for 4 x 5mm Frame Size (Sides) (Diagonal)	
5mm (wide-angle)	47° x 53°	65°
9mm (wide-angle)	25° x 31°	39°
13mm (normal)	18° x 22°	28°
25mm (telephoto)	9° x 11°	15°
50mm (telephoto)	5° x 6°	7°
Standard "C" Mount Focal Lengths	Angular Field for 8 x 10mm Frame Size (Sides) (Diagonal)	
13mm (wide-angle)	34° x 42°	52°
25mm (normal)	18° x 22°	29°
50mm (telephoto)	9° x 11°	15°
100mm (telephoto)	5° x 6°	7°

Table 8. Angular field for various objective lens focal lengths and fiberscope end face dimensions.

A third quantity of interest in the selection of an objective lens is the lens quality. Lenses with a given focal length and diameter are available to provide a broad spectrum of image qualities, as evidenced by the price range which extends from a few pennies for a chipped, rejected singlet to more than one hundred dollars for a well-corrected compound lens. It is necessary to point out that the expensive, precision-made lenses have important uses in the preparation of high quality color motion picture films where the utmost in image quality and detail must be achieved although the higher priced lenses are also often associated with high numerical apertures for use under adverse lighting conditions. In fiberscope applications, the image sharpness provided by a high quality lens is often not needed for present-day fiberscopes do not provide the

resolution afforded by color-sensitive photographic films, and the difference between fiberscope images formed respectively by lenses of high and of moderate quality would be slight.

4.1.2 Magnifying Eyelenses

One ordinarily thinks of a magnifier as having the unusual property of making objects appear larger than they really are. This is not actually the case, for a magnifier is simply a lens or a lens combination which adds some refractive power to the eye lens of the observer and, therefore, lets him place his eye closer to the object and still see it clearly. The apparent increase in size results from the nearness of the observer's eye to the object; if he were especially nearsighted or had good visual accommodation, he could view an object a few inches from his eye without a magnifier and see it apparently magnified. It is important to realize that magnification does not make an object appear "larger than it really is", which, by itself, is meaningless but it makes it appear larger than it appears at ordinary viewing distances. Since this is a relative matter, a particular "ordinary viewing distance" has been adopted by scientists as an arbitrary reference value in order to place the phenomenon of magnification on a quantitative basis. This distance is ten inches and is the distance at which the average person might hold an object in order to scrutinize it closely and yet see it comfortably. The apparent size of an object at ten inches is, therefore, the reference value with which its apparent size is compared when it is at other distances. As an example, if an observer were to view an object five inches away, with or without a magnifier, its apparent linear dimensions would be doubled and, loosely speaking, one might say that the object was being viewed with a magnification of two.

The use of a positive or converging lens enables an observer to place his eye effectively much closer to an object than ordinarily. The stronger the lens (or the shorter its focal length), the closer the eye may be. The distance from the lens to the object is important and most people automatically hold the lens so that they can view the object most comfortably. When this is the case, it happens that the lens-to-object distance corresponds closely to the focal length of the lens. It also happens, then, that the diverging rays from the object are refracted by the lens in such a way that essentially parallel families of rays leave the lens and proceed to the eye. This is important because truly parallel rays ordinarily arise only from objects at great distances -- such as stars.

Parallel rays are of importance to an observer in two ways although the average observer is not ordinarily conscious of them. The first is that when parallel rays enter the eye from a distant object being viewed, the eye lens automatically relaxes, increasing its focal length and the viewing condition is physiologically more comfortable to the observer than when he is viewing a nearby object. The second effect is that truly parallel rays imply an object

essentially "at infinity" (such as a star) so that no matter how much closer to or farther from the object the observer tries to move, he cannot change its apparent size.

These phenomena are important to the matter of how an observer uses a magnifier to "enlarge" an object. The first effect ensures his (inadvertent) tendency to place the lens so that the emergent rays will be parallel. This affords the most comfortable viewing and places the object "optically at infinity". When this is the case, the object is at or very near to the focal point of the lens. Under these conditions, the apparent size of the object will be the same whether the observer's eye is far from the lens or practically touching it. (The only effect that distance will have will be to change the area of object which he can see through the lens; that is, one can see more of the object with his eye closer to the lens, but the magnification will be the same.)

Consequently, when an object is at the focus of a magnifier, the apparent size of the object will be exactly what it would be if the eye were at the optical center of the lens and no lens were present. Thus, a lens with a one inch focal length, when used as a magnifier, simply locates the eye (optically) one inch from the object, regardless of where it is physically. This produces an apparent object size of ten times the linear dimensions compared with its apparent size at ten inches. The magnification is thus said to be 10X which, it will be noted, is obtained simply by dividing ten inches by the focal length of the lens expressed in inches.

It is obvious that the shorter the focal length of the lens or lens combination, the greater will be the magnification. What then, we ask, prevents us from using the highest magnification possible? The answer is that there is another effect which occurs as the focal length of a lens is changed. This involves the size of what is called the exit pupil which is an imaginary disc in space within which the eye must be placed, at whatever its viewing distance, in order to see a given amount of the object. Everything else being equal, a lens affording higher magnification also provides a smaller exit pupil and places a greater burden on the observer in aligning his eye with the lens axis. These opposing effects, magnification, and exit pupil diameter, are a matter of common experience, as the reader will note. For example, when viewing an object at ten inches with no magnifier and with a magnification of unity, one has no exit pupil restriction and may position his head throughout a hemispherical space and still see the object. Conversely, in order to obtain the magnification afforded by high-powered microscope, one must align his eye quite accurately with the small ocular in the eyepiece.

As to the matter of what compromise one must reach in providing magnification for a given fiber bundle, only judgment and experience can determine this for it is based on the personal preference and circumstances of the user of the bundle. In the case of the fighter pilot or astronaut whose physical movements are relatively constrained and whose field of view must be shared by many

instruments simultaneously, a large exit pupil is often necessary, with its attendant low magnification, for the observer would have no opportunity to position his eye close to the magnifier. On the other hand, in the case of the aerospace vehicle with a crew of several men, one of these may be freely able to place his eye close to the lens and profit by the high magnification afforded by a shorter focal length and reduced exit pupil.

The luxury of high eyepiece magnification which is attained at the expense of exit pupil diameter is illustrated in Figure 43 which refers the reader to the following suggestions intended to provide him with an appreciation of the degree of compromise which is necessary:

EXPLANATORY NOTE, FIGURE 43

This figure depicts a typical image on a fiberscope end face as it might appear in actual size, as well as under various eyepiece magnifications. To observe the image sizes as they would appear to the eye, the reader should view the photographs at his "distance of most distinct vision" -- generally ten inches -- using one eye. However, he should also be aware of the corresponding viewing limitations imposed by the smaller lens diameters and other optical factors which accompany higher eyepiece magnifications.

In examining this figure, the reader can attain an appreciation of the more difficult head movement restrictions at higher magnifications if he will perform the following experiment. The thumb and forefinger should be bent to form a makeshift circular aperture which is placed exactly on the perpendicular axis of each photograph and about ten inches from the page. For viewing the 12X photo, the aperture should be no greater than about 1/2 inch in diameter; for the 6X and 3X enlargements, the corresponding aperture diameters should be about one inch and 1-1/2 inches respectively. (These values correspond to the use of an eyelens with an f/1.6 aperture.)

Note that in order to view the 12X photo fully, the reader must place his eye very close to the 1/2 inch aperture. With the other photos and larger aperture diameters, the eye can be moved more freely, both sideways and back from the aperture, without seriously restricting the view of the image. Note also that only one eye can be used at a time.

The topmost photo in the figure should be viewed without a limiting aperture for its size is intended to represent a typical end face as seen in actual size. Note that in this case, both

eyes may view the subject together and head movements are completely unrestricted. (In an actual fiberscope, the eye positions would be limited by the exit angle of the light rays leaving the fiber ends. See Paragraph 3.1.9.)

This experiment simulates the effect of using a simple magnifier with an f/1.6 aperture. Larger aperture eyepieces can be designed which, for the lower magnifications, would permit simultaneous viewing by both eyes but, in any case, a higher magnification eyepiece always implies less eye freedom.

The subject shown in Figure 43 is the image of a jet engine section formed on part of a high resolution fused fiber optics faceplate. Approximately one million fibers are represented in the photograph but are too small to be seen individually.

A further discussion of magnifying eyepieces appears in Section D.3 of the Appendix as related to their use with image tubes.

4.2 Radiation Detection

Where fiber bundle systems are to be used in the detection of aerospace fires or other self-luminous hazards, it is necessary that automatic warning systems be used with them to notify the pilot or appropriate crew-member as to when he should perform a visual check of the bundle image. It is highly desirable that such a warning system be able to discern between optical situations which imply hazardous occurrences and those which do not. A fundamental requirement is that the system subject the pilot to the least possible number of false alarms by discrimination against normal radiative phenomena such as sunlight.

The following paragraphs review the state-of-the-art in optical radiation detection as applied to flame and hot surface conditions. Specific detection techniques are recommended for use with optical fiber systems, including cases in which the detector monitors the remote compartment from the viewing end of the fiber bundle and cases of direct monitoring from within the compartment itself.

4.2.1 Determination of a Detection-mode Philosophy

The primary problem in the automatic radiation detection of flames and hot surfaces is one of discrimination. Modern photo- and thermal-detection systems offer sufficient sensitivity that the detection of a hazard is generally not a problem; rather, the problem is to render the system insensitive to radiative sources of a non-hazardous nature such as the various daylight sources originating in sunlight and various artificial light sources incidental to aerospace operations.

Modern scientific techniques offer several alternative methods of automatically recognizing certain distinguishing features of radiation from hazardous sources and discriminating against normal background radiation. The various methods differ in their adaptabilities to various operational and environmental requirements and the selection for a given situation must be made accordingly.

This discussion comprises a review of such techniques with particular attention to their possible use with fiber optic systems.

Function of Detection System

The function of a fiber optic hazard detection system in a manned flight vehicle should be to afford automatic detection and visual identification of various hazards in remote areas of the vehicle. The primary hazards of interest are those producing changes in visible radiation, such as fires and hot spots resulting from overheating. The identification function is performed by the pilot or other crew member by viewing the remote area through the fiber bundle. The detection function must be performed automatically. This is necessary in order that the remote area be continuously monitored for unusual light level conditions, it being the function of the detection device to notify the pilot of any such conditions. The pilot will then view the remote area through the light pipe and make a visual identification of the hazards involved.

The ideal detection device would warn the pilot of any abnormal radiation conditions caused by fire, overheat, or other hazard, and at the same time would reject all normal radiative phenomena, such as normally hot objects or sunlight, so that false warnings never occur. Such an ideal system is not presently possible, and even a human observer has difficulty in distinguishing certain situations, such as a match flame held up against the sun. However, it is possible to identify many fire conditions against most normal background radiation conditions.

Two types of radiation background that must be discriminated against are sunlight and hot objects. Methods of doing this will be discussed in detail later. Of the environmental conditions that must be taken into consideration in designing the radiation detection device, temperature is the only critical one. The other conditions, such as vibration, shock and humidity, can be accommodated with routine packaging methods. The temperature conditions are determined by the type of vehicle and by the particular location in which the detector is situated. These temperature conditions can greatly affect the choice of a radiation detector, for each presently available detector has its own upper temperature operating limit, all of them being below 600°F.

Types of Detectors

Optical radiation detectors fall into two main classes, notably, photodetectors and thermal-detectors. Photodetectors include the familiar photo-emissive, photoconductive, photovoltaic and photoelectromagnetic detectors and operate through the direct action of radiation upon valence electrons in the detector material. By contrast, thermal detectors operate as the result of becoming warmed by radiation, whereupon their molecular, or thermal, energy is transformed to electronic energy. Thermal detectors include thermocouples, metallic and semiconducting bolometers and a variety of other devices.

A major distinguishing feature between photo- and thermal-detectors is their respective types of spectral response. Each type of photodetector is sensitive only to a specific region of the wavelength spectrum, whereas a thermal detector will respond to energy of any wavelength which its surface can absorb. Another feature is that photodetectors offer a faster response and higher sensitivity in those spectral bands in which they are sensitive than do the thermal detectors in the same bands.

Methods of Fire Detection

There are many possible methods for detecting fires in flight vehicles. Excellent discussions of fire detection principles which can be utilized are given in References 132 and 134. In brief, methods of fire detection can be classified as either the direct contact type or the surveillance type. In the former type, the flame must come in direct contact with the detector in order for an alarm to occur. Such detectors usually alarm at a predetermined temperature level or

rise-rate, but the use of flame conductivity or flame rectification for fire detection has also been suggested. The various methods for accomplishing contact-type fire detection will not be discussed here, for they are felt to be unsuitable for use with fiber optics. The main reason for this is the complexity required when contact with the flame is required for alarm. One of the major advantages of a fiber optic system is that a rather large compartment can be monitored with very few detectors. This advantage would be nullified if a contact-type fire detector were used with fiber optics.

Surveillance can be defined as the act of watching. Thus, a surveillance fire detector can be described as a detector which will watch, or monitor, a large volume of space and which will alarm when a fire is present without its being in actual contact with the fire. Most surveillance detectors are sensitive to the radiant energy from a flame. The main exceptions are surveillance systems for smoke detection use and those using ultrasonic waves and the Doppler shift as a means of detecting fires in large spaces. The latter method will not be discussed here. Smoke detection will be discussed later, since in many situations this could be combined very advantageously with fiber optics.

The following paragraphs discuss the various methods of radiation detection, and state the advantages and disadvantages of detection in the various spectral regions. The several methods of discriminating against the normal radiation background will also be discussed.

The first spectral region which we consider is the infrared one beyond three microns. This region is suitable for the detection of moderately warm objects and of certain prominent spectral bands in premixed flames. Most of the detectors sensitive in this region can be classed as "exotic" types that require operation at very low temperatures in order to offer usable sensitivity. They are widely used in military applications which require either the utmost in sensitivity or a response to fairly low temperature surfaces. Because of their high cost and the complexity of the special cooling equipment required, they are not at this time recommended for use in aircraft fire detection devices. There is enough radiant energy available from fires in other spectral regions so that more conventional detectors can be used satisfactorily. In general the exotic type detectors have not been included in the present study. One detector which is sensitive in this region and does not require cooling is the indium antimonide PEM (photoelectromagnetic) detector. This unit is fairly insensitive and is rather costly, but it could be used where the detection of hot objects at relatively low temperatures is required. This could be necessary where a slight overheat condition must be detected at the earliest possible time.

Both diffusion and premixed flames radiate considerable energy in the near infrared region extending from 0.8 to 3 microns. There is less background radiation from sunlight in this region than in the visible spectrum, but there is more radiation from hot bodies than in the visible region. This situation

changes with the wavelength; at 3 microns, a surface at 250°F might be a problem, while at 0.8 microns, the surface would have to be at about 1000°F to emit sufficient background radiation to compete with the flame radiation. Of the many detectors sensitive in this region, lead sulfide is the one most commonly used, and the most sensitive. At the lower end of this region, silicon photovoltaic detectors, peaking at about 1 micron, can be used. As mentioned before, these would be less sensitive to background hot body radiation.

The visible region, extending from about 0.4 to 0.7 micron, is characterized by high intensity radiation from sunlight and from diffusion flames but much less so from hot bodies below 1000°F or from premixed flames. The detectors that are sensitive to light, both photoconductive and photovoltaic, tend to be relatively stable and very sensitive. The greatest problem in operating in the visible radiation region is that of discriminating against background energy, particularly from sunlight. Possible methods of discriminating against sunlight will be described later.

Fire detection in the region below 0.29 micron has intriguing advantages since there is negligible radiation in this region either from hot engine parts or from sunlight at altitudes to the ozone layer at about 90,000 feet. The only fundamental disadvantage of operating in this region is that the ultraviolet transmission is very greatly reduced by oil films on the detector window. The extreme sensitivity of many of the detectors in this region helps to overcome this. In addition, various automatic window cleaning techniques (see paragraph 4.5) may eliminate the problem. The practical limitation of operating in this region at present is the types of detectors available. These will be discussed in detail later, but they can be classed as a group as fragile, high voltage devices which are rather bulky in comparison to detectors sensitive in other regions. All of them have glass or glass-like envelopes. There is great need for a solid state detector which is sensitive in this region. Optical methods of smoke detection, while classified as surveillance detection, do not make use of self radiation but require, instead, the use of an auxiliary light source. The presence of smoke can be detected either by the increase in the optical scattering or by the decrease in the transmittance of the atmosphere. The adage "where there is smoke, there's fire" is not always true where aircraft smoke detectors are concerned. In addition to smoke, the aircraft smoke detector is subject to alarms from leaks in exhaust lines and from fog conditions. One of the main drawbacks of systems that have been used in aircraft is that they have been too sensitive. When combined with a fiber optic system, smoke detection could have many advantages on an aircraft. The final determination of whether hazardous conditions were present would be left to the crew member who was viewing the compartment through the fiber bundle. In some aircraft compartments excessive smoke could collect before a serious overheat or fire condition existed. With a combination of smoke detection and fiber optics, crew members would be warned of a potentially dangerous situation and could take early corrective action.

Discrimination Methods

In certain wavelengths bands of the spectrum, radiation from sunlight is filtered out by the atmosphere so that these bands contain virtually no solar energy at sea level. Detectors sensitive in these spectral regions are termed "solar-blind".

a. The Ultraviolet Solar-Blind Region

The first such region of interest here is the ultraviolet one below 0.29 micron. The ozone layer at ninety thousand feet above the earth absorbs practically all of the ultraviolet radiation below this wavelength. The radiant energy emitted by a flame in this region is very small compared with the total energy emitted at all wavelengths, but it is very substantial in comparison with sunlight below the ninety thousand foot level. Also, blackbody radiation from hot engine parts is insignificant in this region. Moreover, highly sensitive ultraviolet detectors have been made which will reliably detect a single candle flame at distances up to fifty feet in broad daylight.

These facts would indicate that this is the ideal region for the detection of fires in flight vehicles to be used at altitudes below ninety thousand feet. In theory this is true. However, there are many limitations to any method developed to date utilizing this wavelength region.

The first problem is that oil and grease films are highly opaque to ultraviolet energy. This opacity greatly varies with the type of oil used, but in many cases, a thin film of clean oil can have a transmittance of less than 10%, and in some cases even less than 1% (see Figure 26 in Reference 134). The two possible solutions to this problem are either to use a detector with sufficiently high sensitivity to overcome the loss from the oil film or to use a window cleaning technique that will remove or prevent the formation of the oil film, as discussed in Paragraph 4.5. In many applications, high sensitivity would be sufficient to overcome the problem. Most detectors usable in this region are very sensitive, and, as mentioned previously, the signal-to-background ratio for flame detection is very high. For these reasons, a large portion of the signal could be lost and the system could nevertheless respond to the remainder. Also, most danger-zone locations in jet or rocket engine flight vehicles are relatively clean, especially in comparison with piston engine airplanes. In these cases a periodic cleaning of the detector window at the time of engine overhaul, combined with a high sensitivity detector, would be sufficient. Where there is considerable oil film buildup, or when a low sensitivity detector is used, some type of automatic window cleaning technique will be necessary. If the method used does not remove all the oil, a high sensitivity detector would have to be used because of the ultraviolet attenuation by any residual film.

A second limitation stems from the present "solar-blind UV" detector state of the art, which is yet in its infancy. A prime requirement of the detector is

that it have a sharp cut-off below 0.29 micron and that it have virtually no response above this wavelength. This is necessary since there are no practical filters available for use at this wavelength, and therefore all discrimination has to be in the detector itself. The three available types of detectors that have the required characteristics are Geiger-Mueller tubes, arc discharge tubes, and multiplier phototubes ("photomultipliers"), all of them having glass-like envelopes or windows. All operate at 300 VDC or greater, and in the case of photomultipliers, may require up to 2000V DC. These detectors are discussed in more detail in Paragraph 4.2.2 on photodetectors. There is great need for the development of a UV solid state detector which would overcome the limitations of the presently available ones. Such a detector would have to have a sharp cutoff at 0.29 micron as stated above and be relatively insensitive to temperature changes. If such a detector were developed, with a sensitivity equal to that of the Geiger-Mueller tube, it would be the ideal fire detector for practically all aircraft applications and many space vehicle applications.

b. The Infrared Solar-Blind Regions

A second solar-blind region is the infrared one at 2.7 microns, in which sunlight is absorbed by water vapor and carbon dioxide in the atmosphere. There is practically no radiant energy in a narrow band centered around 2.7 microns from sunlight at sea level. At the same time, a hydrocarbon flame emits considerable energy in the same band due to the emission from the water vapor and carbon dioxide exhaust products. This combination offers a very high signal-to-background ratio and therefore good discrimination against daylight radiation. However, since the absorption is due to the atmosphere, the discrimination is good up to only 30,000 to 50,000 feet, diminishing gradually as the altitude increases. This imposes a severe limitation on this system when used in high altitude aircraft. The same is true in another band centered at 4.3 microns. This band offers slightly improved discrimination since most of the absorption is due to carbon dioxide which is distributed rather evenly through the atmosphere compared with the water vapor which resides at the lower altitudes. However, most of the detectors sensitive at 4.3 microns fall into the high cost, exotic class, requiring special cooling and therefore this band will not be considered here.

In order to utilize the 2.7 micronband, very narrow-band filters must be used to reject all radiant energy outside this band. Such filters greatly improve the signal-to-background ratio, but they are not the perfect solution. The daylight levels normally encountered in flight vehicle compartments can be discriminated against, but the detectors should be located so that they are not subjected to direct sunlight, since it is difficult to discriminate against this at the higher altitudes (50,000 feet and above).

Another problem with the filters is that they obviously limit the amount of energy reaching cell. This means that the signal from the flame would be at a lower level than without the filter, and electrical noise from the circuit becomes

a problem. A third problem is that cells sensitive at 2.7 microns are very temperature sensitive, so that for high temperature use, 2.7 micron band detection must be combined with radiation chopping or with flicker detection. These are discussed in detail later.

The temperature drift of lead sulfide cells, which are commonly used for near infrared detection, is greatly accentuated when they are used to detect radiation in the 2.7 micron solar-blind band. This is caused by the temperature dependence of the long wavelength cutoff of these cells. This cutoff is very sharp and the cutoff wavelength decreases as the cell temperature increases. At room temperature a filtered cell may have a ~~cutoff~~ of 3 microns and a peak response at about 2.7 microns. As the temperature increases, the long wavelength cutoff will shift to well below 2.7 microns, and because of the sharp cutoff the signal will be considerably attenuated. This effect is added to the decrease in over-all response of the cell as the temperature increases. This combination means that to operate a cell over a wide temperature range, the preamplifier used with the detector must have very extensive temperature compensation. This obviously means that the amplifier must be in the same physical environment as the cell. Such placement is also required by the low signal from the cell, since locating the preamplifier remotely would mean excessive electrical pickup in the leads.

One disadvantage of both the ultraviolet and the infrared solar blind systems (for use with fiber bundles) is that the detector would have to be located in the compartment being monitored rather than in the readout module. This is necessary since ordinary glass fiber bundles will not transmit either ultraviolet or 2.7 micron infrared radiation. The use of infrared transmitting fiber bundles would be highly expensive at the present time. Thus, the remote mounting location would impose a severe temperature problem upon the detector. The advantages of locating the detector in the readout module will be discussed later.

c. Radiation Level Sensing

Another method of flame detection depends simply upon the anticipated flame vs. background radiation level in any convenient spectral band, such as the visible or near-infrared ones. In such a system, the detector triggering threshold would be set above any expected background radiation level. With this detector, the spectral characteristics of the signal and background sources are immaterial, since the detector responds only to the amount of radiant energy in the band selected. For this reason the detector must be sensitive in the spectral region where the background radiation is low. The ultraviolet region below 0.29 microns is an ideal example of radiation level detection in a region of very low background energy. In the case being discussed now, however, we are considering detection in other spectral regions where there may be appreciable background radiation present. If hot surfaces are present, the infrared region above 1.5 microns cannot be used. This wavelength limit will

be even lower for hotter objects. If the sunlight level is high, the visible region where most of the energy of the sun is concentrated cannot be used. The usual situation where this method of detection can be used to advantage is where the compartment is almost completely light-tight, and where there are no extremely hot surfaces in the compartment. More specifically, there should be no hot objects above approximately 1000°F (unless the surface emissivity is low) and no direct sunlight in the compartment. The small amount of daylight that would be permissible in the compartment would be determined by the size of the smallest fire to be detected.

With some sunlight present, it would be best to eliminate the region from 0.3 to 0.8 micron since most of the radiant energy from the sun is concentrated there. However, if there is much hot surface radiation in the background it may be necessary to use the visible radiation region. Where the compartment is light-tight, it may be advantageous to use this region, since the problem of hot surface background radiation is almost completely eliminated and there are many high sensitivity, economical detectors available for such use. Very simple circuitry can be used with these detectors, resulting in a very low-cost, light weight system. In situations where extremely high sensitivity is required, the detector may have to be temperature-compensated or the radiation chopped (modulated) in order to eliminate temperature drift. Chopping the radiation will help eliminate temperature problems, but it will not increase the signal-to-background ratio.

Where there is the possibility of an occasional flash of light in the compartment, a time lag of about 0.5 second could be used so that these flashes would not trigger the system. This could be the case where there is only one direction from which sunlight could enter the compartment through a crack. It is more probable, however, that in such a situation there would be a case in which the background radiation level could increase and thus alarm the system. If the compartment were designed so that this could occur only if there were structural damage, it might be desirable to warn the pilot of the situation so that he could view the compartment through the fiber bundle to determine what had happened.

d. Two-band Methods

Where the background radiation level is too high for the use of flame-radiation level as the sole discrimination means, the ratio of radiant intensities in two wavelength intervals can be used for higher discriminability. This method relies on the difference in spectral distribution of the radiant energy from a flame and that from a continuous radiator or blackbody. For example, the spectrum of the diffusion flame has a positive slope from 0.5 micron to 1 micron, while the spectrum of sunlight has a negative slope here. The use of two detectors in a balanced circuit, one sensitive at each end of this region, affords a high degree of discrimination between a diffusion flame and sunlight. However, if the background happened to be a hot object at about 2000°F, this system would provide no discrimination at all. It can be seen that again the

problem is to determine in advance what types of background radiation will be present. It is practically impossible to predict what the ratio will be for the background or flame in an actual aircraft installation, and the problem is compounded by the fact that the ratios for premixed and diffusion flames differ greatly. Also, even if a ratio were found that could not be duplicated by background radiation, a soot or oil deposit on the detector window could change it, causing the detector to false alarm from the background radiation. This would be due to possible selective absorption by the oil or soot films on the window. If a red-blue detector were used, it would be a highly effective yellow-flame detector in locations containing little background light. However, high altitude or premixed flames which are characterized by a blue color could not be detected. Also, high sunlight levels would inhibit the detector response so that it could not detect any flames, and red lights or sunsets could false-alarm it.

e. Flame Flicker Recognition

Chopping the radiation has been mentioned previously in connection with many of the detection methods but is discussed in detail here as a prelude to the discussion of flicker detection.

The electrical characteristics of most photodetectors are very sensitive to small changes in temperature. If the DC output from the cells is used, changes in temperature may cause as much signal as the radiation that is being measured. These changes due to temperature, or temperature drift, can be eliminated by chopping or modulating the radiation. In this way, the radiation being measured is proportional to an AC signal from the cell and the temperature drift problem is eliminated. In some cases the basic sensitivity of the cell as well as its DC resistance may change with temperature, in which case temperature compensation of the amplifier will still be necessary. It must be stressed that the radiation must be chopped, and not the electrical signal, in order to have any effect on the temperature drift. Also, it is best to chop only the radiation being detected rather than the total radiation spectrum. For example, if 2.7 micron infrared radiation is being detected, a chopper blade of plastic material can be used so that visible light is not modulated. The plastic blade will transmit visible light but will block out the 2.7 micron energy almost completely. The direct approach to radiation modulation is to use a motor driven chopper. This may be the most economical method but it has many disadvantages. The motor adds weight to the system and requires electrical power; it is subject to bearing wear, and may create excessive electrical noise. The problem of electrical noise can be reduced to some extent by synchronous rectification.

A second mechanical chopping means which shows promise but which has not been developed extensively is the use of a coil-driven tuning fork for modulation. This might be more practical than a motor and there are no parts to wear out. Also, the chopping rate would be very constant.

Most other radiation chopping methods are impractical for fire detection because of the cost. These include Kerr cells and other birefringent modulators, scanning interferometers, and semiconductor free-carrier modulators. All of these devices are relatively complex and expensive, and all are limited to rather narrow fields of view. There are many other proposed methods of radiation modulation that have not been tried, but these will not be discussed here.

There is one method of getting an AC signal from a flame without chopping that also takes advantage of a unique characteristic of all flames. This is by means of flame flicker recognition. The AC signal from the photodetector resulting from the flame flicker is just as effective in eliminating the temperature drift problem as is a chopped radiation signal. The most important reason for using flicker detection, however, is that it is a characteristic of a flame that in most cases will not be duplicated in the background radiation. The flicker is always present in accidental fuel fires and is always of sufficient modulation ratio to be distinguishable against ordinary backgrounds. The flicker frequencies of such flames are at a maximum at between 2 and 20 cycles per second. Higher frequencies are also present in premixed flames, but there is generally enough modulation amplitude in this range to be detectable. If a high sensitivity detector is located where the temperature conditions are not too severe, relatively simple circuitry can be used. AC amplifiers are usually less complex than DC amplifiers with corresponding gain. Obviously, if the signal from the detector is very small due to a low sensitivity detector or because of temperature compensation, the circuitry will be more elaborate and costly. In flicker detection, the total radiation from the flames is incident upon the cell. For this reason, a cell must be used that does not saturate at high radiation levels. If otherwise, when a large flame front was present the total radiation from the flame might be sufficient to lower the sensitivity of the detector so that it would not see the flame flicker. In such a situation, the detection system would clear when there was still a large fire present.

Flame flicker recognition cannot be used where background radiation is excessively high. There is always the chance that the background radiation may be modulated by vibrating reflecting surfaces, by reflections from water waves, by air currents or by rain. Sunlight is sometimes modulated by hot air currents in the flicker frequency band. Most of these problems can be avoided by proper placement of the detectors.

When used wisely, flicker detection can be the simplest and most reliable single method of flame detection for use in flight vehicles. When used in conjunction with visible-band or near-infrared detectors, it allows the possibility of detector placement within the fiber bundle readout module.

f. Combination Methods

Where an extremely high degree of reliability is required, two different methods or channels of discrimination can be combined. Usually this would consist of

flicker recognition combined with one of the discrimination methods described earlier. By such means, if each channel had a chance of false alarm once in "n" flight hours, the combination of two such channels would offer a probability of false alarm only once in " n^2 " flight hours.

Possible combinations are flicker and initial flame rate of rise, or flicker and radiation level. Both of these rely on the fact that the modulation ratio due to flicker is always less than unity. When either of these systems is used, great care must be taken to ensure that the second channel is really adding additional information. In the case of detecting the initial rate of rise of the flame, the time constant must be adjusted so that the flicker rate cannot trigger this channel of the detector. Otherwise, flame flicker will be actuating both channels, and there will be actually only one source of information. In the case where the radiation level is used as the second channel, the background radiation may be sufficient to trigger this channel, in which case the only property of the flame being detected is the flicker. Also, with this system it may be difficult to temperature-stabilize the radiation level part of the circuit. One very satisfactory fire detection system uses flame flicker recognition in the solar blind 2.7 micron band. This system affords very high discrimination against most normally encountered radiation background conditions. However, it still has the altitude limitation of 30,000 to 50,000 foot altitudes where solar absorption is reduced, and the spectral pass bands of modern glass fibers would not permit the detector to be placed in the readout module. Using flicker in this band does eliminate the need for chopping the radiation, but the circuit required is still relatively complex. Also there is the temperature limitation of about 250°F for detectors sensitive in this band. Cooling methods to raise this temperature limit will be discussed shortly.

Detector Location

When used in conjunction with a fiber optic system, the detection system offers the choice of being located either in the remote compartment being surveyed or in the readout module. Both have definite advantages depending on the circumstances. The main advantage of mounting the detector in the fiber bundle pick-up head, where it views the compartment directly, is that the detector is not limited by the spectral transmission capabilities of the fiber bundle. This location would be required for ultraviolet, 2.7 micron infrared, heat, or possibly smoke detection.

If detectors sensitive in the spectral pass-band of glass were mounted remotely, the signal would be greater than otherwise since it would not be attenuated by the fiber bundle.

One limitation of locating the detector in a remote area might be the maintenance problem. Of even greater importance could be the temperature problem in this area. As the performance capabilities of modern flight vehicles are expanded, there is a corresponding increase in the environmental temperatures encountered

in hazard detection problems. If a detector is found that will endure the high temperatures, it is probable that the associated circuitry will have to be located in a cooler region. This implies long electrical lead lengths between the detecting cell and the amplifier and possible electrical pick-up problems on these leads. With some cells, this can be overcome by using very low impedance circuits. Where the temperature in a compartment is unsuitable for the detector, some method of cooling would have to be used. In many cases this would add unwarranted complexity to the system, but in others it would be the only means of providing reliable fire detection. In some cases where high temperatures are encountered for only brief periods, thermal lagging by means of insulation may be sufficient to overcome the problem. Thermoelectric coolers have been improved extensively during the last few years, and these are probably the best cooling devices for use with thermal detectors. Temperature differences of one hundred or more Fahrenheit degrees are obtainable with them at moderate operating power levels. These devices in effect pump heat from the unit being cooled to the surrounding environment. One limitation is that the ambient temperature in which presently obtainable devices will work is limited to about 300°F. Also, they require very large currents at very low voltages which would necessitate the use of heavy lead wires from a specially designed power supply.

Another device of possible interest for cooling photodetectors and which has not been extensively developed is the Hilsch or vortex tube which has been described extensively in the literature, such as in References 119 to 123. In this device compressed air, possibly from a jet engine compressor section, would be used as the power source. By expansion through a vortex configuration, two streams of air are obtained, one being hotter and the other cooler than the incoming air. Single experimental units have achieved a temperature reduction as of much as 140 Fahrenheit degrees from the inlet air. Extensive cooling might be achieved by cascading such units.

In most cases, cooling systems add considerable complexity to a detection system. This can be avoided by locating the detection system in the readout module rather than in the remote compartment. Since this module will be in a manned compartment, temperatures obviously cannot be too extreme. One drawback of such a system is that the photodetector is limited to a wavelength band that can be transmitted by the fiber bundle. Also, the signal will be somewhat attenuated by the fiber bundle. In most cases these limitations are more than compensated for by the lower ambient temperature, reliability (elimination of lead wires, shorting and pickup problems), and ease of maintenance in this location. One advantage to this system is that a detector can be chosen that will see what the pilot sees. Another advantage of locating the detector in the readout module is that testing the system is made easier; all that is necessary is a test light located at the remote end of the fiber bundle where it can verify both bundle integrity and system response at one time.

Detection Systems For Use With Fiber Optics

As can be seen from the previous discussion, the detection system to be used in a particular installation will depend to a great extent upon the environmental conditions in the area, particularly the background radiation. Three systems for different locations will be described.

The most common situation in modern high performance flight vehicles is the relatively light-tight compartment. This is in contrast with the piston engine airplane where the engine compartment is relatively open. For the jet engine case, we assume that there is no direct sunlight, no extremely hot or glowing surfaces, and only a low daylight background level. In such a situation, the recommended system detects light-level only, with the detector located in the readout module, and "looking" through the fiber bundle. If an occasional flash of light might enter the compartment, such as through a crack in the skin, a time delay of 0.5 second could be incorporated into the circuitry. Such a system would offer ease of maintenance and low-cost, simple circuitry with its attendant high reliability and low weight. Also, when operating in the visible radiation region, the system will "see" what the pilot sees. This is the system selected for use in the experimental breadboard assembled for evaluation and described in Section 5. The circuitry will be discussed in Paragraph 4.2.3.

The second situation to be considered is where there is no direct sunlight, but where there is considerable background light or hot body radiation. In this case, radiation level detection would not suffice, the recommended method of discrimination being the use of flicker detection. For simplicity, the detectors should be in the readout module, as before. The circuitry would be only slightly more complex than that of the light-level detector. If occasional high background light levels should be anticipated in the target compartment under certain situations, such as if the vehicle were flying directly toward the sun, a two-color system could be used. In this case, the two-color system would not be for discrimination against normal backgrounds, as described previously, but for "locking out" the system under unusual background radiation conditions. In other words, normal detection would be by means of flicker recognition, but if the background level were extremely high, such as from direct sunlight, the system would be inactivated. In some cases, however, high light levels might occur only if there were physical damage to the vehicle. In this case, the pilot might want to have an alarm so that he could view the remote area to determine the extent of the damage. For such a situation, the two-color lockout would not be necessary.

A conclusion to be drawn from the discussion so far is that an array of photo-electric hazard detection techniques is available, but that in order for one to derive the fullest value from the capabilities which they have to offer, he must give considerable thought to the types of signal radiation and background radiation which must be distinguished, and he must select the system accordingly. Modern technology does not offer an "automatic, universal hazard detector";

even a trained human observer can be deceived by complex visual situations. Thus, the effectiveness of an automatic detection system in a given application depends largely upon the ability of the designer to anticipate every unusual combination of radiation or other environmental conditions which might occur in that application, no matter how improbable their occurrence might be.

The third situation which we consider is where there is a high background radiation level present. As discussed earlier, some distinguishing characteristic of the flame must be selected as the basis for automatic detection and discrimination. In extreme cases of high background light, an oriented bundle, or fiberscope, may have to be used in order for the pilot to distinguish the flame from the background. An ultraviolet detector in the pickup head would be an ideal detector, but it is not practical at this time. The best system for this application would be flicker detection in the 2.7 micron infrared band. This system is relatively expensive and is limited to ambient temperatures of about 250°F, but it offers very high reliability.

In the foregoing discussion, many references have been made to "low" or "high" light levels to "relatively" dark compartments. Quantitative values have not been quoted for either flame or background radiation levels. Unfortunately it is impossible to specify the exact flame size that should be detected or the background level which should be rejected in various flight vehicles, for these vary widely from one case to the next. This is unfortunate, for it is very difficult to specify a reliable surveillance fire detector for a given application without having such knowledge. A program should be initiated to measure the radiation in discrete spectral bands in various critical areas of flight vehicles. This would greatly increase the reliability of fire detectors, and the information would also be useful in the design of other components and assemblies.

4.2.2 Evaluation of Existing Photodetectors

An evaluation has been made of existing photodetectors that might conceivably be useful for aircraft fire detection in conjunction with fiber optic verification systems. An attempt has been made to obtain data on all useful cells manufactured in the United States and on cells manufactured by some well known foreign firms. Characteristics which were evaluated included electrical, spectral and physical characteristics and suitability for aircraft environments. In addition, special characteristics such as solar-blind cells were also considered.

There are two types of cell that were not studied in detail in this report, although some of them are listed for comparison purposes. The first type includes the standard photoemissive and multiplier tubes. These are provided with glass envelopes, are relatively large, operate on high voltages and are generally unsuitable for aircraft environments. Also they have no inherent advantages over the photocurrent or photovoltaic cells. Their spectral responses, which are usually given "S" numbers (S-1 to S-21), cover the spectral region from the near

ultraviolet to the near infrared, which is in general the same region covered by photoconductive cells. An exception has been made with solar-blind ultraviolet-sensitive phototubes which have unique characteristics for fire detection.

The second class of cells that has not been covered are the cooled cells, sensitive in the intermediate and far infrared. Representative types are photoconductive or photovoltaic indium antimonide, lead telluride, and the doped germanium and germanium-silicon cells. These require cooling by liquid nitrogen or other methods to cryogenic temperatures for operation. The expense and complexity of both the cells and the cooling devices are not warranted for fire detection use; cells that operate at room temperature or above will give just as satisfactory results, considering the relatively large radiation signals provided by accidental fires and the rather nearby locations from which they may generally be detected.

Two charts have been constructed for comparison of the various types of cells. The first chart, shown as Table 9, lists certain photocell characteristics. These include the sensitive material, the mode of operation, peak response and 50% response wavelengths, the sensitivity, impedance, time constant, sensitive area, price and operating temperature.

The second chart, shown as Figure 61, shows the principal wavelength response regions of the various types of cells, between the half-power points, and the peak response wavelengths are indicated also. A plot of the spectral transmittance of a six-foot fiber bundle is drawn on this chart for comparison purposes.

These charts are useful as a comparison between the various types of cells and as an aid in selecting a cell for a particular application. However, the data sheets for the individual cells are needed to obtain complete information. In the sensitivity column of Table 9, it is often difficult to make a direct comparison between the cells because different units are used for different types of cell.

In general, the charts are self-explanatory. However, some of the photo-detectors have unique characteristics which are difficult to put in chart form. This is particularly true of the solar-blind ultraviolet sensitive photo cells. There are four types of tubes in this classification: the vacuum photodiode, the multiplier phototube, the photon counter or Geiger-Mueller tube and the glow discharge tube. The first three types use cesium telluride, rubidium telluride or pure metal cathodes. The Geiger-Mueller tubes are available in self-quenching or externally-quenched types. In the fourth classification is the glow discharge tube. This device has a glass-like envelope, as do all the other solar blind ultraviolet tubes, but it is rated to stand 20 G acceleration up to at least 1000 cycles per second. Its main disadvantages are its relatively large size, (1-1/8 inches in

<u>Type</u>	<u>Kind</u>	<u>Peak</u>	<u>50%</u>		<u>Sensitivity</u>	<u>Im</u>
		<u>Response</u> <u>Wavelength</u> <u>(microns)</u>	<u>Response</u> <u>Wavelength</u> <u>(microns)</u>	<u>Response</u> <u>Wavelength</u> <u>(microns)</u>		
UVT	Photoemissive Diode	0.18	0.16	0.26	----	
UVTI	Photon Counters	0.23	0.20	0.26	1,800-60,000 counts/sec. microwatts/cm ²	
UVT2	Photomultiplier	0.24	0.21	0.26	3000A/watt	
PbS	Photoconductive	2.0	0.20	3.5	D* (500, 750, 1) = 10 ⁹	6E
Se	Photovoltaic	0.56	0.36	0.64	0.5 - 4.8A/ftc	
Ge	Photoconductive	2.2	0.37	8.5	0.001 - 1.6A/ftc	0.1
GaAs	Photovoltaic	0.85	0.40	0.90	0.03A/W	1
Si	Photovoltaic	0.85	0.40	1.1	0.1 - 5A/ftc	0
CdS	Photoconductive	0.57	0.45	0.79	4-31 mA/ftc	1.
PbTe	Photoconductive	4.0	0.60	6.0	D* (500, 400, 1) = 8 x 10 ⁸	1
CdSe	Photoconductive	0.72	0.66	0.83	1000-3000 A/ftc	0
PbSe	Photoconductive	3.0	1.0	5.0	D* (500, 750, 1) = 3 x 10 ⁷	
InSb	Photoconductive or voltaic	5.5	2.0	7.0	D* (500, 500, 1) = 1 x 10 ⁹ - 15 x 10 ⁹ for p-pn cell: D* = 10 ⁷	
Thermistor		---	flat	response ---	1.6 - 60 volts watt	0.



TABLE 9. COMPARISON OF

<u>Sensitivity</u>	<u>Impedance</u>	<u>Time Constant</u>	<u>Sensitive Area (mm²)</u>	<u>Price Range</u>	<u>Operating Temperature</u>
----	----	----	103	\$350	----
,800-60,000 counts/sec. microwatts/cm ²	----	----	68-505	\$25-32	-65°C to +200°C
3000A/watt	----	----	1410	\$55	100° max.
D* (500, 750, 1) = 10 ⁹	6K-20 meg. ohms	5-2000 sec.	.62 x 10 ⁻³ -1000	\$4.25-32.50	-196° to +90°
0.5 - 4.8 μa/ftc	6-60K	----	1.93 - 1580	\$20-30	-60° to +140°
0.001 - 1.6 μa/ftc	0.1 - 100 meg.	1-100 sec.	0.01-8.63	\$6-1000	-196° to +75°
0.03 a/ W	1.5 meg.	1.0 msec.	----	\$100	120° max.
0.1 - 5 μa/ftc	0.5 ohm 10 meg	0.1 - 20 sec.	2.5 x 10 ⁻³	\$5.35 - 1000	-65° to +175°
4-31 ma/ftc	1.5 K-1000 meg	1.0-460 msec.	2.32 - 360	\$2.65-5.00	-75° to +77°
D* (500, 400, 1) = 8 x 10 ⁸	1-50 meg	10 sec.	10	----	-195°
1000-3000 μa/ftc	0.24 ohm -133K	12 - 34 msec.	1.13 - 226	\$4.00	-70° to +75°
D* (500, 750, 1) = 3 x 10 ⁷	15 ohm -100K	2 sec.	6	----	25°
D* (500, 500, 1) = 1 x 10 ⁹ -15 x 10 ⁹ for pcm cell: D* = 10 ⁷	5 ohms -50K	0.5-2.0 sec.	0.04 - 25	\$45-1700	-196° to +25°
1.6 - 60 volts watt	0.2-3 meg	1 - 10 msec.	0.4 - 2.25	----	----

TABLE 9. COMPARISON OF PHOTODETECTORS



diameter by 1-1/4 inches long), and the fact that it has to operate on 700 volts AC. In contrast to the very low-current Geiger-Mueller tubes, this tube is self-quenching and can conduct up to 25 ma. In the visible region of the spectrum, the two types of cell useful for fire detection are photovoltaic and photoresistive (or photoconductive). The materials customarily used for photovoltaic cells are selenium, silicon and gallium arsenide. They have the advantage over photoresistive cells that the signal is self-generating so that no bias voltage is needed, but the output signal is small so that considerable amplification is needed.

The most commonly used photoresistive cells are cadmium sulfide and cadmium selenide. Also, some of the photovoltaic cells can be used photoresistively by back-biasing them. In the demonstrator constructed under this contract, a cadmium selenide cell was used. It has excellent temperature characteristics and a peak spectral response that corresponds to the peak radiation of the diffusion flames. This more than offsets the fact that the spectral response of cadmium sulfide corresponds better to the transmittance of the fiber bundle. These cells have very high output so that very little amplification of the signal is needed.

In the near and intermediate infrared region, the most commonly used cells are lead sulfide, lead selenide and indium antimonide. Lead sulfide is by far the most widely used. All of these cells show higher sensitivity when cooled, but they can be used at room temperature or above. Lead sulfide cells have been used up to 400°F, but the signal is extremely dependent on temperature and extensive temperature compensation is needed. Since the long wavelength cut-off is also heat-sensitive, the temperature dependence is accentuated when lead sulfide is used in the solar blind configuration with a 2.7 micron filter. For this use, the upper temperature limit is about 250°F. Indium antimonide photo-electromagnetic cells are sensitive out to about seven microns and can be used at room temperature or slightly above.

Although these cells have a much lower signal to noise ratio than lead sulfide, they might be useful as solar blind fire detectors in the 2.7 or 4.3 micron bands.

4.2.3 Photodetection Circuitry

The discussions in the foregoing paragraphs have pointed out that each detection problem must be solved by the selection of an appropriate detector and by the choice of a suitable electronic method of using the detector. Once these decisions have been made for a given system, the selection or design of an appropriate circuit must be undertaken.

Many standard circuits are available in the technical literature for use with the known photodetectors. In the commercial design of photoelectric fire detectors, it is common practice to employ modified forms of the standard circuits or, more often, to design completely new ones to meet specialized environmental or detection problems which are not encountered in other applications of photodetectors.

Several "detection-mode philosophies" have been described in Paragraph 4.2.1 and some of them have been investigated in detail during this effort with attention to special problems posed by the possible use of a fiber bundle as an integral component in the detection system. The principal problem introduced by the use of fiber bundles is the loss of radiant energy in long bundles and the reduced signal available to the detector when it is used at the viewing end. The problem is not insurmountable; it is merely uncommon in ordinary photoelectric fire detection design practice where one is accustomed to dealing with larger flame signals. Solutions to the reduced-flame-signal problem are readily achieved with some extra thought on the part of the circuit designer.

As an example, we shall describe a particular circuit which has been developed under this effort as a part of the fiber optic demonstrator described in Section 5. The design criterion was based on the "radiation level" sensing of diffusion flames as viewed by the detector through a 25-foot length of light pipe. The detector chosen was of the cadmium selenide type with a peak response at about 735 millimicrons and with appreciable sensitivity to long-wavelength visible light and to short-wavelength near-infrared radiation. The system was designed to operate at low to moderate levels of background radiation, as might be encountered in jet engine spaces and in parts of some piston engine spaces. To accommodate various background levels, the breadboard model was provided with a "High-Low" sensitivity selector so that the circuit would alarm when the detector was illuminated by either 50 or 10 foot candles of flame signal. Test lamps were provided within the fiber bundle objective lens assembly (see Fig. 58c) and are activated by a "Press to Test" switch on the control panel (see Fig. 59).

The circuit diagram is presented in Fig. 44. Briefly, the photodetector is located in a bridge circuit -- its electrical resistance decreasing in response to a light signal -- providing an increase in the signal current entering a current amplifier. When the amplifier output reaches a predetermined level, it triggers a free-running multivibrator which operates at a rate of five cycles per second. The multivibrator output is fed into a switching circuit which actuates the alarm lamps on the control panel.

In greater detail, the circuit operates as follows. The detector comprises one of two legs of a bridge circuit whose output is fed to the base of the transistor Q_1 . In response to a light signal, the increased photodetector current is fed into the base of Q_1 and amplified. A voltage is thus established across CR2 and sufficient current is supplied through R_4 to the base of transistor Q_2 to switch it partially on. With Q_2 partly conducting, a current is fed through R_6 and the thermistor to the base of Q_3 and, in turn, amplified by transistors Q_3 and Q_4 . Positive feedback from the collector of Q_4 through R_8 causes Q_2 to switch fully on. A voltage is built up across C_1 as a result of current flow through R_{12} from Q_4 . This voltage across C_1 yields sufficient current through R_9 to tunnel diode CR3 to switch it from its low voltage state to its high voltage state.

Transistor Q₂ is then switched off by the voltage developed across CR3 and the voltage across capacitor C₁ is allowed to decay, thus returning CR3 to its low voltage state. Transistor Q₂ will again begin to conduct provided that sufficient signal is supplied through R₄. The network consisting of Q₂, Q₃, Q₄, CR3 and other related components acts as a free running multivibrator at a rate of 5 cps provided that sufficient current is supplied through resistor R₄.

A thermistor activated temperature-compensating network in the collector circuit of Q₂ provides a stable operating point over the temperature range from -65° F to +165° F. Zener diode voltage regulation has been provided in the first transistor stage to stabilize the light sensitivity of the alarm circuit in the event of supply voltage variations of ±10%. In the collector circuit of Q₄ (a power transistor) are lamps which provide the visual indication of an alarm condition.

4.2.4 Combined Photo and Thermal Detection

Modern electronic hazard detection techniques provide aircraft designers with the options of a "flame-only" detector and a "flame-plus-overheat" detector. The former would be used where fires were to be detected against backgrounds of surfaces whose normal operating temperatures were fairly high or where, for some other reason, an overheat alarm was not desired from the detector. In the other situation, it may be desired that the detector respond not only to accidental fires but also to engine-overheat conditions above a certain temperature threshold.

Depending upon whether or not that threshold were compatible with the flame-detection threshold as "seen" by the detector, it is often possible to combine the separate functions into a single one by a suitable choice of the photodetector and circuitry. In particular, those photodetectors which are sensitive to energy of greater wavelengths in the infrared region will also be able to respond more readily to hot surface radiation in the lower temperature range; by contrast, the ultraviolet sensitive flame detectors mentioned earlier would respond to incandescent surface radiation of only the highest order.

A combined flame-plus-overheat detector would provide an alarm in the case of either a fire or an overheat condition, but it would not distinguish between the two. If such a distinction were required of the system, then a minimum of two detection-transducers should be used. If they were electrically compatible, their output signals could be amplified by a single (but sophisticated) circuit which could then actuate either a "flame" or an "overheat" alarm, as appropriate. If the detectors were widely different, as in the case of a fast-responding, low-impedance photodetector versus a slower, high-impedance thermal detector, separate circuits would be more appropriate. In such a case, the thermal or overheat detector is best located at the far end of the fiber bundle if temperatures far below the incandescent range are to be

indicated for most of the energy radiated by such surfaces is in the longer wavelength infrared region which is not transmitted by glass fiber bundles. (However, see Paragraph 3.1.10 for a discussion of infrared-transmitting fibers.)

On the other hand, if the overheat threshold temperatures are just below or within the incandescent range, the substantial near-infrared transmission capabilities of glass fibers will often permit the placement of the overheat detector at the viewing end of the bundle. However, as the overheat threshold temperature is raised, there is a greater likelihood that the flame detector will respond to an overheat condition, and if this situation is not desirable, then particular thought must be given to the choice of flame detection system so that it will respond more selectively.

In any case, the earlier suggestions applying to the location of the flame-sensing transducer (pickup-end versus viewing-end) are still applicable except as dictated by extreme requirements of flame-versus-overheat discrimination, in which case an appropriate flame sensor would be an ultraviolet detector placed directly within the danger zone.

4.2.5 Detector-to-Fiber-Bundle Couplings

In cases where the detector is to be located within the readout module in order to view the danger zone through the fiber bundle, the question arises as to how the detector and the human observer can most efficiently share a view of the bundle end face. An obvious solution suggests itself if one considers that after the detector has provided a warning of an unusual radiation condition as transmitted by the bundle, it has discharged its intended function and can be temporarily moved aside in order to provide the observer with an exclusive view of the end face. This consideration suggests the idea of "sequential sensing" in which either the detector or the observer is permitted a full view of the end face at the discretion of the observer. Many simple mechanical arrangements are possible through which the detector can be located intimately against the end face but can be quickly moved aside at the wish of the observer. This technique has been incorporated into the experimental system described in Section 5.

An objection to the above technique may be that a manual operation is required on the part of the observer and that this would interfere with other manual duties, particularly in the case of an individually manned vehicle. In such a case, sequential viewing is nonetheless possible but can be achieved more conveniently through use of an electromechanical device which automatically moves the detector aside after it has signaled an alarm condition. The alarm signal itself would be the actuating agency, and the detector could be restored manually to its position at any convenient time afterward.

If a further objection to sequential sensing exists, on the basis of the inclusion of moving parts, a "no-moving-parts" simultaneous-sensing system is possible through the use of an optical beam splitter. Such devices are conventional partial-mirrors which can "split" a beam of light into two differently-directed parts with any desired ratio of intensities. For example, a "fifty-fifty" neutral beam splitter placed at 45 degrees to the axis of a light beam will allow half of the energy to continue on its path essentially undeflected while the other half is deviated 90 degrees from the original beam. Moreover, by means of well-known "thin film" techniques, spectrally-selective beam splitters (or "dichroic mirrors") can be made which will reflect radiation in one wavelength region only, allowing radiation of other wavelengths to continue on its course.

An objection to the neutral beam splitter is that it provides images of reduced intensity to both the detector and the observer. In this case, the more sophisticated dichroic beam splitter can be invoked in order to capitalize on the fact that the spectral sensitivity regions of the detector and observer may differ although both are included within the spectral passband of the optical fibers. For example, if the detector is of the near-infrared-sensitive type, it may derive adequate optical signal energy within the infrared spectral region transmitted by the fibers but not utilized by the human eye. In this case, one might specify a beam splitter with a high infrared reflectance and a high visible-band transmittance with a sharp cutoff near 700 millimicrons. This "mirror" might be located very near to the bundle end face, making a 45° angle with it; it could then deflect the infrared signal energy into a nearby detector at 90° to the ray path while detracting very little from the visible signal proceeding through it to the eye of the observer. Such a system would make highly efficient use of the radiant energy which is transmitted by a fiber bundle but which is ordinarily useless to a human observer. However, because of geometrical considerations, the detector would not be located as near to the bundle end face as otherwise and would not intercept the entire emittance cone; in such a case, an appropriate condensing lens, located between the mirror and the detector, would be useful in diverting to the detector much of the energy which would otherwise by-pass it.

References 43 and 44 present discussions on optically coupling a fiber bundle to an image tube. Certain aspects of these discussions are of interest to the problem of fiber-bundle to photodetector couplings.

4.3 Unusual Bundle Configurations

The bundle configurations considered so far in this report have involved simple bundle lengths for conveying radiation from a single objective lens directly to the viewing end.

Many variations of this basic configuration are both conceivable and feasible for use in special applications. A practical configuration which might find wide application in aerospace problems involves the branching of a bundle somewhere along its length, the separate branches terminating in individual objective lenses at various physical locations within an aerospace vehicle. The separately collected optical information could then be displayed on the single readout face, making it possible to monitor several object scenes with a minimum of visual scanning or of required instrument panel area.

The method is applicable both to fiberscopes and to light pipes although the fabrication problems may be somewhat simpler in the latter case.

Several such possible configurations are shown in Figure 45. For simplicity, the drawings depict the fiber bundles only but not the associated optical or photoelectric alarm components.

Figure 45a shows a configuration suitable, for example, for the surveillance of two zones of a power plant. In this case, the split would be located near the objective lenses in the power plant and light entering from Zones A and B would be transmitted to the viewer through a single bundle end face. Here the fibers would be separated by a suitable means so that the observer can identify the zone of origin.

Figure 45b shows a configuration where several views of a single zone are required. The three objective ends may survey partially overlapping areas. In this arrangement the split may be in or at the bulkhead of the zone being surveyed and the fibers proceeding from the three objective lenses would terminate in random positions over single viewing end face. This would provide an observed array of scintillating dots if a flame were to exist anywhere in the zone.

A third configuration, shown in **Figure 45c** would provide for surveillance of many separated zones individually identifiable and requiring a minimum of instrument panel area for visual observation. This arrangement would consist of a number of individual light pipes joined together at the viewing end to provide a compact viewing face with a clearly defined and identifiable area for each zone under surveillance. For purposes of economy, such a system would comprise individual light pipes of various lengths coupled at the viewing end where the individually transmitted images would be joined together as a single compound image. Each image would occupy its own separate and clearly defined section on the viewing face.

Depending upon the requirements for a specific application, any or all of the three above-mentioned configurations can be combined into a single system in order to meet the requirements. However, the use of multiple bundles should be reserved for specific problems which cannot be solved through the use of an appropriate number of single bundles for the additional cost of joining several bundles of glass fibers together within a single jacket for a part of their length may not be justified. Particular cases in which the use of multiple bundles may justify the added cost are (1) where panel space must be conserved, and (2) where, in view of weight considerations, it would be important to combine the protective jacketings of separate bundles into a single jacket over a great portion of the bundle length especially in the case of long bundles.

4.4 Bundle-to-Bundle Couplings

Where a great length of fiber bundle is to be used in a given application, it is worthwhile to consider the fabrication of the bundle in modular sections which can be joined together during installation. The use of such lengths would simplify the problems of installation, inventory maintenance, and replacement of a damaged section. The method is applicable to both fiberscopes and light pipes although some image degradation occurs in both cases depending upon the number of joints used and the optical quality of each.

If the end faces of two fiber bundles are simply pressed together, the effect of a continuous bundle length will be simulated very closely. (See Figures 31 and 32.) Some degradation of detail occurs because the light emanating from a single fiber in one bundle will, on the average, fall on several fiber ends in the second bundle. Moreover, if the end faces are not in direct optical contact, the spreading of rays from each "donor" fiber will cause a further dilution of energy over the "receiver" fiber ends. In cases of bundles containing large numbers of fibers, where each fiber makes a very small contribution to the total image, the lateral spreading of light rays is relatively minor and degrades only the finest image detail; however, the degradation is progressive as the image traverses further optical joints. A discussion included in Reference 36 concerning fiber point-spread functions, is of particular interest to the matter of fiber couplings.

From the optical standpoint, then, it is desirable that the butted end faces be in intimate contact. From the aerospace environmental standpoint, however, it may be wiser to avoid physical contact which might invite a chafing situation under vibrational influences. In such a case, a slight separation of the end faces is permissible, provided that the gap width is not appreciably larger than the diameter of a single optical channel. Thus, for fiber bundles composed of two mil monofilaments, an end face spacing of two or three mils can be tolerated; however, accurate control of the spacing required for a multi-fiberscope would be much more difficult.

The burden of spacing-control falls upon the design of the connector which is to be used in the coupling arrangement. The connector must be rugged and "foolproof" and yet must be fabricated with optical precision. The present effort has yielded a connector design aimed at meeting such criteria. This connector has been fabricated as a part of the demonstration system described in Section 5 and it will be discussed more fully therein.

There is an alternative procedure to providing an air gap between the end faces and that is to fill the space with a transparent solid or a fluid material instead. In the case of a permanent joint, any of several optical resins or cements may be used. For a demountable joint, one would insert a drop of an appropriate oil on one end face before making the connection. The narrowness of the gap would be expected to retain the oil film through capillary action, avoiding the need for a fluid seal.

The advantage of using a gap material other than air is that it provides the possibility of matching its refractive index to that of the core material. Such an index match would achieve a more optically continuous transition across the joint, reducing surface reflectance losses as well as the lateral spreading of light rays between end faces. In the case where oil is used, there is a variety of optical "immersion oils" with a choice of closely calibrated refractive index values, making it possible to select one whose index matches that of a given glass to several decimal figures.

4.5 Self-Cleaning Windows

The possibility that films of various fluids and/or soot particles will accumulate on the exposed surface of a fiber bundle window or lens situated in an engine compartment is a problem that should be considered. Such an accumulation would tend to distort or obscure the view of the engine section under surveillance and reduce the effectiveness of the fiber optic system.

A program was initiated to find various ways of either preventing the formation of such deposits or of automatically removing them once they had formed.

A twelve-inch cubicle container was fabricated from sheet metal to simulate a compartment containing contaminants in vapor or particulate form. The container was provided with removable end panels, a number of viewing ports, a pressurized jet to atomize fuel (light motor oil or kerosene) and internal lighting, as shown in Figure 46.

Several tests were conducted using a number of simple laboratory type devices designed for the purpose of preventing film formation or of removing the films automatically, using glass plates as the test surfaces.

Some advantages and limitations of the various types of devices constructed and tested during this program are reviewed briefly below and are discussed more fully in subsequent paragraphs.

1.) Air Flow Devices

Certain devices utilizing air flow can be used to prevent, but not remove, accumulations of contaminating films on an exposed surface of a glass lens or window, if operated continuously. Of the various types tested, the plenum chamber devices appear to be the most satisfactory.

The device illustrated in Figure 52, having a long sleeve which acts as a plenum chamber, can be used where wide angular coverage is not important and sufficient mounting depth is available. The devices illustrated in Figure 53, having large diameter plenum chambers, can be used in locations which have limited mounting depth and for applications where wide angular coverage is important.

2.) Electromechanical Windshield Wipers

A device of this type can be used both to prevent and to remove oil and soot films on the exposed surface of a glass lens or window and will not necessarily limit the angular coverage.

There is a possibility that high engine temperatures and certain types of engine fluids could adversely affect a Neoprene rubber wiper blade. Certain other materials, perhaps Teflon, would be affected to a lesser degree than Neoprene.

3.) Heated Windows

All of the devices utilizing self-heating appear successful in preventing but not in removing accumulations on the exposed surfaces if operated continuously (see Figures 47 to 49). The temperatures involved for successful operation, 300° to 500°F, might present some problems. Air gaps (cooled areas) might be required between the heated glass and nearby or associated equipment adversely affected by high temperatures.

4.5.1 Thermal Methods

A number of simple, elevated temperature devices were constructed to determine whether heat could be used to prevent and/or remove an accumulation of condensed fluid vapors and/or soot-like particles on the exposed surface of a glass lens or window mounted within an aircraft engine space under surveillance.

The upper photographs of Figure 50 illustrate a device similar in construction to those illustrated in Figure 51. Two layers of glass plate were used, however, instead of one. The glass plates were separated from each other by an asbestos gasket. An air gap, approximately 1/32" high and 1-3/4" in diameter, was provided at the center between the two glass plates. Two openings, from opposite sides of the gap, were provided to allow the passage of heated air between the glass plates. No accumulation of the test fuel (kerosene) was observed on the exposed surface of the glass plate when the temperature of this surface was maintained near 350°F. Accumulations of kerosene were observed, however, when the temperature of the exposed surface dropped below 250°F. A brown residue was observed on the exposed surface of the glass plate upon heating the glass to 350°F after allowing the kerosene to accumulate on the exposed surface of the glass at room temperature. The lower photograph in Figure 50 illustrates a device similar to that shown in the upper photographs. The major difference is that an electrically heated, flat, metallic heater element, in the shape of a ring, has replaced the air gap in the previous model. This device functions in the same manner as the previous model. If the temperature of the exposed surface of the glass is maintained at approximately 350°F continuously, no fuel accumulation or residue is apparent.

A third class of devices, shown in Figures 47, 48 and 49, was constructed similar to those illustrated in Figure 50. The major difference was that a transparent, electrically conductive film of tin oxide was used in place of the metallic heater ring. This electrically heated film affords much the same results as the previous models discussed. Considerable experimentation was

involved in the preparation of these films and the fabrication of electrical contacts. Because the use of transparent conductive coatings offers an alternative heating method which might find wide application to the window problem, we believe that a somewhat detailed account of our findings on tin oxide films will serve a useful purpose.

Tin Oxide Conductive Coating

If a water solution of stannous chloride is sprayed on to a hot glass surface, a thin, transparent coating of tin oxide is formed. This film is capable of electrically heating the entire glass up to a temperature as high as 650°F, depending on the resistance of the film and the applied voltage. The tin oxide film is prepared in the following manner. Three milliliters of concentrated hydrochloric acid are added to 500 milliliters of distilled water. Twenty-five grams of stannous chloride are then dissolved in the solution. The solution should be filtered if it is not clear and used only when it has been freshly prepared. It is then sprayed on to Pyrex glass plates which have been heated to about 1300°F. A tin oxide film will result, with a resistance of about 700 to 20,000 ohms per square. Three inch square plates were used in these experiments.

It can be difficult to achieve a film with the desired resistance and still obtain a clear transparent film, since the resistance depends on the thickness of the film. The transparency of the films prepared here was good, but the sample films were not uniform.

Electrical Contacts

The application of suitable contacts presented several problems. The first contacts which were tried utilized silver paint and brass foil. The brass foil was cemented to the film by use of the silver paint and then lead wires soldered directly to the foil. The contacts were air dried and no baking was necessary since a low-temperature silver conducting paint was used. If these contacts were placed about 3/4" apart, a resistance of about 1000 ohms could be obtained with a good film. (See photo of Test Window #1, Figure 49)

Other glass plates were prepared and an effort was made to minimize the amount of brass foil used since it did not adhere too well. (See photo of Test Window #2, Figure 49) Thermal insulation was added between the two plates of glass and between the glass and metal holder. A third type of contact was tried, formed from a silver paste that was baked at 1000°F and to which wire leads were soldered directly. This method was not too successful because the wire leads did not adhere very well and there was also the problem of finding a solder with a high enough melting temperature as not to melt when the glass plate was heated. A sample prepared by this method is shown as Test Window #3, Figure 49.

Efficiency of the Heated Windows

Despite possible non-uniformities in the film, it was found that the entire glass plate will heat up very well. With 140 volts applied, a current of anywhere between 120 and 400 ma may be measured. Heat can be detected in the glass after applying the voltage for only about one minute. The maximum temperature that the glass will reach, with a given voltage, depends on the resistance of the film. The resistance of the glass plates varied anywhere from 20K ohms, which was not low enough to allow the glass to heat, to less than 700 ohms, which allowed the glass to reach a temperature of 650°F.

The values presented below are the observed surface temperatures for various coated glass samples with 140V AC applied across them.

<u>Film Resistance</u>	<u>Observed Film Temperature, °F</u>
20,000 ohms	Room Temperature
3,000 ohms	240
1,500 ohms	385
700 ohms	650

If a resistance of 1000 ohms or less is achieved, the glass plates will heat enough to prevent an oil film from forming. A surface temperature of 375°F (T_1 in Figure 47), was found to be needed to keep an engine film from forming on the glass. A temperature greater than this must initially be supplied since when a mist of oil is blown onto the glass plate, it acts as a cooling agent and reduces the temperature by as much as 200°F. The face of the glass plate that is toward the oil mist must maintain a temperature of 375°F (T_1). In order to do this under our testing conditions, the film itself had to reach a temperature of about 560°F (T_2 in Figure 47).

If the heat and oil mist begin simultaneously, then the glass remains clear of any oil film or droplets. If, however, the oil mist is allowed to form droplets on the glass before it is heated, the heat is not sufficient to remove these droplets. If the source of the oil mist is removed and the glass continues to be heated, then these oil droplets disappear, leaving a residue of impurities. If the oil contains a high amount of non-volatile impurities, it can be expected that these impurities would form films and eventually cut down the transmittance of the glass.

The possibility of eliminating the conductive film itself and just using a circular conductive path of silver material was investigated. A semicircular path was sandblasted in the glass plate and then a silver paste was applied to this groove and baked. Leads were soldered on directly to the silver material. A temperature of about 350°F was reached, but the silver material decomposed during all attempts to heat the glass in this manner. No other materials besides the silver conducting paste have been investigated.

4.5.2 Pneumatic Methods

A number of simple air flow devices were constructed for evaluation as possible self-cleaning window methods. Several of them and their air flow patterns are illustrated in Figures 51, 52 and 53.

The light arrows shown in these illustrations indicate the direction of flow for pressurized air feeding and proceeding from the device. The dark arrows indicate areas of negative pressure which allow fuel and/or soot to be drawn into the device and to collect on the lens surface.

All of the devices to be discussed were attached to a metal sleeve bonded to the metal container (Figure 46) used for simulating a section of a jet engine. They have in common a glass lens, lens holder, rubber sealing ring, mounting sleeve and a connecting tube for supplying pressurized air.

Figure 51a includes a tubular ring having several rows of small air holes located around the inner diameter. The ring is located in the mounting sleeve between the glass lens and the metal container mentioned previously.

When the device was activated, droplets of fuel (kerosene) were drawn into the device instead of being repelled, and accumulated on the exposed surface of the glass lens. Air at low pressure (2 to 5 psi gage) reduced the rate of accumulation but did not prevent or remove it. Air at high pressure (6 to 60 psi gage) increased the rate of accumulation.

Figure 51b is similar to Figure 51a except for showing a reduced orifice between the tubular ring and the metal container. Results were the same as those obtained with the first device except that the rate of accumulation was reduced.

Figure 51c is similar to Figures 51a and 51b except that a smaller orifice was provided. No accumulation of fuel was observed regardless of the air pressure used. However, due to the location and diameter of this orifice, the optical angular coverage was reduced.

Figure 51d shows a tubular ring having a thin air slot running around its inner diameter. The connecting tube is fastened to the ring at less than a right angle to impart circular motion to the flow of air. The result was a cyclonic type of air flow with a high negative component at its center. Fuel (kerosene) again collected on the exposed surface of the glass lens, regardless of air pressure used.

Figure 51e illustrates a conical inner sleeve, joined at the large diameter to the end of the mounting sleeve farthest from the glass lens. A small air gap was provided between the small end of the inner sleeve and the exposed surface of the glass lens. The connecting tube was attached to the mounting sleeve at right angles for this particular test. A negative pressure area was also observed

with this device with the accompanying accumulation of fuel (kerosene) on the exposed surface of the glass lens.

Figure 51f is identical to Figure 51c, except for the connecting tube which was attached to the mounting sleeve at less than a right angle. A cyclonic type of air flow resulted with a high negative component at its center. A collection of fuel droplets was again observed on the exposed surface of the glass lens, with the rate of accumulation depending on the air pressure used.

With the exception of the device shown in Figure 51c, all of the air flow devices tested were found to attract rather than repel the spray droplets and none will effectively remove accumulations from the exposed surface of a glass lens.

A second series of air flow devices, incorporating plenum chamber designs, was fabricated and tested. The purpose of the chambers is to create a positive pressure gradient between the glass lens and the engine.

Figure 52 is quite similar to the devices illustrated in Figure 51. The major difference is that a sleeve approximately 8" long has been added between the glass lens and the engine chamber. With no air flow, fuel droplets were seen to accumulate on the exposed surface of the glass lens. With low-to-medium-pressure air flow (3 to 20 psi gage), no accumulation was observed. However, with this device the optical angular coverage was substantially reduced.

Figure 53a illustrates a plenum type chamber 6" in diameter and 1" deep, located between the glass lens and the simulated engine chamber. With low-pressure (2 to 3 psi gage) air flow, a negligible accumulation of fuel was observed on the exposed surface of the glass lens. With high pressures (4 to 30 psi gage), substantial accumulations were observed due to the cyclonic effect of the air stream. A smaller opening to the engine chamber would prevent accumulation at higher pressures, but would also reduce the angular coverage.

Figure 53b illustrates a plenum type chamber, 4" in diameter and less than an inch deep. With low-pressure (2 to 5 psi gage) air flow, no accumulation of fuel was observed on the glass lens. At higher pressures (6 to 30 psi gage), some accumulation was observed but less than on the previous model, Figure 53a. Again, a smaller opening would prevent accumulations but at the expense of angular coverage.

4.5.3 Electromechanical Methods

A windshield wiper, consisting of a 12 RPM motor, cam, cam follower, drive shaft, shaft bearing, wiper arm and wiper blade (neoprene rubber), was mounted on a panel having a glass window. The panel assembly was then attached to the metal container (Figure 46) with the wiper arm, wiper blade (bearing on the glass window) and a portion of the drive shaft inside.

Light motor oil, and later kerosene, was forced through an atomizing jet into the metal container and allowed to accumulate on the exposed surface of the glass window. The wiper was then activated and appeared to clear the window completely on two passes.

The exposed surface of the glass window was next covered with a mixture of light oil and soot. On two passes of the wiper, the window appeared clear. Figures 54 and 55 are photographs taken from both sides of the panel, and show the glass before, during and after one pass of the wiper.

Repeated tests indicate that a windshield wiper can effectively clear a glass window of oil, kerosene and/or soot under laboratory conditions. High engine temperatures or jet engine fuel, however, might adversely affect a neoprene rubber wiper blade.

4.6 Image Tubes

It has been pointed out in Paragraph 3.1.11 and elsewhere that practical length limitations on fiber bundles for ordinary viewing conditions are in the 50 to 100 foot range.

An interesting possibility of either broadening the usable spectral range or extending the useful length of a fiber bundle is presented if one considers the possible use of commercially available electronic image processing devices. Such devices fall into two main functional classes. The first class includes the image amplifiers or intensifiers, with the ability to present a greatly brightened version of a very weak image. The devices in the other class, which are probably of greater interest to the present problem, are able to convert invisible infrared energy into visible light, being referred to as image converters. Both types of device are presently available in the form of evacuated glass enclosures and are generally referred to here as "image tubes", although various solid state versions are under development which would not rightfully be called "tubes".

It should be understood that various sacrifices are involved in the use of image tubes with fiber bundles, so that their use should be contemplated only where the anticipated gains offset the losses. In particular, present image tubes provide only a monochromatic image and, therefore, sacrifice the color-transmitting ability of present glass fibers. The image color depends upon the choice of output phosphor used in the device, presently available colors being confined to a choice of blue-green or yellow-green. Another feature is the inevitable loss of image detail which generally results from the introduction of an additional optical element into an imaging system, although the extent of the lost detail need not be appreciable in a properly designed system. The only other sacrifices which need to be mentioned are the obvious ones of economy, reliability, size, weight, and so forth.

However, in cases where it is necessary to extend a bundle length beyond its ordinary limit for a given viewing situation, the use of an image intensifier can be well justified, provided that the optical information in the scene being viewed resides primarily in the visible spectral region. In cases where this information is carried largely by energy in the infrared region, an infrared image converter can serve the same purpose in extending the usable bundle length.

Another purpose served by image converters is the broadening of the useful spectral transmission band afforded by most fibers. Transmittance curves such as those of Fig. 19 reveal that a substantial part of the energy transmitted by fiber bundles is in the near-infrared region and is not used by the human eye. Moreover, a knowledge of the spectral emission characteristics of most flames and hot surfaces indicates that their emitted energy is proportionally

higher in this region than in the visible band. In addition, it is known that the reverse is true of daylight sources (direct and indirect sunlight) whose radiant energy in the visible region exceeds that in any infrared band of the same spectral width. One could thus profit by using the near-infrared transmitting capability of optical fibers in conjunction with infrared-sensitive image converters, not only in making flames and hot surfaces appear brighter, but also in increasing the contrast between them and any daylight-illuminated surrounding surfaces, thereby increasing their visibility further.

This phenomenon is illustrated in Figs. 56 and 57 which compare the direct views of various scenes containing incandescent surfaces with the indirect views provided by infrared image conversion. The converted images were provided by means of a 1P25 image converter tube of the type used in World War II "sniperscopes", this tube having an S-1 photosurface and a P-20 phosphor, which are explained in Appendix A and whose characteristic spectral curves are shown in Figs. A-1 and A-3.

The photographs were prepared directly and not through a fiberscope, but they illustrate the brightness gain and contrast gain which would be afforded in conjunction with fiberscope use. The converter tube used in preparing these figures is shown in Fig. 56.

The same figure presents a direct view of a familiar domestic scene in which the object of present interest is an incandescent burner coil. The lower figures are direct photographs of this image as presented by the converter tube, the difference being that the image shown in the lower right was prepared through the use of an infrared filter placed before the receiving surface of the converter tube. This filter (Polaroid Corporation, No. XRX) blocks most of the visible light and transmits highly in the near infrared region. Its purpose was to emphasize the high radiance of the burner coil in the near-infrared region as compared with the daylight radiation provided by the background in the same spectral region. Examination of the two lower photographs in this figure will verify the increase in contrast which is achieved as one limits the scene radiation to the near-infrared band.

Figure 57 presents reference photographs and converted images of various familiar scenes containing diffusion flames whose incandescent carbon-particle emission is at a maximum in the near-infrared region where daylight radiance is on the decline. The monochromatic images provided by the image converter tube are not as colorful but are unquestionably more efficient in emphasizing the presence of the flames than are the direct photographs.

The subject of image tubes and their uses is a broad one, requiring a detailed analysis which is more logically placed outside of the main body of this report. Such an analysis is, therefore, presented as an appendix to the report.

The highlights are that, in cases where flames and overheated surfaces must be observed through fiberscopes of great lengths or under adverse conditions of daylight backgrounds, it would be highly profitable to consider the use of image tubes, particularly infrared image converters, at the viewing end of a fiberscope or light pipe. Under conditions of extreme fiber bundle length or low object radiance, it might be necessary to locate such a tube part way along the length of the bundle, remote from the viewing end, although this would undo any advantage of simplicity and reliability afforded by maintaining the tube at the viewing end.

4.7 Test Circuits

In operational use, the physical continuity of a fiber bundle can readily be verified by a glance at the readout surface in cases where the pickup end is viewing a luminous scene. In many instances, however, the bundle may normally "look" into a darkened area which does not provide a self-checking capability. In such cases, it is desirable or even necessary that an independent light source be available at the pickup end to allow the observer to check the bundle continuity at will.

Several simple test-light arrangements are possible; in many cases they can serve the double purpose of verifying bundle continuity as well as providing a check on the response of an automatic photoelectric detection system which may often be used with the fiber bundle. Test lights may be designed as an integral part of the objective lens assembly with the electrical leads integral with the fiber bundle assembly, as in the experimental detection system described in Section 5. Alternatively, a test light may be placed anywhere in or near the field of view of the bundle with its power leads routed along any convenient path and it will serve adequately.

In cases where an automatic alarm system is used which may be designed to respond selectively to certain light sources such as flames, the test light arrangement would have to take this into account in order to provide a detection system response check. For example, if the detection system is designed to respond only to flame flicker in the 5 to 20 cps frequency region, then the test light power source would have to be modulated in this frequency region, such as at 13 cps, in order to provide a radiant signal with characteristics similar to those of a flame in order to alarm the detection system. If a "two-color" detection system were used (see Paragraph 4.2.1), the color of the test light would have to be chosen appropriately.

4.8 Dynamic Scanning Devices

The discussion which follows refers to an electromechanical technique which can be used to improve the image quality of a given fiberscope. For reasons to be seen, the method is not suggested for use with light pipes.

The earlier discussions and accompanying photographs have made it clear to the reader that a typical fiberscope superimposes a texture or graininess upon the image which it transmits. This is especially true if the fiberscope contains fewer fibers which are viewed at higher magnification, and it is even more true if many broken or missing strands are apparent. Conversely, a fiberscope containing several hundred thousand or more very fine fibers, especially with fused end faces, would introduce only negligible grain into the picture. Such fiberscopes, however, would require considerable cross-sectional area, because the individual fibers cannot be below a certain minimum diameter for effective light transmission; moreover, the cladding losses (see Paragraph 2.1.3) would be appreciable.

In those aerospace fiberscope applications where the utmost in visual acuity is required without undue sacrifice of weight considerations, it is inviting to consider the use of a technique called "dynamic scanning". This technique has been discussed at length by several authors (33, 36, 37, 46, 56 and 64) and has been instrumented by several commercial firms.

The method makes use of the "persistence of vision" of the human visual mechanism, or the ability of the eye to "time-average" the brightness of an image which is flickering at a rate faster than about 15 or 20 cycles per second. (This rate is called the "flicker fusion frequency" and depends largely upon the scene brightness, the modulation ratio, and the part of the retina involved.) The flicker fusion mechanism is responsible for many illusions in our daily experience, including the apparent continuous motion observed in television presentations, motion pictures, theater marquee lights, and many animated lighting displays.

As applied to improving the image quality of a fiberscope, the dynamic scanning technique involves the use of mechanical means to vibrate the fiberscope end faces in synchronism, each in its own plane, but leaving the terminal optics stationary with regard to both the object scene and the observer's eye. Each image point is, therefore, transmitted consecutively by many fibers on a time sharing basis. The scanning of the image plane is done in a circular manner and at a rate higher than the flicker fusion frequency for most viewing situations. Consequently, the shapes of the individual fibers, as well as local fiberscope defects, are "averaged out" and the improvement in apparent image quality is a substantial one. The effect is similar to that of viewing a scene through a coarse grid, such as the teeth of a pocket comb or the outstretched fingers, and oscillating the grid rapidly as compared with holding it still.

Commercial dynamic scanners have not been evaluated as a part of this effort. They are mentioned only in passing as being of possible interest to certain aerospace fiberscope problems, for the size and cost of the scanner instrumentation might be prohibitive in ordinary applications. However, they might prove to be practical for certain critical applications, especially where long fiberscope lengths are involved for they would provide the image quality of large diameter (static-scanning) fiberscopes while using only small diameter ones, and the net weight savings could be appreciable.

SECTION 5. AN EXPERIMENTAL MODEL

Several of the findings of this study have been articulated in the form of a research model intended to represent a typical fiber optic hazard detection system which might be used in aerospace applications. The unit has been delivered to the Contract Initiator for his laboratory evaluation.

From the variety of possible configurations, one was selected which used a 1/8" diameter light pipe as the light-bearing element, containing about 1700 two mil fibers. Bundle lengths of six and seventeen feet, respectively, were suitably jacketed and provided with end fittings so that they could be used simultaneously or interchangeably with the objective lens assembly and control box which were also provided. A "radiation level" photodetection system was incorporated at the viewing end; the system circuitry is discussed in Paragraph 4.2.3.

A more detailed discussion of this system follows.

5.1 Design Considerations

The experimental optical detection system was designed to demonstrate the ability of light pipes to act as light transmitting media to aid in the detection of flames or variations in light intensity, by actuation of an automatic alarm, and to permit visual inspection for rationalization and confirmation of such an incident occurring in a remote zone.

The control unit was designed to be a compact, portable unit with self contained batteries for the test lamp circuit and with terminals for attaching a 28 volt DC source for the alarm circuit. The front panel contains a minimum number of components, namely (1) the on-off switch with two "on" positions, for the selection of either a low or a high sensitivity; (2) the warning indicator lamp assembly which is also the "press to test" switch for testing the entire system; (3) the viewing lens assembly for providing a magnified image of the bundle end face, and (4) a lever for moving the photodetector aside so as to allow the observer to view the end face directly.

The rear of the control unit is provided with a hand hole to permit access to the rear plate of the alarm unit for attaching the light pipe to the light pipe adaptor and for changing the test circuit dry cells.

In order to provide for various arrangements of light transmission from the objective lens to the viewing unit, a system of light pipes and connectors was incorporated. The viewing unit light pipe adaptor, the connector, and the objective lens adaptor are all similar and can be coupled to either end of either light pipe.

In order to provide a compact system with no external wiring for the test lamp circuit and yet keep the light pipe diameter and weight to a minimum, coaxial conductors were incorporated. The external braid of the light pipe jacket was used for one conductor and an internal braid, added just inside the Teflon tubing, was used as the other conductor for illuminating the test lamps located in the objective lens adaptor.

The light fiber bundles selected were standard American Optical Light Guides except that they were in non-standard lengths. They consist of 1/8 inch diameter bundles, each covered initially with a plastic jacket and with shrink-on sleeves at the ends, and are mounted within No. R-101-6 Titeflex Teflon Hose. The shrinkable sleeves provide maximum fiber density at the end faces, with a minimum of voids.

From the discussion in Paragraph 4.4 on the properties of the various types of optical couplings, the dry coupling with a 0.001" to 0.003" spacing between the end faces of the fiber bundles was selected as the most practical because of the relatively practical tolerances, the simplicity of maintenance, and the fact that a relatively minor reflectance loss would be introduced, equivalent to the transmission loss of only a few inches of fiber length. The electrical aspects of the connector are essentially two rings coaxial to the fiber bundles, thus eliminating external wiring. This method is compatible with the use of the external and internal braid in the composition of the light pipe.

The method for providing an alarm, incorporating electronic circuitry, was selected so that an alarm light will flash when light of a predetermined intensity enters through the objective lens within its cone of vision. The high-low selection switch enables the system to detect at two different light levels. In general, the "low" position will require a light intensity greater than ordinary room light to indicate an alarm. The "high" position will result in an alarm at ambient room light intensities. This is somewhat dependent upon the light pipe length and the intensity of the room ambient light. With the selection switch in the "high" position, only one of the three test lamps in the objective lens adaptor assembly is needed to alarm the system, whereas in the "low" position, at least two of them must be activated. A third test lamp provides a margin of safety, ensuring an alarm under all conditions, including slightly worn test lamp dry cells.

5.2 Configuration of Experimental Model

The control unit is housed in a sloping panel utility cabinet with the alarm unit and viewer assembly mounted on the front panel, as shown in Figures 59 and 60. The various controls, indicator, and viewer are shown in both figures. The dry cells for the test circuit are not shown but are located

on the inside of the rear panel of the cabinet. These are readily accessible, as well as the alarm unit light pipe adaptor, through the hand hole located in the rear panel. Terminals for the 28 volt DC supply, with the polarity indicated, are located at the top center of the rear panel.

Figure 58 shows sectional views of alarm unit light pipe adaptor, light pipe end fittings, connector and the test light and objective lens adaptor assembly. From these views, continuity of the two electrical circuits for the test lamps can be traced through the adaptors, the connector, and the light pipes. The light transmission, from the test lamps, or light through the objective lens, can also be traced through the light guides and connector to the cell. With the cell moved aside by pressing the observation lever, the image on the end of the light pipe can be viewed through the eyepiece assembly.

The eyepiece assembly was designed to bring the image end of the light pipe into proper focus when its mounting thread is completely engaged in the front panel. The image may be observed through this eyepiece when the cell is moved aside by pressing the viewing lever. Three eyepiece assemblies are provided so as to enable the observer to view the image with 3X, 5X, or 10X magnification.

The objective lens supplied as part of the system is an Elgeet No. WC727 8mm motion picture camera lens, with a focal length of 7mm, to permit broad angular coverage, and with a focal ratio of f/2.7. The standard "D" mount thread provided with the test light assembly permits any of a variety of 8mm camera lenses to be readily interchanged.

Figure 60a is an oblique front view of the control unit assembly. Figure 60b is an exploded view of the light pipe assembly showing the two light pipes of different lengths, the connector, the objective lens adaptor (test lamp assembly) and the objective lens. Figure 60c is a rear view, with the rear plate removed, of the alarm unit. This view shows the arrangement of components and electronic circuitry within the unit.

5.3 Operation of Experimental Model

Three configurations of the present demonstrator are possible with regard to fiber bundle length. They are (1) control unit with the six foot light pipe and the objective lens assembly, (2) control unit with the seventeen foot light pipe and the objective lens assembly, and (3) control unit with both light pipes joined with the connector and the objective lens assembly.

Using any of these three configurations, operation is as follows:

- (1) Connect a 28 volt DC supply to the terminals provided on the upper center of the rear panel, observing proper polarity.

- (2) Check to ascertain that the test circuit "D" cells are properly installed in their holders inside of the rear panel.
- (3) Place the OFF-LOW-HIGH switch to the LOW position.
- (4) Press the test light assembly. Observe the warning lamp. This should flash approximately five times per second while in the test position.
- (5) Press the observation lever and observe the end face through the eyepiece. The end face will appear as a pale green array of luminous points under room lighting.
- (6) With the observation lever still depressed and while observing through the eyepiece, press the test light assembly. The end face will change from the pale greenish appearance to a relatively bright yellow-green.

These first six steps verify that the system is functioning properly.

- (7) Locate a flame or light source in the cone of vision of the objective lens. This will put the system into alarm condition as indicated by the flashing of the indicator light. With the observation lever depressed, a flickering flame or moving light will appear as a pattern of scintillating dots. A steady flame or light will show up as a steady array of bright dots. The larger the flame or light, and the closer it is to the objective lens, the greater will be the number of illuminated dots (individual fibers) and conversely. With a little experience, the observer will be able to discriminate between ambient light, various flames, and other sources of light.

The HIGH position on the selector switch is provided for detecting and observing small flames and light sources under fairly low room lighting conditions or with the full-length light pipe configuration.

SECTION 6. CONCLUSIONS AND RECOMMENDATIONS

Our studies have indicated that the new technology of fiber optics can make a substantial contribution to present techniques of detecting, verifying, or identifying various vehicular malfunctions which may occur aboard aerospace vehicles. The compatibility of suitably protected glass fibers with a broad range of possible aerospace environments has been established in the laboratory.

In situations where detailed pictorial information must be transmitted, present fiberscope fabrication techniques can provide the transfer of extremely high quality images. Where visual signals of a lower information content must be transmitted, such as in the identification of an accidental fire in a dark engine compartment, a light-weight, economical light pipe configuration can be used to great advantage. In either case, where flames or overheated surfaces are to be observed, the transmission capabilities of fiber bundles can be greatly extended through the use of image tubes.

Our studies have also indicated directions in which future improvements might profitably be sought in the further development of the optical fiber art for aerospace applications. Transmittance variations among fibers might be reduced as a result of further study, leading to higher quality images. Mechanical strength is another area of concern to the fiber industry, for it is believed that present fibers do not exhibit the durability which they ultimately should; mechanical weaknesses exert their greatest threat during the fabrication and assembly of the fibers, resulting in production yields which are lower than they might be, with consequent adverse effects upon delivery and cost.

With regard to the over-all aspects of radiative hazard detection, it has been pointed out that the photodetection problem is essentially a discrimination problem, and that further information on the radiative background signals to be found in modern aerospace vehicle danger zones would be of great value in establishing design criteria for automatic detection systems to be used with fiber bundles.

Despite future improvements which might be achieved, it is our firm belief that the fiber optics art as it now exists is ready for the "flight test" stage and that the greatest immediate advance in our knowledge of fiber optic aerospace applications would be found in the actual preparation and testing of various fiber bundle configurations aboard flight vehicles.

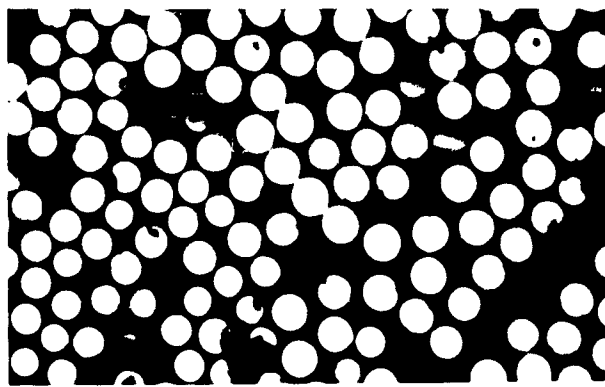
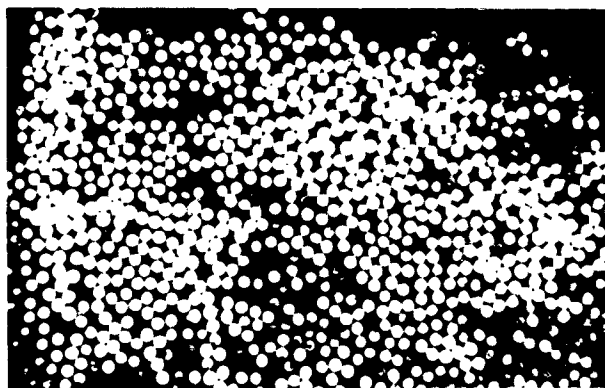
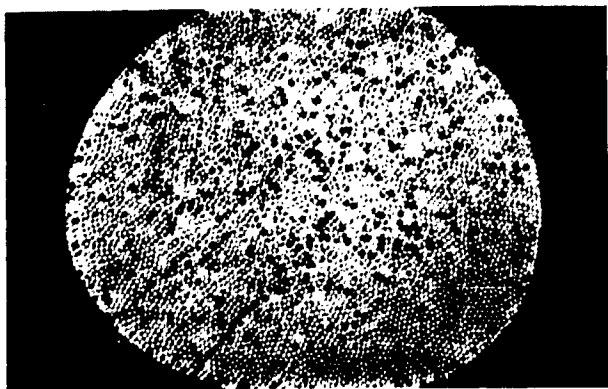


FIGURE 1a. END FACES OF MONOFILAMENT FIBER BUNDLES AT VARIOUS MAGNIFICATIONS.

Bundle in middle photograph is unevenly illuminated.

Discussion in Paragraph 2.1.1.

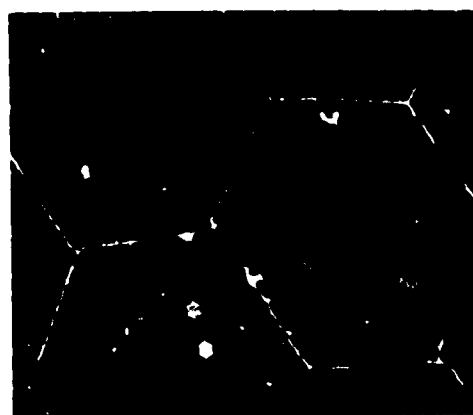
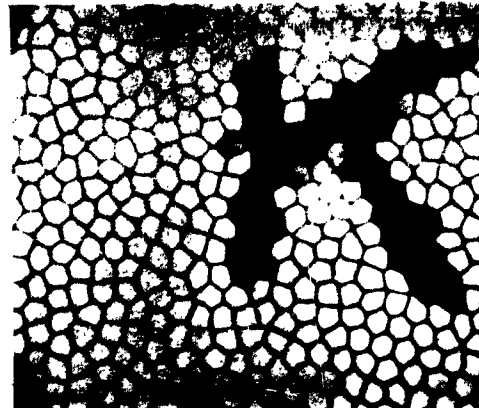


FIGURE 1b. SEVERAL FUSED PLATES UNDER VARIOUS MAGNIFICATIONS AND CONDITIONS.

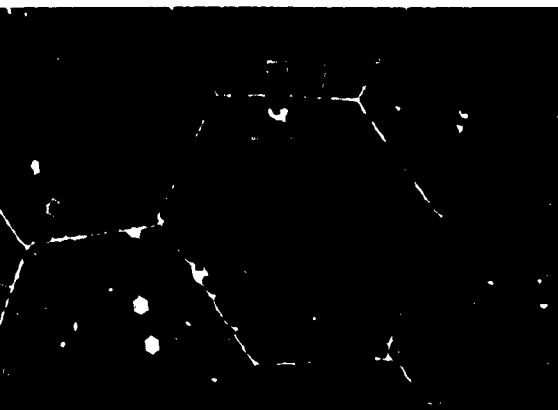
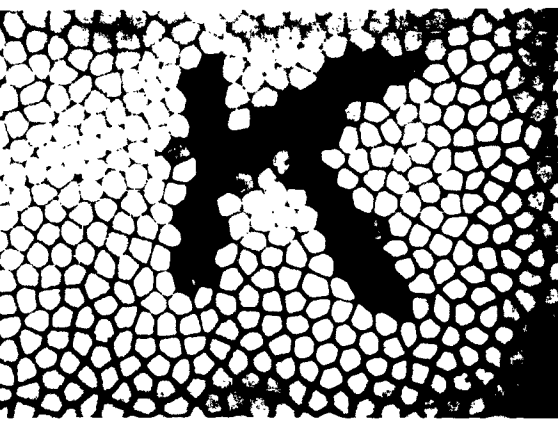


FIGURE 1b. SEVERAL FUSED FIBER FACE-PLATES UNDER VARIOUS MAGNIFICATIONS AND LIGHTING CONDITIONS.

110

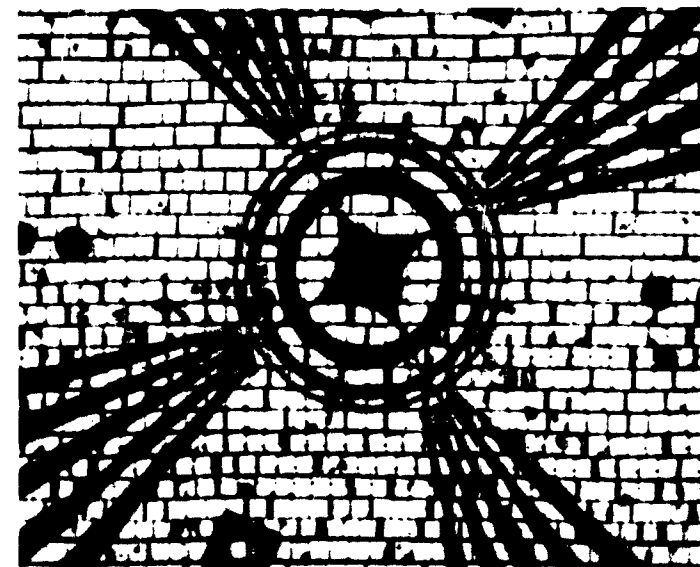
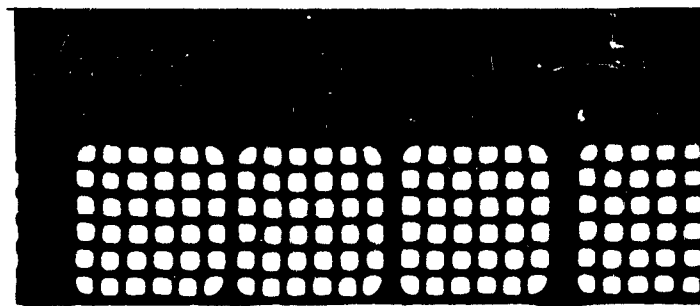


FIGURE 1c. MULTIFIBERS UNDER HIGH MAGNIFICATION.

Lower photograph is 40X actual size.



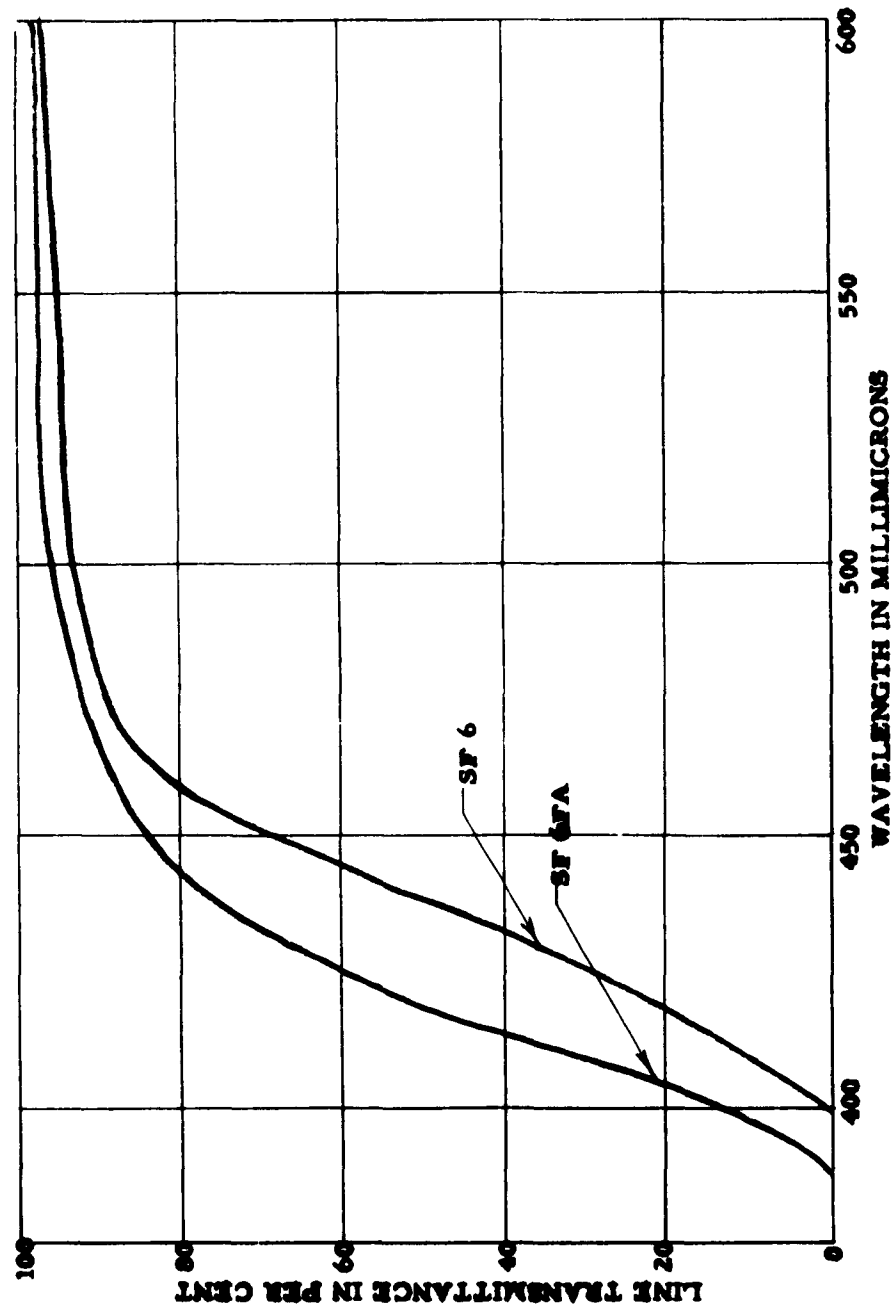


FIGURE 2.
SPECTRAL TRANSMITTANCE OF TWO TYPES OF SCHOTT GLASS IN FOUR INCH THICKNESSES
(End surface losses not included)

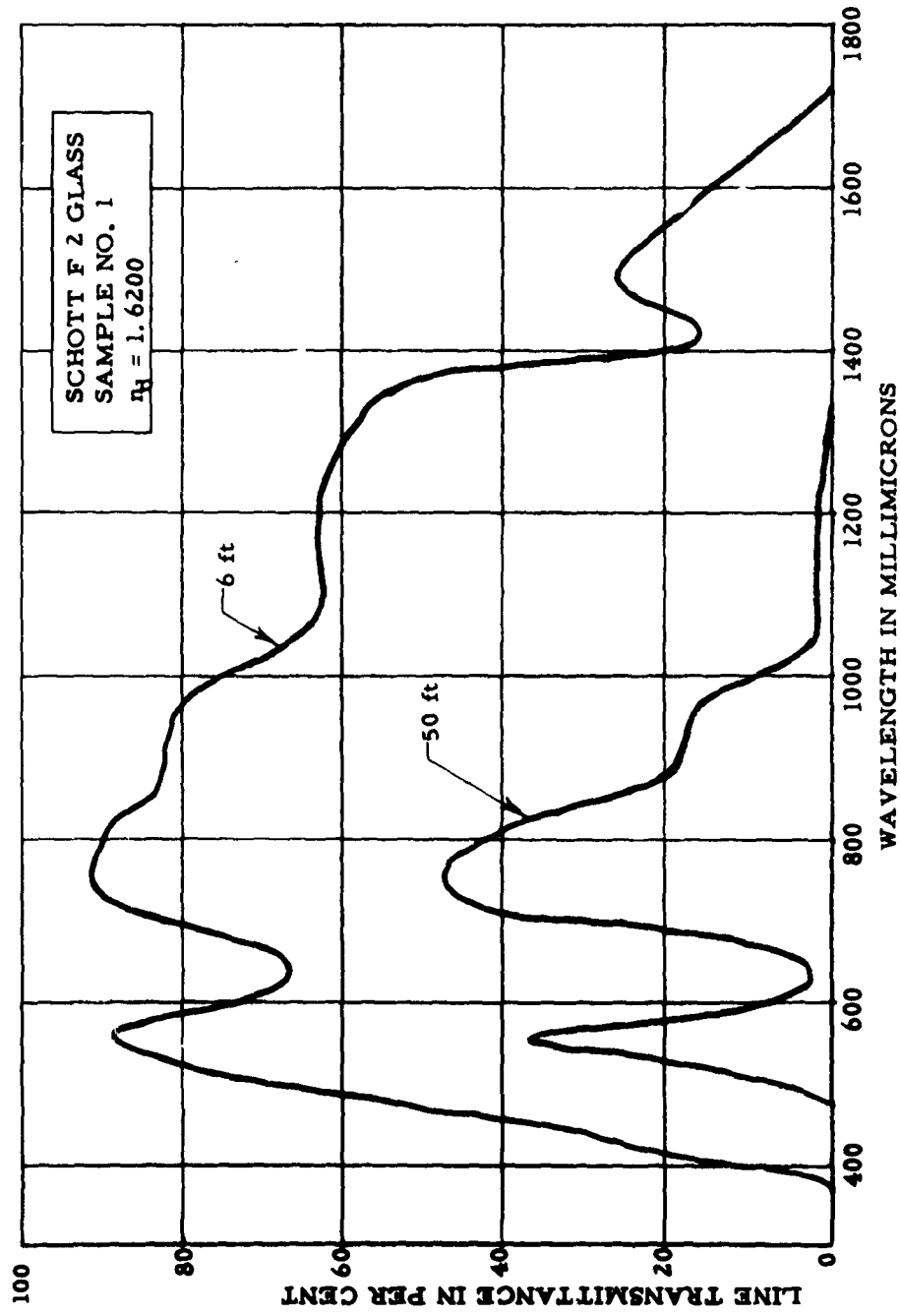


FIGURE 3.
SPECTRAL TRANSMITTANCE OF SOLID GLASS EXTRAPOLATED
TO 6 AND 50 FOOT THICKNESSES FROM MEASUREMENTS ON A 4 INCH BLOCK

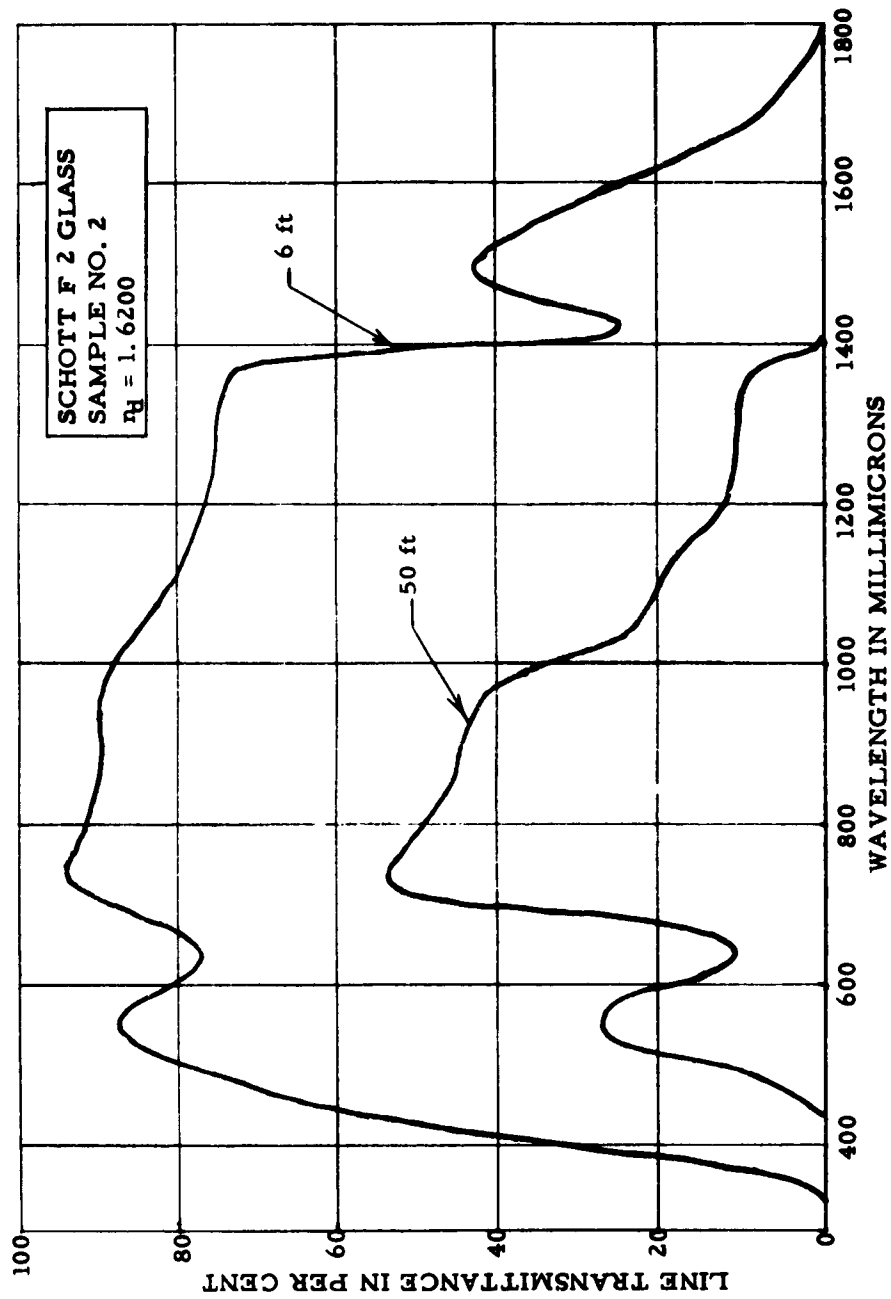


FIGURE 4.
 SPECTRAL TRANSMITTANCE OF SOLID GLASS EXTRAPOLATED
 TO 6 AND 50 FOOT THICKNESSES FROM MEASUREMENTS ON A 4 INCH BLOCK

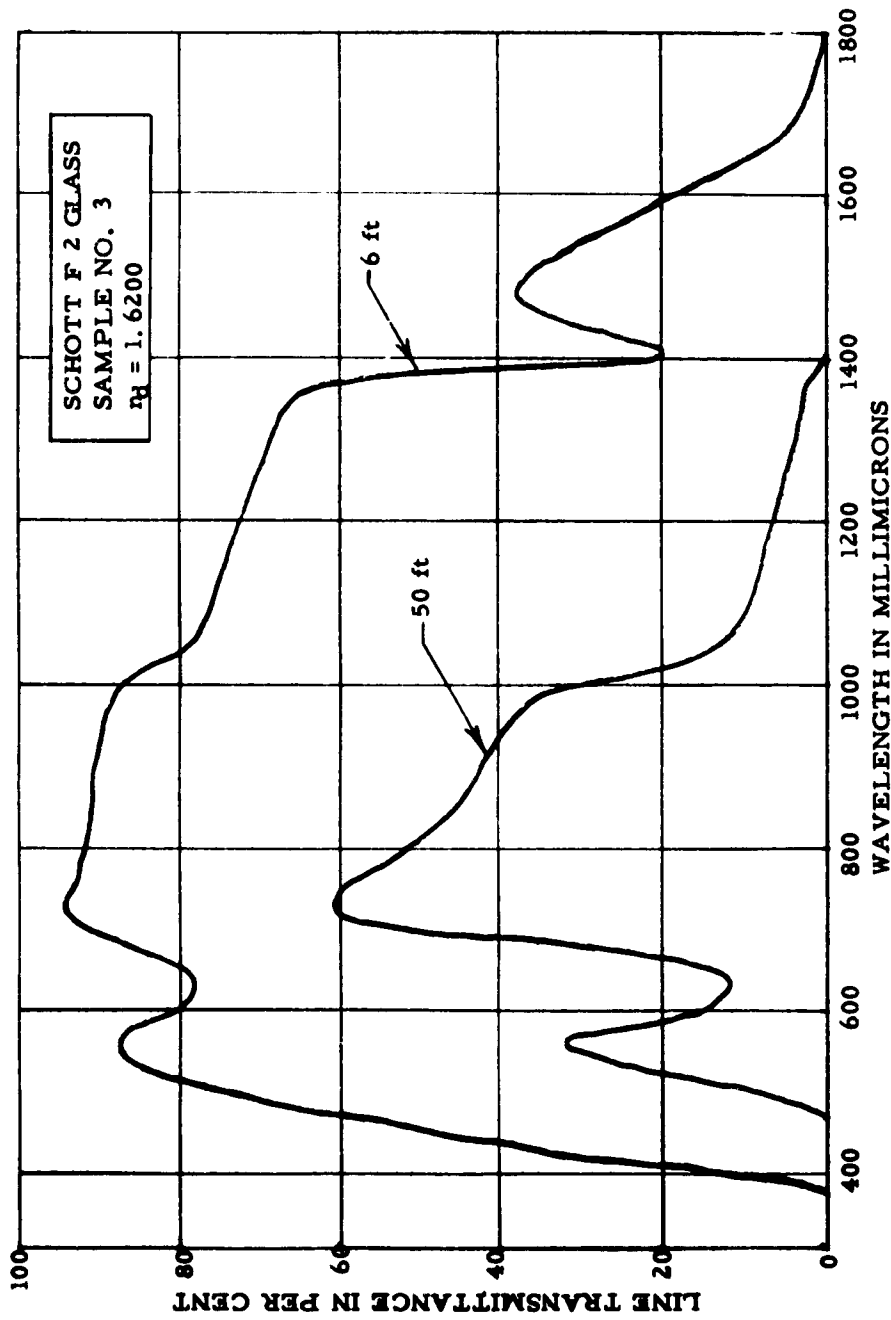


FIGURE 5.
 SPECTRAL TRANSMITTANCE OF SOLID GLASS EXTRAPOLATED
 TO 6 AND 50 FOOT THICKNESSES FROM MEASUREMENTS ON A 4 INCH BLOCK

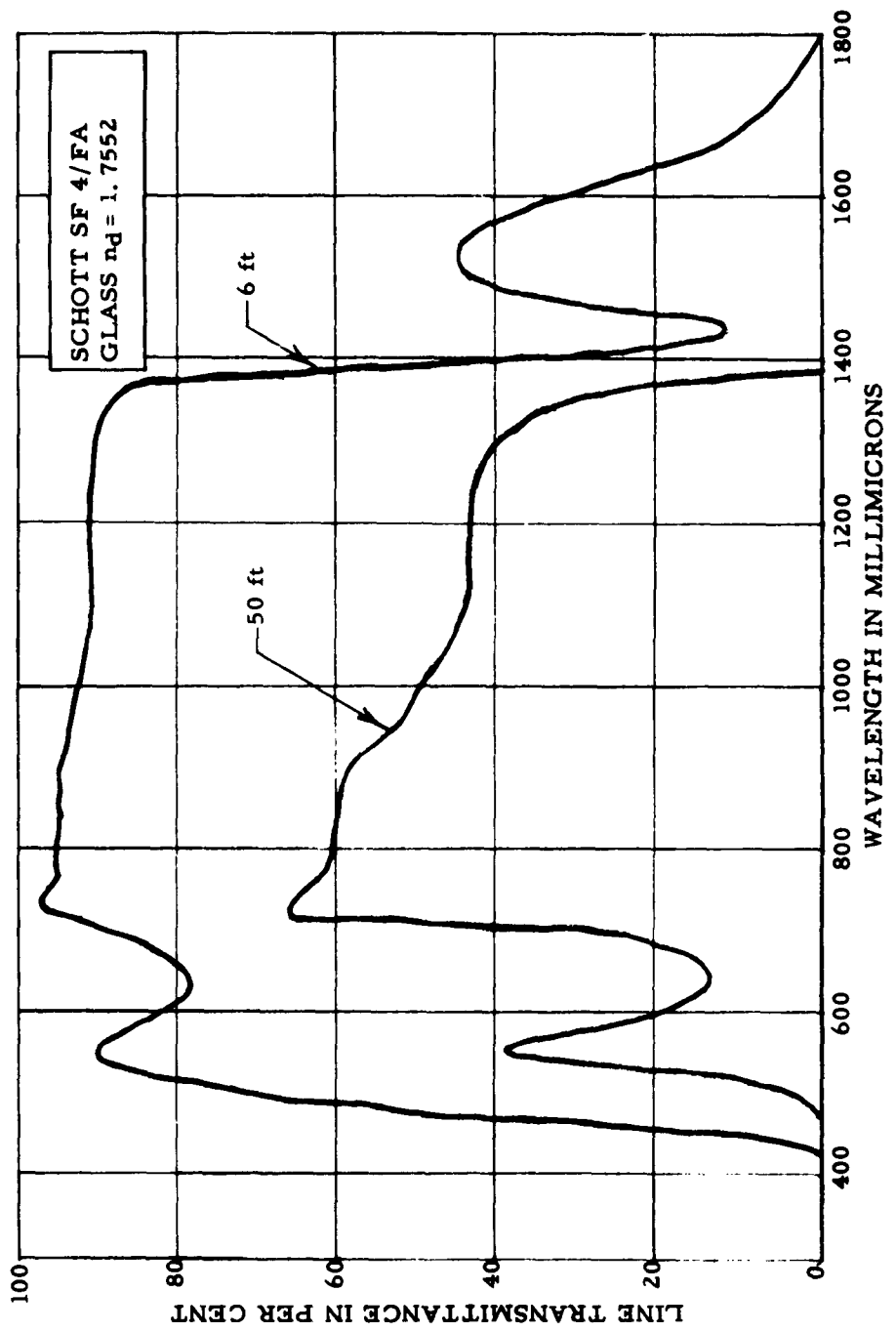


FIGURE 6.
 SPECTRAL TRANSMITTANCE OF SOLID GLASS EXTRAPOLATED
 TO 6 AND 50 FOOT THICKNESSES FROM MEASUREMENTS ON A 4 INCH BLOCK

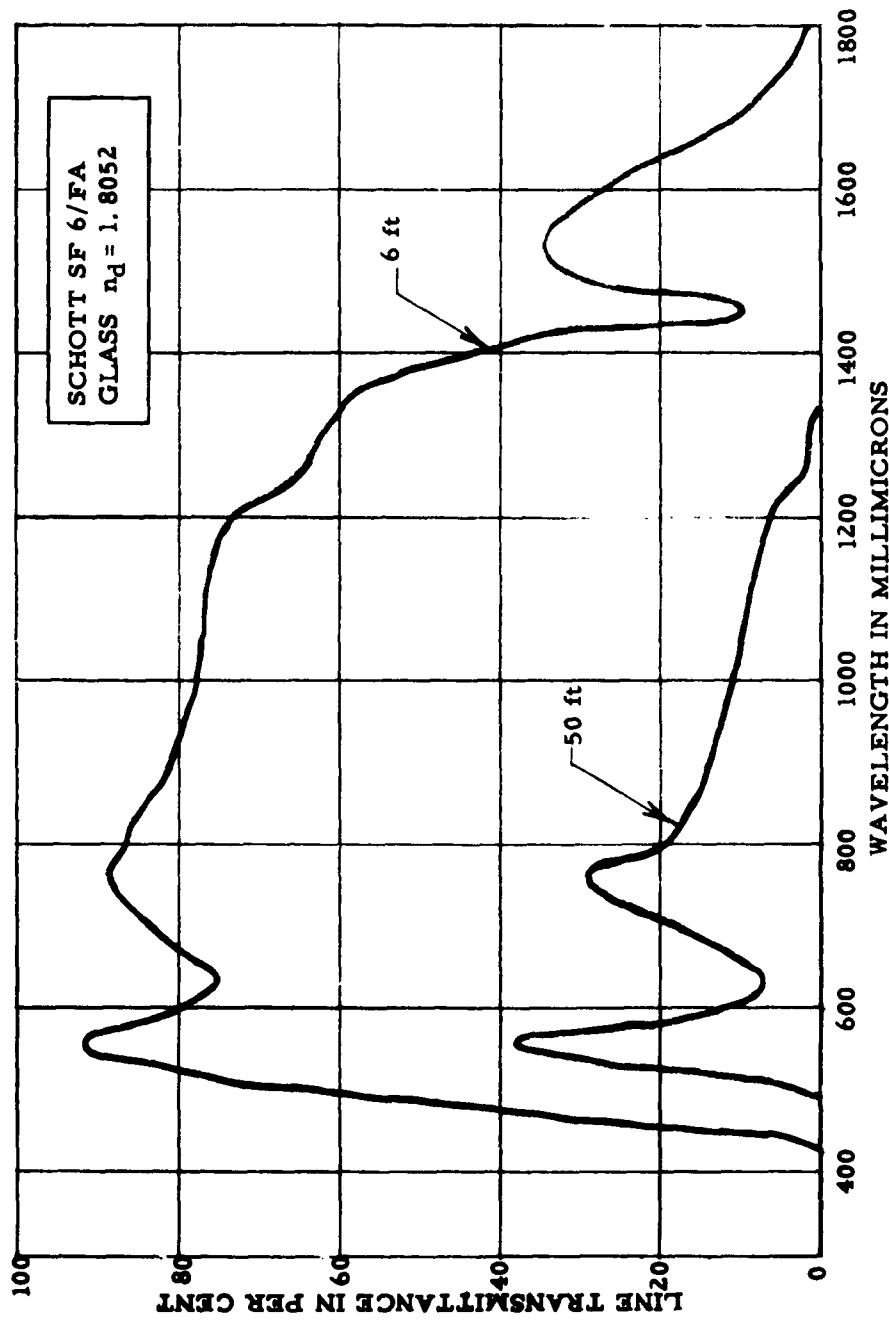


FIGURE 7.
 SPECTRAL TRANSMITTANCE OF SOLID GLASS EXTRAPOLATED
 TO 6 AND 50 FOOT THICKNESSES FROM MEASUREMENTS ON A 4 INCH BLOCK

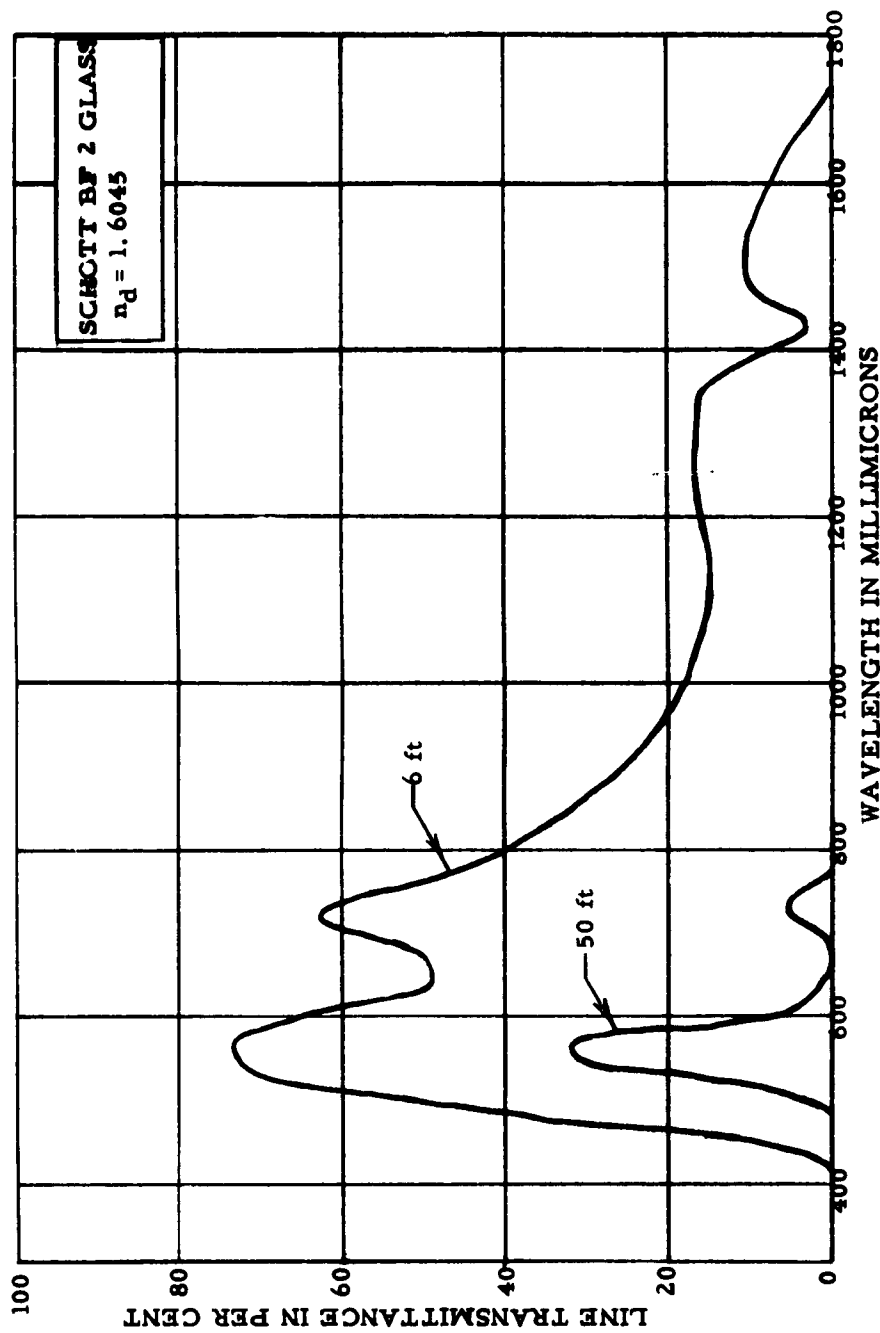


FIGURE 8.
 SPECTRAL TRANSMITTANCE OF SOLID GLASS EXTRAPOLATED
 TO 6 AND 50 FOOT THICKNESSES FROM MEASUREMENTS ON A 4 INCH BLOCK

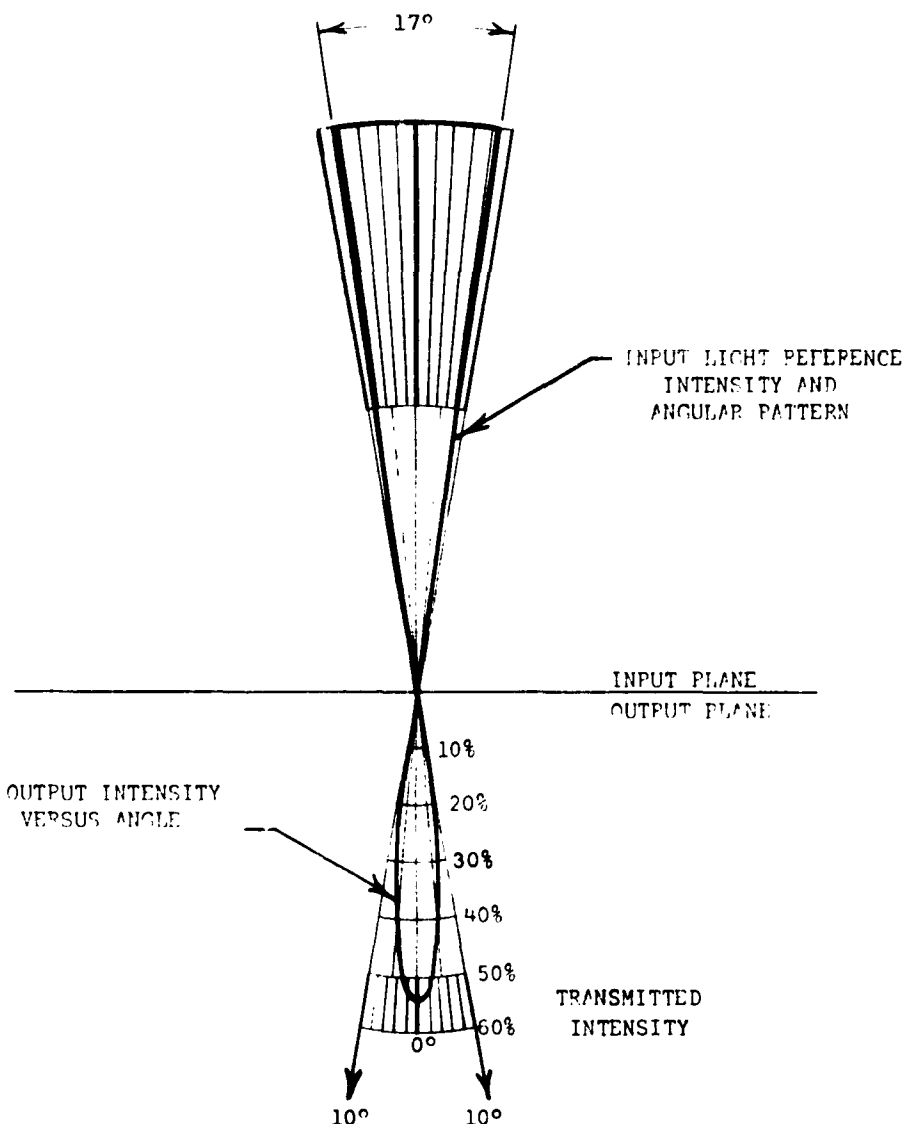


Figure 9. Fiber radiation pattern with 17° input cone.
 Core: SF 4 glass ($n=1.755$)
 Cladding: R-6 glass ($n=1.520$)

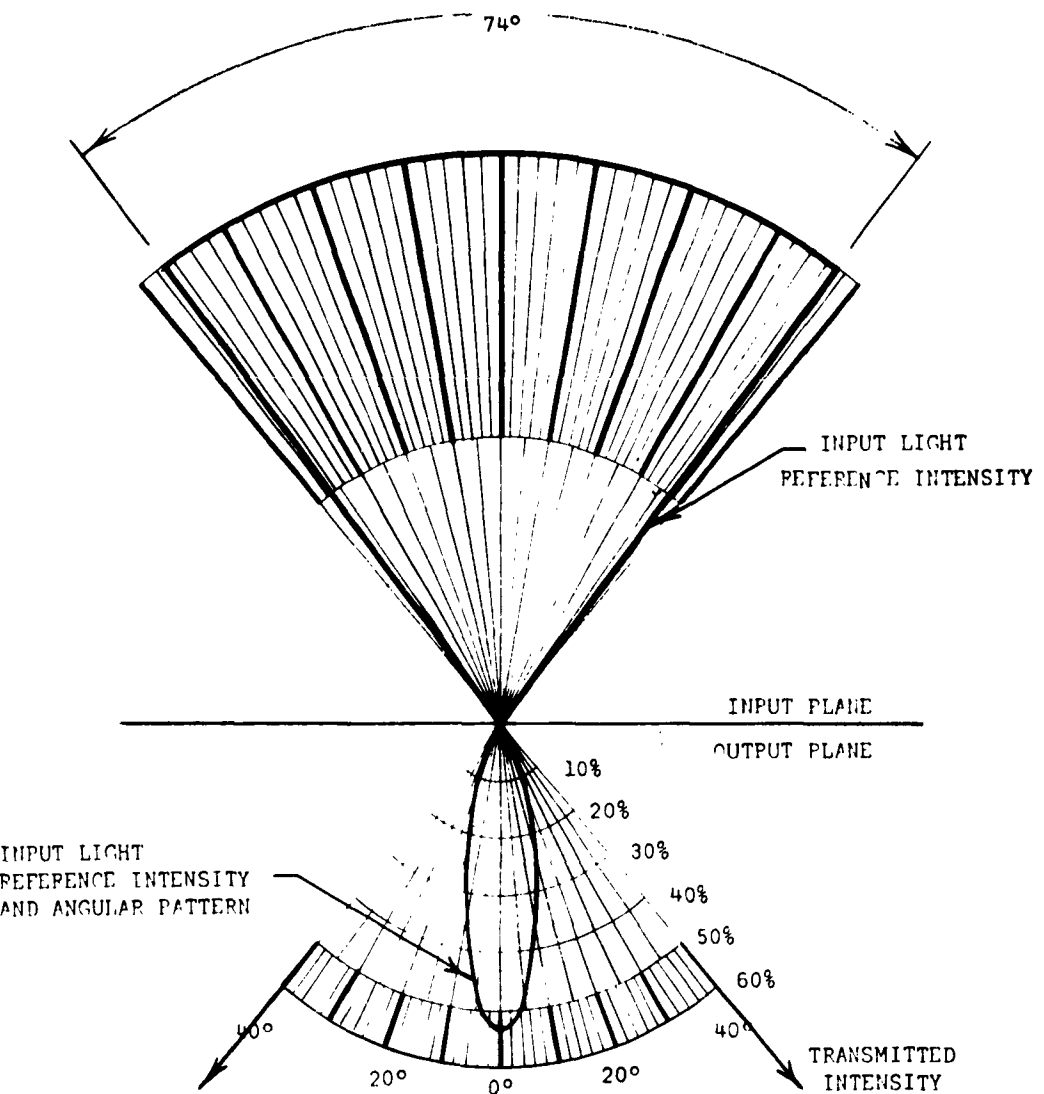


Figure 10. Fiber Radiation Pattern with 74° input cone.

Core: SF 4 glass ($n=1.755$)

Cladding: R-6 glass ($n=1.520$)

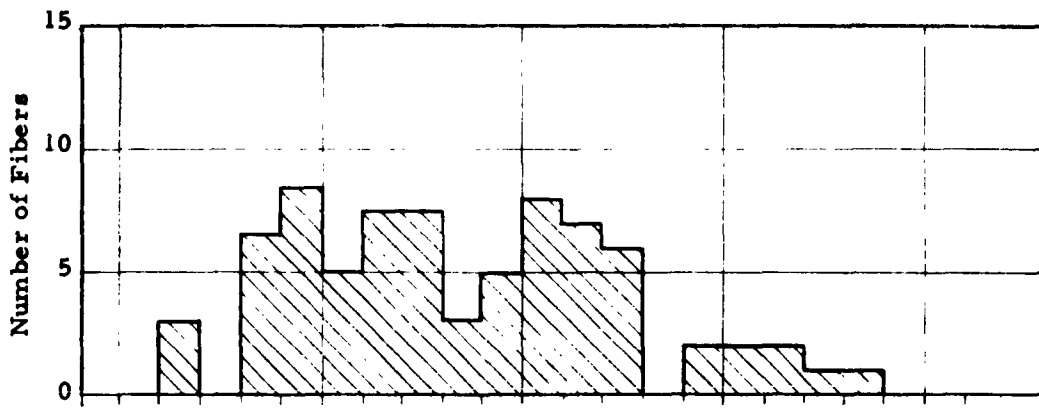


Figure 11a.

F 2/R-6/KG-12 Multifibers (total: 75).

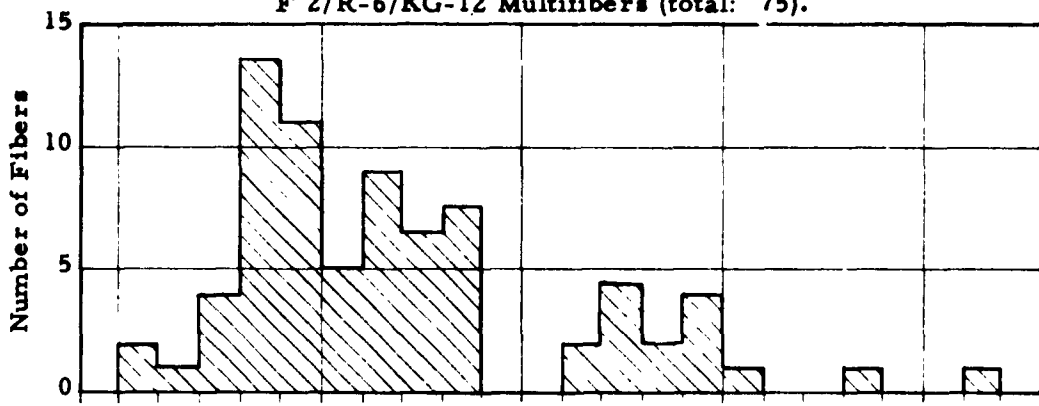


Figure 11b.

F 2/R-6/KG-12 Multifibers (total: 75).

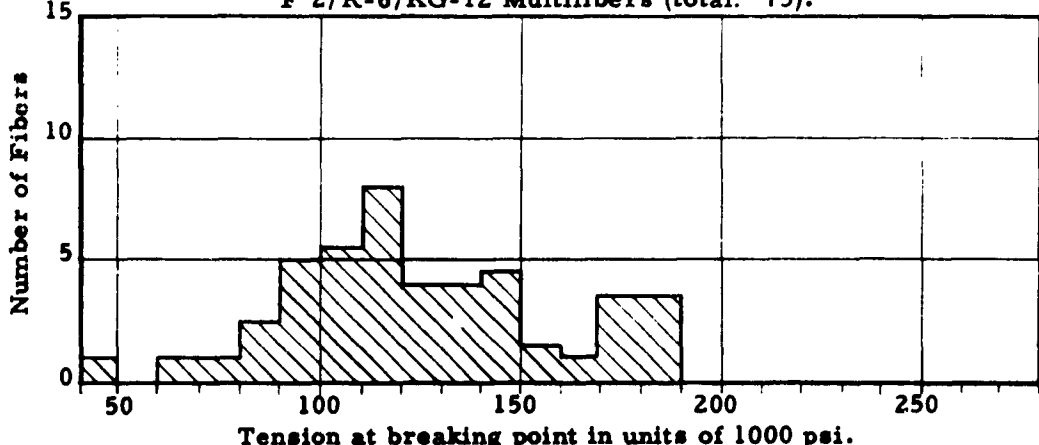


Figure 11c.

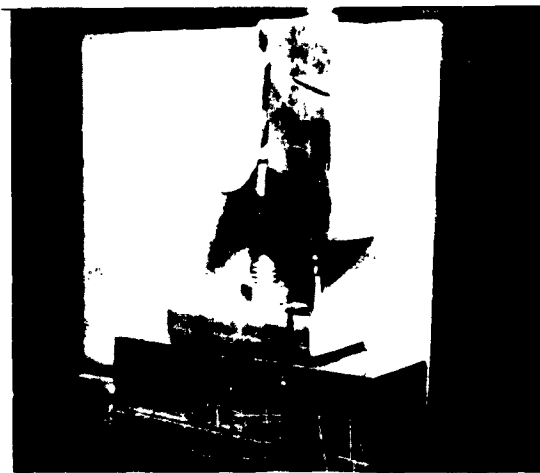
BF-2/KG-12 Monofibers (total: 50).

FIGURE 11. FREQUENCY OF BREAKAGE VS. TENSION FOR THREE GROUPS OF FIBERS.

Glass fiber positioned on mounting plate of shear test jig. Clamp and shearing pin in open position. →



← Glass fiber locked in position on jig. Shearing pin resting on fiber.



Force on shearing pin being increased slowly to determine shear point of glass fiber. →

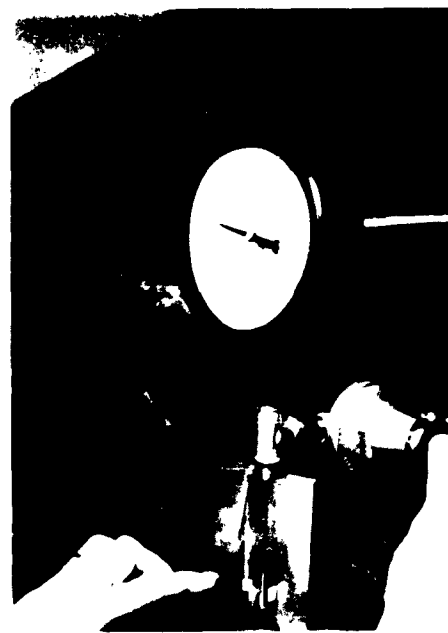


FIGURE 12. SHEAR STRENGTH APPARATUS

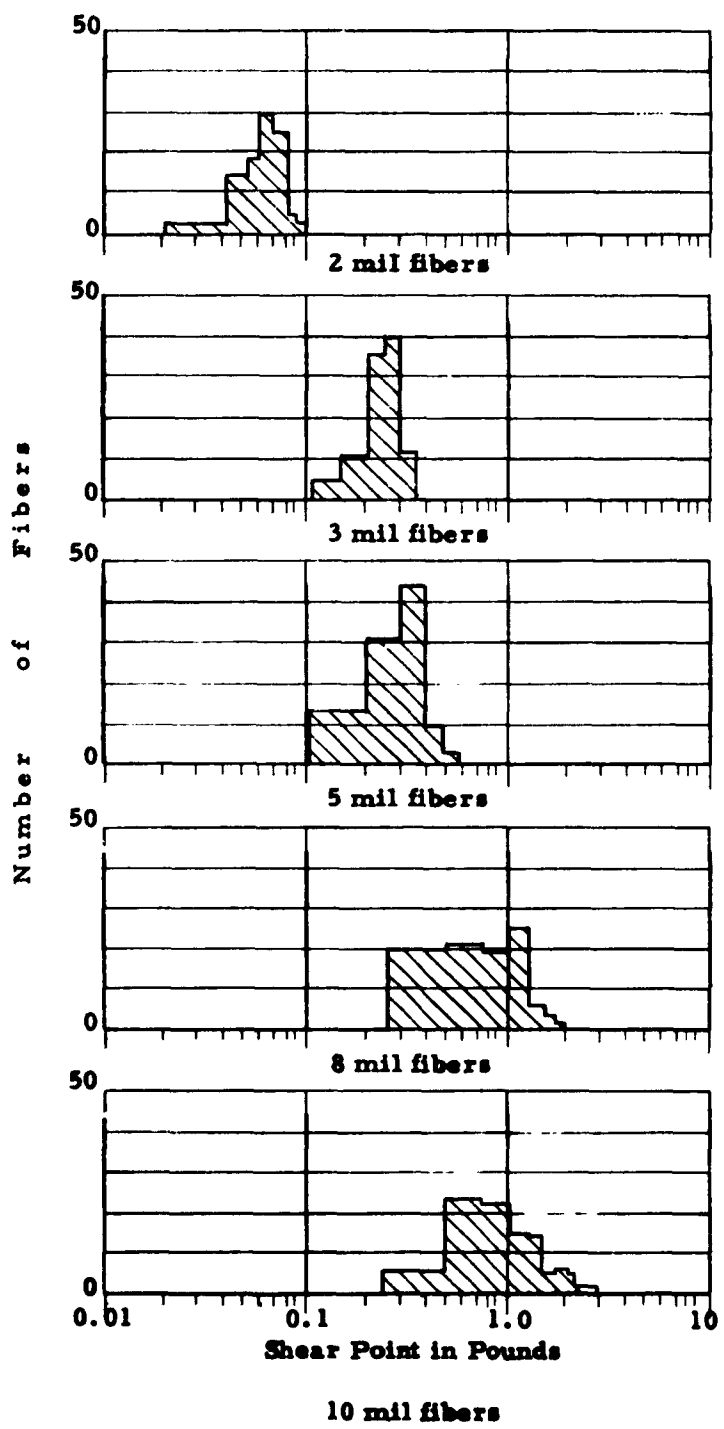


FIGURE 13. DISTRIBUTION OF SHEAR POINTS FOR MONO-FIBERS OF VARIOUS DIAMETERS.

Test fiber being guided around guide ring to form loop.



Ends of fiber grasped, and tension applied.



**Diameter of fiber loop decreasing under tension.
(Wire used in photo for visibility.)**



FIGURE 14. TEST FOR MINIMUM BEND RADIUS OF GLASS FIBERS.

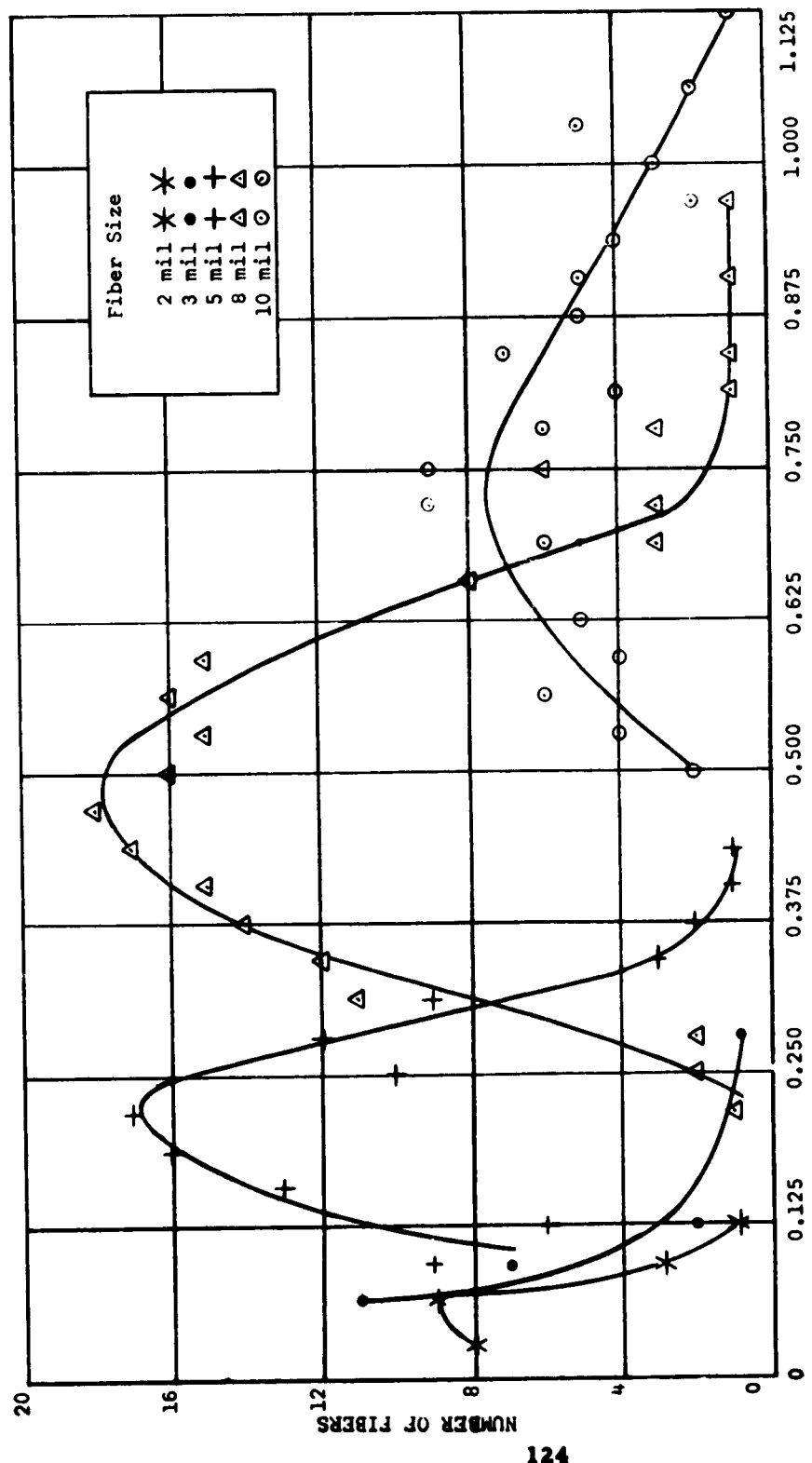


Figure 15. Frequency of breakage vs. radius for several fiber diameters.

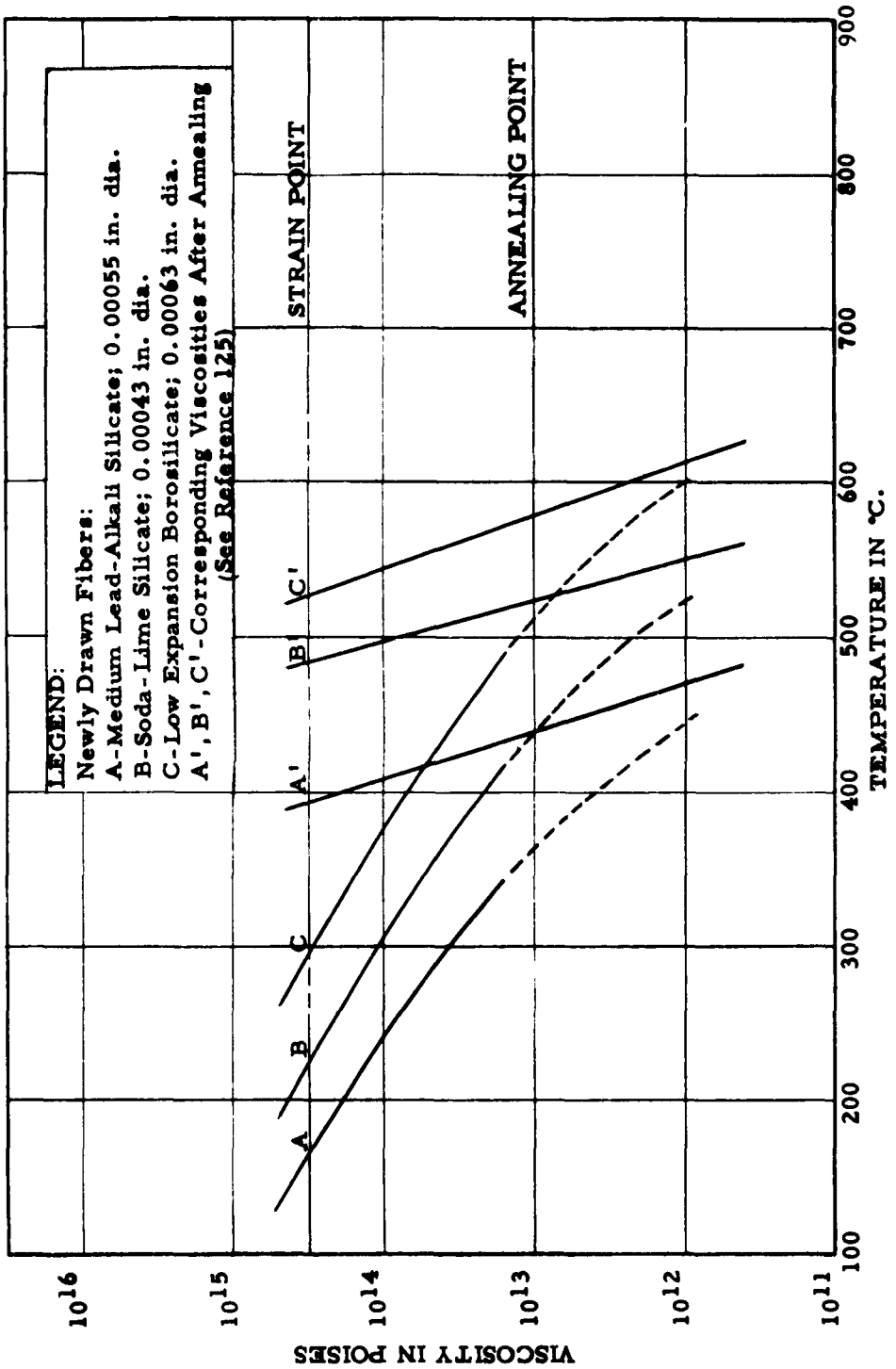


FIGURE 16. TYPICAL FIBER VISCOSITIES VS. TEMPERATURE

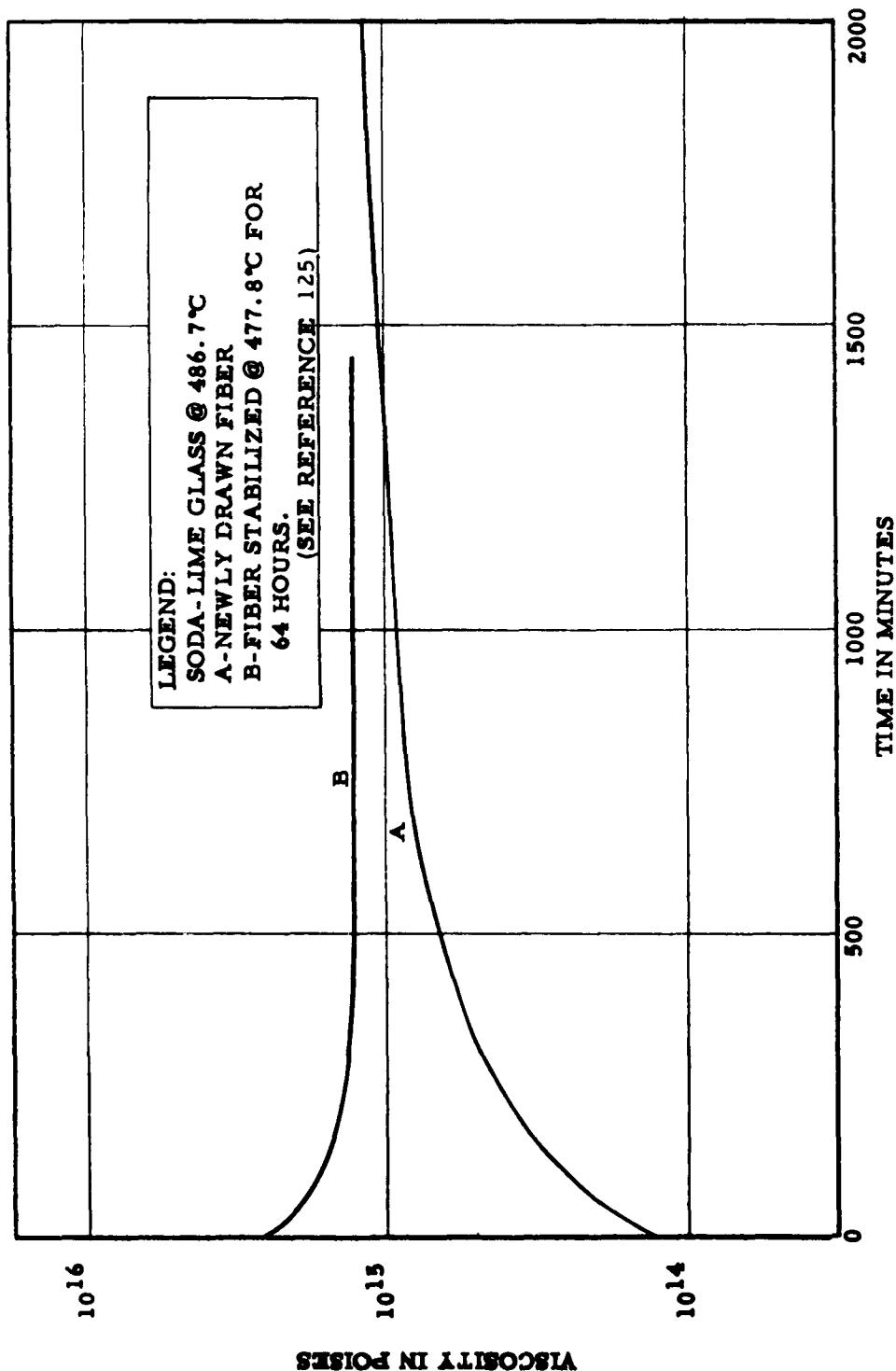


FIGURE 17. TYPICAL VISCOSITY-TIME CURVES

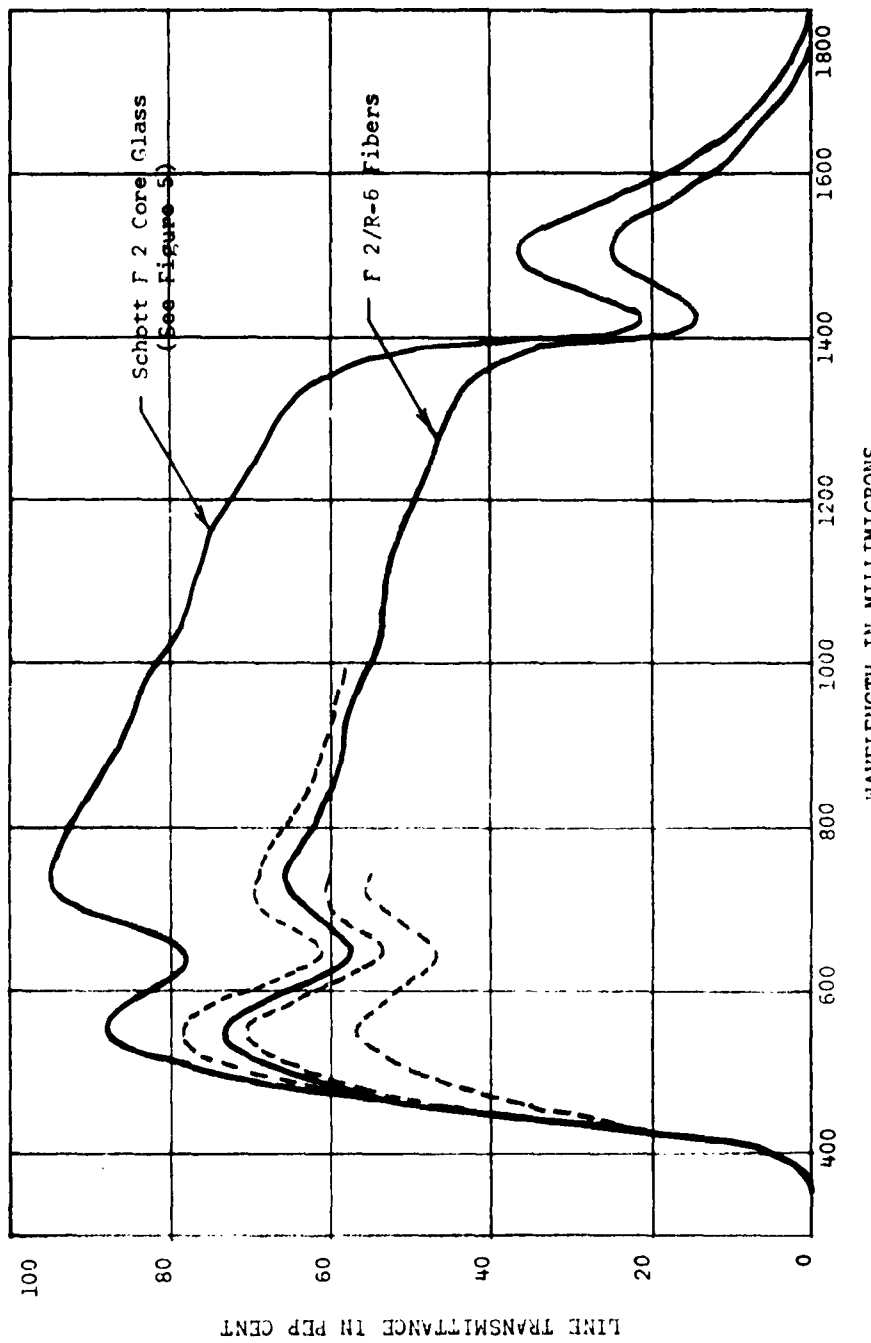


Figure 18. Comparison of core and clad-core transmittance (theoretical).

Broken lines show observed values for three "F 2/R-6" light pipes. See Paragraph 3.1.1.

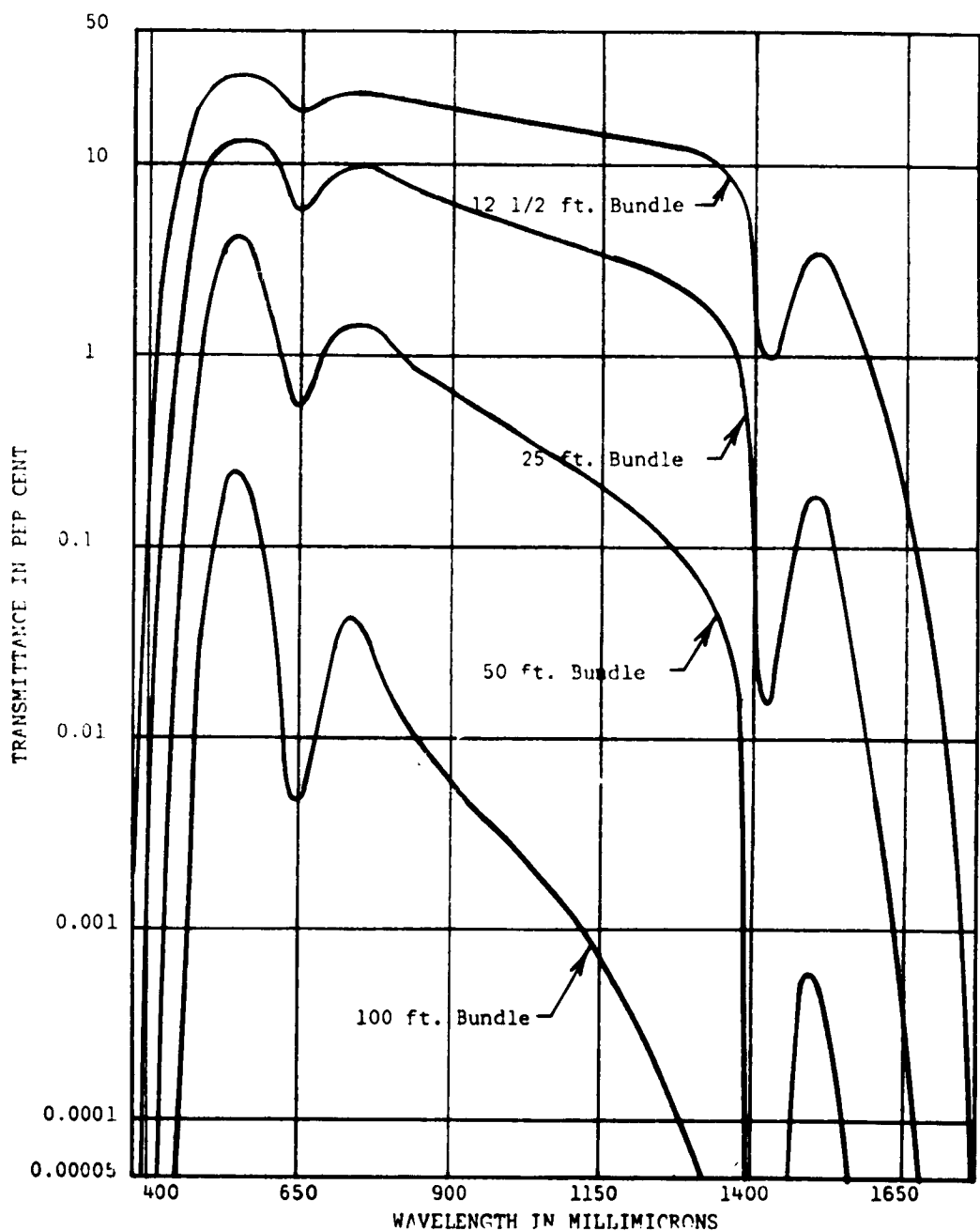


Figure 19. Theoretical spectral transmittance of four fiber bundles with 70% area factor. (See Paragraph 3.1.1.)

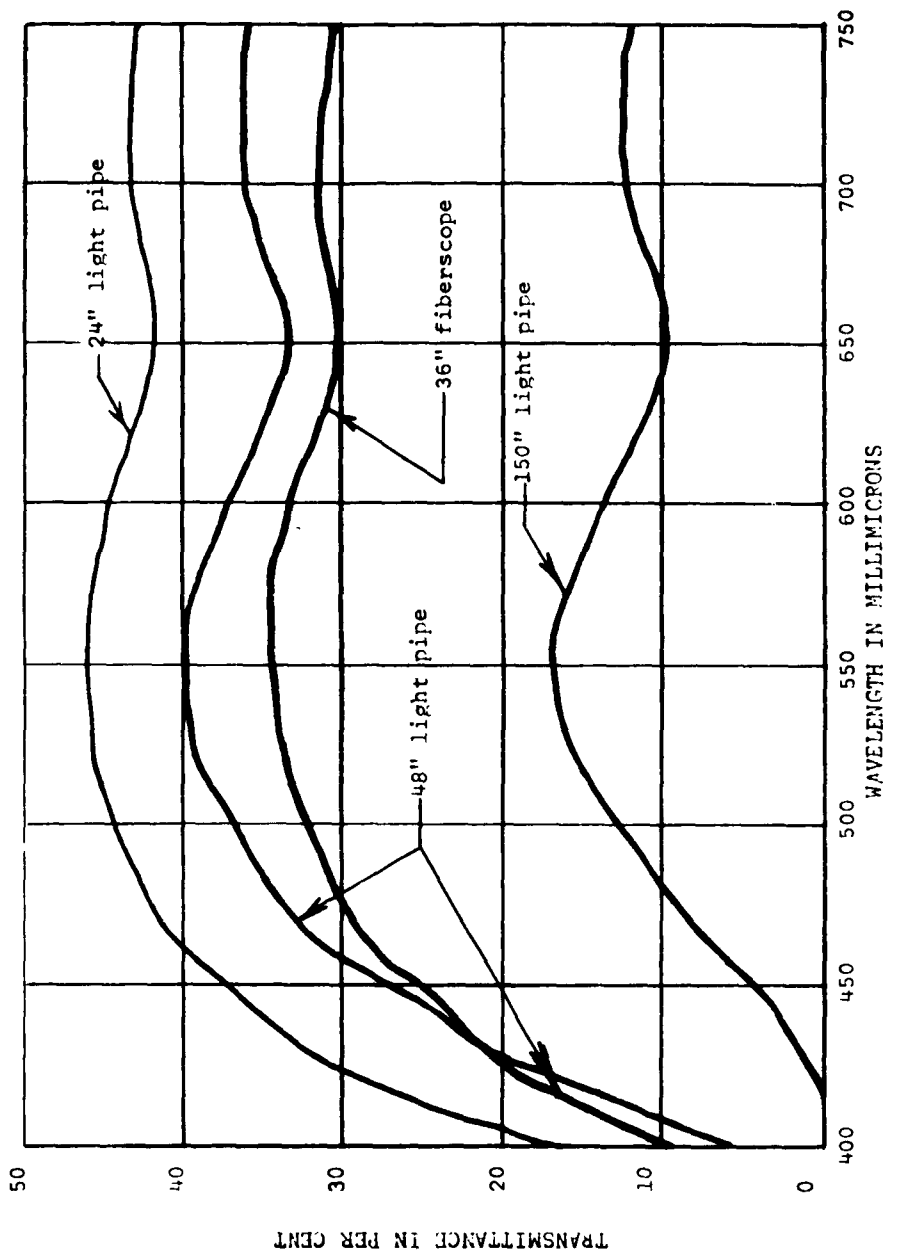
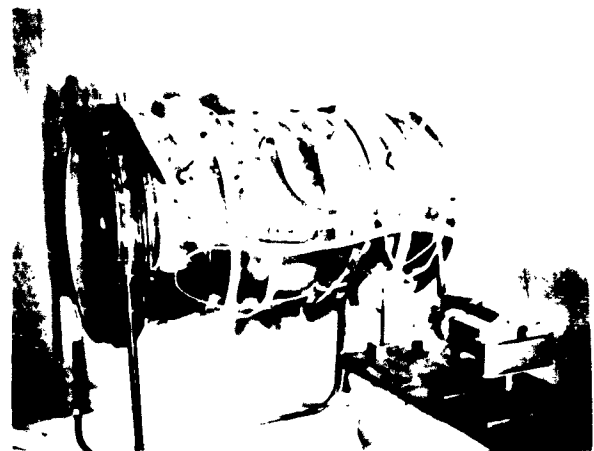
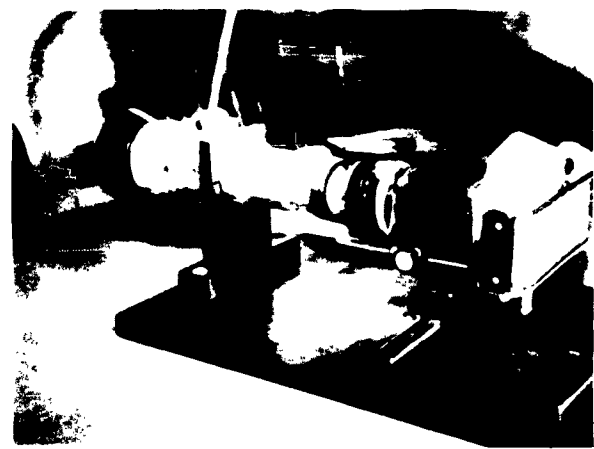


Figure 20. Reproduction of direct spectrophotometric curves for four fiber bundles, including lens losses (See Paragraph 3.1.1, Table 3.)

Jet engine mockup and optical imaging setup.



Imaging setup, showing zoom lens, a fiberscope faceplate, and camera.



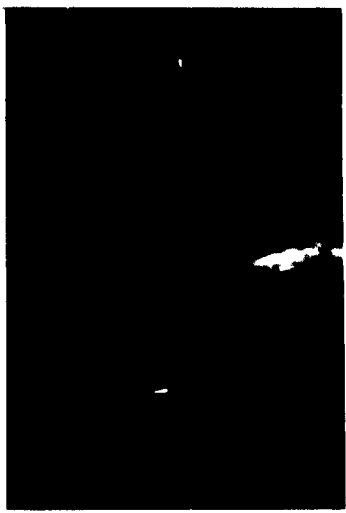
Another view, with simulated engine fire visible.



FIGURE 21. TYPICAL ARRANGEMENT FOR FIBER IMAGE STUDIES.



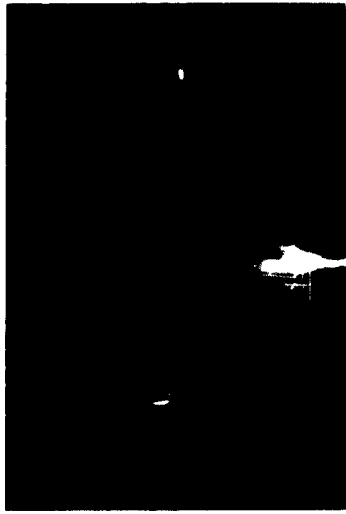
10 feet



20 feet



5 feet

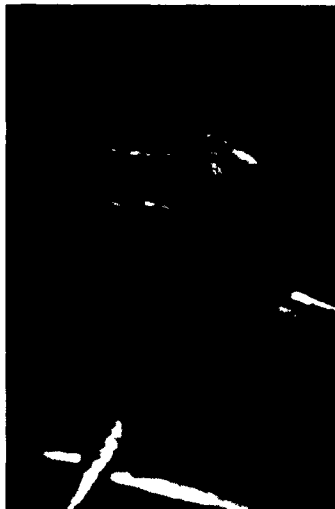


15 feet

FIGURE 22. APPEARANCE OF ENGINE FIRE THROUGH SIMULATED THICKNESSES
OF FUSED FIBER FACEPLATE
Approximately one million fibers shown. See paragraph 3.1.1.



5 feet



10 feet

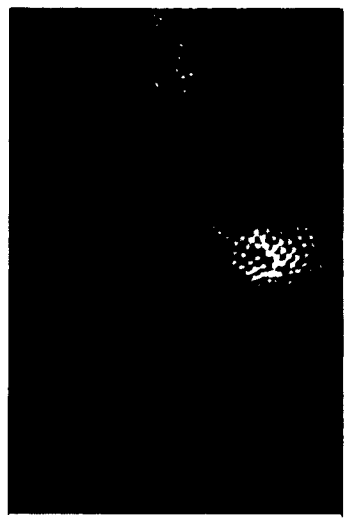


15 feet

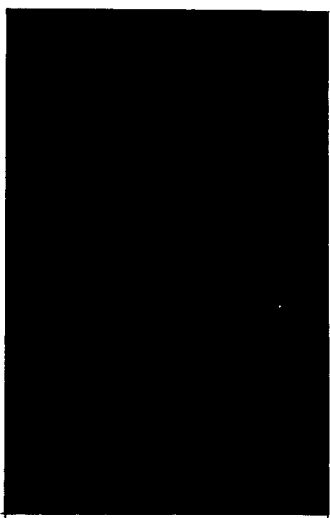


20 feet

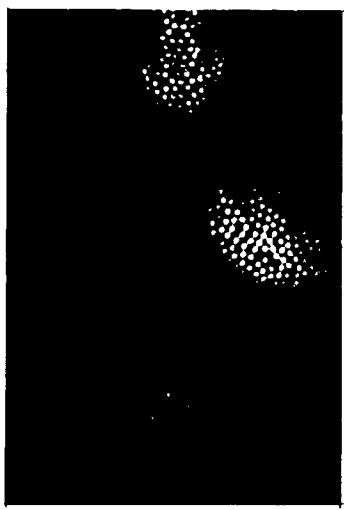
FIGURE 23. APPEARANCE OF ENGINE FIRE
THROUGH SIMULATED LENGTHS OF MULTIFIBERSCOPE
Approximately 100,000 image points shown. See Paragraph 3.1.1.



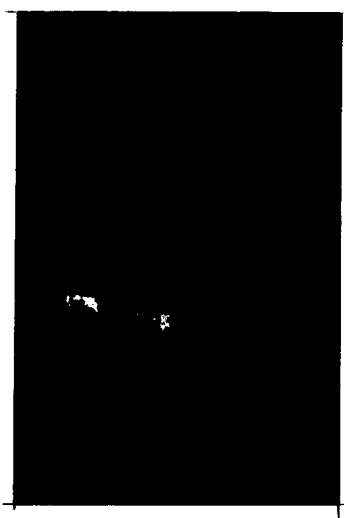
10 feet



20 feet

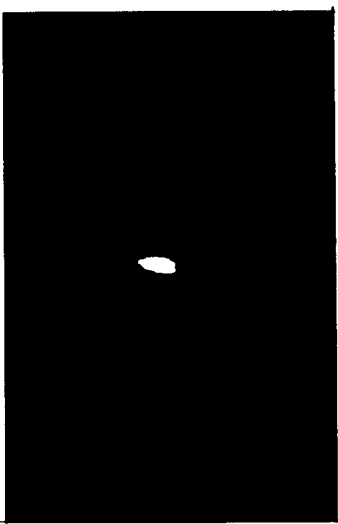


5 feet

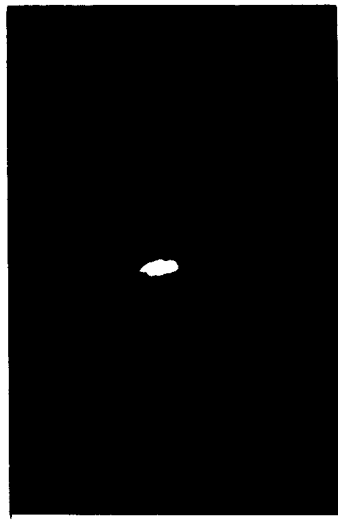


15 feet

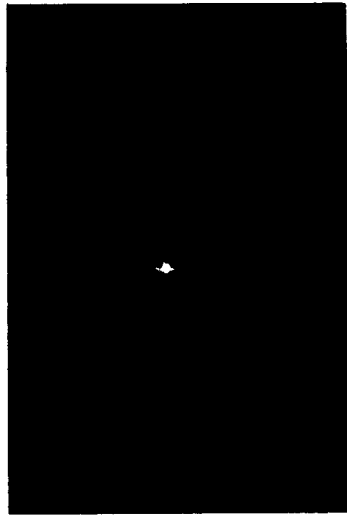
FIGURE 24. LOW RESOLUTION FLAME IMAGE TRANSMITTED BY
SIMULATED LENGTHS OF MONOFILAMENT FIBERSCOPE
(See Paragraph 3.1.1.)



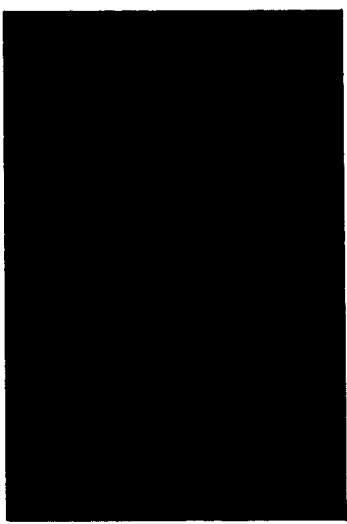
10 feet



20 feet



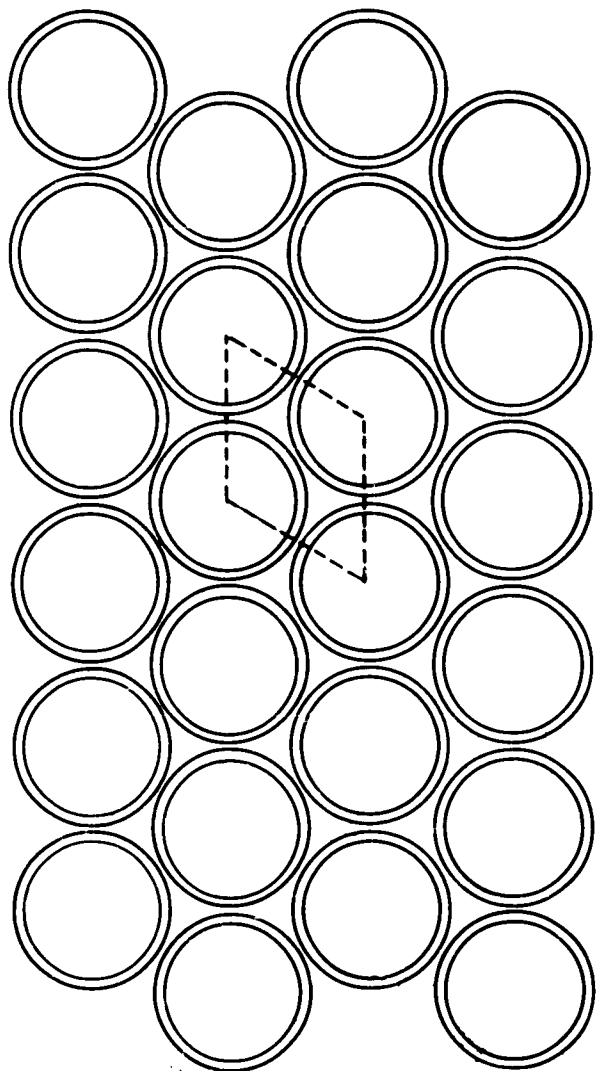
30 feet



40 feet

**FIGURE 25. SMALL FLAME AND GLOWING TURBINE CASING SEEN THROUGH
SIMULATED LENGTHS OF MULTIFIBERSCOPE
(See Paragraph 3.1.1.)**

FIGURE 25. CLOSELY PACKED ARRAY OF FILTER ENDS, TYPICAL, OF LIGHT PIPES.



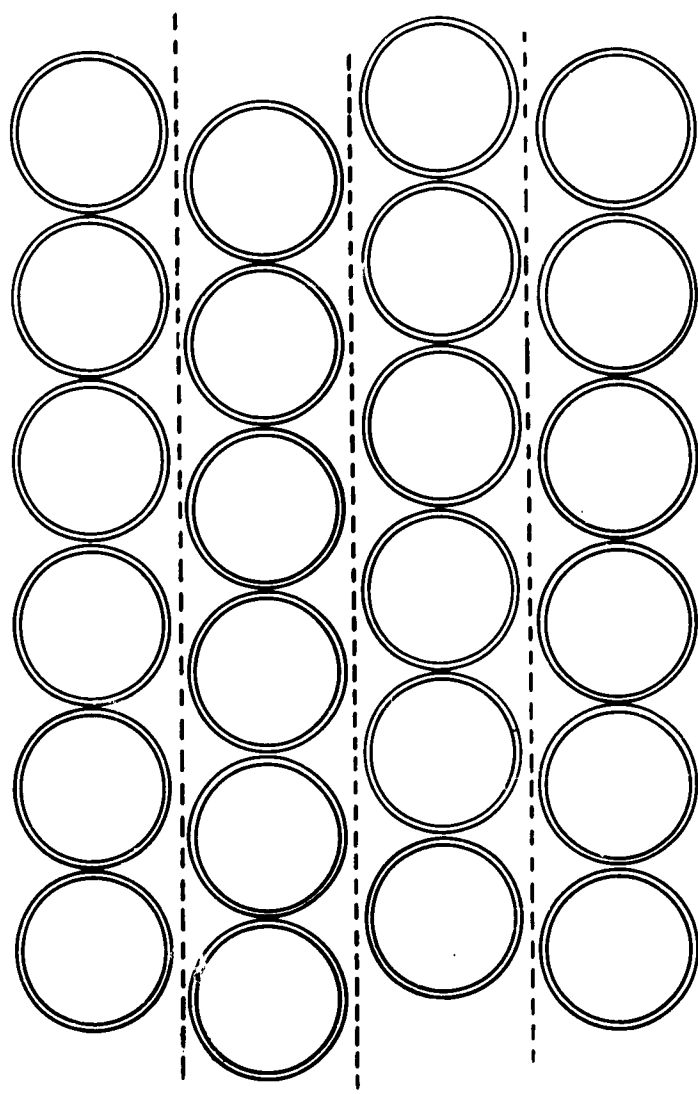


Figure 27. END FACE ARRAY TYPICAL OF MONOFILAMENT FIBERSCOPE.

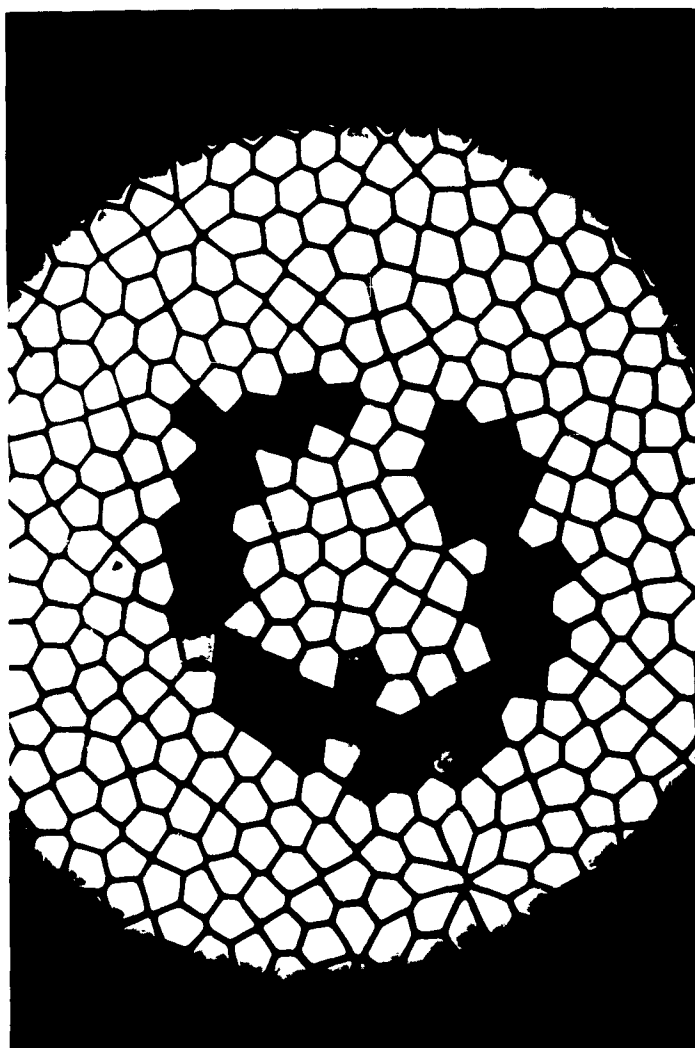


FIGURE 28a. TEST PATTERN IMAGED BY FUSED FACEPLATE WITH "FOUR MIL" FIBERS.

Magnification: approximately 50X.
For comparison with Figures 28b
and 28c.

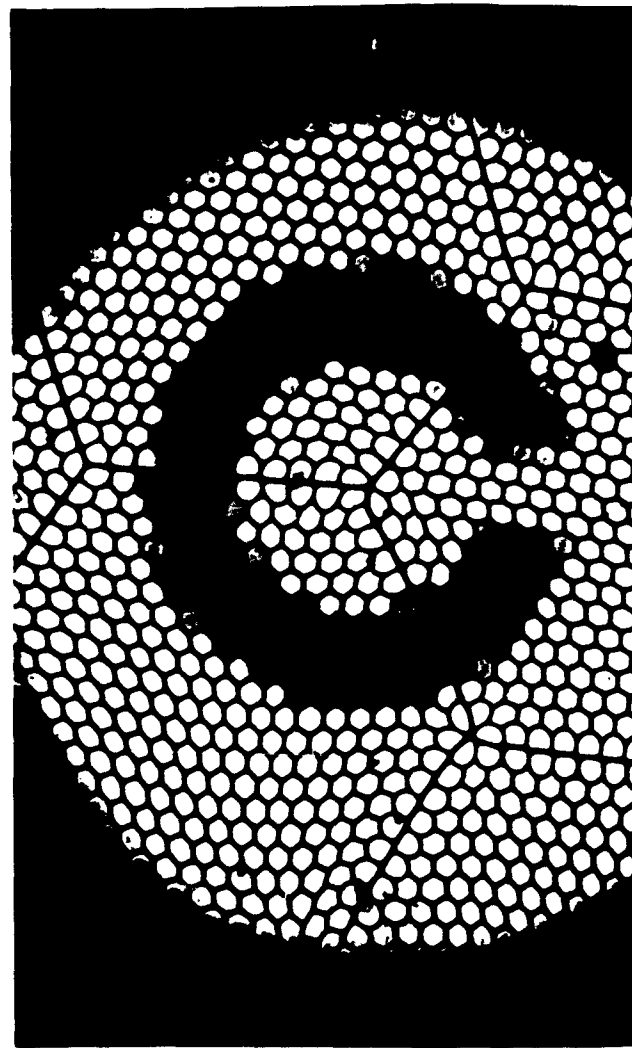


FIGURE 28b. TEST PATTERN IMAGED BY 1 FACEPLATE WITH "TWO MIL FIBERS.

Magnification: approximately 50X.
For comparison with Figures 2
and 28c.

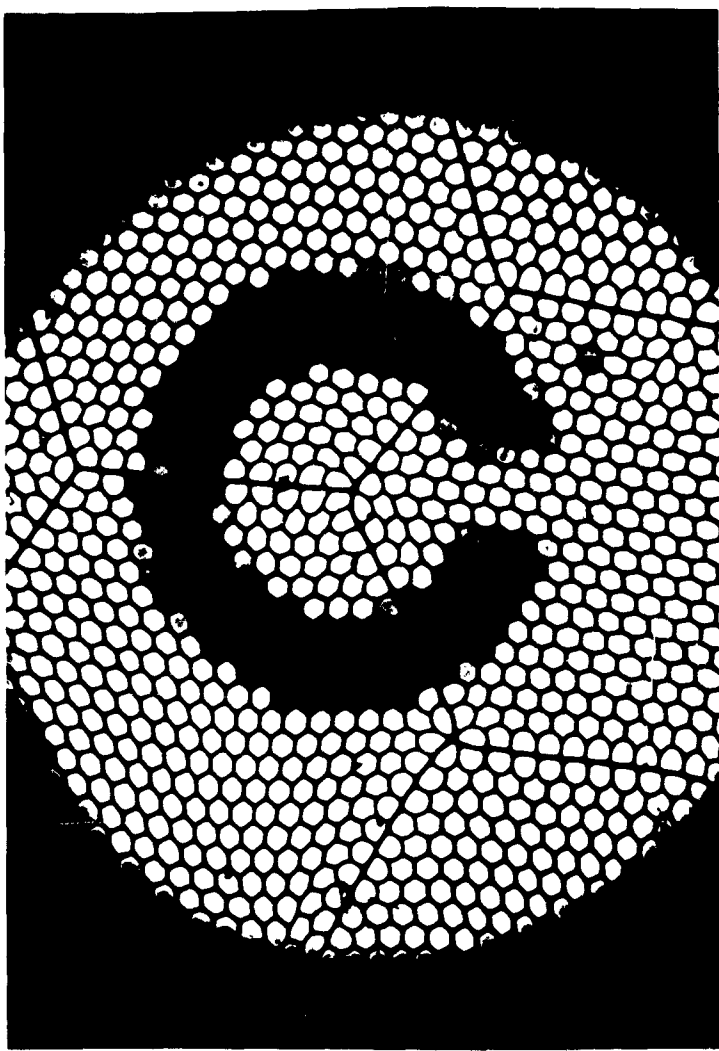


FIGURE 28b. TEST PATTERN IMAGED BY FUSED FACEPLATE WITH "TWO MIL" FIBERS.

Magnification: approximately 50X.
For comparison with Figures 28a
and 28c.

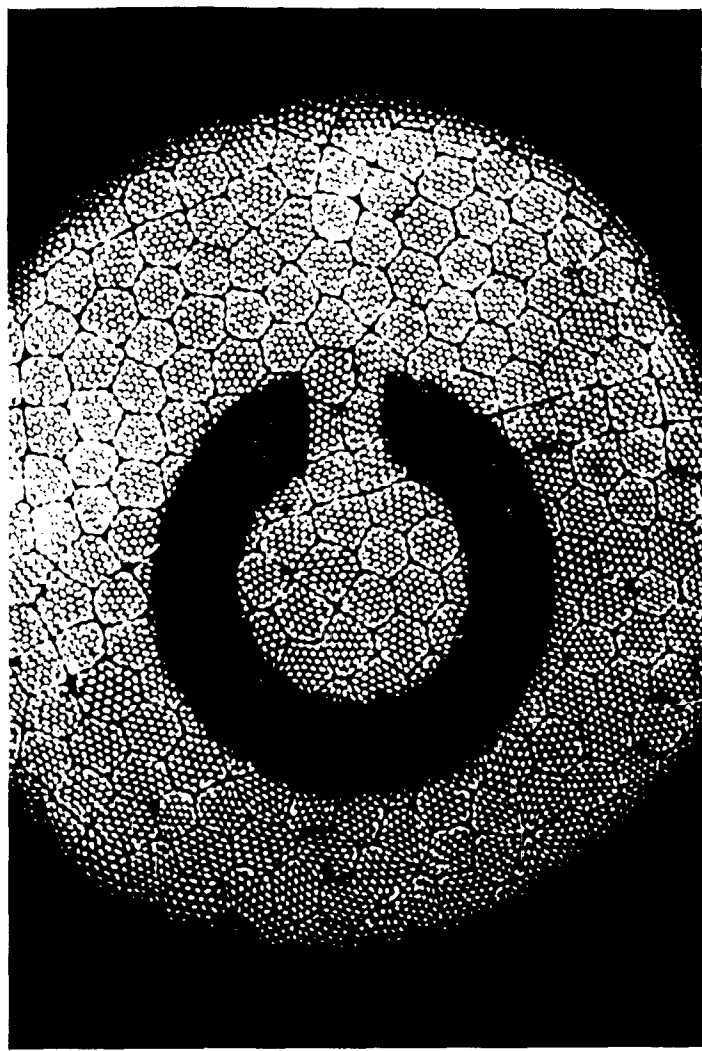
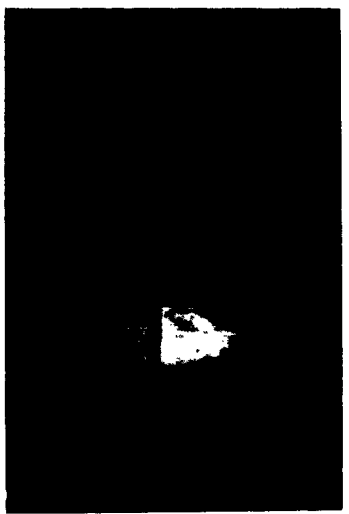


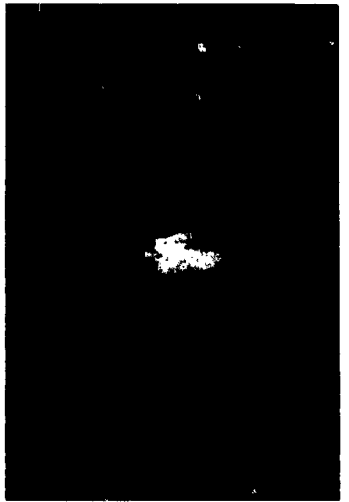
FIGURE 28c. TEST PATTERN IMAGED BY FUSED FACEPLATE WITH "HALF MIL" FIBERS.

Magnification: approximately 50X.
For comparison with Figures 28a
and 28b.

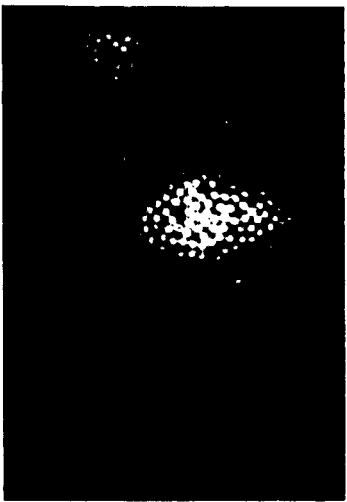
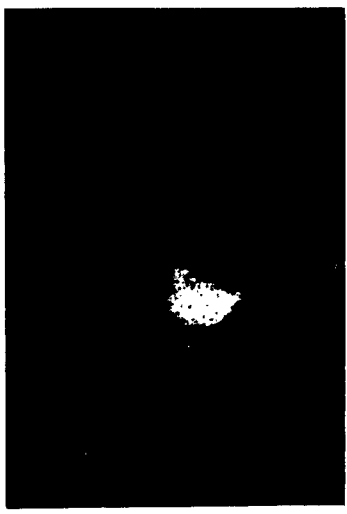




One Million (estimated) Half-mil Fibers.



Fifty Thousand (estimated) One-mil Fibers.



Ten Thousand (estimated) Two-mil Fibers.

One Thousand (estimated) Eight-mil Fibers.

FIGURE 29. IMAGE CLARITY AS AFFECTED BY NUMBER OF FIBERS PER IMAGE
(See Paragraph 3.1.3.)



FIGURE 30. PERCEPIBILITY OF INCANDESCENT TURBINE CASING VERSUS APPARENT IMAGE SIZE.
(See Paragraph 3.1.4.)

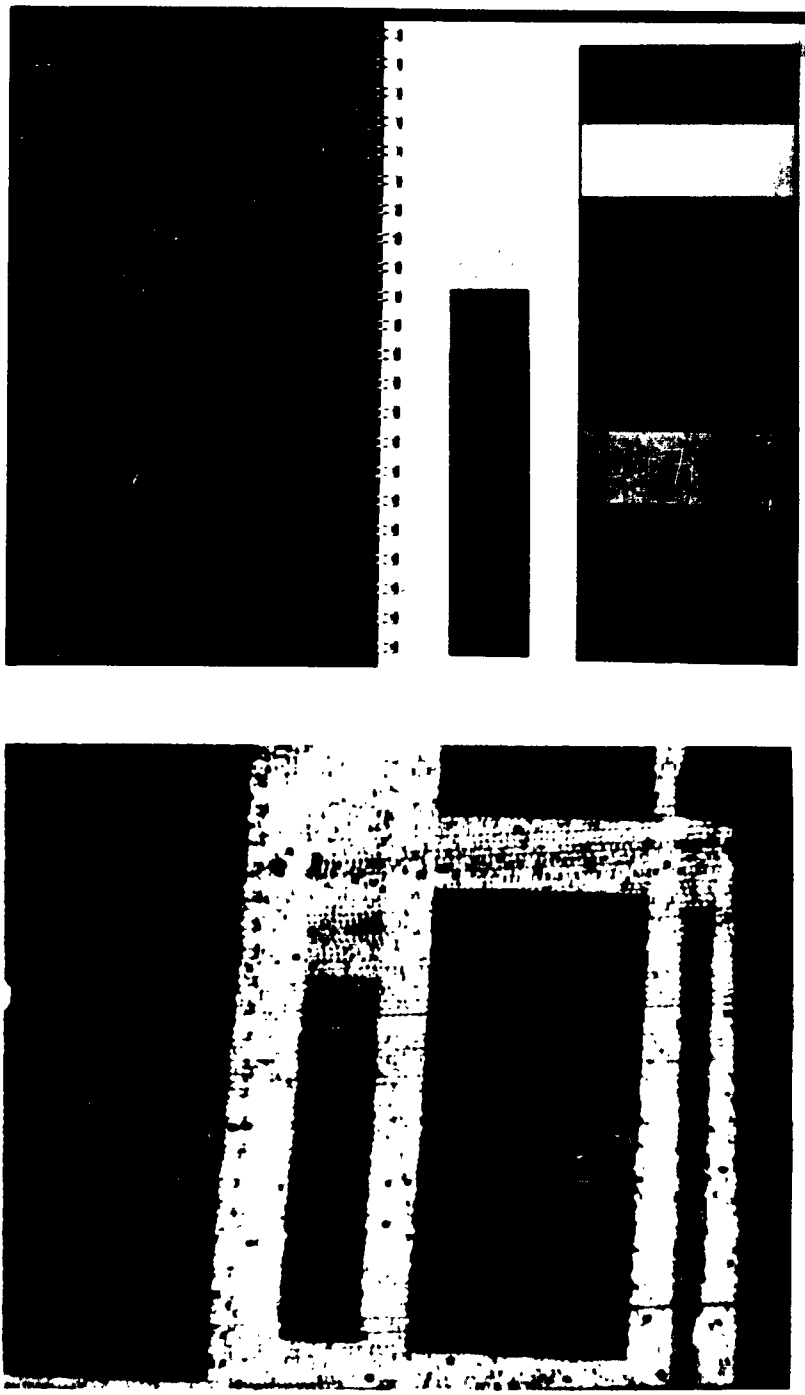


Figure 31. Color test chart photographed directly and through 25 foot fiberscope.

(See Paragraph 3.1.6.)

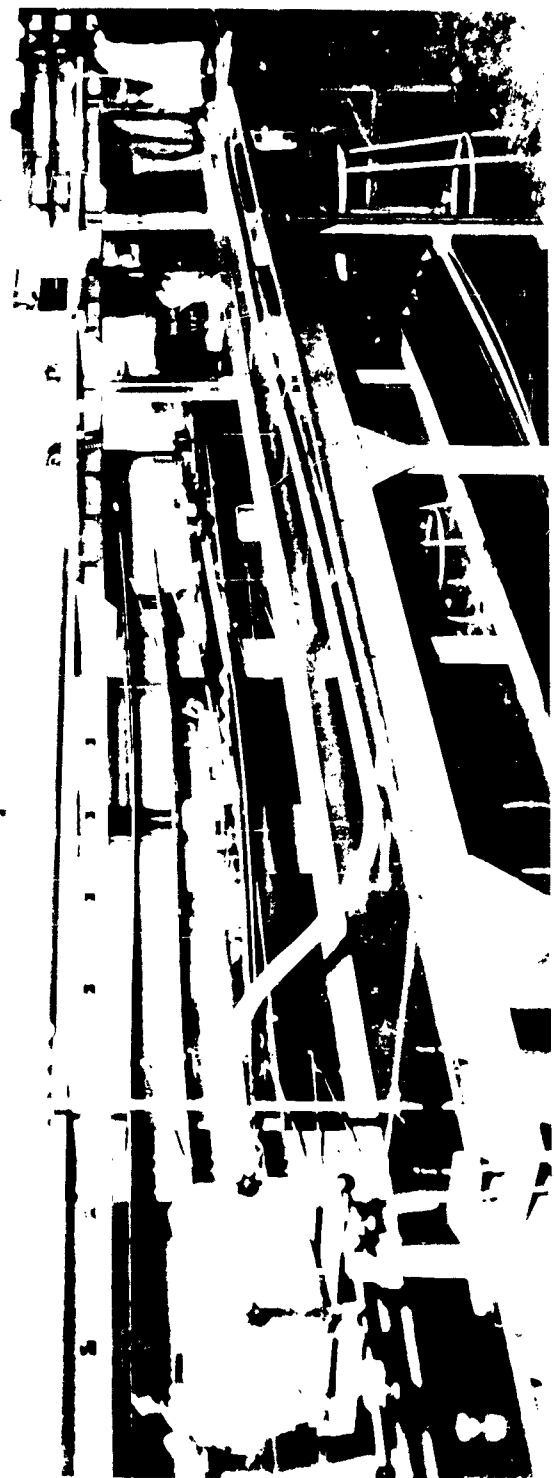


FIGURE 32. PAIR OF JOINED 12½-FOOT FIBERSCOPES USED IN PREPARING FIGURE 31.

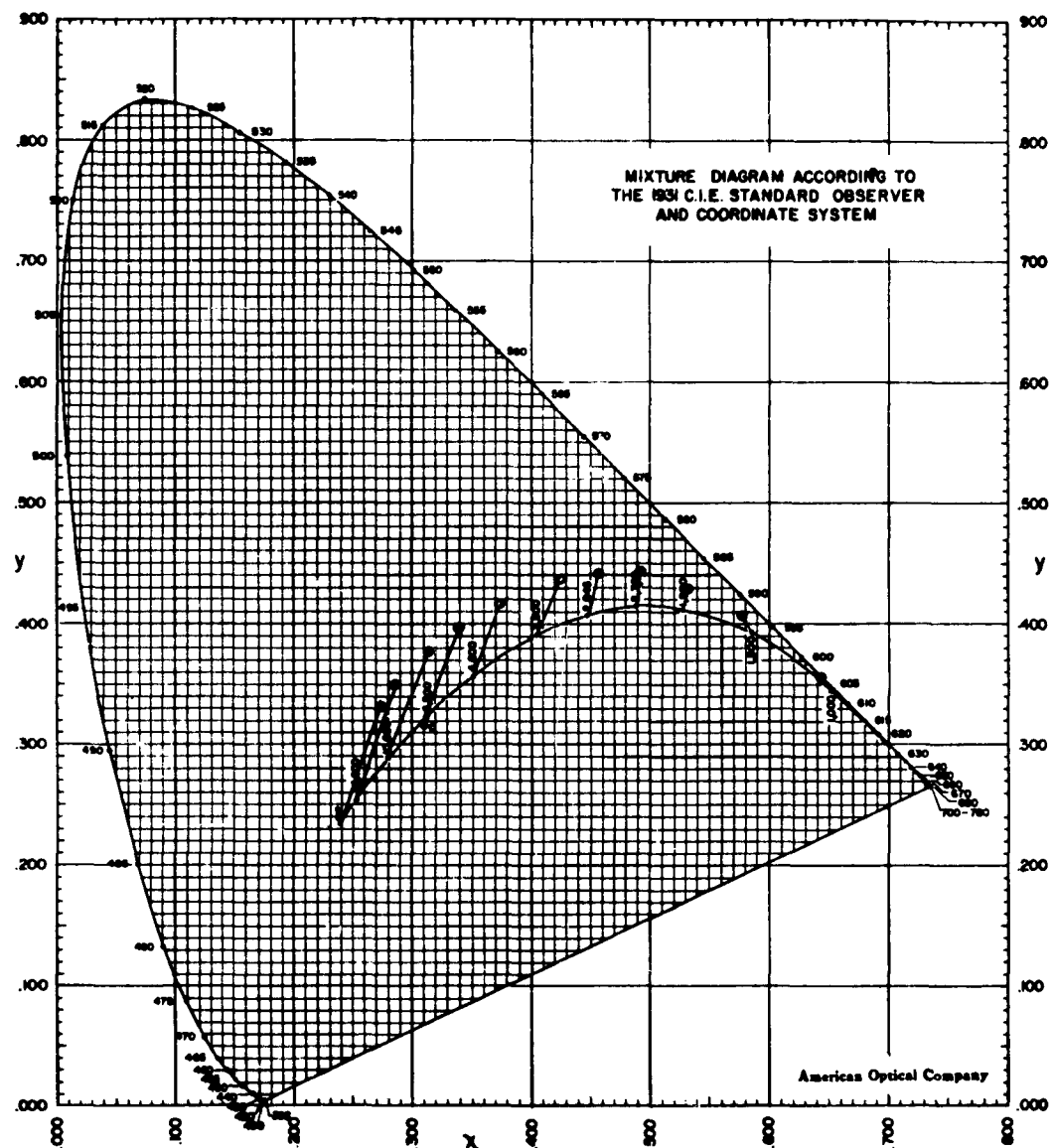
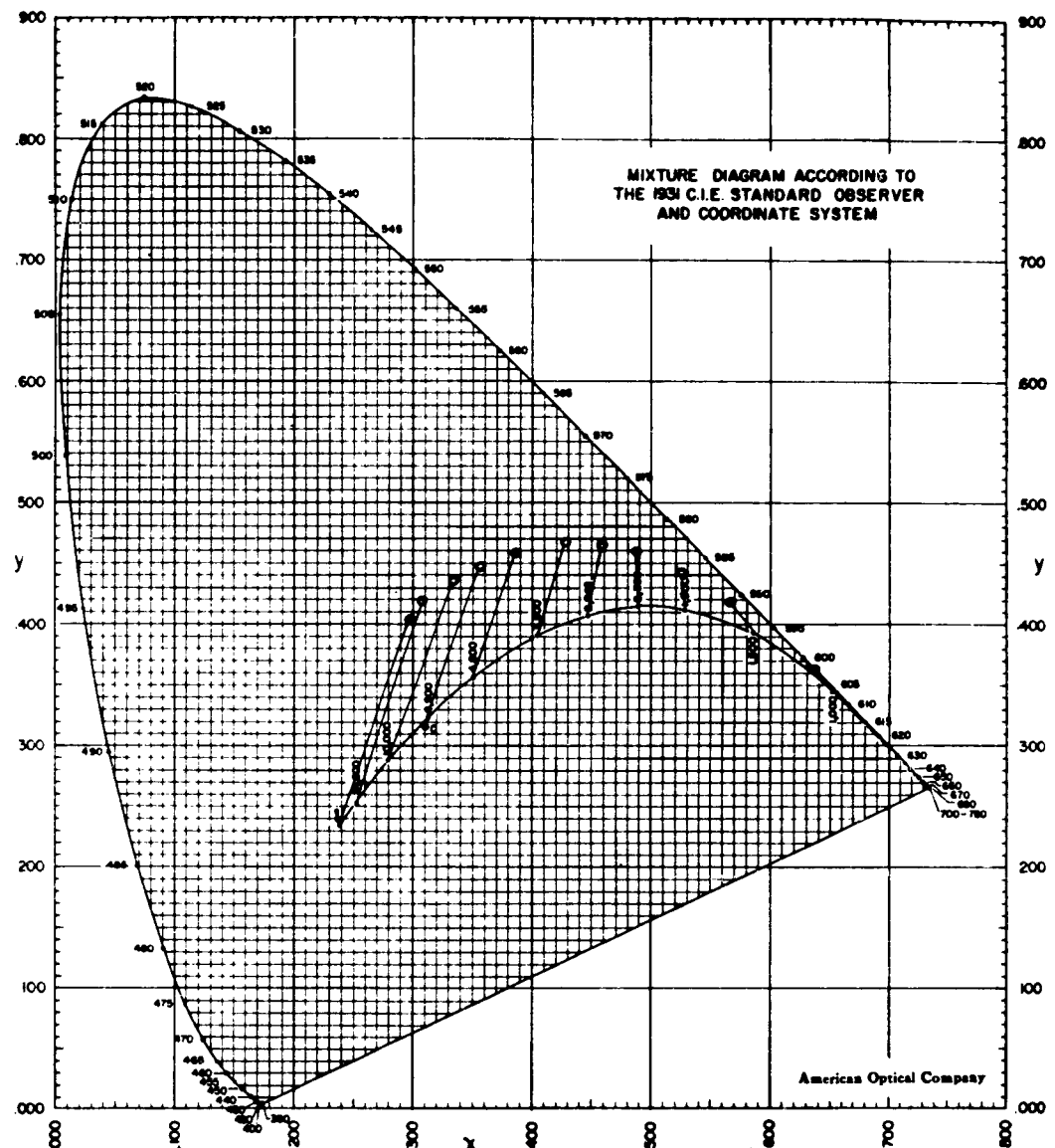


Figure 33. Color effects of 6-1/4 foot long fiber bundle on selected blackbody temperatures (See Paragraph 3.1.6.)



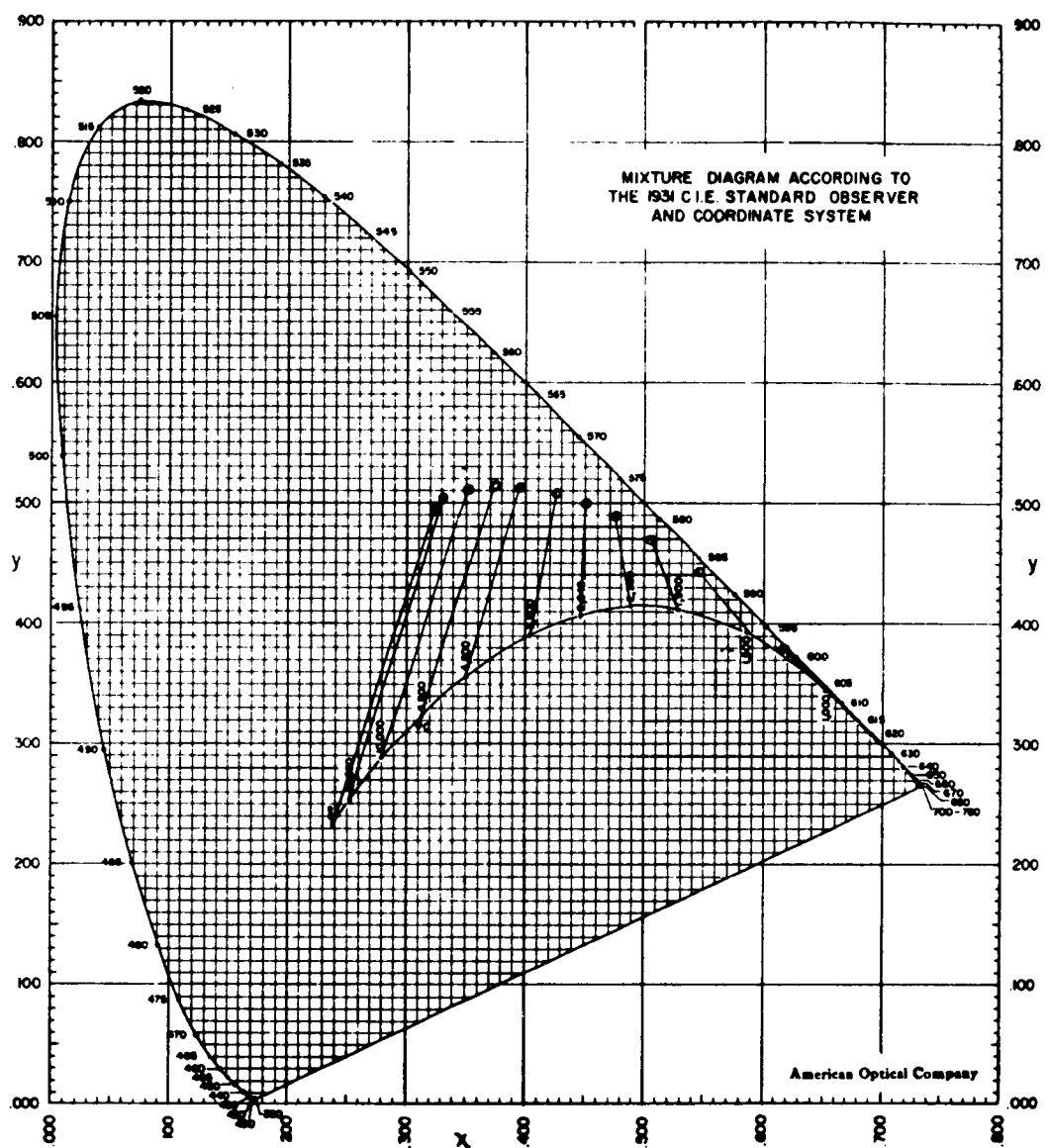


Figure 35. Color effects of 25 foot long fiber bundle on selected blackbody temperatures (See Paragraph 3.1.6.)

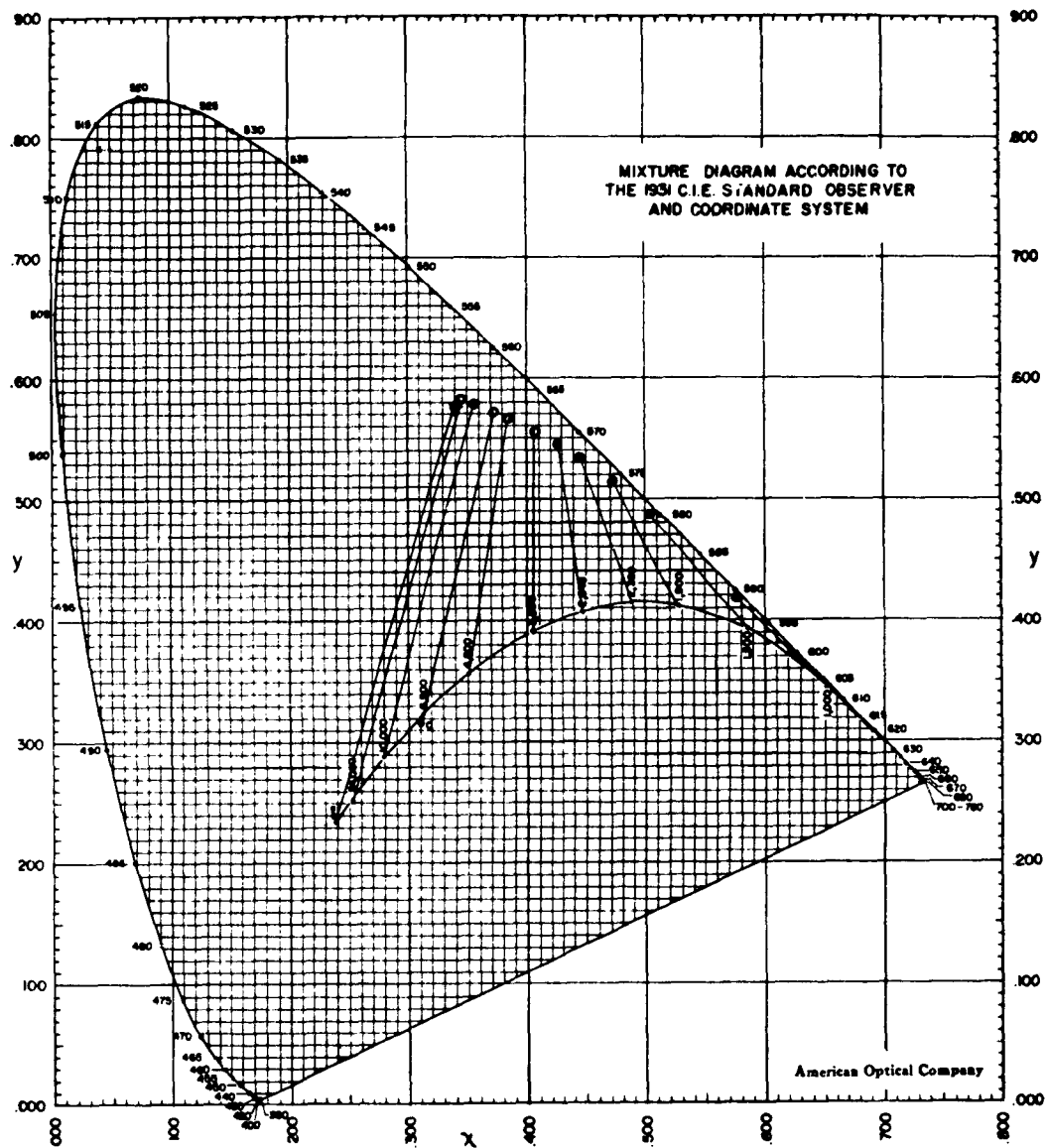


Figure 36. Color effects of 50 foot long fiber bundle on selected blackbody temperatures (See Paragraph 3.1.6.)

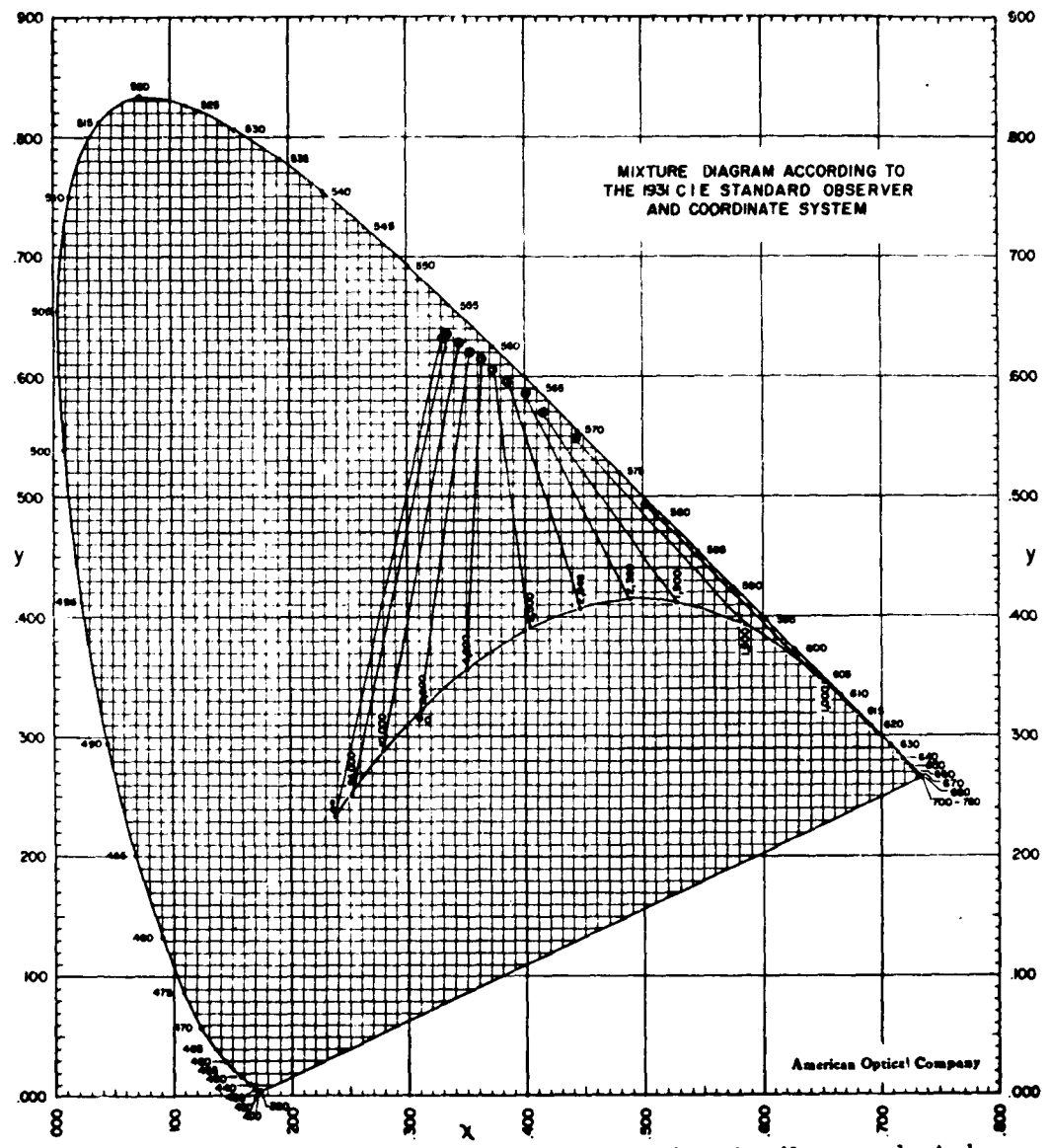


Figure 37. Color effects of 100 foot long fiber bundle on selected blackbody temperatures. (See Paragraph 3.1.6.)

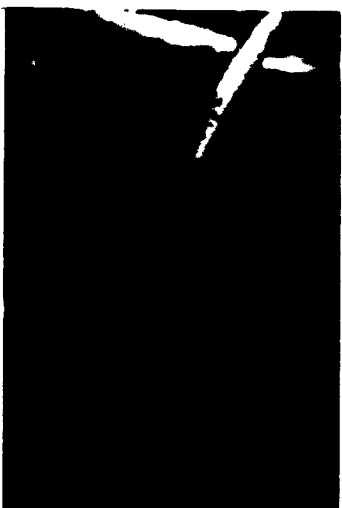


0 foot candles



50 foot candles

10,000 foot candles



0 foot candles



1000 foot candles

FIGURE 38. "IMAGE WASHOUT" DUE TO AMBIENT LIGHT FALLING ON END FACE.
The indicated end-face illuminance values are approximate. (See Paragraph 3.1.7.)



f/2 aperture



f/4.5 aperture



f/8 aperture



f/16 aperture

FIGURE 39. INCREASED IMAGE MOTTLING WITH REDUCED OBJECTIVE LENS APERTURE.

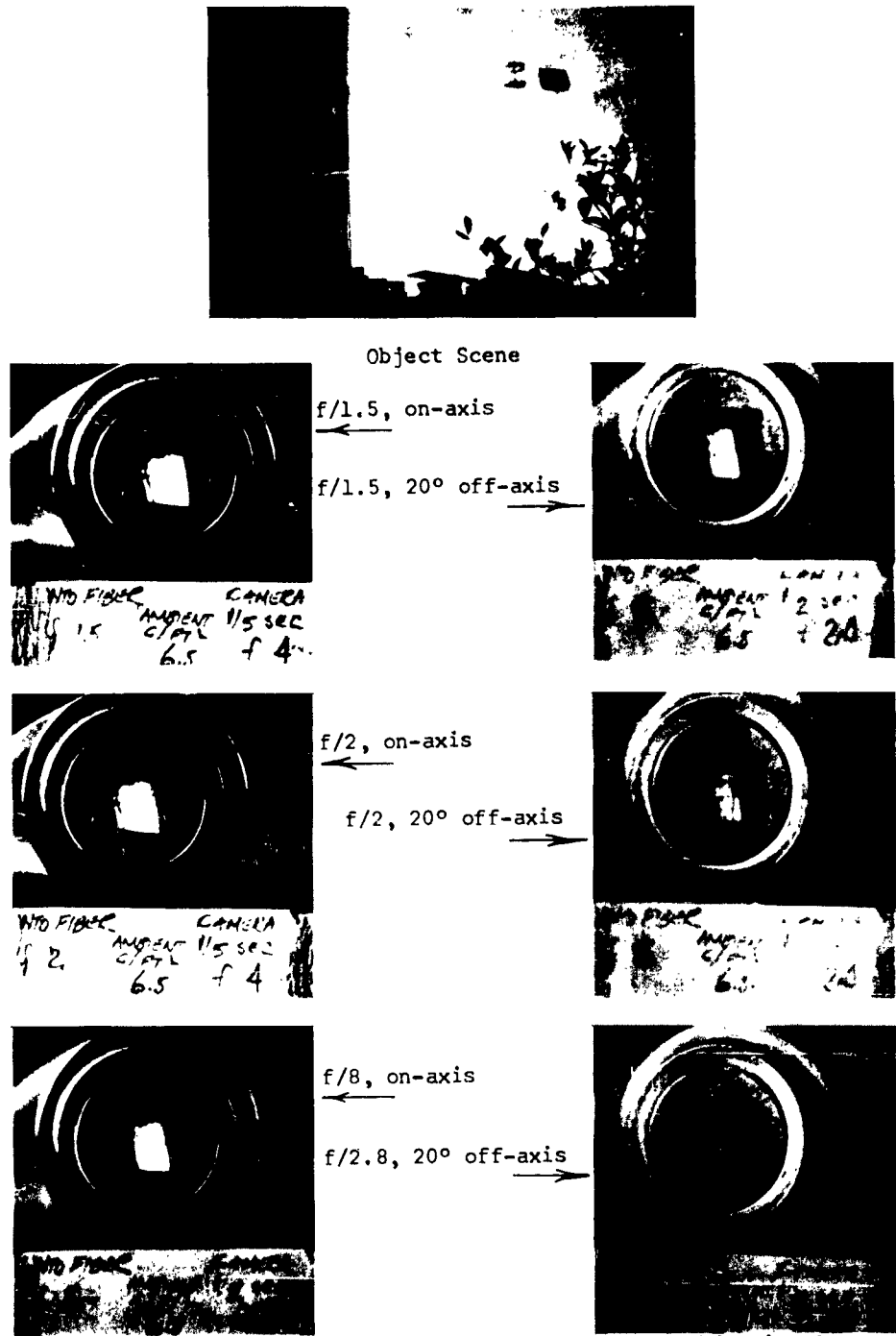


Figure 40. Image brightness vs. viewing angle and objective lens aperture ratio.
 (See Paragraph 3.1.9.)

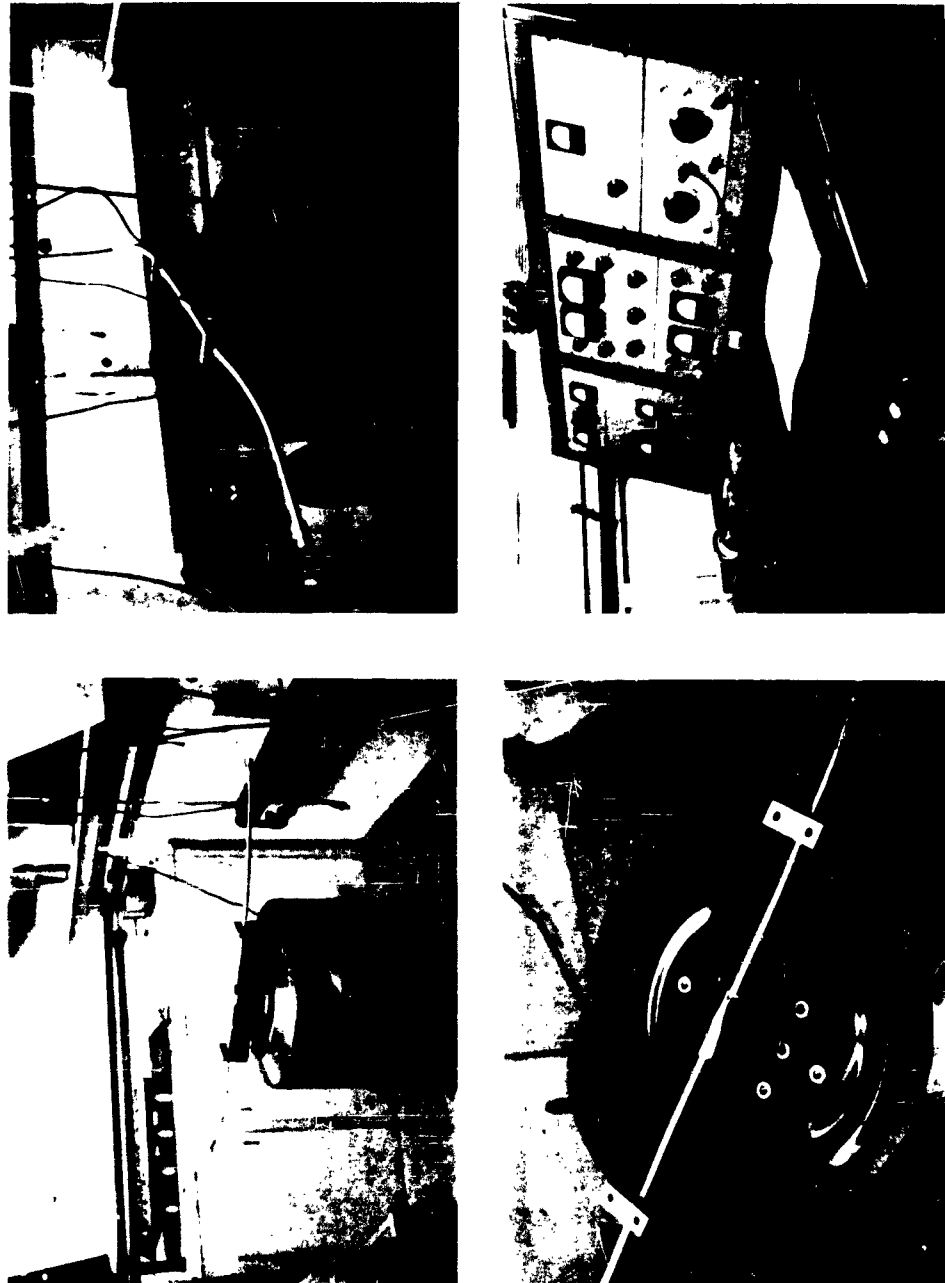


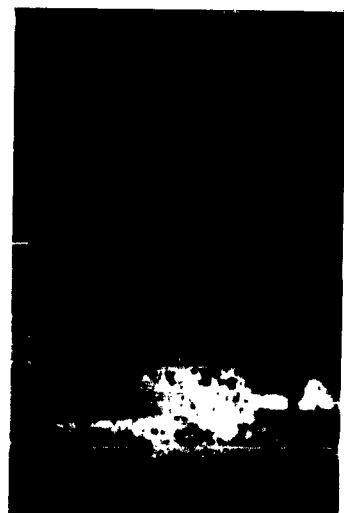
FIGURE 41. TYPICAL VIBRATION TEST ARRANGEMENT, SHOWING SHAKER TABLE AND CONTROL CONSOLE. (See Paragraph 3.2.2)



Reference focal length, L



3L

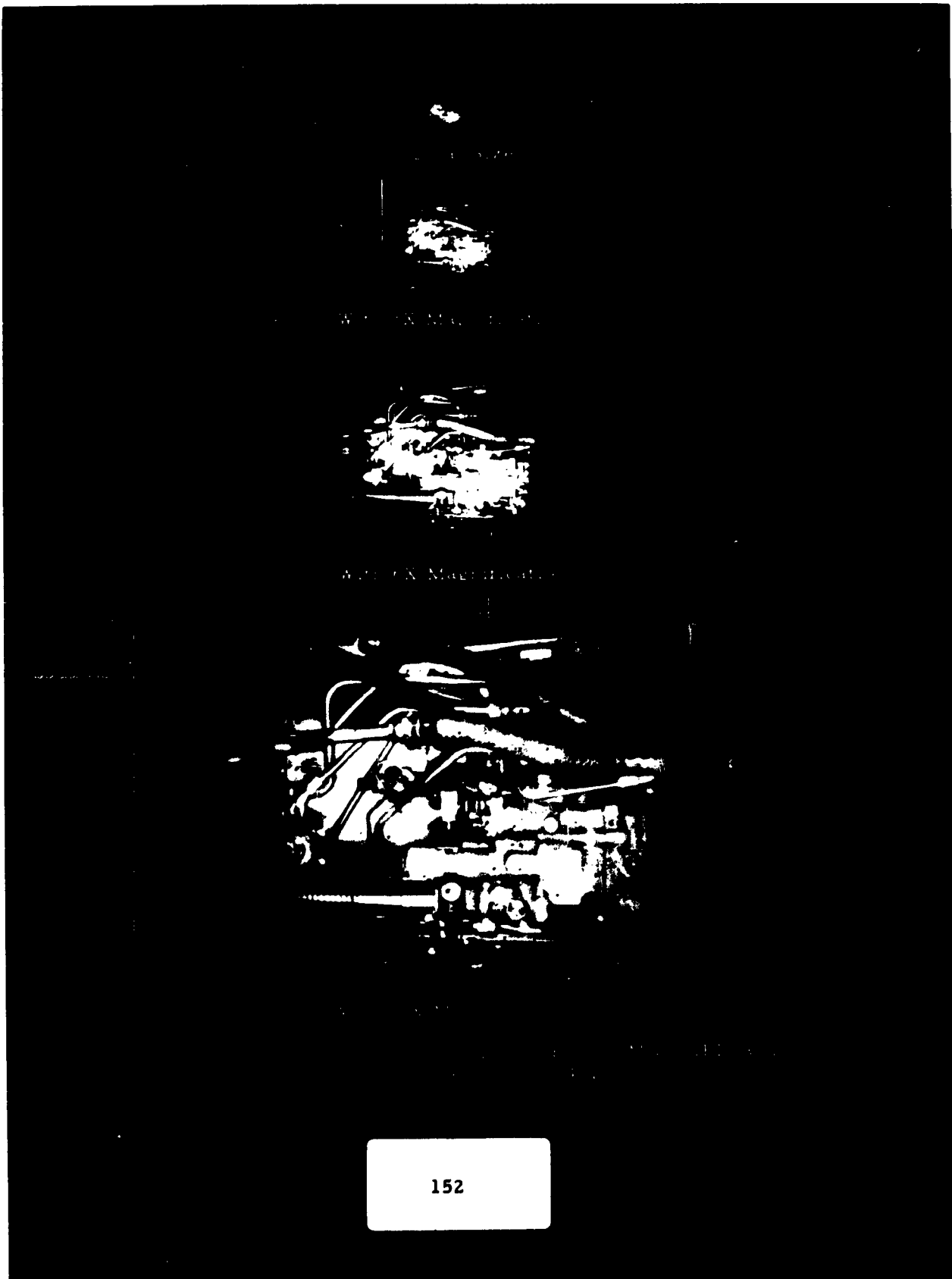


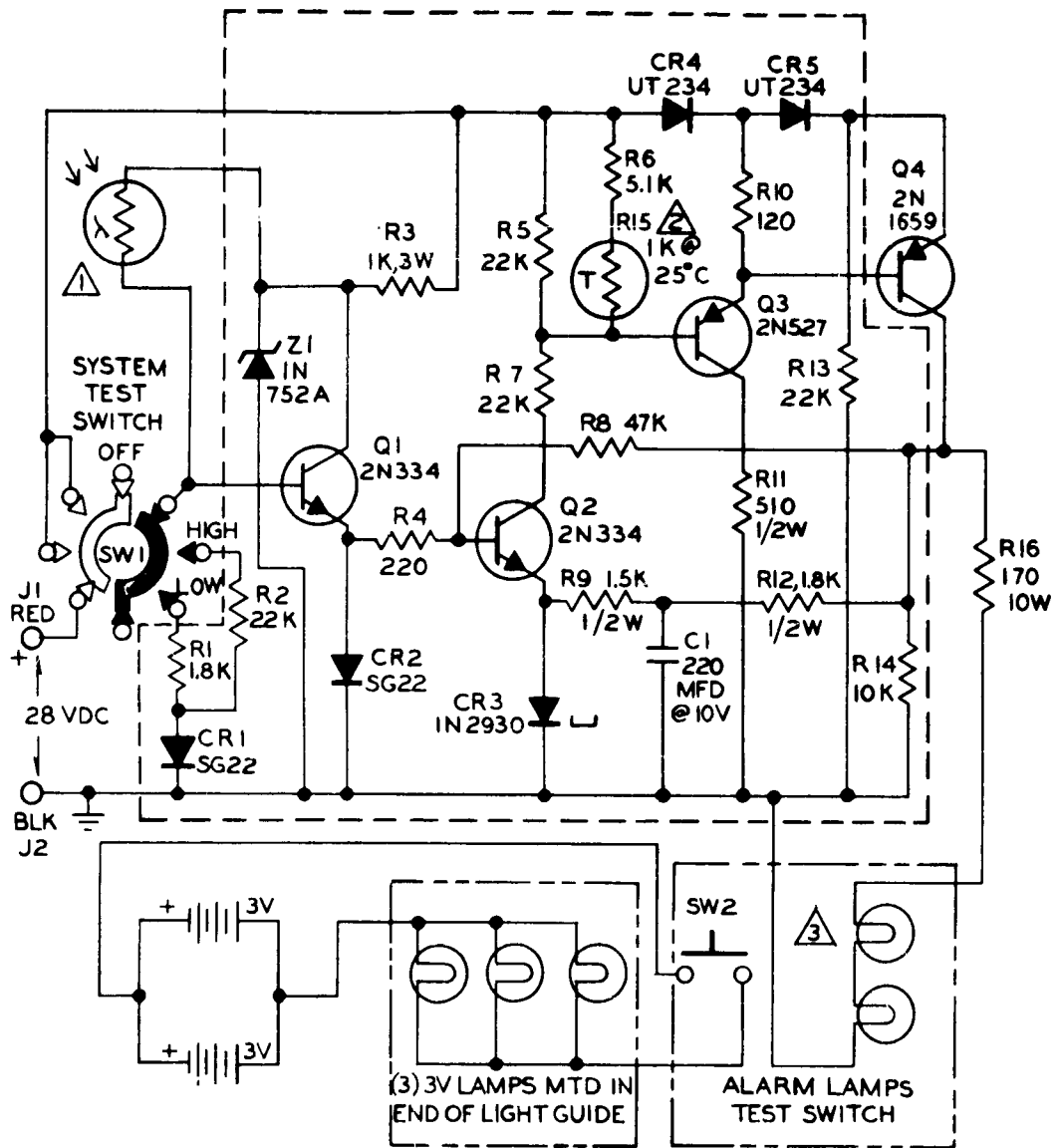
1.5L



5L

Figure 42. Effect of varying the objective lens focal length.
(See Paragraph 4.1.1.)





NOTE UNLESS OTHERWISE SPECIFIED

1. ALL RESISTOR VALUES ARE IN OHMS, $\pm 5\%$, $1/4$ W
2. COMPONENTS ENCLOSED THUS --- ARE MOUNTED ON PC BOARD.
3. CELL TYPE, CLAIRED #CL603AL.
4. THERMISTOR TYPE, FENWAL ELECT. #KA31LI.
5. MICROSWITCH (SW2) TYPE, MINNEAPOLIS HONEYWELL #302PBI-T-RR

FIGURE 44. PHOTODETECTION CIRCUIT USED IN EXPERIMENTAL BREADBOARD. (See Paragraph 4.2.3)

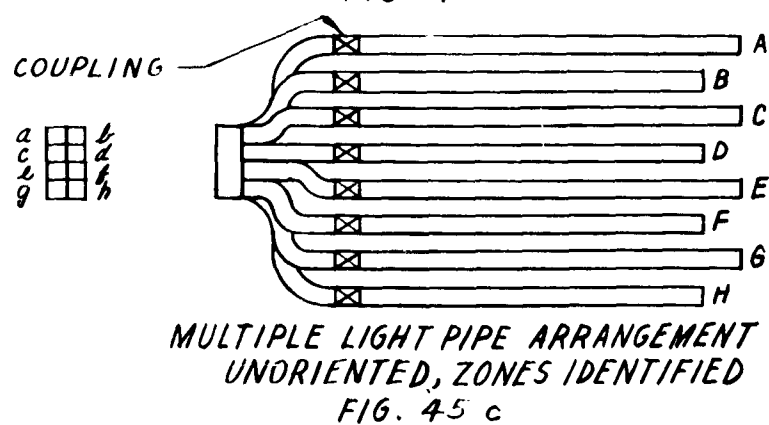
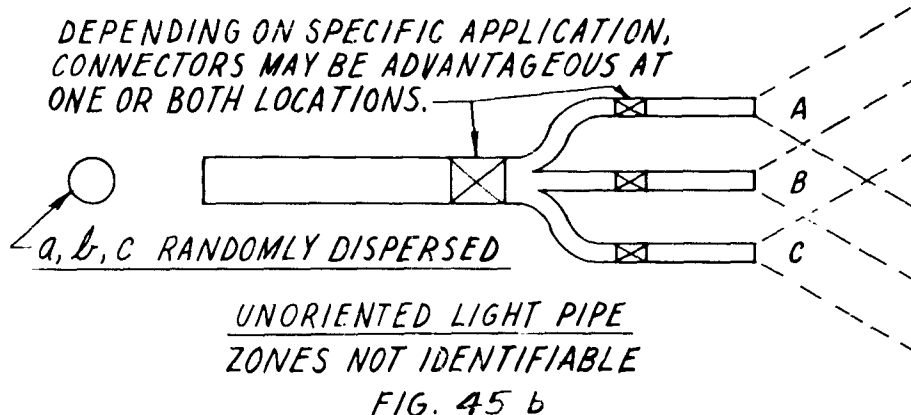
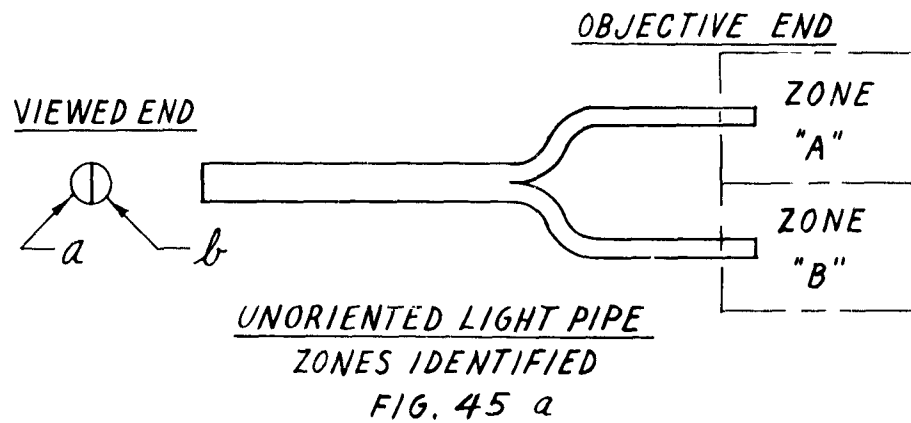


FIGURE 45. THREE POSSIBLE MULTIPLE BUNDLE CONFIGURATIONS.
 (SEE PARAGRAPH 4.3.)

**View of container used
for simulating a section
of a jet engine. Fuel
container, fuel atomizing
jet, one self-cleaning
window and lighting con-
nections also shown.**



**View of container with
self-cleaning windows
attached.**



**Another view of container
with self-cleaning windows
attached.**



FIGURE 46. SELF-CLEANING WINDOW TEST ARRANGEMENT.

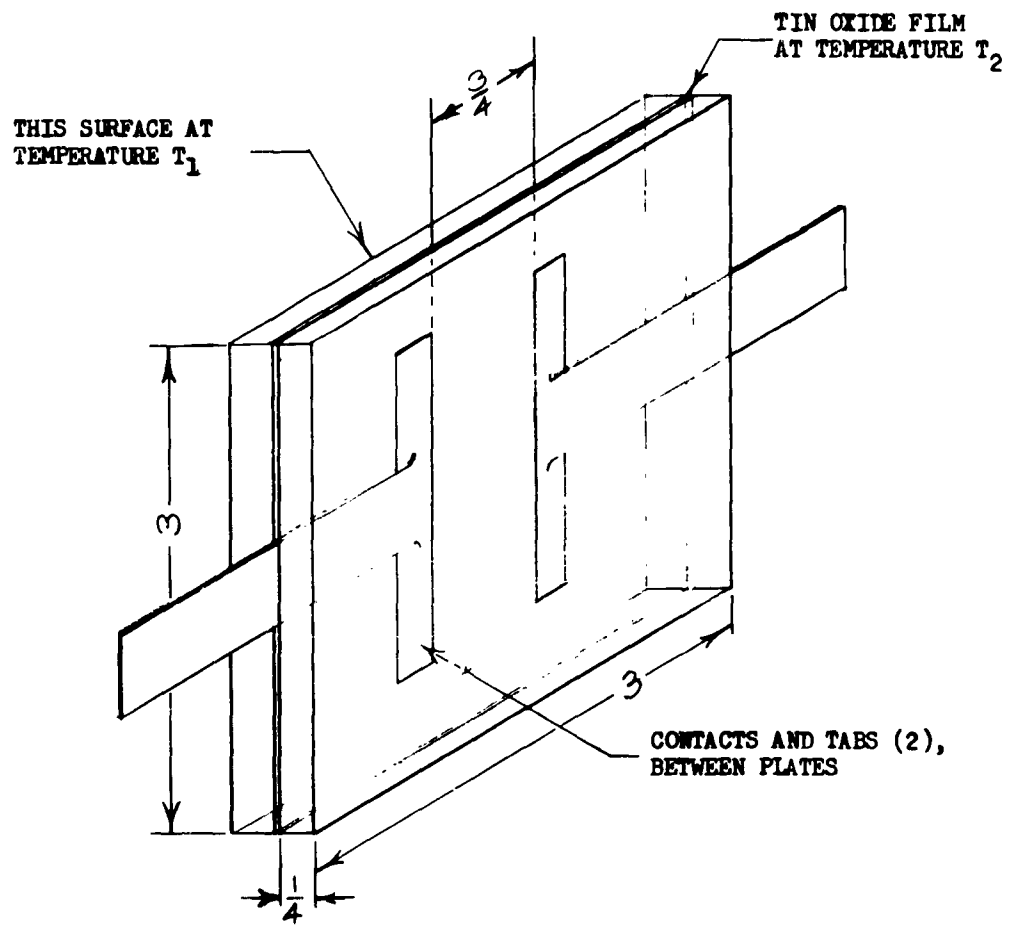


FIGURE 47. ONE FORM OF THERMAL SELF-CLEANING WINDOW.

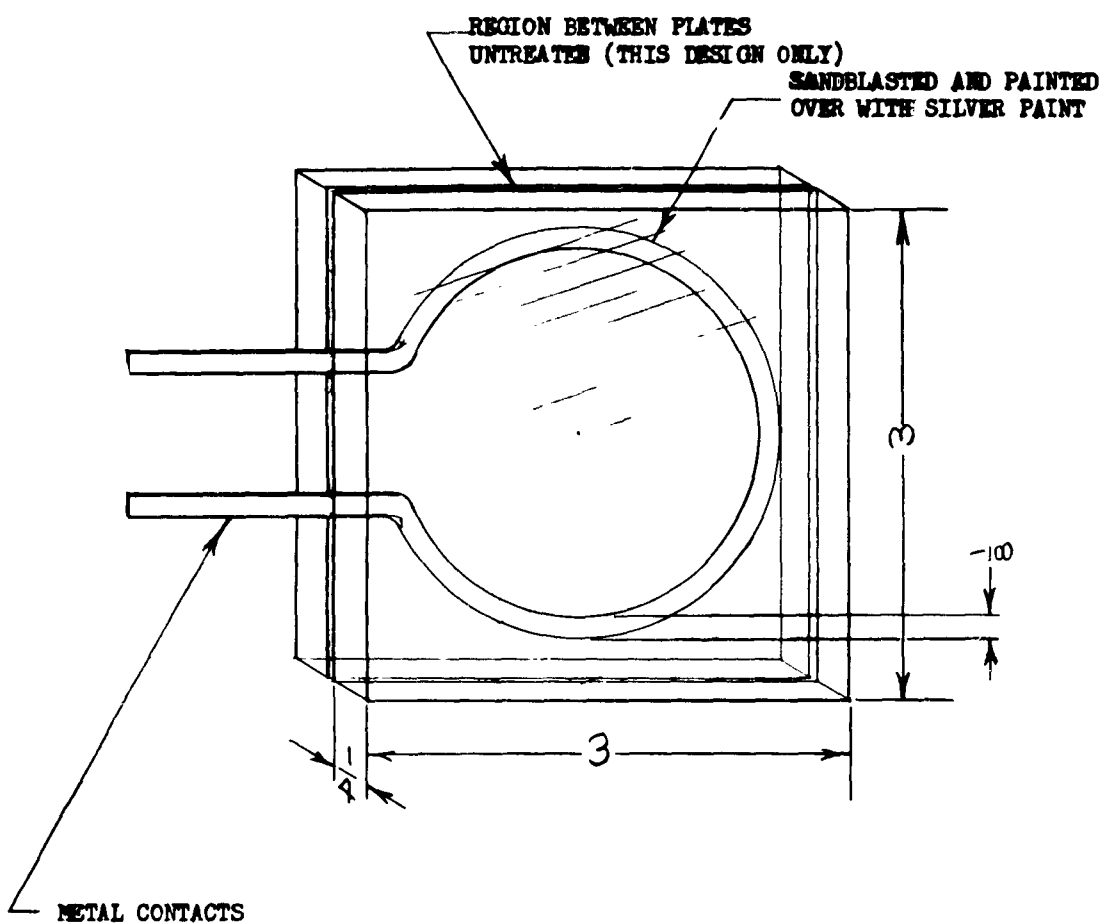
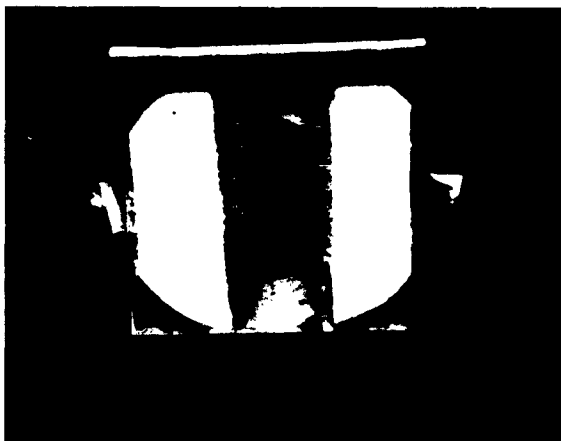


FIGURE 48. ANOTHER FORM OF THERMAL SELF-CLEANING WINDOW.

Test Window #1
with brass foil and
silver paint contacts.



Test Window #2
with different contacts
and added insulation.



Test Window #3
with baked silver contacts
and leads soldered directly.

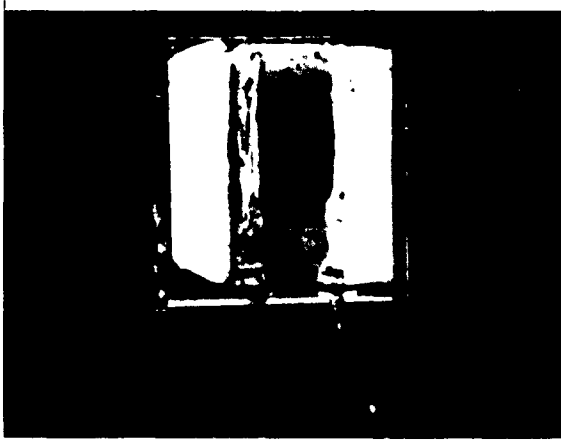
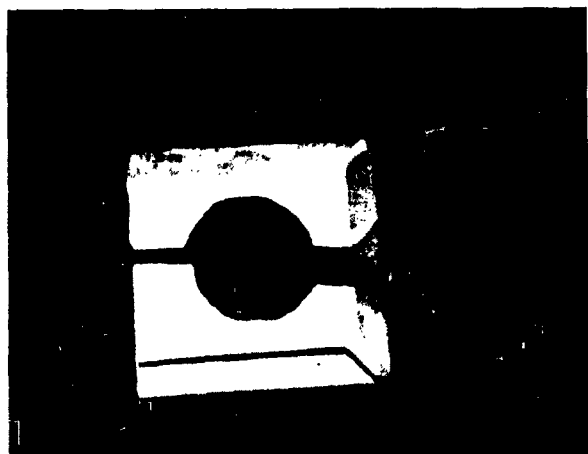


FIGURE 49. VARIOUS SELF-HEATED TEST WINDOWS.

**Self-cleaning window
using flow of hot air
between two glass plates.**



**Same window shown with
air line, heater chamber
and heater transformer.**



**Self-cleaning window with
electrical ring heater
sandwiched between two
glass plates.**

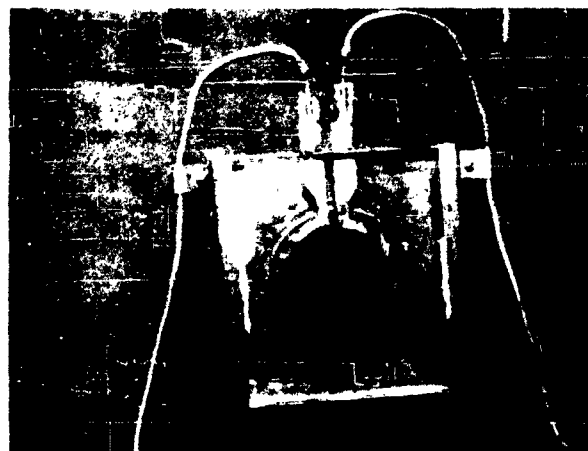


FIGURE 50. TWO OTHER FORMS OF SELF-CLEANING WINDOWS.

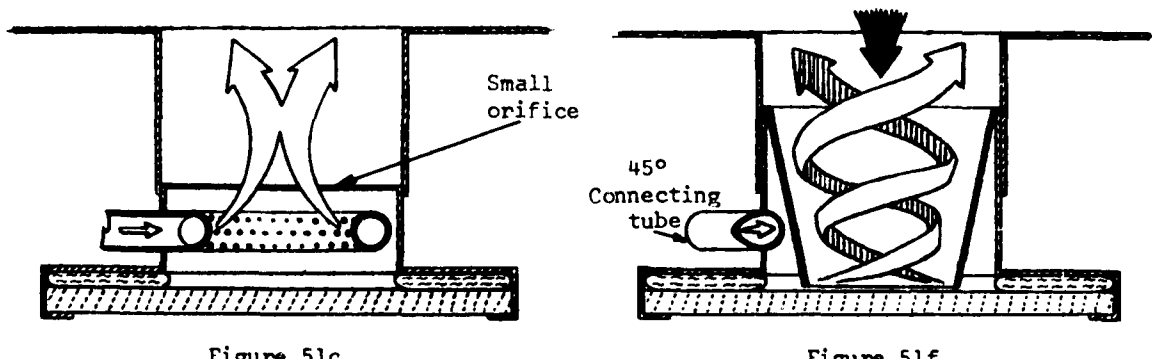
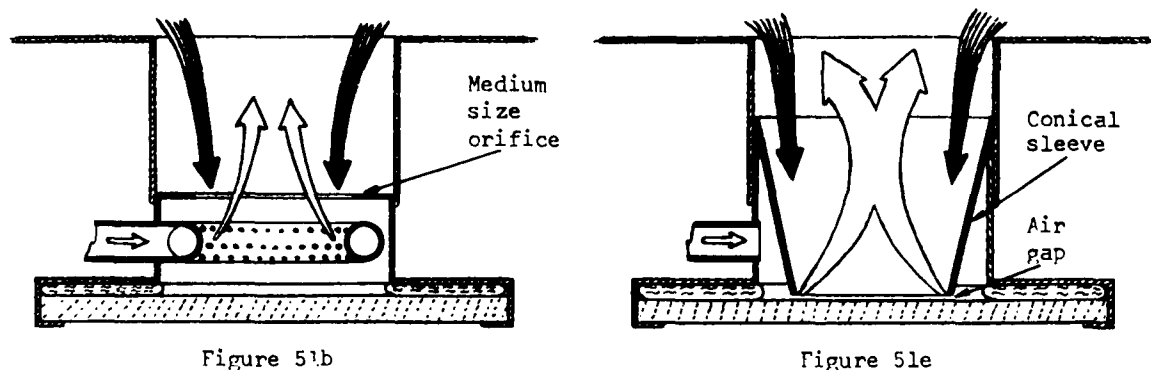
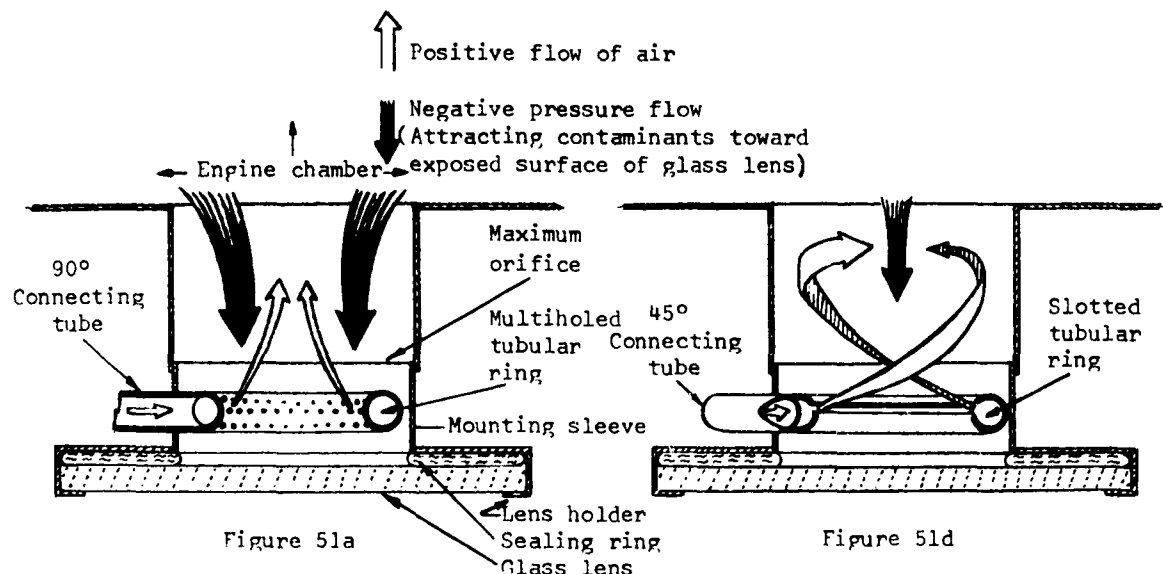


FIGURE 51. SELF CLEANING WINDOWS; AIR FLOW DEVICES

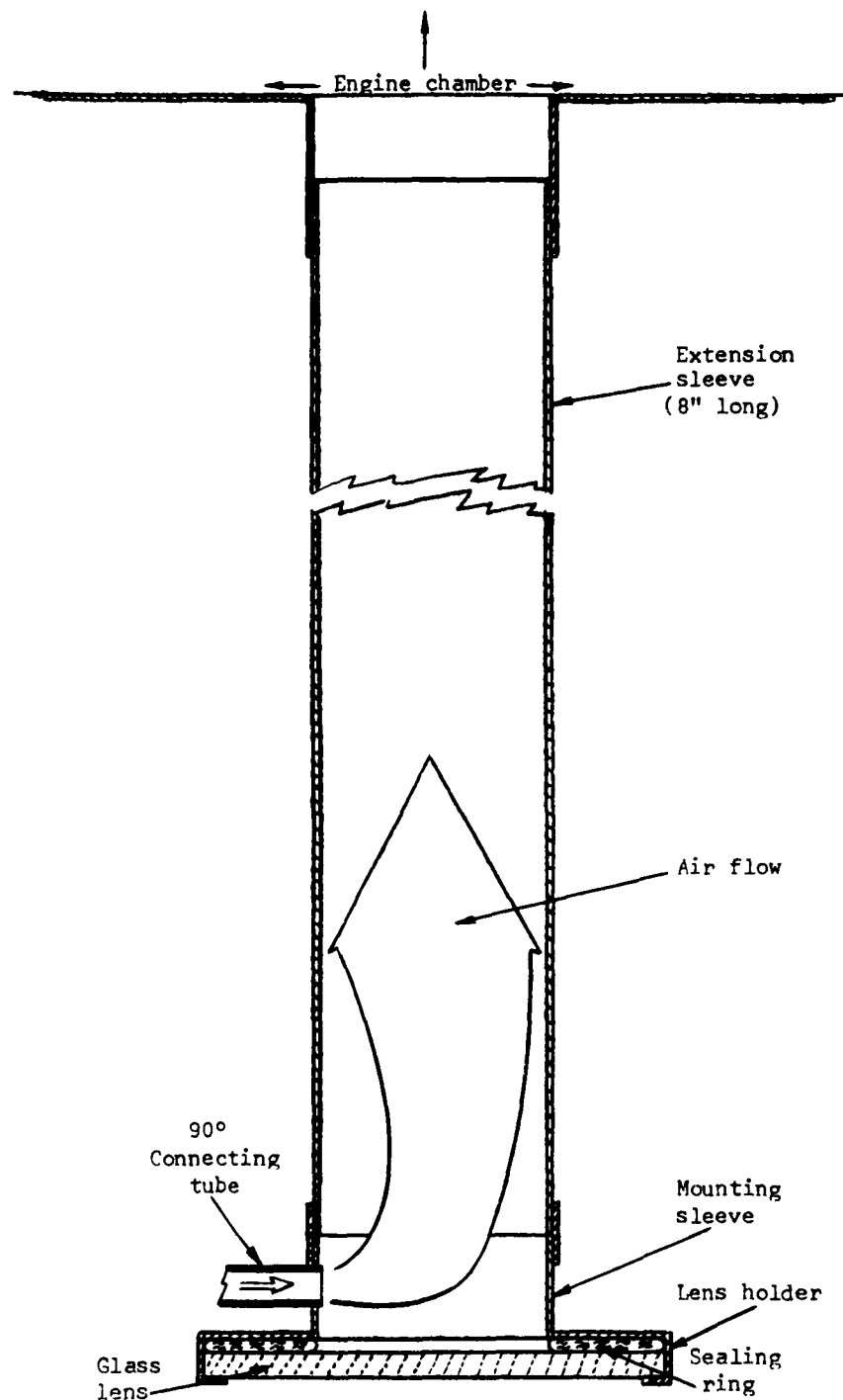


FIGURE 52. SELF-CLEANING WINDOWS; AIR FLOW DEVICES

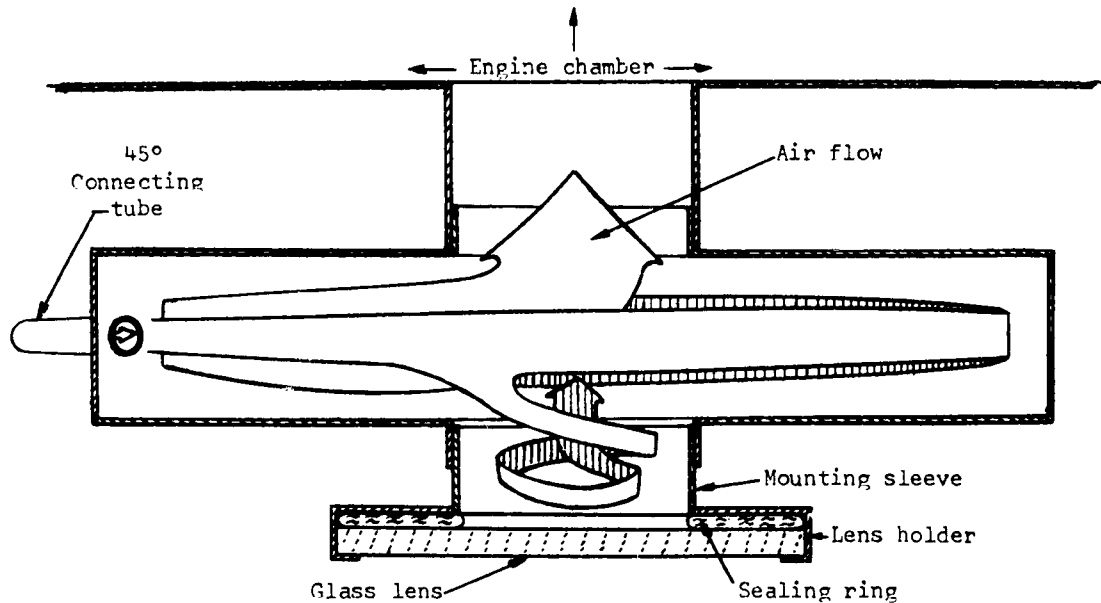


Figure 53a

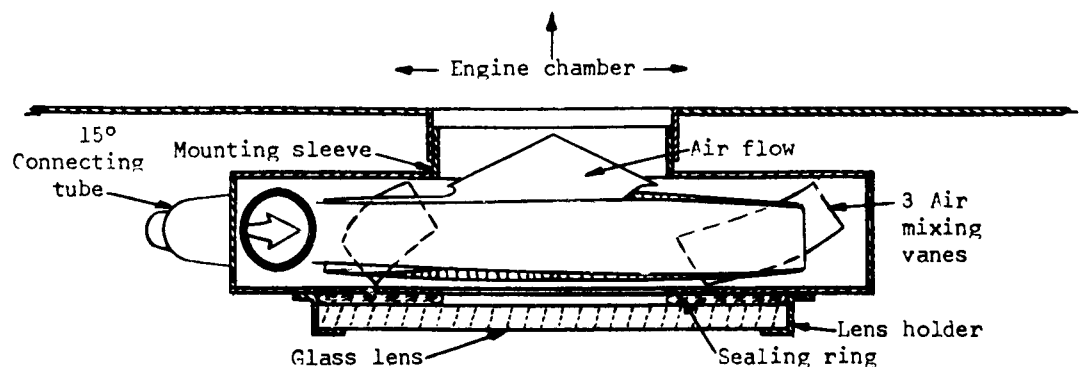


Figure 53b

FIGURE 53. SELF CLEANING WINDOWS; AIR FLOW DEVICES

Oil and soot covered window, from wiper side.



Window partially cleared of oil and soot with one-half pass of wiper.



Window virtually cleared of oil and soot with one pass of wiper.



FIGURE 54. OPERATION OF ELECTROMECHANICAL SELF-CLEANING WINDOW. EXTERIOR VIEW.

Oil and soot covered
window, from wiper
motor side.



Window partially cleared
of soil and soot with
one-half pass of wiper.

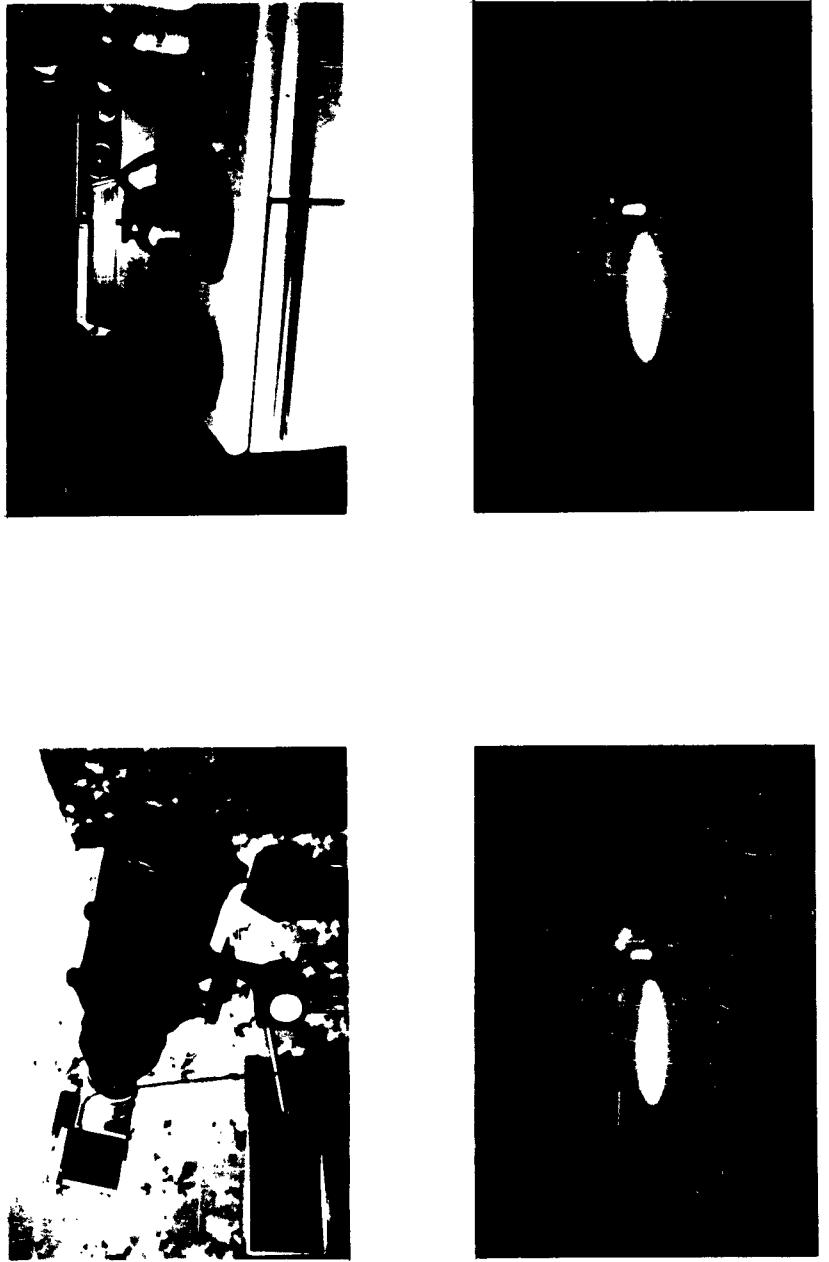


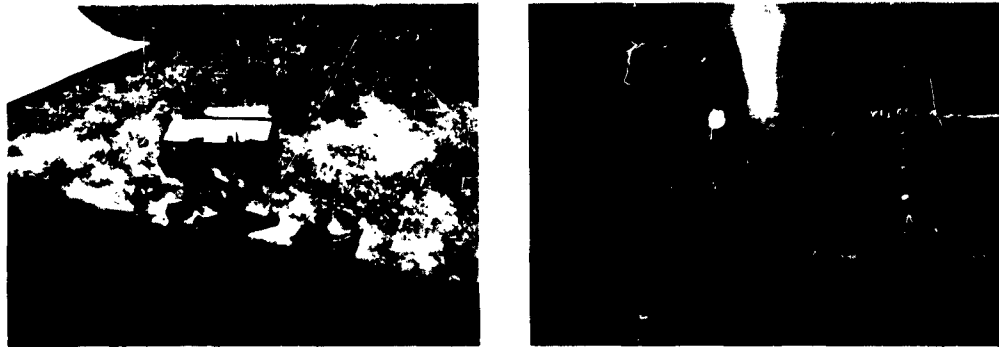
Window virtually cleared
of oil and soot with one
pass of wiper.



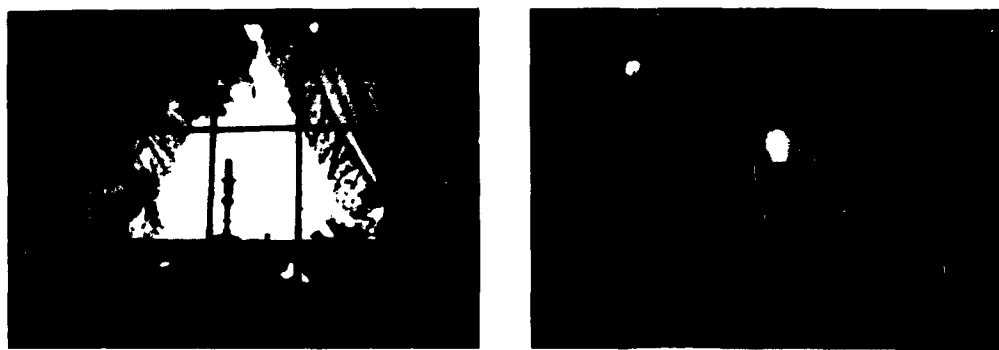
FIGURE 55. OPERATION OF ELECTROMECHANICAL SELF-CLEANING
WINDOW. INTERIOR VIEW.

FIGURE 56. AN INFRARED IMAGE CONVERTER, A REFERENCE PHOTOGRAPH, AND TWO CONVERTED IMAGES.
(See Paragraph 4.6.)

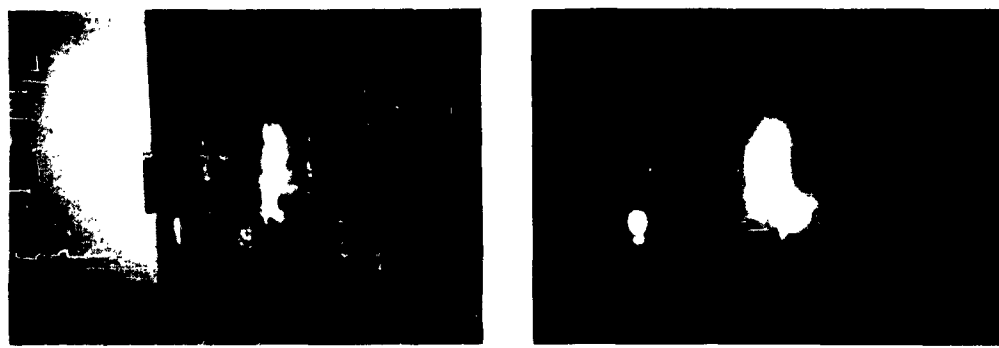




Scene under direct daylight illumination



Indirectly illuminated scene



Scene under incandescent lighting

FIGURE 57. CONTROL PHOTOGRAPHS (LEFT) AND CONVERTED INFRARED IMAGES (RIGHT) OF VARIOUS SCENES CONTAINING ORGANIC DIFFUSION FLAMES.
(See Paragraph 4.6.)

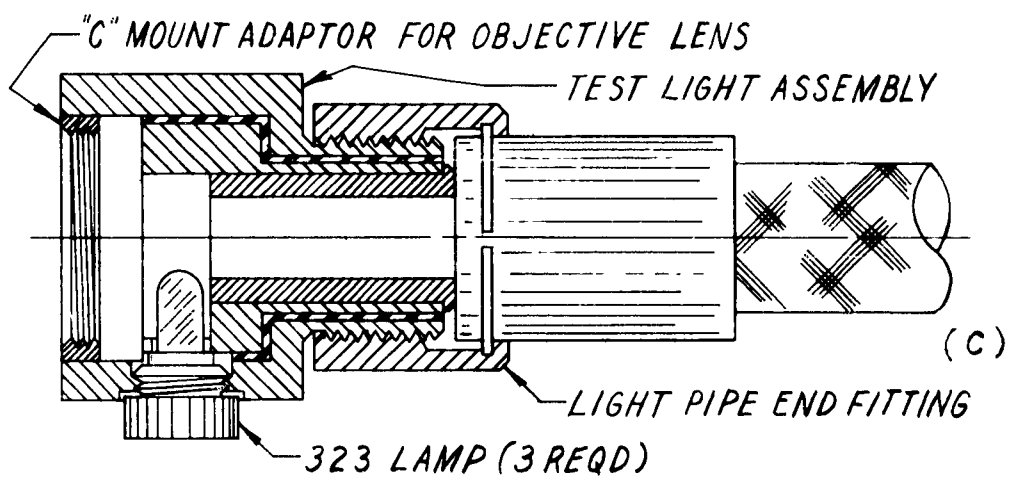
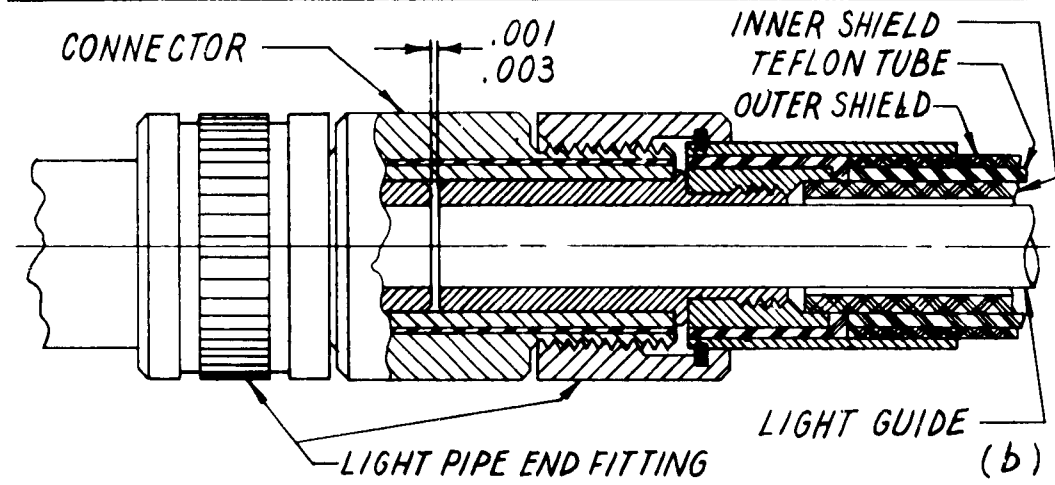
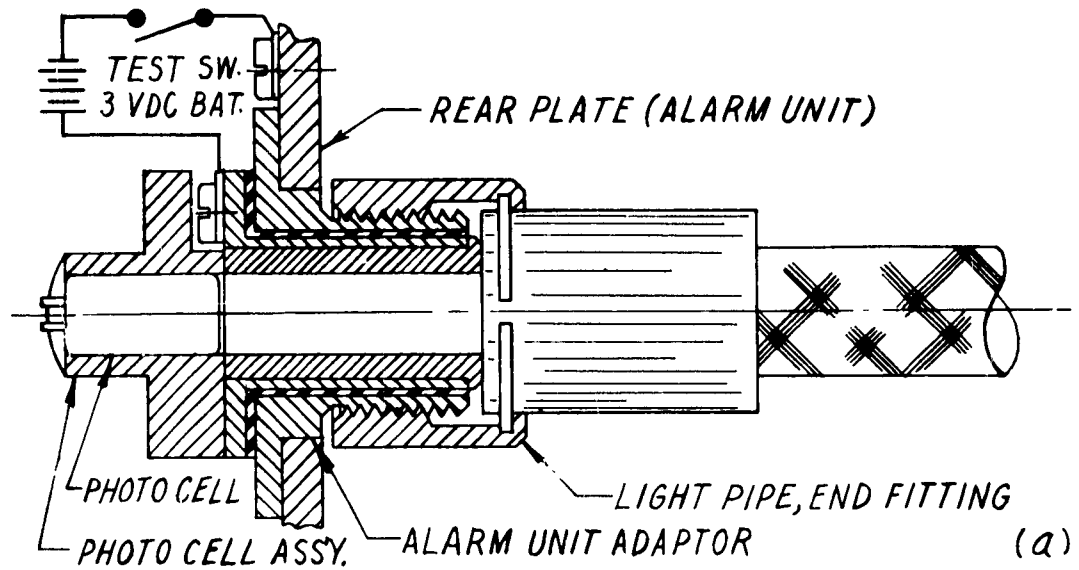


FIGURE 58. ALARM UNIT ADAPTOR (a); CONNECTOR (b); AND TEST LIGHT ASSEMBLY (c). (See Section 5)

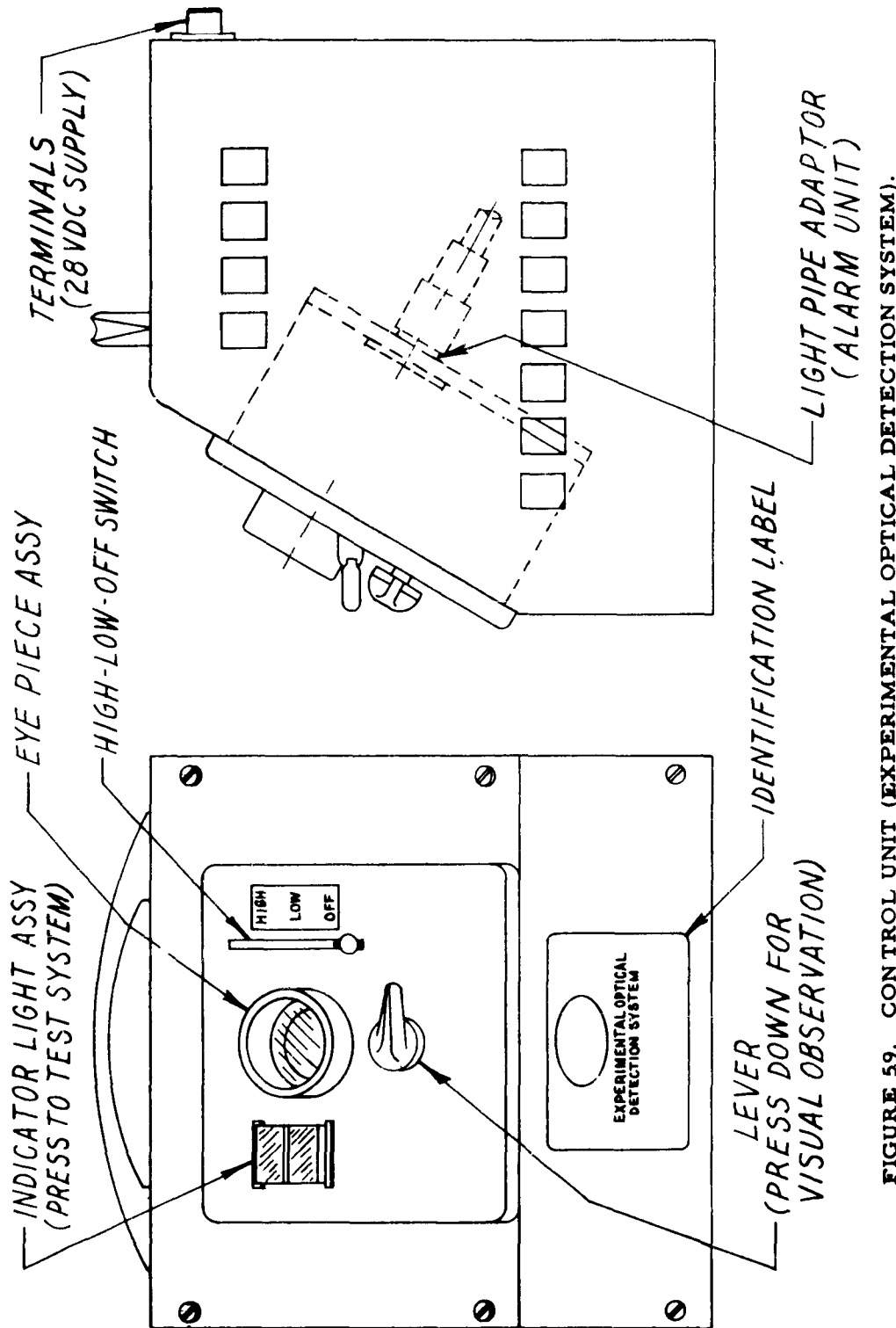


FIGURE 59. CONTROL UNIT (EXPERIMENTAL OPTICAL DETECTION SYSTEM).

Fig. 60a
Control unit assembly

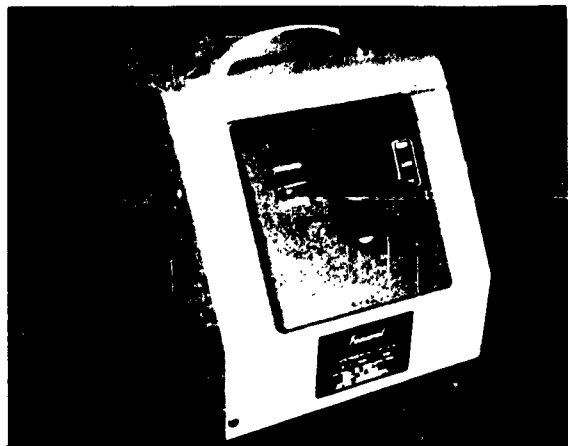


Fig. 60b
Light pipe assembly

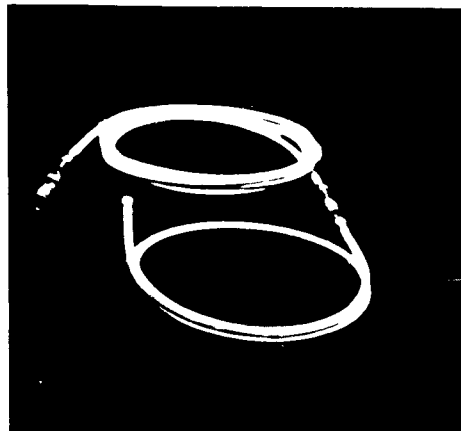


Fig. 60c
Internal view of alarm unit

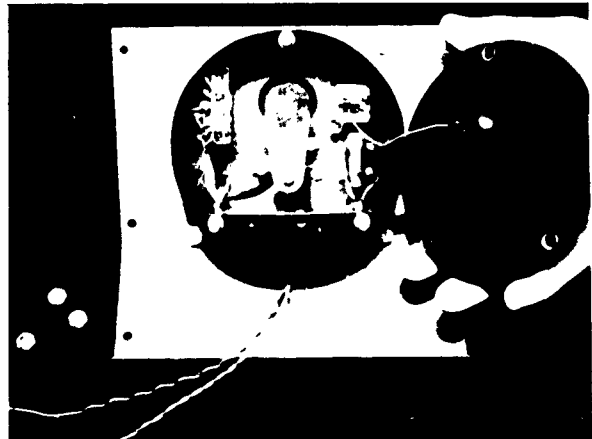
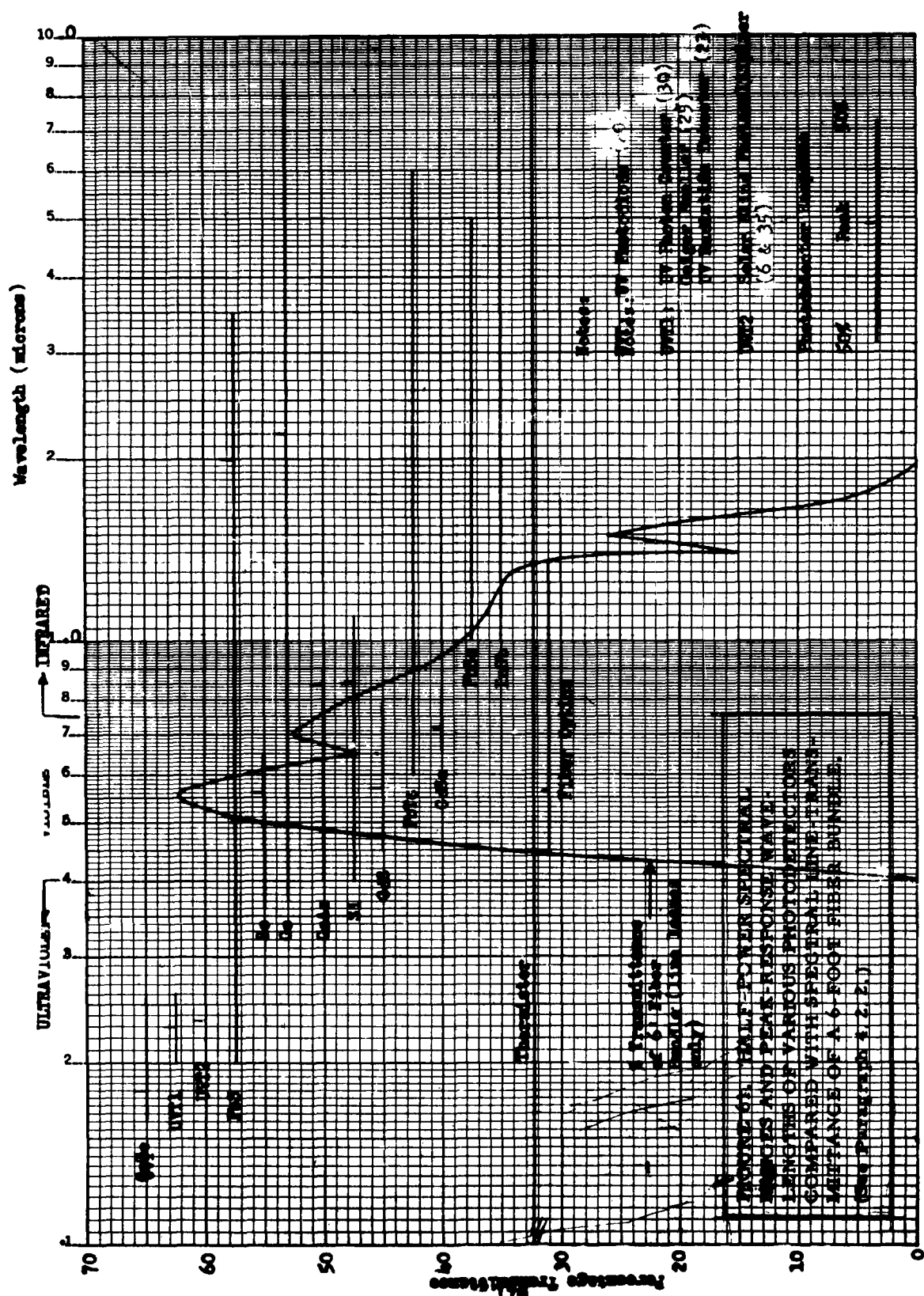


FIGURE 60. EXPERIMENTAL FIBER OPTIC HAZARD DETECTION SYSTEM



APPENDIX

IMAGE TUBES

**This appendix was prepared by Mr. Robert M. Burley,
Concord, Massachusetts, serving as a consultant to the
contractor.**

APPENDIX

IMAGE TUBES

TABLE OF CONTENTS

Section	Page
A. Introduction.....	175
B. Approaches	175
C. Image Changes Introduced by Image Tubes	176
1. Change in Color.....	176
2. Change in Angular Distribution of the Rays	176
D. Viewing Optics	177
1. Eye Freedom	177
2. Resolution	177
3. Lens Magnifier or Eyepiece.....	178
4. Fiber Optics Magnifier.....	178
5. Coupling Optics.....	178
E. Image Tube Performance Data	179
1. Image Converter Magnification.....	180
2. Image Converter Resolution and Information.....	180
3. Conversion Index	181
F. Fiber Optics - Image Converter Combinations	182
1. Coupling Optics.....	182
2. Example Combination	182
3. Gain of Cascaded Image Converters.....	186
G. Spectral Filtering.....	186
1. Infrared Region.....	186
2. Ultraviolet Region	186
H. Summary	187

(continued)

SUB-APPENDIX

Section	Page
A. Transmission through a Long Fiber Bundle	188
B. Formulae for Image Intensification and Conversion	188
1. Development of Formulae for Scene Brightness.....	189
2. Development of Formulae for System Brightness Gain.....	190
3. Evaluation of Scene Brightness in Terms of the Photodetector.....	190
4. System Brightness Gain.....	191
5. Sample Calculation.....	192

APPENDIX

IMAGE TUBES

LIST OF ILLUSTRATIONS

Figure		Page
A-1	Relative Spectral Response of S-1 Photosurface	193
A-2	Relative Spectral Response of S-21 Photosurface	193
A-3	Spectral Emittance of a Typical Commercial Phosphor Material, P-20	194
A-4	Resolution of No. 6411 Image Converter Tube.....	194
A-5	Use of an Eyepiece Magnifier.....	195
A-6	Use of a Tapered Fiber Bundle Magnifier.....	195
A-7	Combination of an Objective Lens with an Image Tube.	196
A-8	Objective Lens and Image Tube with Fiber Optic Faceplate.....	196
A-9	Objective Lens, Fiber Bundle, and Lens-Coupling to Image Tube	196

APPENDIX A. IMAGE TUBES

A. Introduction

As was made evident in Paragraph 3.1.1, an image transmitted by a long bundle of optical fibers suffers a substantial loss of brightness. This brightness may be restored at least in part by means of electronic image intensification. Other benefits may be obtained as outlined below.

B. Approaches

There are two general approaches to electronic image intensification. One accomplishes an image brightening process completely within a single physical unit. The other utilizes an image pickup tube to transform the image information into a video signal which is transmitted by wires or by radio signals to a remote cathode ray presentation unit. While the latter provides greater flexibility, its relative complexity and power requirements make it less attractive for flight safety instrumentation. Only the former approach is treated in the present report.

For purposes of analysis, the image intensifier may be treated as a "black box" which can be inserted in an optical image transmission system. The input element is a photosensitive surface and the output element is a phosphor-coated surface which is excited by a beam of electrons to emit a luminous image. In use, the input surface is placed at an image plane of the optical system such as at the focal plane of an objective lens or in contact with the end face of a glass fiber bundle. The output phosphor image may be viewed directly or through a magnifying eyepiece, or may be fed into a glass fiber bundle by direct contact or by means of re-imaging optics. When it is introduced into the middle of an optical transmission system, an image intensifier may be likened to an amplifying relay unit in a communications transmission line.

Image intensifier tubes presently available use a high voltage in the neighborhood of 6 to 20 kilovolts, depending upon the tube type and upon the brightness gain desired. Using electrostatic focussing, most of the tubes consume very little electrical current, usually less than one microampere. The high voltage can therefore be developed in a small vibrator-transformer-rectifier unit, as is presently done in the hand-held snooperscope.

For flight safety equipment purposes, the entire assembly, including all high voltage leads, can be housed in an explosion-proof enclosure. Since the required operating power is less than one watt at low voltage, the device can be powered by a self-contained rechargeable cell such as a nickel-cadmium cell, making it independent of vehicle power failure.

C. Image Changes Introduced by Image Tubes

When an image intensifier is introduced into an optical transmission system, the output is not simply equal to the input intensified by some factor. Besides being intensified, the picture is generally altered in at least four ways: (1) a color translation takes place; (2) a change in the angular distribution of the rays occurs; (3) magnification may be changed, and (4) a loss in resolution may occur.

1. Change in Color

The color translation involves the spectral sensitivity of the input photosurface and the spectral emission of the phosphor. Since, in ordinary image tubes, the color of the output is determined by the characteristic emission of the particular phosphor used, regardless of the spectral distribution of the input image, the color content of the image is ordinarily lost. (Color information could be retained by resorting to the complexity of a scanning system such as a color television system.) On the other hand, the color translation inherent in the process opens up possibilities of relaying information contained in the image in wavelengths invisible to the eye. For example, infrared rays from a hot object or ultraviolet rays from a flame can be translated to form a visible image of the object on the phosphor screen. By selective filtering, the system can be made insensitive to visible-band wavelengths. Expedients which may be used to make a system that sees only a hazardous scene will be discussed later in this Appendix.

Commercially available image converter tubes are made with a cesium-oxide-silver photosurface designated S-1 by the manufacturers and with a cesium-antimony surface designated S-21. The former, used in World War II snooperscopes, has low sensitivity in the visible spectrum, but has some sensitivity in the near infrared out to about 1.1 micron. The S-21 surface has good sensitivity to blue, violet and near-UV, but is blind to red and to longer wavelengths. Spectral response curves are shown in Figure Nos. A-1 and A-2. The quantum efficiencies at their peak response wavelengths are about 0.4% and 7% respectively. The P-20 phosphor is generally used for the output surface. Its emission curve is shown in Figure No. A-3.

2. Change in Angular Distribution of the Rays

This is inherent in the phosphor emission process. Phosphor emission is nearly Lambertian; a cathode ray tube picture can be seen with nearly the same brightness from any direction. (The newer transparent phosphors such as the P-5 follow more closely a Lambertian distribution than the ordinary settled phosphors such as the P-11, but in either case the departure is nearly negligible.) The fact that an image tube scene can be viewed

from any direction may be important in a practical installation, as discussed under Viewing Optics, which follows.

D. Viewing Optics

1. Eye Freedom

A point image conveyed by a system of lenses or mirrors, either with or without fiber optics, as long as it contains no diffusion (ground glass) element, can be viewed only from within a restricted cone determined by the numerical aperture of the system. (Numerical aperture, or N.A., is equal to the inverse of twice the f/ratio of the system.) Other points in the image can be viewed only from within a different cone. The circular area where all of the cones from all points in the image intersect defines the exit pupil of the system. If the eye is placed within the circle, it can see the whole scene. If not, it can see only as much of the scene as it could see through an imaginary hole located at the exit pupil. In installations where the observer must be some distance away from the nearest optical element, this becomes a problem; either the magnification must be made small or the optical elements large, since the exit pupil diameter is equal to the objective element diameter divided by the magnification.

If diffusion is introduced by a ground glass or opal glass or a white matte projection screen, the image becomes visible from anywhere in the hemisphere cut by the image plane. The price paid is in image brightness, which for the case of perfect diffusion becomes reduced to $(N.A.)^2$ times the brightness that would appear with direct undiffused viewing.

The difference between direct and diffused viewing is familiar to users of reflex cameras having a ground glass focussing area in a "bright field" view-finder. Because ground glass is not a perfect diffuser (forward scattering exceeds oblique scattering) the loss of brightness is not as great as if it were; but by the same token the brightness varies with viewing angle. The latter effect is also familiar to reflex camera users and is the reason for the usual inclusion of a field lens to direct the forward scattered light into the eye.

2. Resolution

Combinations of fiber optics and image tubes can be made to yield picture resolution elements 0.005" in diameter or smaller, such as by using 0.005" or smaller fibers with one of the image tubes listed in Table A-1 in Paragraph E.3., for example.

Limiting angular resolution of the eye for a high contrast bright scene (about 10-foot lamberts or more) is on the order of $\frac{1}{2}$ milliradian. This

falls off markedly at much lower levels. The resolution of the eye at low light levels, and the related ability to detect and to identify objects is treated in Reference 135, starting on Page 249.

Considering the eye's resolution as $\frac{1}{2}$ milliradian, a picture having 0.005" elements can just be resolved at a distance of ten inches when viewed directly without a magnifying lens or eyepiece. For some installations, at least, ten inches is undesirably close to the observer's eye; hence some form of magnification is required if the resolution capability of the image tube - fiber bundle combination is to be fully exploited. A treatment of magnifiers is given below.

3. Lens Magnifier or Eyepiece

Figure A-5 shows an object having a linear dimension h magnified by a lens L to a virtual image of dimension h' . If F is the focal length of the lens, then by simple geometrical optics it can be shown that the linear magnification is:

$$\frac{h'}{h} = \frac{a'}{a} = \frac{F}{F - a}$$

The angular magnification is

$$\frac{a' (d + a)}{a (d + a')}$$

For the example shown, which illustrates the use of a simple magnifier, the eye can be moved from the axial position at e_0 as far as position e_1 , and still see the whole object through the lens, since the point L_1 falls within the edge of the lens, provided that the angle θ_2 does not exceed the maximum angle at which rays emanate from the image h .

From Figure A-5 it is obvious that for greatest eye freedom, a' should be kept as small as possible (consistent with the magnification required) in relation to the lens diameter. This calls for a lens of short focal length in relation to diameter. The lens may be made up of several elements to gain f/ratio, but the practical limit is not much faster than f/1.

Figure A-5 and the magnification formulae apply also when the lens is considered as an eyepiece, but in this case the eye is generally closer, the angular field of view larger, and the lens components are arranged differently to minimize aberrations throughout the larger angular field of view.

The lens can be placed at an object distance "a" which is greater than its focal length F. In this case h' and a' become negative, which means that an

inverted image is formed on the eye side of the lens. This arrangement is suitable only when d is necessarily large, because the eye must focus on the nearer image.

4. Fiber Optics Magnifier

A tapered fiber bundle may be used as a magnifier as shown in Figure A-6. The phosphor should be deposited directly on the small end of the bundle, to avoid loss of resolution. The linear magnification is equal to the ratio of the output to input fiber diameter. Eye freedom is determined substantially by θ_2 , where $\sin \theta_2 = \frac{\sin \theta_1}{\text{magnification}}$

When the image being magnified is emitted by a phosphor screen with a nearly Lambertian light distribution, $\sin \theta_1$ is limited only by the maximum numerical aperture of acceptance of the fiber, which can readily be made as high as 0.8; hence good eye freedom along with substantial magnification can be realized.

Aside from reflection and absorption losses and the effect of fuzzing of the exit pupil, which are slight in a very short fiber bundle, neither the tapered fiber bundle nor the lens magnifier affects the brightness of an image viewed directly (i. e., without diffusion) through them.

5. Coupling Optics

Brightness gain with cascaded image converters is treated in Sub-Appendix B.2 on the basis of unity magnification in the coupling optics between them. With such coupling, because of the minification provided by the image tubes themselves, the full face of only the first tube in the series is utilized, and system resolution is affected more by the last tube because the resolution losses in the first become scaled down.

If magnification is introduced in the coupling between cascaded image tubes, a reduction occurs in image brightness gain from that stated, according to the square of the input/output numerical aperture ratio of the magnifier, which is according to the square of the magnification.

E. Image Tube Performance Data

Treatments of the dependence of image tube performance upon internal parameters have been presented in the literature (see References 135 to 147). These include discussions of various configurations, electrostatic and magnetic focussing, sandwich construction, and so forth. In the present report only the external performance data on available tubes are presented and evaluated.

The performance of image converter tubes is specified in terms of magnification, resolution, spectral response and conversion index (output image light flux in lumens divided by input image flux). Also of interest in some applications are the distortion and screen background brightness. The latter sets a lower limit on input intensity that can be distinguished and determines the dynamic range of the device when related to the maximum output phosphor brightness.

1. Image Converter Magnification

Available image converter tubes have a magnification of about 0.75, i.e., the linear dimensions of the output image are about 3/4 those of the input image. This reduction can be compensated for by optical magnification as discussed elsewhere.

2. Image Converter Resolution and Information

Resolution capability for image converters is expressed in a manner similar to that used for photographic films. A test pattern is imaged onto the photocathode by a high quality lens, the pattern having lines with various spacings, and line widths equal to those of the spaces. The resolving power is given as the limiting number of line pairs per millimeter at the photocathode that can be distinguished in the output phosphor image.

In present image converter tubes, resolution is limited chiefly by focus of the electron beam onto the screen, and by spreading of the image in the screen. Resolution is somewhat degraded by beam focus of off-axis electron beams, as shown in Figure A-4, which results in a somewhat less well defined image at the edges of the field of view than at the center.

Nevertheless, a great deal of information can be conveyed by a single tube. Integrating over the entire surface, there are typically about 40,000 distinguishable picture elements in available tubes. Stated another way, based on Figure A-4, the image tube could convey substantially all of the optical information which can be carried by a uniform fiber optics bundle of 0.007" fibers 0.8" in diameter at its input end, or a bundle of 0.005" fibers 0.6" in diameter at its output end. More information could be conveyed by grading the size of the fibers to match the finer resolution of the image tube at the center.

This is still somewhat less information than can be utilized rapidly by the human eye. The eye could absorb the optical content of several units placed side by side, by rapid visual scanning.

3. Conversion Index

The radiant conversion index M_r of an image converter in terms of phosphor-screen-lumens output divided by effective-watts input is determined by the product of the radiant sensitivity of the photocathode in amperes per effective watt of incident radiation times the phosphor screen-to-cathode voltage times the phosphor screen "luminous efficiency" in lumens per watt of electron beam power.

The quantum efficiency and hence the cathode sensitivity of suitable photocathode surfaces are fairly well established from a number of years' experience with photomultiplier tubes and television pickup tubes. Considerable work has been directed at developing surfaces of low work function for high sensitivity in the visible and infrared. Aside from the multi-alkali development (leading to quantum efficiencies as high as 25%) there have been few improvements in available materials in recent years; the S-1 surface has stood as the only photoemissive material used in commercially produced tubes which respond to wavelengths longer than one micron.

The improvement in conversion index which has been achieved in recent image converters has therefore resulted primarily from use of higher screen potentials and from cascading of stages.

Values of conversion index of various available image converters are given in Table A-1. For most of the tubes, published values are given of the visual conversion index for a 2870°K color temperature, in lumens output divided by lumens input

Type No.	Cathode					Resolution		
		Spectral Response	Screen Volts	Diameter Inches	Conversion Index	Resolution At Center ³	0.3" From Center ³	Screen Background
6914	S-1	16,000	1.00		15 ¹	28	13	0.25 ⁴
6929	S-1	12,000	0.75		10 ¹	33	9	0.33 ⁴
7404	S-21	12,000	0.75		6000 ²	38	9	10^{-10}^5

Table A-1. Operating data on three commercial image converter tubes.

For all three types listed: Magnification (output/input image size) ≥ 0.75 .

Screen Phosphor - P20 (See Figure No. A-3).

See following page for explanatory notes referred to in above table by superscripts.

Notes:

1. Ratio of output lumens to incident 2870° K lumens at photocathode.
2. Ratio of output lumens to incident radiant flux at 2537 angstroms.
3. Resolution in line pairs per mm at photocathode.
4. Screen background brightness/conversion index, in incident microlumens/cm².
5. Screen background brightness/conversion index, in incident watts/cm².

F. Fiber Optics-Image Converter Combinations

1. Coupling Optics

In transferring an image between a fiber bundle and an image tube, one must consider a particular problem imposed by the geometry of conventional image tubes, such as those described in Table A-1. Both the photosensitive surfaces and the phosphor surfaces of these tubes are deposited on the insides of glass walls which are many thousandths of an inch thick. If one attempted to couple an image tube and fiber bundle simply by placing them in contact, the lateral spreading of light rays as they passed through the glass walls of the image tube would cause a substantial resolution loss.

Coupling must therefore be accomplished through the use of conventional optics, that is, by using a lens or mirror system to form an image of the bundle end face on the appropriate image tube surface, and conversely.

The present state of the art permits the fabrication of an image tube with the glass walls replaced by thin sections of fused fiber optics faceplates. This would optically bring the image surfaces of the tube to the exterior wall surfaces, permitting image coupling with fiber bundles by simply butting the appropriate surfaces together. Such image tubes are not yet commercially available, but are now under development by various companies. A comparison of fiber optics coupling with Schmidt mirror coupling is discussed in Reference 43 and the matter of coupling is also reviewed in Reference 44.

2. Example Combination

A combination of interest in the fire detection problem makes use of a long fiber bundle to relay an image of an area under surveillance, followed by an image intensifier tube to brighten the image and to make up for losses in the long bundle. An image tube having an S-1 photocathode is selected for the

example because its response in the near-infrared makes it capable of picking up overheated objects as well as flames. The output phosphor image can be viewed through a lens magnifier. This combination has several possible advantages over the alternative arrangement of placing the image tube at the input end:

- (1) The image intensifier tube would be remote from the environmental problems within the engine space and would be safely mounted within the cockpit.
- (2) Intensifying the image after it has been attenuated avoids the saturation of the tube that would result from bright objects such as flames which may be imaged at full brightness on the picture surface. (See Table A-2).
- (3) Fiber optics transmission losses are less for the red-infrared end of the spectrum (useful with the S-1 photocathode) than for the blue-green phosphor output emission of the image tube.
- (4) The complication of using long electrical leads is avoided.

Using generally available tubes having conventional glass faceplates, the above combination requires an imaging system to couple the output end of the long fiber bundle to the photocathode of the image tube. As stated in Sub-Appendix A, the exit numerical aperture is ill defined with the light intensity tapering off from the angle shown in Figure No. A-9 as $(\theta_1 - \Delta\theta)$ to $(\theta_1 + \Delta\theta)$.

The second half of the above combination is identical to that shown in Figure A-7; hence the brightness gain of the second half is as given in the formulae in Sub-Appendix B and tabulated for particular conditions in Table A-3.

For the first half, the losses are of two types, those due to attenuation in the fibers and those due to numerical aperture fuzzing. The attenuation loss is discussed in detail in Paragraphs 2.1.1 and 3.1.1 of the main body of this report. For a 60-foot length the transmission may be expected to be on the order of 0.2%. The extent of the loss due to numerical aperture limitations in very long bundles is not as well known and varies from bundle to bundle, but it can probably be limited to 50%.

Combining these two values to give 0.1% for the first half, the over-all performance of the system including the image intensifier can be determined by dividing the values given in Tables A-2 and A-3 by 1000.

From these data, the 1900° flame shows brightly on the phosphor screen at a level of 75 foot-lamberts. The 1000° K source also shows well, at a level

		Blackbody at 1000° K					
λ in microns	σ_{s-1} Relative Response S-1 Photocathode	Unfiltered		Filtered		Unfiltered	
		N_λ	$\frac{\sigma_{s-1}(\lambda) \times N_\lambda}{N_\lambda \text{ max}}$	$F(\lambda)$	$\frac{F(\lambda)\sigma_{s-1}(\lambda) \times N_\lambda}{N_\lambda \text{ max}}$	$\frac{N_\lambda}{N_\lambda \text{ max}}$	$\frac{\sigma_{s-1}(\lambda)}{N_\lambda}$
1.1	0.06	42×10^{-3}	2.5×10^{-3}	1	2.5×10^{-3}	22×10^{-4}	13×1
1.0	0.30	19 "	5.7 "	1	5.7 "	6.5 "	20 "
0.9	0.80	6.3 "	5.0 "	0	0	1.3 "	10 "
0.8	1.00	1.6 "	1.6 "	0	0	0.18 "	2 "
0.7	0.80	0.2 "	0.2 "	0	0	0	0
$\int \sigma_{s-1}(\lambda) F(\lambda) \frac{N_\lambda}{N_\lambda \text{ max}} d\lambda$		$1.5 \times 10^{-3} \mu$		0.82×10^{-3}		4.5×10	
$\int \frac{N_\lambda}{N_\lambda \text{ max}} d\lambda = 1.5 \lambda \text{ max}$ (for any blackbody)		4.3μ		4.3μ		5.7μ	
$\rho_{s-1} = \text{ratio of above integrals}$		3.4×10^{-4}		1.9×10^{-4}		7.8×1	
$N_s \text{ watts}/(\text{cm}^2 \text{ ster.})$		1.82		1.82		0.58	
$N_{s-1} = \rho_{s-1} N$		6.2×10^{-4}		3.5×10^{-4}		4.5×10	
Screen brightness Type 6411 image tube, $N.A. = 0.5, \text{candles}/\text{cm}^2$		$6.2 \times 10^{-1} *$		$3.5 \times 10^{-1} *$		4.5×10	
Foot-lamberts		1800*		1000*		13	

TABLE A-2. RESPONSE OF S-1 PRO

*signifies overload



	Blackbody at 750°K				Blackbody at 600°K			
	Unfiltered		Filtered		Unfiltered		Filtered	
$\frac{x N_\lambda}{\max}$	$\frac{N_\lambda}{N_\lambda \max}$	$\frac{\sigma_{s-1}(\lambda) \times N_\lambda}{N_\lambda \max}$	$F(\lambda)$	$\frac{\sigma_{s-1}(\lambda)}{N_\lambda \max} F(\lambda) \times N_\lambda$	$\frac{N_\lambda}{N_\lambda \max}$	$\frac{\sigma_{s-1}(\lambda) \times N_\lambda}{N_\lambda \max}$	$F(\lambda)$	$\frac{\sigma_{s-1}(\lambda) F(\lambda) \times N_\lambda}{N_\lambda \max}$
0 ⁻³	22 x 10 ⁻⁴	13 x 10 ⁻⁶	1	13 x 10 ⁻⁶	10 x 10 ⁻⁸	6.0 x 10 ⁻⁸	1	6.0 x 10 ⁻⁸
"	6.5 "	20 "	1	20 "	1.8	5.4 "	1	5.4 "
	1.3 "	10 "	0	0	0.19	1.5 "	0	0
	0.18 "	2 "	0	0	0	0	0	0
	0	0	0	0	0	0	0	0
		4.5 x 10 ⁻⁵		3.3 x 10 ⁻⁵		1.3 x 10 ⁻⁶		1.14 x 10 ⁻⁶
		5.7μ		5.7μ		7.2μ		7.2μ
		7.8 x 10 ⁻⁶		5.8 x 10 ⁻⁶		1.8 x 10 ⁻⁷		1.6 x 10 ⁻⁷
		0.58		0.58		0.24		0.24
		4.5 x 10 ⁻⁶		3.4 x 10 ⁻⁶		4.2 x 10 ⁻⁸		3.8 x 10 ⁻⁸
		4.5 x 10 ⁻⁵		3.4 x 10 ⁻⁵		4.2 x 10 ⁻⁸		3.8 x 10 ⁻⁸
		13		10		0.12		0.11

RESPONSE OF S-1 PHOTOCATHODE TO VARIOUS SOURCES.



λ in Microns	σ_{s-1} Relative Response S-1 Photocathode	Daylight 5800° K		Daylight 5800° K		Tungsten 2870°	
				Filtered			
		$\frac{N_\lambda}{N_\lambda \text{ max.}}$	$\frac{\sigma_{s-1}(\lambda) \times N_\lambda}{N_\lambda \text{ max.}}$	$F(\lambda)$	$\frac{F(\lambda)\sigma_{s-1}(\lambda) \times N_\lambda}{N_\lambda \text{ max.}}$	$\frac{N_\lambda}{N_\lambda \text{ max.}}$	$\frac{\sigma_{s-1}}{N_\lambda}$
1.1	0.06	0.32	2×10^{-3}	1	2×10^{-3}	0.98	6×1
1.0	0.30	0.40	12. "	1	12 "	1.00	30
0.9	0.80	0.50	40. "	0	0	0.97	77
0.8	1.00	0.63	63. "	0	0	0.87	87
0.7	0.80	0.77	62. "	0	0	0.70	56
0.6	0.45	0.92	41. "	0	0	0.46	20
0.5	0.20	1.00	20. "	0	0	0.22	4
0.4	0.50	0.89	45. "	0	0	0.06	3
$\int \sigma_{s-1}(\lambda) F(\lambda) \frac{N_\lambda}{N_\lambda \text{ max.}} d\lambda$		$285 \times 10^{-3} \mu$		$14 \times 10^{-3} \mu$		$283 \times$	
$\int \frac{N_\lambda}{N_\lambda \text{ max.}} d\lambda = 1.5 \lambda \text{ max}$ (for any blackbody)		0.75 μ		0.75 μ		1.5 μ	
$\rho_{s-1} = \text{ratio of the two above integrals}$		0.38		1.87×10^{-2}		0.19	
$N_{s-1} = \rho_{s-1} N \text{ (watts/cm}^2 \text{ ster.)}$		← not applicable					
$\rho_v L$ (lumens per watt)		90		90		16.3	
System brightness gain Type 6411 image tube N. A. = 0.5		4.2		0.2		12	

TABLE A-3. RESPONSE OF S-1 PHOTOCATHODE



Tungsten
2870° K

Tungsten
2870° K

Candle Flame 1900° K
Emissivity 0.025

		Filtered		Unfiltered		Filtered	
$\frac{F(\lambda) \times N_\lambda}{N_\lambda \text{ max.}}$	$\frac{\sigma_{s-1}(\lambda) \times N_\lambda}{N_\lambda \text{ max.}}$	$F(\lambda)$	$\frac{F(\lambda)\sigma_{s-1}(\lambda) \times N_\lambda}{N_\lambda \text{ max.}}$	$\frac{N_\lambda}{N_\lambda \text{ max.}}$	$\frac{\sigma_{s-1}(\lambda) \times N_\lambda}{N_\lambda \text{ max.}}$	$F(\lambda)$	$\frac{\sigma_{s-1}(\lambda) \times N_\lambda}{N_\lambda \text{ max.}}$
10^{-2}							
	0.98 6×10^{-2}	1	6×10^{-2}	0.77	4.6×10^{-2}	1	4.6×10^{-2}
	1.00 30 "	1	30 "	0.63	18.9 "	1	18.9 "
	0.97 77 "	0	0	0.45	36.0 "	0	0
	0.87 87 "	0	0	0.29	29.0 "	0	0
	0.70 56 "	0	0	0.15	12.0 "	0	0
	0.46 20 "	0	0	0.05	2.3 "	0	0
	0.22 4 "	0	0	0.01	0.2 "	0	0
	0.06 3 "	0	0				
$10^{-3}\mu$							
	$283 \times 10^{-3}\mu$		$36 \times 10^{-3}\mu$		$103 \times 10^{-3}\mu$		$23.5 \times 10^{-3}\mu$
	1.5 μ		1.5 μ		2.3 μ		2.3 μ
$< 10^{-2}$							
e	0.19		2.4×10^{-2}		4.5×10^{-2}		1.0×10^{-2}
	16.3		16.3		2.6 $\times 10^{-2}$		5.8×10^{-3}
	12		1.5		1		1
					45		10

RESPONSE OF S-1 PHOTOCATHODE TO VARIOUS ILLUMINANTS.



of 1.8 foot-lambert. The 750° K source, at slightly over 1/100 foot-lambert, can be seen, but at this level it would not be noticeable unless the phosphor screen were well shielded from ambient light and interference from face mask reflections was absent.

3. Gain of Cascaded Image Converters

For a two-stage cascaded system of cesium-antimony tubes, with direct interstage coupling, the over-all visual conversion index has been derived in the paper starting on Page 1 of Reference 135 and has been computed to be 1965, though measured to be only 1000 in a particular sample. This is somewhat greater than the square of the conversion index of a single tube, since the cesium-antimony spectral response of the second stage is well matched ($\rho = 91\%$) to the P-11 phosphor spectral emission of the first tube.

G. Spectral Filtering

1. Infrared Region

Although sensitivity to daylight of the S-1 photocathode is relatively small, ambient daylight could interfere with the seeing of low temperature overheated objects. Spectral filtering can in this case substantially improve the contrast between an overheated object and the ambient-lit background. For example, referring to Table A-2, if all radiation short of 0.95 micron is filtered out, response to sunlight is reduced by a factor of 20, while response to a 750° K source is reduced only by 1.4. With such filtering, effective brightness of a 750° K source is equivalent to that of a 14 candles/ ft^2 (Weston exposure meter reading) scene illuminated by ambient daylight. Even more drastic filtering could be used but this would entail appreciable loss in sensitivity. The effect of filtering is shown in Figure 56.

2. Ultraviolet Region

The possibility exists of using one of the existing ultraviolet-sensitive image converters or others being developed, together with a filter passing only UV, to detect the UV emission from a flame. The spectral pass band could be chosen to render the system partially or completely blind to ambient daylight by restricting the band to the ozone-absorption region short of 0.29 micron. Even though the UV radiation from the flame may be very small, it may be possible to detect it because of the inherently high sensitivity and low noise of photocathodes responding to this region. The disadvantages are (1) the large amount of gain required in order to

present a visible image, (2) the inability to detect overheat conditions if necessary, and (3) the requirement that the image detector be located physically close to the scene, because of strong UV absorption in glass fibers.

H. Summary

In this report, formulae and tables are developed from which one may calculate the brightness of images presented by image converter tubes in combination with lenses, mirrors or fiber bundles, when such systems are used to view overheated objects, flames, and scenes illuminated by ambient daylight. Formulae are also offered for calculating the other important factors of image portrayal: image size, resolution, and eye freedom.

Example calculations show that an existing image converter with an S-1 infrared-sensitive photocathode is capable of presenting an easily visible image of a hazard such as a flame or an object heated to 750° K or above. These calculations have been confirmed qualitatively in experiments, which showed that a source at 600° K could be seen under dark ambient conditions.

The calculations show that even after attenuation by a factor of 1000 as might occur in a long fiber bundle, a flame or an object glowing dull red can be seen with an image converter presently available; but in order to see readily an object at about 750° K under these conditions, one would have to add another image tube in cascade.

Another conclusion of importance is that in using an existing image tube with an S-1 photocathode filtered to reduce daylight response, there should be no question of one's being able to see and distinguish an ordinary flame from background even when under direct sunlight illumination. A high altitude blue flame shows up above ambient background illumination of approximately ~~one~~ foot-candle.

How cool an object can be detected in an actual installation will be determined by ambient light conditions and by the discrimination techniques that can be utilized. Some improvement is realized by filtering out visible radiation as indicated in Section G. One further possible technique is to chop (mechanically modulate) the scene radiation falling on an infrared-sensitive image converter by means of a two-color chopper; if both of the

color filters are made to transmit the same amount of ambient light, the image tube output picture of the ambient-lit scene remains constant; but if one of the filters is made opaque to infrared while the other is made transparent, then an overheated object or flame emitting infrared appears to flicker at the chopping frequency, whereas the rest of the scene remains steady.

SUB-APPENDIX A

Transmission through a Long Fiber Bundle

Theoretically, in a perfect long optical fiber, rays striking the fiber from a point source at an angle θ from the axis of the fiber emanate from the other end in an annular beam of radius θ . (This effect is due to skew rays entering the fiber.) If this were so actually, the exit numerical aperture of the bundle of rays leaving the fiber would be the same as that entering. Also, if this were so, the exit pupil of an optical imaging system using such fibers to convey the image would be homogeneous like the entrance pupil, even though the point to point correspondence between entrance and exit pupils that exists in conventional optical systems is destroyed by the action of skew rays in the fiber. Practically, because of surface imperfections in long fibers, the exit annulus is smeared from a sharply defined ring to a broad, weaker and less defined ring (111). The effect on the exit pupil is to spread it out to a larger, weaker, less-defined exit pupil. While this phenomenon does not greatly affect performance, it needs to be taken into account in the optical system design.

SUB-APPENDIX B

Formulae for Image Intensification and Conversion

To evaluate image intensification, it is necessary to consider the spectral distribution of the energy in the scene, since different tubes respond differently to the various wavelengths and all of them respond differently from the human eye.

The procedure followed below is to (1) relate the scene spectral radiance to the scene visual brightness, as in Eq. (a), by means of a visual effectiveness factor ρ_V and the mechanical equivalent of light L , in the manner customarily followed in computing luminous efficiency (lumens per watt) of a source (Cf: Smithsonian Tables, 9th Ed., Page 96.); (2) in a parallel

manner, relate the scene spectral radiance to the scene's effective "brightness" as viewed by the photodetector, as in Eq. (b).

To evaluate the above, two different cases are considered: (1) a scene illuminated by a source where color temperature is known, and (2) a source which emits radiation associated with its elevated temperature and which may or may not be visible. In the former case we combine Eqs. (a) and (b) to relate effective radiance, as received by a photodetector, to a brightness which can be expressed in familiar terms and measured by a light meter such as a photographic exposure meter, as in Eq. (c). This leads to formulae for image intensification, when the optical geometry is introduced, as in Eq. (e) below.

In the latter case, we evaluate Eq. (b) directly on the basis of blackbody temperature and emissivity. This leads to formulae for image conversion, when the optical geometry is introduced, as in Eq. (d).

1. Development of Formulae for Scene Brightness

The visual brightness of a scene viewed directly can be related to the radiance of the scene by the expression

$$b_v = \rho_v L N \quad (a)$$

where L = the constant 680 lumens/watt = the mechanical equivalent of light

N = $\int N_\lambda d\lambda$
= radiance of the scene, total watts emitted per (cm^2 ster).

b_v = visual brightness of the scene, candles per cm^2 =
lumens per (cm^2 ster).

ρ_v = visual effectiveness factor of the scene radiation

$$\rho_v = \frac{\int \sigma_v(\lambda) N_\lambda d\lambda}{N}$$

N_λ = spectral radiance of the scene, w/(cm^2 ster micron).

$\sigma_v(\lambda)$ = normalized spectral response of eye.

λ = wavelength in microns

The value of $L\rho_v$ is sometimes called the luminous efficiency of the radiation, tabulated for various color temperatures in handbooks.

2. Development of Formulae for System Brightness Gain

The "brightness" of a scene as detected by a typical photosensitive surface, such as the S-1, can be expressed as an effective radiance N_{s-1} which is the total scene radiance multiplied by an effectiveness factor ρ_{s-1}

$$N_{s-1} = \rho_{s-1} N \quad (b)$$

where N_{s-1} = S-1 effective radiance of scene in S-1 effective watt/(cm² ster).

$$\rho_{s-1} = \text{effectiveness of the scene radiation} = \frac{\int \sigma_{s-1}(\lambda) N_\lambda d\lambda}{N}$$

$\sigma_{s-1}(\lambda)$ = normalized spectral response of S-1 photosurface.

$F(\lambda)$ = spectral transmission of optical filter. If no filter is used, $F = 1$.

3. Evaluation of Scene Brightness in Terms of the Photodetector

For scenes whose color temperatures are known, such as those illuminated by sunlight (5800° K color temperature) and whose visual brightness may be measured by an exposure meter (in candles per ft²), the photodetector effective radiance is obtained by combining equations (a) and (b) above, giving:

$$N_{s-1} = \frac{\rho_{s-1} b_v}{\rho_v L} \quad (c)$$

Values for $\rho_v L$ are published in Smithsonian Physical Tables, 9th Ed. Page 96. Values for ρ_{s-1} are tabulated in Tables A-2 and A-3 for various sources and illuminants. If b_v is measured by an exposure meter, calibrated in candles per sq. ft., its reading must be divided by 930 cm²/ft² to convert to candles/cm² (or lumens/cm²-steradian).

For self-emitting objects of known emissivity and temperature, equation (b) above has been evaluated to yield values of ρ for some objects of interest. These values have been tabulated in Table A-2.

Values are also calculated for the case where an idealized optical filter is used having a sharp cutoff at 0.95 microns. ($F = 0$, $\lambda < 0.95\mu$, and $F = 1$, $\lambda > 0.95\mu$). This is approximately the cutoff wavelength of Corning Filter #2540 and Polaroid RX, but the actual filters have a somewhat less sharp cutoff characteristic.

4. System Brightness Gain

Having determined the effective radiance of the illuminated scene or self-emitting object, it is only necessary to consider the optical geometry and the radiant conversion index M_r of the image tube to arrive at a value for the output phosphor brightness and, when applicable, the image intensification or brightness gain of the system. These are given in Equations (d) and (e) below.

For the minimum system illustrated in Figure A-7, consisting of a lens of numerical aperture N.A. forming an image of the scene on the cathode of an image converter, the effective irradiance I_{s-1} of the input image in S-1 effective watts/cm² is, by geometry,

$$I_{s-1} = \pi(N.A.)^2 N_{s-1} \text{ (watts per cm}^2\text{)}$$

and the phosphor screen output brightness is

$$b_p = \frac{M_r I_{s-1}}{\pi m^2} \text{ (candles per cm}^2\text{)}$$

The factors of π and m , the image tube magnification, enter because the conversion index M_r is defined in terms of total luminous output (into 2π steradians) and because b_p is expressed as a brightness.

The response of the system to a self-emitting object is therefore: phosphor screen output brightness

$$b_p = \frac{M_r (N.A.)^2 N_{s-1}}{m^3} \text{ (candles per cm}^2\text{)} \quad (d)$$

Table A-2 lists computed screen brightness for a Type 6411 tube with a 0.5 N.A. optical system, for various sources.

The visual brightness gain of the system is obtained by combining Eqs. (c) and (d) as

$$\frac{b_p}{b_v} = \frac{M_r (N.A.)^2 \rho_{s-1}}{m^3 \rho_v L} \quad (e)$$

For the special case of 2870°K tungsten illumination, brightness gain may be obtained more directly using published values of visual conversion index

$$\frac{M_v}{b_v} = \frac{M_r \rho_{s-1}}{\rho_v L} \text{ (lumens per watt)}$$

This leads to

$$\frac{b_p}{b_v} = \frac{M_v(N.A.)^2}{m^2}$$

5. Sample Calculations

For a N.A. = 0.5 optical system with a Type 6411 image tube: Brightness gain when the scene is illuminated by 2870°K color temperature tungsten lamps:

$$\begin{aligned}\frac{b_p}{b_v} &= \frac{(N.A.)^2 M_r}{m^2} \times \frac{(p_{s-1})}{(p_v L)} \\ &= \frac{(0.5)^2 2000 \text{ lumens/watt}}{(0.7)^2} \times \frac{0.19}{16.3 \text{ lumens/watt}} \\ &\approx 12\end{aligned}$$

For a N.A. = 0.5 optical system with a Type 6411 image tube and an idealized optical filter cutting off sharply all radiation below 0.95 micron in wavelength, the phosphor screen image brightness due to an object at 750°K emitting as a blackbody is:

$$\begin{aligned}b_p &= \frac{(N.A.)^2 M_r N_{s-1}}{m^2} \\ &= \frac{(0.5)^2 2000 \text{ lumens/watt}}{(0.7)^2} \times 3.4 \times 10^8 \frac{\text{watts}}{\text{cm}^2 \text{ ster}} \\ &= 3.4 \times 10^{-3} \text{ lumens/cm}^2 \text{ ster.} (= \text{candles/cm}^2) \\ &= 10.7 \text{ foot-lamberts}\end{aligned}$$

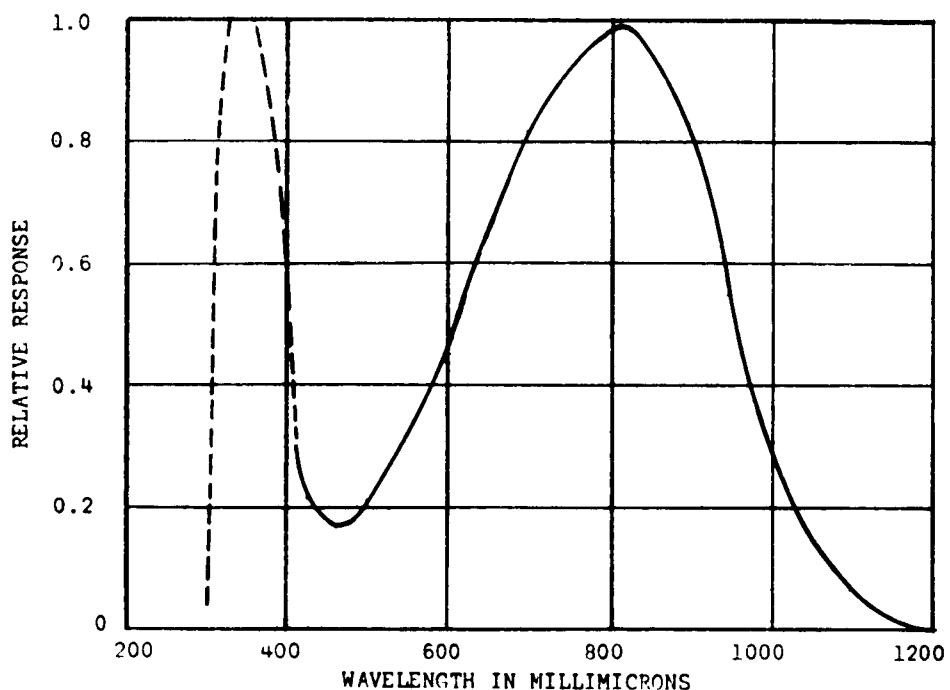


Figure A-1. Relative spectral response of S-1 photosurface. Solid line shows usable portion.

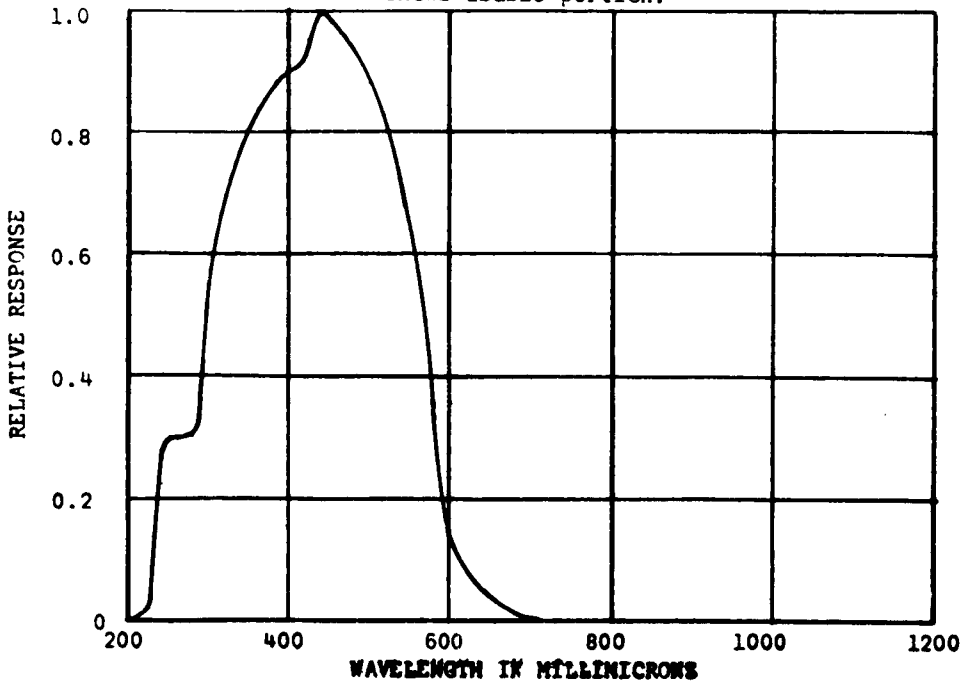


Figure A-2. Relative Spectral response of S-21 photosurface.

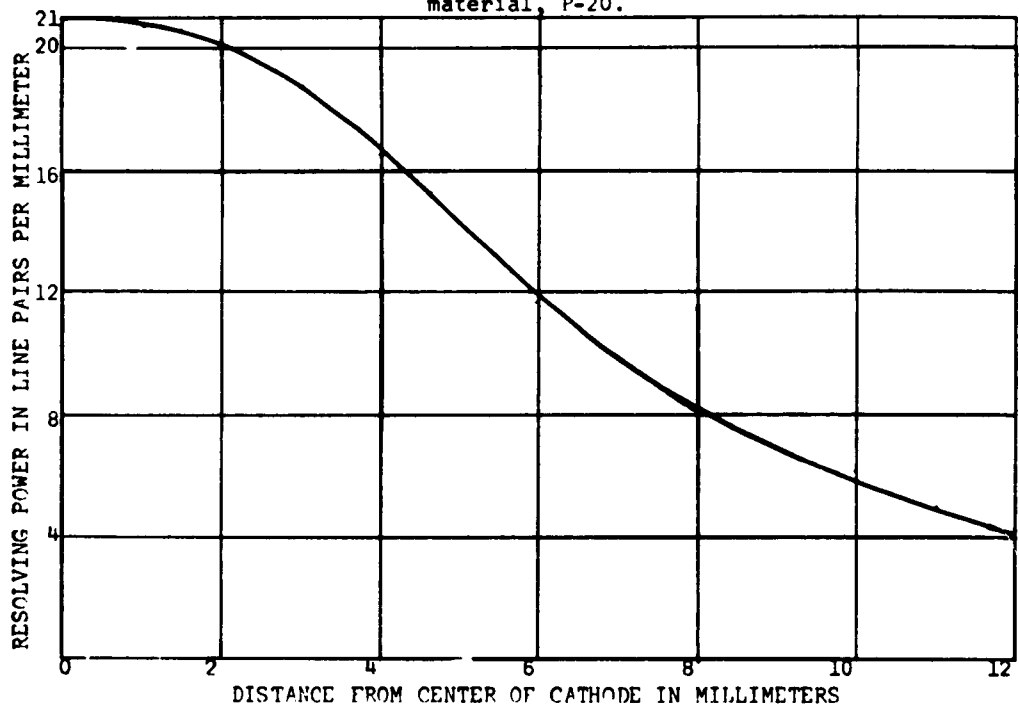
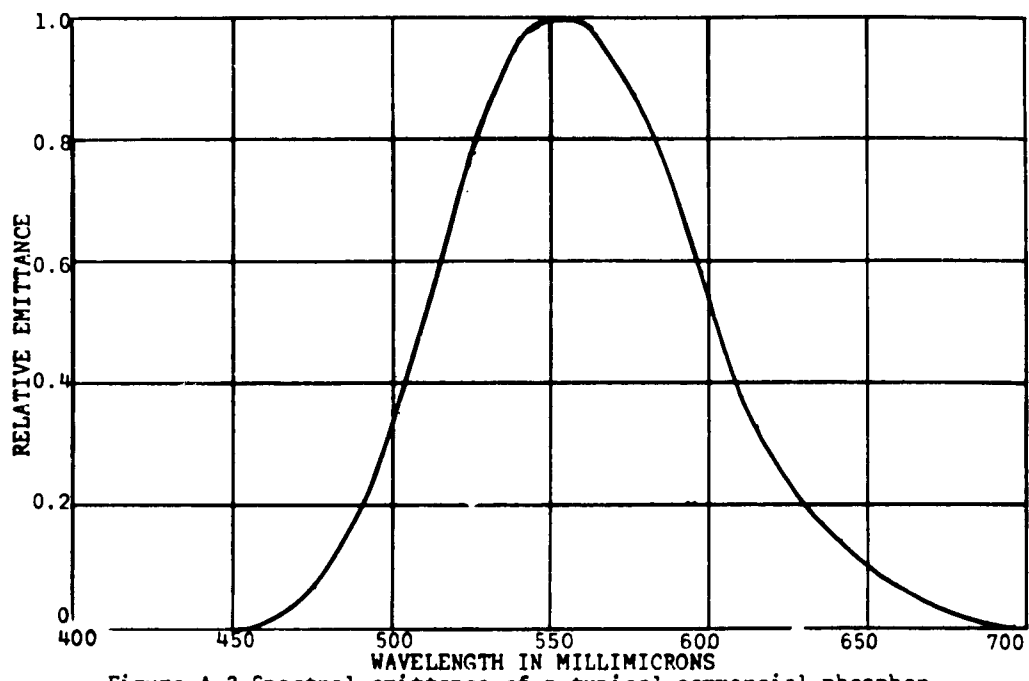


Figure A-4. Resolution of No. 6411 image converter tube.

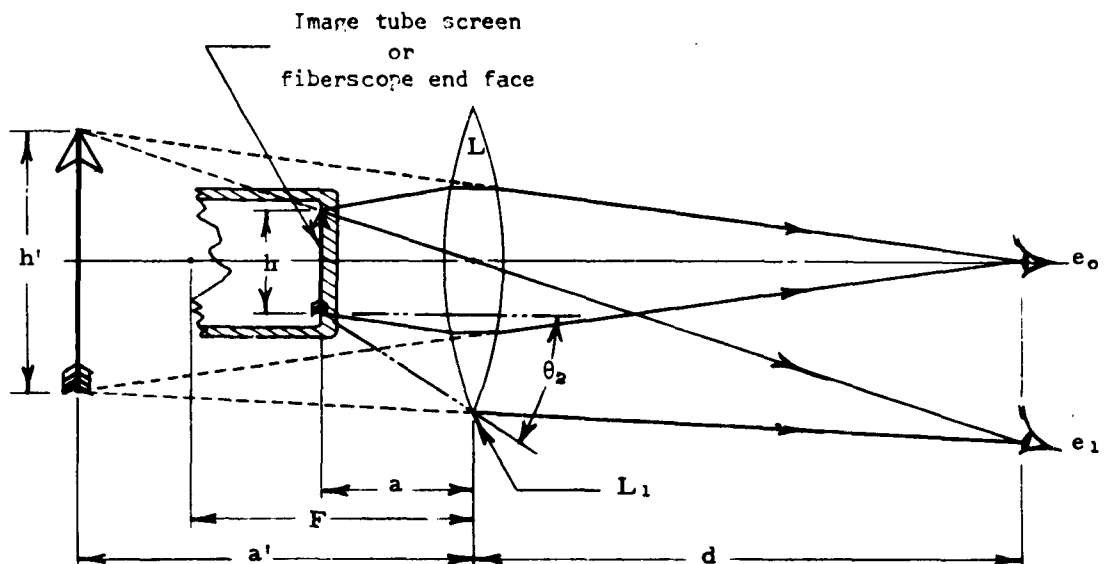


Figure A-5. Use of an eyepiece magnifier.

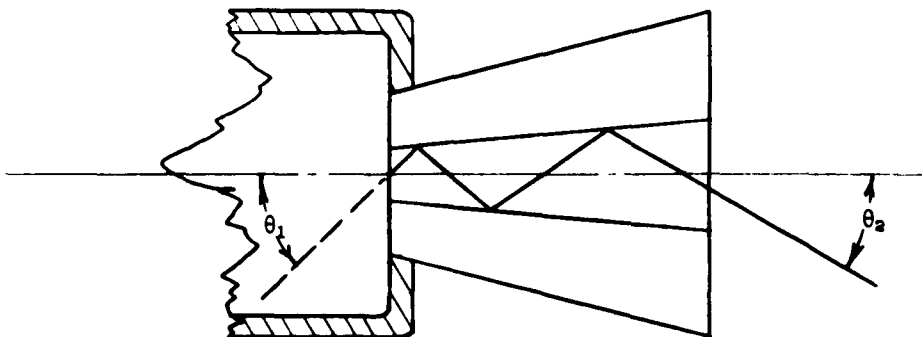


Figure A-6. Use of a tapered fiber bundle magnifier.

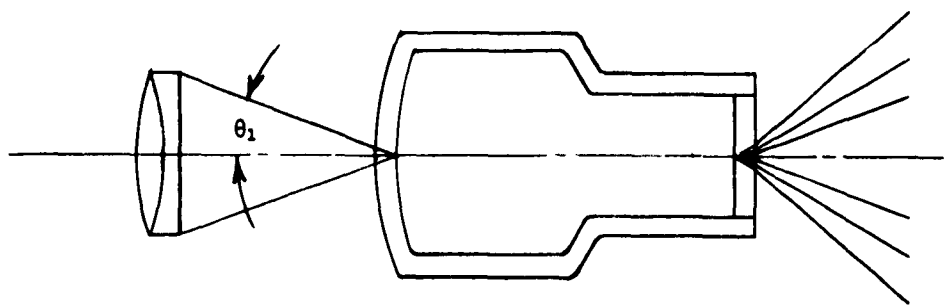


Figure A-7. Combination of an objective lens with an image tube.

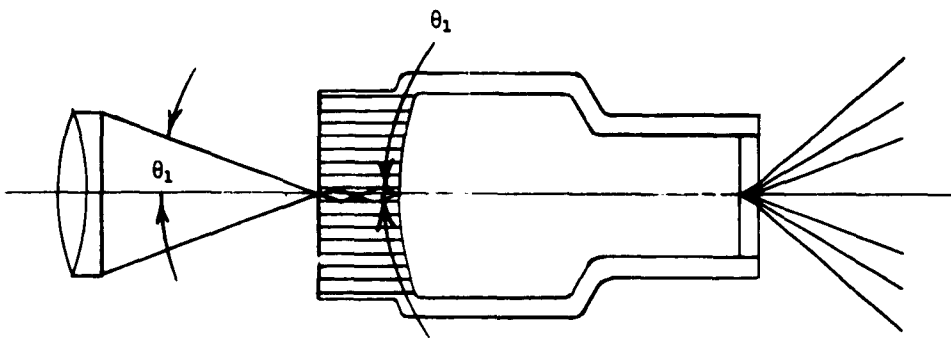


Figure A-8. Objective lens and image tube with fiber optic faceplate.

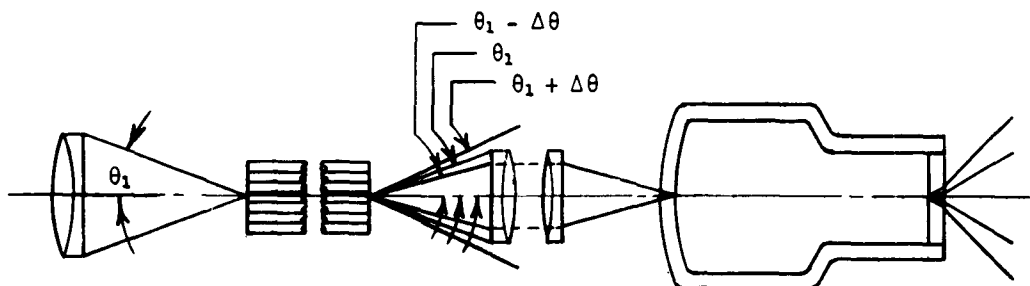


Figure A-9. Objective lens, fiber bundle, and lens-coupling to image tube.

BIBLIOGRAPHY AND REFERENCES

A. EARLY RESEARCH PAPERS, THROUGH 1955

1. Bowen, I. S.
The image-slicer, a device for reducing loss of light at
slit of stellar spectograph
Astrophys. J. 88, 113-124 (1938).
2. Brouwer, W. and van Heel, A. C. S.
Two-dimensional coding of optical images
Optica Acta 2, 49 (1955).
3. Hopkins, H. H. and Kapany, N. S.
A flexible fiberscope using static scanning
Nature 173, 39-41 (1954).
4. Hopkins, H. H. and Kapany, N. S.
Transparent fibers for the transmission of optical images
Optica Acta 1, 164-170 (February, 1955).
5. Jean, J. N.
A microwave analogue to the Stiles and Crawford effect
University of Rochester Thesis, Rochester, N. Y. (1949).
6. Kapany, N. S.
Optical systems with flexible axes
Ph. D. Thesis, Imperial college, London (January, 1955).
7. Lamm, H.
Biegsame Optische Geraete
Z. fuer Instrumentenkunde 50, 579-581 (1930).
8. Lindberg, P.
Measurement of contrast transmission characteristics in
optical image formation
Optica Acta 1, 80-89 (1954).
9. Schriever, O.
Elektromagnetische Wellen an dielektrischen Drachten
Ann. Phys. 63, 645-673 (1920).
10. van Heel, A. C. S.
Optical representation of images without use of lenses or mirror
De Ingenieur 24, 26 (1953) (in Dutch).
(Royal Institute of Engineers, The Hague, The Netherlands).

11. van Heel, A. C. S.
A new method of transporting optical images without aberrations
Nature 173, 39 (1954).

B. PATENTS

12. Allen, R. P.
Image-forming, transmitting, and reproducing apparatus
U. S. 1,848,814 (1932).
13. Baird, J. L.
An improved method of and means for producing optical images
British Patent Spec. 285,738 (1927).
14. Goldsmith, A. N.
Television apparatus
U. S. 2,354,591 (1944).
15. Hansell, C. W.
Picture transmission.
U. S. 1,751,584 (1927).
16. Hardesty, G. K. C.
Indicating device
U. S. 2,128,246 (1937).
17. O'Brien, B.
Optical image forming devices
U. S. 2,825,260 (1958).
18. Young, F. G., Jr.
Light projector
U. S. 1,642,187 (1927).

C. CURRENT RESEARCH PAPERS, 1956-PRESENT

19. Daich, A. R. et al
Passage of light through lightguides
Optics and Spectroscopy viii, 375-379 (1960).
20. Harris, C. C. and Bell, P. R.
Transmission characteristics of light pipers
IRE Trans. Nuclear Sci. 87-89 (November, 1956).
21. Hett, J. H. and Curtiss, L. E.
Fiber optics duodenoscope and ureterscope
J. Opt. Soc. Am. 51, 581,582 (1961).

22. Hirschowitz, B. I.
Endoscopic examination of the stomach and
duodenal cap with the fiberscope
Lancet (London, April, 1961).
23. Hirschowitz, B. I., Curtiss, L. E., Peters, C. W. and Pollard, H. M.
Demonstration of a new gastroscope, the "fiberscope"
Gastroenterology 35, (1) (July, 1958).
24. Hopkins, H. H. and Kapany, N. S.
Transparent fibers for the transmission of optical images
Problems in Contemporary Optics, pp. 150-167
Proceedings of the Florence Meeting, September 10-15, 1954.
Istituto Nazionale di Ottica, Florence, Italy (1956).
25. Kapany, N. S.
A light funnel for stellar spectrograph
Proceedings of a Symposium on Astronomical Optics and Related
Subjects held in Univ. of Manchester, April 19-22, 1955,
North-Holland Publ. Co., Amsterdam pp. 288-292 (1956).
26. Kapany, N. S.
Fiber optics
Concepts of Classical Optics, edited by John Strong
Appendix N, pp. 553-579
W. H. Freeman & Co., San Francisco (1958).
27. Kapany, N. S.
High-resolution fiber optics using sub-micron multiple fibers
Nature 184, 881-883 (1959).
28. Kapany, N. S.
Electro-optical systems using fiber optics
Optica Acta 8, 201 (1960).
29. Kapany, N. S.
Fiber optics for data recording
Twelfth Annual Meeting of the Technical Ass'n of the Graphic Arts,
June 20-22, 1960 pp. 95-101.
30. Kapany, N. S. and Mergerian, D.
Infrared fiber optics (Unclassified article)
Proc. IRIS 5 (2) 139 (April, 1960). (SECRET)

31. Kapany, N. S.
Endoscopes using fiber optics
Proceedings of the International Congress of Gastroenterology 1960
Excerpta Medica Foundation (in press, 1961).
32. Kapany, N. S.
Fiber optics. Part I. Optical properties of certain dielectric cylinders
J. Opt. Soc. Am. 47, 413-422 (1957).
33. Kapany, N. S., Eyer, J. A. and Keim, R. E.
Fiber optics Part II. Image transfer on static and dynamic
scanning with fiber bundles
J. Opt. Soc. Am. 47, 423-427 (1957).
34. Kapany, N. S. and Hopkins, R. E.
Fiber optics. Part III. Field flatteners
J. Opt. Soc. Am. 47, 594-598 (1957).
35. Kapany, N. S. and Pike, J. N.
Fiber optics. Part IV. A photorefractometer
J. Opt. Soc. Am. 47, 1109-1117 (1957).
36. Kapany, N. S.
Fiber optics. V. Light leakage due to frustrated total reflection
J. Opt. Soc. Am. 49, 770-778 (1959).
37. Kapany, N. S.
Fiber optics. VI. Image quality and optical insulation
J. Opt. Soc. Am. 49, 779-787 (1959).
38. Kapany, N. S. and Capellaro, D. F.
Fiber optics. VII. Image transfer from Lambertian emitters
J. Opt. Soc. Am. 51, 23-31 (1961).
39. Kapany, N. S.
Fiber optics. VIII. The focon
J. Opt. Soc. Am. 51, 32-34 (1961).
40. Kapany, N. S. and Burke, J. J.
Fiber optics. IX. Waveguide effects
J. Opt. Soc. Am. 51, 1067 (1961).
41. Potter, R. J.
A theoretical and experimental study of optical fibers
U. S. Atomic Energy Comm. Report NYO-9033 (April 1, 1960).

42. Potter, R. J.
Transmission properties of optical fibers
J. Opt. Soc. Am. 51, 1079-1089 (1961).
43. Potter, R. J. and Hopkins, R. E.
Fiber optics and its application to image intensifier systems
Proc. Image Intensifier Symposium, pp. 91-109
U. S. A. E. R. D. L., Ft. Belvoir, Va. (1958).
44. Potter, R. J. and Hopkins, R. E.
The optical coupling of a scintillation chamber to an image-intensifying tube
IRE Trans. Nuclear Sci. NS-7, 150 (1960).
45. Reiffel, L. and Kapany, N. S.
Some considerations on luminescent fiber chambers and intensifier screens
Rev. Sci. Instr. 31, 1136-1142 (1960).
46. Roetling, P. G. and Ganley, W. P.
Observations on the dynamic frequency response of fiber bundles
J. Opt. Soc. Am. 52, 99 (1962).
47. Snitzer, E.
Proposed fiber cavities for optical masers
J. App. Phys. 32, 36 (1961).
48. Snitzer, E.
Cylindrical dielectric waveguide modes
J. Opt. Soc. Am. 51, 491 (1961).
49. Snitzer, E. and Osterberg, H.
Observed dielectric waveguide modes in the visible spectrum
J. Opt. Soc. Am. 51, 499 (1961).
50. Siegmund, W. P.
Infrared transmitting fiber optics
6th Technical Symposium
Soc. Photographic Instrumentation Engineers
Los Angeles, California, August, 1961
Proceedings (to be published).
51. Simpson, G. R., Upton, L. O. and Campbell, W. C.
High transmission infrared fiber optics (Unclassified article)
Proc. IRIS 6 (3), 151-158 (August, 1961). (SECRET)
(Also published as an American Optical Co. report).

D. ABSTRACTS FROM J. OPT. SOC. AM. (Papers presented at meetings of the Optical Society of America)

52. Burke, J. J.
Elementary modes of circular dielectric waveguide
J. Opt. Soc. Am. 51, 1473 (1961).
53. Burke, J. J. and Kapany, N. S.
Waveguide theory in fiber optics
Ibid. 50, 1128 (1960).
54. Capellaro, D. F. and Kapany, N. S.
Fiber optics--image transfer from Lambertian emitters
Ibid. 49, 1129 (1959).
55. Capellaro, D. F. and Kapany, N. S.
Proximal scanning using fiber optics
Ibid. 51, 1474 (1961).
56. Chitayat, A.
Optical-scanning methods for the improvement of images through fiber optics
Ibid. 52, 607 (1962).
57. Curtiss, L. E., Hirschowitz, B. and Peters, C. W.
A long fiberscope for internal medical examinations
Ibid. 47, 117 (1957).
58. Finkelstein, N. A.
Fiber optics - a progress report
Ibid. 48, 870 (1958).
59. Hett, J. H. and Curtiss, L. E.
Some applications of fiber optics to medical instruments
Ibid. 50, 1128 (1960).
60. Hicks, J. W., Hopkins, R. E., and Potter, R. J.
Fiber optics. I. Optical design considerations
Ibid. 49, 506 (1959).
61. Hicks, J. W. and Potter, R. J.
Fiber optics. IV. Electromagnetic theory
Ibid. 49, 507 (1959).

62. Hopkins, R. E. and Kapany, N. S.
Field flatteners made of glass fibers
Ibid. 47, 117 (1957).
63. Lewis, R. E. and Sheldon, G. J.
Flexible fiber optics bundles
Ibid. 49, 507 (1959).
64. Kapany, N. S.
An introduction to fiber optics
Ibid. 47, 117 (1957).
65. Kapany, N. S.
Role of optical insulation in fiber optics
Ibid. 48, 870 (1958).
66. Kapany, N. S. and Burke, J. J.
Experimental studies of waveguide effects in fiber assemblies
Ibid. 50, 1128 (1960).
67. Kapany, N. S. and Burke, J. J.
Light conduction along absorbing fiber by evanescent boundary wave
Ibid. 51, 1474 (1961).
68. Kapany, N. S. and Capellaro, D. F.
Fiber optics - some recent techniques
Ibid. 49, 1128 (1959).
69. Kapany, N. S., Eyer, J. A. and Keim, R. E.
Fiber optics - Image transfer on static and dynamic
scanning with fiber bundles
Ibid. 47, 117 (1957).
70. Kapany, N. S. and Oberheim, W. A.
Microwave analogs of fiber optics
Ibid. 48, 870 (1958).
71. Kapany, N. S. and Pontarelli, D. A.
On dielectric cylinder photorefractometer
Ibid. 48, 870, (1958).
72. Kapany, N. S. and Pontarelli, D. A.
Fiber optics - detection of absorbing media using modified
photorefractometer
Ibid. 49, 1129 (1959).

73. Osterberg, H. et al
Optical wave-guide modes in small glass fibers. II. Experimental
Ibid. 49, 1128 (1959).
74. Pontarelli, D. and Brushenko, A.
Fiberscope utilizing coaxial illumination
Ibid. 51, 1473 (1961).
75. Pontarelli, D. A. and Kapany, N. S.
Infrared fiber optics
Ibid. 50, 1128 (1960).
76. Potter, R. J.
Numerical aperture of an optical fiber
Ibid. 51, 1473 (1961).
77. Potter, R. J. and Hicks, J. W.
Fiber optics. III. Geometrical theory
Ibid. 49, 507 (1959).
78. Potter, R. J. and Hopkins, R. E.
Properties of optical fibers
Ibid. 49, 1128 (1959).
79. Siegmund, W. P.
Fiber optics. II. Properties of some fiber optics assemblies
Ibid. 49, 507 (1959).
80. Siegmund, W. P. and Wight, R.
Ultra-high speed photographic objective utilizing fiber optics
Ibid. 49, 1128 (1959).
81. Snitzer, E.
Optical coupling between two parallel dielectric wave guides
Ibid. 49, 1128 (1959).
82. Snitzer, E.
High-order dielectric waveguide modes in the visible
Ibid. 50, 505 (1960).
83. Snitzer, E. and Hicks, J. W.
Optical wave-guide modes in small glass fibers, I. Theoretical
Ibid. 49, 1128 (1959).
84. Snitzer, E. and Hoffman, F.
Glass fibers acting as receiving dielectric endfire antennas
in the visible spectrum
Ibid. 51, 1463 (1961).

E. TECHNICAL AND POPULAR ARTICLES

85. Anon.
Piping pictures with fibers
Product Engineering, p. 14 (April 20, 1959).
86. Anon.
Glass fiber optics
Design News 14 (14), 18-19 (July 6, 1959).
87. Anon.
Fiber optics could solve many electronic design problems
Electronic Design, p. 10ff (August 19, 1959).
88. Anon.
Fiber optics improves scan systems
Missiles and Rockets 7 (8), 32-33 (August 22, 1960).
89. Anon.
New way to see around curves
LIFE, p. 5 lff (December 17, 1960).
90. Edman, L. S.
Glass fibers that see around corners
INDUSTRY (January, 1961).
91. Frey, H. B.
Fiber optics
Soc. Aircraft Materials & Process Engrs.,
(P. O. Box 5582, Arlington 5, Va.), presented
at Fall Meeting, Eastern Division, Washington, D. C.,
November 17, 1959.
92. Gernsback, H.
Microtelevision
Radio-electronics, p. 25 (August, 1960).
93. Hodapp, E. J. Jr.
Dyna-Soar safety problem
Aerospace Safety, p. 2-4 (December 1960).
94. Hicks, J. W., Jr. and Kiritsy, P.
Fiber optics
(Part I: The Glass Industry 43 (4), 193 (April, 1962)
(Conclusion: Ibid. 43 (5), 263 (May, 1962).

95. Kapany, N. S.
Fiber optics
Sci. Am. 203, 72-81 (November, 1960).
96. Kapany, N. S.
Fiber optics activity expanding
Electronic News 6 (265), 4(June 12, 1961).
97. Kapany, N. S.
Fiber optics
Research/Development 12, 64 (July, 1961).
98. Krolak, L. J.
Fiber optics and its use in electro-optical devices
Sixth Avionics Technical Panel Meeting, Advisory Group for
Research and Development, NATO. Paris, France, July 6-10, 1962
(to be published).
99. Krolak, L. J., Siegmund, W. P., and Neuhauser, R. G.
Fiber optics - a new tool in electronics
J. SMPTE 69, 705-710 (October, 1960).
100. Lynch, C. J.
Fiber optics grows up
Product Eng. p. 636 (October 30, 1961).
101. MacNeille, S. M.
Fiber optics - new twists in an old science
Am. Soc. Tool & Mfg. Eng., Tech. Paper No. 368
Vol. 61, Book 1 (1961).
102. Miller, A. J. and Hartshorne, R.
Fiber optics in motion-picture printing
J. SMPTE 70, 701 (1961).
103. O'Brien, B.
Physics in the optical industry
Physics Today 13 (1), 52-56 (January, 1960).
104. Revi, A. C.
Miniature portraits in glass rods
The Glass Industry (June, 1947).

105. Salati, O. M.
Handling light with fiber optics
Electronic Industries 20, 102 (December, 1961).
106. Siegmund, W. P.
Fiber optics
The Glass Industry 41 (9), 502 (September, 1960).
107. Siegmund, W. P.
Fiber optics - Principles, properties, and design considerations
Sixth Avionics Technical Panel Meeting, Advisory Group for
Research and Development NATO. Paris, France, July 6-10, 1962
(to be published).
108. Siegmund, W. P.
Unconventional fiber optics
Proc. Image Intensifier Symposium
U. S. A. E. R. D. L., Ft. Belvoir, Va., October, 1961
(to be published).
109. Siegmund, W. P.
Fiber optics at American Optical Company - a progress report
6th Technical Symposium
Soc. Photographic Instrumentation Engineers
Los Angeles, California, August, 1961
Proceedings (to be published).
110. Stewart, H.
The new optics
International Sci. & Technology (4), 15-26 (April, 1962).
111. Stow, R. L.
Fiber optics and their application to electronic tubes
Electrical Design News 6 (12), 30-51 (December, 1961).

F. INDUSTRIAL REPORTS

112. Anon.
Bundling
Industrial Bulletin, A. D. Little, Inc., Cambridge, Mass.
No. 378 (September, 1960).
113. Anon.
Fiber optics
American Optical Co., Southbridge, Mass. (1960).
(Also, see Ref. 51).

114. Anon.
Image enhancer for optical fiber cables
OPTOMECHANISMS, Inc., Plainview, N. Y. (1961).
115. Hicks, J. W. and Kiritsy
Fiber Optics Handbook
Mosaic Fabrications, Inc., Southbridge, Mass.
2nd ed. (1961).
116. Hovnanian, H. P. and Haswell, D. B.
An electro-optical dental monitor
Research & Advanced Development Div., AVCO Corp.,
Wilmington, Mass. (1959).
117. Karkow, W. B. and Baker, A. M.
Fiber optics
Report I
Chicago Aerial Industries Inc. (1961).
118. Traub, A. C.
Fiber optics and the safety problem
Fenwal Inc., Ashland, Mass. (1960).

G. GENERAL WORKS

I. Vortex Tubes

119. Dornbrand, H. (Republic Aviation Corp.)
Theoretical and experimental study of vortex tubes
AF Tech. Report 6123 (June, 1950)
Wright Air Development Center,
Wright-Patterson Air Force Base, Ohio.
120. Hilsch, R. (contributor)
Scientific developments of interest for the
detection of radiation by supraconductors
Tech. Report No. 557-45 (October, 1945)
U. S. Naval Technical Mission in Europe
(PB 23091, distr. by Office of the Publication
Board, Dept. of Commerce, Washington 25, D. C.).

121. Jeffries, N. P. and Wichman, R. E.
Vortex tube modifications
ASD Technical Note 61-79 (1961)
Flight Accessories Lab, ASD,
Air Force Systems Command, USAF,
Wright-Patterson Air Force Base, Ohio.
122. Roebuck, J. R.
A novel form of refrigerator
J. Applied Physics 16, 285-295 (1945).
123. Stong, C. L.
(Section on Hilsch tubes in
The amateur Scientist dept.)
Sci.- American 199 (5), 145 (November, 1958).

II. Properties of Glass

124. Morey, G. W.
The Properties of Glass
Reinhold Publishing Company, New York, 1954.
125. Shand, E. B.
Glass Engineering Handbook
McGraw-Hill Book Co., Inc. New York
Second edition, 1958.
126. Schulman, S.
Elevated temperature behavior of fibers
WADD Technical Note 60-298 (1961)
ARDC, U.S. Air Force
127. Taylor, H. E., author of Ch. 9, "Glass"
Birks, J. B. (Editor)
Modern Dielectric Materials
Academic Press, Inc., New York, 1960.
128. Volf, M. B.
Technical Glasses
Sir Isaac Pitman and Sons, Ltd., London, 1961.

III. Vision

129. Howell, W.C. and Draft, C.L.
Size, blur, and contrast as variables affecting the legibility of
alpha-numeric symbols on radar-type displays
WADC Technical Report 59-536 (1959)
Aerospace Med. Lab., WADD, ARDC, USAF.

130. Traub, A.C. and Balinkin, I.
Proximity factor in the Judd color difference formula
J. Opt. Soc. Am. 51, 755 (1961).

131. Wulfeck, J.W., et al
Vision in military aviation
WADC Technical report 58-399 (1958)
WADC, ARDC, U.S. Air Force.

IV. Aircraft Fire Hazards

132. Carlton, C. et al
Study of explosion and fire suppression of
aircraft engine sections
WADC Technical Report 57-300
Equipment Lab., WADC, ARDC, USAF.

133. Lockheed-California Co. (Div. of LAC)
Study on minimization of fire and explosion
hazards in advanced flight vehicles
ASD Technical Report 61-288 (1961)
Aero. Systems Div., AFSC, U.S. Air Force.

134. Roeser, W.F. and McCamy, C.S.
Principles of fire detection in aircraft engine spaces
WADC Technical Report 54-307 (1954)
Equipment Lab., WADC, ARDC, USAF.

V. Image Devices

135. Image Intensifier Symposium (Proceedings)
U.S. Army E.R.D.L., Ft. Belvoir, Virginia
(October 6-7, 1958)
O.T.S. PB 151813.

136. Anderson, A.E., Goetze, G.W. and Kanter, H.
The Astracan tube and its application to
high-speed photography
J. Soc. M.P.T.E. 70, 440-442 (1961).

137. Gebel, R.K.H.
The limitations for nighttime detection of celestial bodies
employing the image orthicon and the intensifier image orthicon
WADC Technical Note 59-131 (1960)
Aero. Res. Lab., WADD, ARDC, U.S. Air Force.

138. Gebel, R.K.H.
The limitations in resolution and discrimination in brightness
differences for light amplifier systems using contrast enhancement
ARL-12 (1961)
Air Force Res. Div., ARDC, USAF.

139. Gebel, R.K.H. and Devol, L.
 The limiting detectivity of optical amplifying equipment
 WADC technical Note 59-405 (1959).
140. Keyes, R.J.
 Photoconductive-photoemissive far-infrared image tube
 Proc. IRIS 6 (3), 75-78 (August, 1961).
141. Lempert, Jr.
 Research and reports on an optical amplifier
 ARL Technical Report 60-283 (1960)
 Air Force Research Division, USAF.
142. Morton, G.A.
 Infrared photoemission
 Proc. I.R.E. 47, 1467-1469 (1959).
143. Morton, G.A. et al
 Brightness intensifier study
 ARL technical Report 60-284 (1960)
 Air Force Research Division, USAF.
144. Nakamura, T. and Kasai, T.
 Image converter tube for high-speed photography
 Electronics 33 (50), 76-78 (December 9, 1960).
145. Orthuber, R.K. and Ullery, L.R.
 A solid-state image intensifier
 JOSA 44, 297-299 (1954).
146. Perl, M.L. and Jones, L.W.
 Very-high-gain image-intensifier systems and the photography
 of single photons with microsecond time resolution
 J. Soc. M.P.T.E. 70, 704-709 (1961).
147. Wiseman, R.S. and Klein, M.W.
 Photoemissive image-forming systems
 Proc. I.R.E. 47, 1604-1606 (1959).

VL Entries Added In Proof

148. Potter, R.J.
 Transmission properties of optical fibers
 Research Paper RC-330 (September 16, 1960)
 International Business Machines Corp.
 Thomas J. Watson Research Center
 Yorktown Heights, New York
 (See Ref. 42).

149. Potter, R.J., Donath, E. and Tynan, R.F.
The light collecting properties of optical fibers -
Part I. The perfect circular fiber
Research Paper RC-656 (March 15, 1962)
Ibid. (see 148)
(To be published).
150. Novotny, G. V.
Fiber optics for electronics engineers
Electronics 35, 37-42 (June 1, 1962).
151. Stookey, D. S.
Modern glass
International Science and Technology, No. 7, 40-46 (July, 1962).

Aeronautical Systems Division, Dir/Materials
and Processes, Flight Accessories Lab.,
Wright-Patterson AFB, Ohio.
Rpt Nr ASD-TDR-62-731, FIBER OPTICS IN
AEROSPACE VEHICLE HAZARD DETECTION, Final
report, Dec 62, 212p., incl illus, 151 refs.

Unclassified report
I. AFSC Project 6075
Task 607506
II. Contract AF 33(616)-
8165
III. Femval Inc.,
Ashland, Mass.
IV. Terry Trumble
V. Avail for OTS
VI. In ASTIA collection

I. Waveguides
2. Fiber optic systems
3. Aerospace hazard
detection
4. Electromagnetic
radiation
5. Optics
I. AFSC Project 6075
Task 607506
II. Contract AF 33(616)-
8165
III. Femval Inc.,
Ashland, Mass.
IV. Terry Trumble
V. Avail for OTS
VI. In ASTIA collection

Aeronautical Systems Division, Dir/Materials
and Processes, Flight Accessories Lab.,
Wright-Patterson AFB, Ohio.
RPT NR ASD-TDR-62-731, FIBER OPTICS IN
AEROSPACE VEHICLE HAZARD DETECTION, Final
report, Dec 62, 212p., incl illus, 151 refs.

Unclassified report
I. AFSC Project 6075
Task 607506
II. Contract AF 33(616)-
8165
III. Femval Inc.,
Ashland, Mass.
IV. Terry Trumble
V. Avail for OTS
VI. In ASTIA collection

Information concerning possible engine fires,
smoke and other malfunctions in remote parts
of an aircraft.

System configurations are recommended which
would extend the capabilities of the basic
fiber bundle in meeting the diverse require-
ments of installation, operation and main-
tenance in various applications. An experi-
mental fiber optical system for flame de-
tection is described. It uses a 25 foot long
bundle and incorporates a special photo-
electric detection system and other embed-
ments of our findings.

(over)

Information concerning possible engine fires,
smoke and other malfunctions in remote parts
of an aircraft.

System configurations are recommended which
would extend the capabilities of the basic
fiber bundle in meeting the diverse require-
ments of installation, operation and main-
tenance in various applications. An experi-
mental fiber optical system for flame de-
tection is described. It uses a 25 foot long
bundle and incorporates a special photo-
electric detection system and other embed-
ments of our findings.